

INVESTIGATION OF THE MECHANISMS OF
URIDINE 5' TRIPHOSPHATE INDUCED
CONTRACTION OF RAT MESENTERIC ARTERY
SMOOTH MUSCLE

Thesis submitted for the degree of
Doctor of Philosophy
at the University of Leicester

by

Fouzia Panhwar M. Pharmacy

Department of Cell Physiology & Pharmacology
University of Leicester

July 2011

ABSTRACT

Fouzia Panhwar

Investigation of the mechanisms of uridine 5' triphosphate induced contraction of rat mesenteric artery smooth muscle.

Uridine 5' triphosphate (UTP) is a pyrimidine nucleotide which is released from a variety of cells including platelets and endothelial cells. The release of UTP can lead to vasoconstriction if there is damage to the endothelial layer and hence its actions on the vasculature are important areas of investigation.

The research presented in this thesis describes the measurement of isometric contractile responses of rat mesenteric arteries to UTP and of the electrophysiological measurements of ionic currents of smooth muscle cells isolated from these arteries.

UTP induced contractions were recorded using various pharmacological tools to investigate the possible signaling mechanisms leading to the contractile response. Particular attention was given to the identification of the ion channels involved in generating the UTP induced contraction. It was clear that the contraction was dependent on Ca^{2+} influx and my results indicated that this influx was only partly due to an increased activity of voltage-gated Ca^{2+} channels and that non-selective cation channels were also important. The involvement of PLC is likely as using U73122, a PLC blocker, significantly reduced the UTP induced response. However, the potential involvement of PKC is less convincing as several PKC isoform peptide inhibitors, linked to the carrier peptide Tat(47-57) to render them membrane permeable, failed to affect the contraction.

The ionic basis of the UTP induced contraction was studied by measuring the effect of UTP on various ionic currents measured in enzymatically isolated mesenteric artery smooth muscle cells using the whole-cell patch-clamp technique. UTP was found to inhibit both K_v and K_{ATP} currents, though in parallel to the contraction results, the UTP induced inhibition of these currents remained even in the presence of PKC block, suggesting a lack of involvement of PKC. Finally, application of UTP resulted in the activation of a non-selective current. An inhibition of K^+ currents and the activation of a non-selective cation current would lead to membrane depolarization, the activation of voltage-gated Ca^{2+} channels and, dependent on the permeability of the non-selective channels, an additional route for Ca^{2+} influx and hence contraction.

Acknowledgements

I would like to thank my Mum Fatima Panhwar and Dad Faiz Muhammad Panhwar for their motivation and prayers. A very special thanks and love to my husband Aqeel Ahmed Qureshi, and children Safia, Manzoor and Ramsha, without their cooperation, love, and encouragement I could never achieved my goal.

I would like to thank my supervisor, Dr. Noel Davies for all his help and support over the last four years especially in electrophysiology, data analyses and during writing up my thesis. I also extend my thanks to Dr Bob Norman for the Tat-PKC inhibitor peptides. I am thankful to Mrs Diane Everitt for all her technical support from learning dissection of rat mesenteric arteries to myography technique. I would like to thank Dr Nina Storey and all my lab fellows Jenny Brignell, Yusuf Bhagatte, Helen Turrell, Carl Nelson, Richard Rainbow, and Sadaf Afreen for having a fantastic time together.

I would like to thank my employer, University of Sindh and my sponsor, Islamic development Bank for providing me opportunity and financial support for the entire course of study.

ABBREVIATIONS

EXPLANATIONS

4-AP	4-aminopyridine
ADP	adenosine diphosphate
Ang-II	Angiotensin II
ATP	Adenosine triphosphate
BK _{Ca}	calcium activated potassium channels
CGRP	calcitonin gene related peptide
C-terminus	carboxyl terminus
DMSO	dimethylsulphoxide
EDHF	endothelium derived hyperpolarizing factor
EGTA	ethyleneglycol-bis(β -aminoethylether)-N,N,N',N' tetracetic acid
EK	potassium equilibrium potential
E _K	equilibrium potential for K ⁺
eNOS	endothelial nitric oxide synthase
ER	endoplasmic reticulum
Gd ³⁺	gadolinium
GPCRs	G-protein coupled receptors
GTP	guanosine triphosphate
HEPES	N-[2-hydroxyethyl]piperazine-N9-[2[ethanesulphonic acid]
IP3	inositol 1,4,5-triphosphate
K _{ATP}	ATP sensitive potassium channels
K _{ir}	inwardly rectifying potassium channel
K _v	voltage gated potassium channel
MLCK	myosin light chain kinase
MLCP	myosin light chain phosphatase
mM	millimolar
nM	nanomolar
NO	nitric oxide

ABBREVIATIONS EXPLANATIONS

N-terminus	amino terminus
PIP2	phosphatidyl inositol bisphosphate
PKA	protein kinase A
PKC	protein kinase C
PLC	phospholipase C
RyR	ryanodine receptor
S.E.M	standard error of the mean
SR	sarcoplasmic reticulum
STOCs	spontaneous transient outward current
TRP channel	transient receptor potential channels
TRPC	canonical transient receptor potassium channels
UTP	Uridine 5' triphosphate
μ M	micromolar

Table of Contents

CHAPTER 1	INTRODUCTION	10
1.1	GENERAL INTRODUCTION	11
1.2	THE CARDIOVASCULAR SYSTEM	12
1.3	ARTERIOLES: STRUCTURE AND FUNCTION	14
1.4	REGULATION OF PERIPHERAL BLOOD FLOW	15
1.4.1	<i>Extrinsic regulation</i>	15
1.4.2	<i>Intrinsic regulation</i>	17
1.4.3	<i>The myogenic response of blood vessels</i>	21
1.5	SMOOTH MUSCLE	22
1.5.1	<i>Smooth muscle contraction</i>	23
1.5.2	<i>Regulation of contraction in vascular smooth muscle</i>	24
1.5.3	<i>Smooth muscle membrane potential and its role in regulating contraction</i>	25
1.5.4	<i>Ion channels and smooth muscle contraction</i>	27
1.5.5	<i>Receptors involved in regulating smooth muscle contraction</i>	38
1.6	SIGNALING PATHWAYS INVOLVED.....	41
1.6.1	<i>G-protein coupled receptor (GPCR) signaling pathways</i>	41
1.6.2	<i>Ca²⁺ regulation</i>	48
1.7	PURINERGIC SIGNALING	49
1.7.1	<i>Introduction to purinergic signaling</i>	49
1.7.2	<i>Purinergic signaling</i>	51
1.8	AIMS AND OVERVIEW OF THE THESIS	54
CHAPTER 2	MATERIAL AND METHODS	56
2.1	DISSECTION OF RAT MESENTERIC ARTERIES.....	57
2.2	MYOGRAPHY	60

2.2.1	<i>Principles of small vessel myography</i>	60
2.2.2	<i>Mounting of mesenteric arterial segment</i>	62
2.2.3	<i>Normalization</i>	64
2.2.4	<i>Measurement of contractile responses</i>	65
2.2.5	<i>Analysis</i>	68
2.2.6	<i>Experimental Solutions:</i>	68
2.3	PATCH CLAMP ELECTROPHYSIOLOGY	70
2.3.1	<i>Cell isolation:</i>	70
2.3.2	<i>Principles of patch clamp electrophysiology</i>	71
2.3.3	<i>Whole cell patch clamp configuration</i>	75
2.3.4	<i>Practical aspects of the whole cell patch clamp technique</i>	75
2.3.5	<i>Data collection and analysis</i>	79
2.3.6	<i>Chemicals</i>	81
2.3.7	<i>PKC inhibitor peptides:</i>	82
2.3.8	<i>Experimental solutions for electrophysiology</i>	86
CHAPTER 3 UTP INDUCED CONTRACTILE RESPONSE OF RAT MESENTERIC ARTERIES		88
3.1	INTRODUCTION	89
3.1.1	<i>Uridine 5' triphosphate</i>	89
3.2	GENERAL CONDITIONS	91
3.2.1	<i>Contractile response</i>	91
3.2.2	<i>Analysis</i>	91
3.3	RESULTS	92
3.3.1	<i>UTP induced contraction was sustained and reproducible</i>	92
3.3.2	<i>Cumulative dose response curve for UTP</i>	94
3.3.3	<i>Role of extracellular Ca²⁺ influx in UTP induced contraction</i>	96
3.3.4	<i>Involvement of voltage gated Ca²⁺ channels</i>	98
3.3.5	<i>UTP induced contractions and activation of PLC</i>	101
3.3.6	<i>PKC involvement in the contractile response of mesenteric arteries to UTP</i>	103

3.3.7	<i>Are non-selective cation channels involved in UTP induced contraction?</i>	116
3.4	DISCUSSION.....	119
3.4.1	<i>UTP induced sustained contraction depends on extracellular Ca²⁺ influx</i>	119
3.4.2	<i>Voltage gated L-type Ca²⁺ channels and UTP induced vasoconstriction</i>	121
3.4.3	<i>UTP activates PLC to initiate a signaling cascade leading to contraction</i>	121
3.4.4	<i>Contribution of PKC to UTP induced vasoconstriction</i>	122
3.4.5	<i>Are non-selective cation channels involved in UTP induced contractions?</i>	124
3.5	SUMMARY	125
CHAPTER 4 INVESTIGATION OF THE MODULATION OF IONIC CURRENTS BY UTP		126
4.1	INTRODUCTION	127
4.2	KV CURRENT AND UTP	128
4.2.1	<i>Isolation of Kv current</i>	128
4.2.2	<i>Modulation of Kv current by UTP</i>	128
4.2.3	<i>Effect of low intracellular Ca²⁺ on Kv current modulation by UTP</i>	136
4.2.4	<i>Effect of PLC on Kv current modulation by UTP</i>	139
4.2.5	<i>Does UTP modulate Kv current via PKC?</i>	141
4.2.6	<i>K_{ATP} current and UTP</i>	144
4.3	MODULATION OF K _{ATP} CURRENT BY UTP	146
4.3.1	<i>Effect of Ca²⁺ on K_{ATP} current modulation by UTP</i>	146
4.3.2	<i>Does UTP modulate K_{ATP} current via PKC</i>	150
4.4	NONSELECTIVE CATION CURRENT EVOKED BY UTP.....	153
4.5	ISOLATION OF VOLTAGE GATED CA ²⁺ CURRENT.....	159
4.6	DISCUSSION.....	161
4.6.1	<i>Kv current and effect of UTP</i>	161
4.6.2	<i>K_{ATP} current and UTP</i>	163
4.6.3	<i>NSSC current and UTP</i>	164
4.6.4	<i>Voltage gated Ca²⁺ current</i>	164

CHAPTER 5	OVERALL DISCUSSION	166
5.1	DISCUSSION.....	167
5.1.1	<i>UTP induced contraction depends largely on extracellular Ca²⁺ influx</i>	<i>168</i>
5.1.2	<i>Voltage gated Ca²⁺ channels are partly involved in UTP induced contraction</i>	<i>169</i>
5.1.3	<i>UTP mediates contraction via PLC activation.....</i>	<i>170</i>
5.1.4	<i>Is PKC involved in generating the UTP induced contraction?.....</i>	<i>171</i>
5.1.5	<i>UTP activates non selective cation channel</i>	<i>174</i>
5.1.6	<i>UTP modulates Kv current.....</i>	<i>175</i>
5.1.7	<i>UTP modulates K_{ATP} current</i>	<i>177</i>
5.2	CONCLUSION AND FUTURE PERSPECTIVES	179
CHAPTER 6	REFERENCES	181

Chapter 1 Introduction

1.1 General Introduction

The research presented in this thesis involves the study of the mechanism of UTP induced contraction in rat mesenteric arteries. UTP is a pyrimidine nucleotide which is released from various cells including endothelial cells and platelets. The release of UTP, as well as other nucleotides, increases upon shear stress and cardiac ischemia (Erlinge and Burnstock, 2008). The research presented in this thesis describes the measurement of isometric contractile responses of rat mesenteric arteries to UTP and of the electrophysiological measurements of ionic currents of smooth muscle cells isolated from these arteries. The smooth muscle which is present in the middle layer of the arterial vessel plays a major role in the contractions of blood vessels and maintenance of blood pressure.

It is now well understood that membrane potential plays an important role in the regulation of myogenic tone. K^+ channels are involved in regulating the membrane potential and hence the myogenic tone and blood flow. Various vasoconstrictors, including UTP, are known to decrease K^+ channel activity, reducing the K^+ efflux thereby causing contraction of vascular smooth muscle cells (Standen and Quayle, 1998). Because of this particular attention was given to K_V and K_{ATP} channel function under normal physiological conditions and in the presence of UTP.

In the rest of this chapter I aim to provide an introduction to some cardiovascular concepts with special reference to small resistance arteries, smooth muscle contraction and the regulation of membrane potential.

1.2 The cardiovascular system

The cardiovascular system was first demonstrated to be a circulatory system by William Harvey an English physiologist. It comprises the heart (pump) and a network of distributing and collecting blood vessels. The main function of the cardiovascular system is to transport oxygen and essential nutrients to the tissues and to remove CO₂ and other metabolites.

The heart is composed of four chambers; the right atrium, right ventricle, left atrium and left ventricle. Both atria receive blood whereas the ventricles act as pumps. The heart operates as two pumps, the right ventricle and the left ventricle, which act in series to maintain the pulmonary and systemic circulation respectively. The presence of valves in the heart ensures that the unidirectional flow of blood is maintained. The aorta along with other arteries ensures the rapid distribution of blood to the systemic circulation, while the pulmonary artery delivers blood to the lungs where exchange of carbon dioxide with oxygen takes place.

Blood vessels form an extensive network to transport blood throughout body by the pumping action of the heart. The network of blood vessels comprises arteries, arterioles, capillaries and veins. These vessels differ in their physical dimensions, morphology and functional specialization. The inner lumen of the blood vessels is lined with a layer of cells called the endothelium. With the exception of capillaries, the walls of blood vessels are made up of three layers: tunica intima, tunica media and tunica adventitia. The main components of all blood vessels are (with the exception of capillaries): endothelial cells, elastic fibers and connective tissue and smooth muscle cells. Capillaries comprise endothelial cells and a basal lamina.

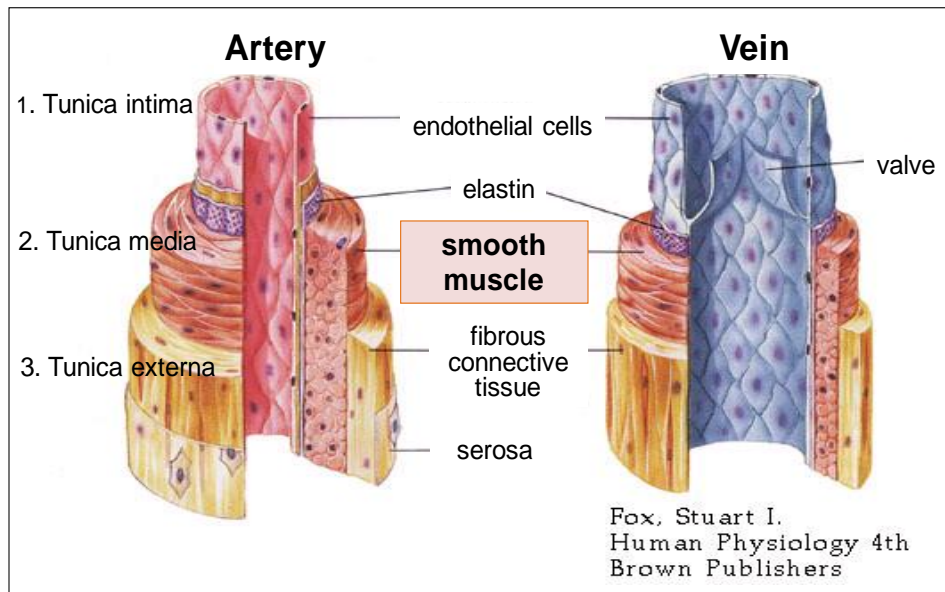


Fig: 1.1 Figure representing the anatomical structure of an artery and a vein.

Tunica intima This is the inner most layers of blood vessels and consists of a single layer of endothelial cells surrounded by collagenous fibers and an elastic membrane called elastic interna.

Tunica media In the tunica media of large arteries, a compact layer of smooth muscle is arranged in a helical or spiral manner with a layer of connective tissue and matrix. The relative abundance of smooth muscle and other components of the tunica media may vary among different blood vessels. The proportion of smooth muscle is higher in the smaller arteries as compared to large arteries. However elastic fibers in the media decrease as the size of the arterial vessel decreases. Only a single layer of smooth muscle cells is present in small arteries of 15-100 μm internal diameters (Greger, 1996). In contrast to arteries veins are thin walled vessels containing a thinner and loosely arranged media.

Tunica adventitia The tunica adventitia is the outer layer of blood vessels which forms the attachment to nearby organs. It is made of elastic and collagenous fibrils arranged longitudinally. This layer may also contain fibroblasts and macrophages.

1.3 Arterioles: structure and function

Arterioles are small diameter blood vessels that form a network of microcirculation along with capillaries. Arterioles are comprised of one to two layers of smooth muscle that forms their muscular portion and are considered the stopcock of the circulation as they provide the primary site of vascular resistance. Arterioles branch out to capillaries which are the site of exchange of gases and nutrients from blood to the tissue.

The contractile activity of smooth muscle controls the tone of the resistance and terminal arteries and thereby plays an important role in the regulation of blood flow and blood pressure. Contraction of smooth muscle cells reduces the radius of the blood vessels and according to Poiseuille's equation:

$$Flow = \Delta P \cdot r^4 / 8\eta \cdot L \quad 1.1$$

Where ΔP is the pressure difference, r is the radius of the vessel, η is blood viscosity and L is length of the blood vessel. According to equation 1.1, the radius has a large effect on blood flow and hence a small decrease in radius will result in a large increase in the resistance to flow. The tonic contraction of vascular smooth muscle has great influence on the vascular resistance and maintains the local blood flow, arterial pressure, capillary filtration and central venous pressure (Levick, 2003).

1.4 Regulation of peripheral blood flow

The peripheral blood flow is regulated by two mechanisms, an extrinsic mechanism and an intrinsic or local control.

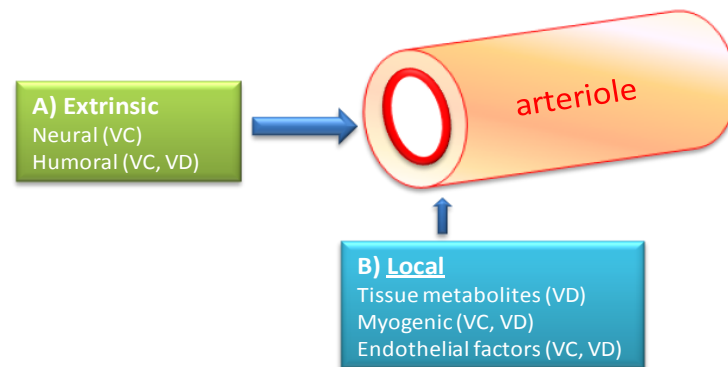


Fig: 1.2 Peripheral blood flow is under extrinsic and local or intrinsic control

1.4.1 Extrinsic regulation

1.4.1.1 Neuronal control

Smooth muscle cells of blood vessels are under the control of the autonomic nervous system and are innervated by post-ganglionic sympathetic nerve fibers. These sympathetic post ganglionic nerve fibers release noradrenaline and ATP.

Noradrenaline acts on different adrenergic receptors to cause either vasodilation or vasoconstriction. Noradrenaline evoked responses are mediated by α and β adrenergic receptors present on the smooth muscle of blood vessels. Noradrenaline has a higher affinity towards α receptors as compared to β receptors. Generally α_1 -receptors are present on most blood vessels but in vessels supplying the heart, liver and skeletal

muscle β_2 receptors are found. Stimulation of α_1 receptors by noradrenaline causes vasoconstriction whereas β_2 receptor stimulation leads to vasodilation of arteries in skeletal muscle and liver. β_1 receptor stimulation by noradrenaline causes vasodilation in rat basilar arteries possibly by activating ATP-dependent K^+ channels (Kitazono et al., 1993). In mesenteric arteries the α_1 adrenergic receptor response predominates.

The release of noradrenaline can be altered by several factors. Ang-II increases the release of noradrenaline by acting on presynaptic angiotensin receptors, thereby increasing the effectiveness of sympathetic transmission. Other modulators depress the release of noradrenaline, including noradrenaline itself acting on α_2 receptors, adenosine, K^+ , and H^+ (Levick, 2003). ATP is released as a co-transmitter with noradrenaline from the sympathetic varicosities in the blood vessels and acts on purinergic receptors. Other neurotransmitters released from nerve terminals present in blood vessel walls include substance P, which causes vasodilation via release of nitric oxide, and calcitonin gene related peptide (CGRP). CGRP is known to be involved in autoregulation and has been shown to causes vasodilation in, for example, mesenteric and ophthalmic arteries of rabbits (Nelson et al., 1990, Quayle et al., Zschauer et al., 1992).

1.4.1.2 Hormonal control

The control of blood circulation by hormones is comparatively less important than neuronal control under physiological conditions; nevertheless, hormones play an important role in the control of blood flow, especially so during pathological conditions such as hemorrhage.

Adrenaline, a methylated form of noradrenaline, is secreted from the adrenal gland situated above the kidneys. Adrenaline and noradrenaline are collectively known as catecholamines and their plasma concentrations under resting conditions are 0.1 to 0.5 nM and 0.5 to 3.0 nM respectively (Levick, 2003). At rest adrenaline has relatively little effect on the cardiovascular system. However, as the concentration of adrenaline rises, for example during exercise, it causes muscle vasodilation and skin vasoconstriction via activation of β_2 and α_2 receptors respectively. Angiotensin II and vasopressin are two peptide hormones that are involved in regulation of blood volume; both of these peptides act as powerful vasoconstrictors also.

1.4.2 Intrinsic regulation

Intrinsic regulation or local control refers to the mechanisms that regulate vascular tone to meet the metabolic needs of nearby tissues. Additionally, local control also describes the responses to pathological conditions such as vasospasm and inflammation. The close interaction between the endothelial layer and smooth muscle exerts an important form of local regulation of vascular tone.

1.4.2.1 Endothelial factors

Various vasodilators such as nitric oxide (NO), endothelium derived hyperpolarizing factor (EDHF) and prostacyclin (PGI_2), are synthesized and released from endothelial cells. In addition, endothelial cells also synthesize and release endothelin-1 (ET-1), which is a very powerful peptide vasoconstrictor.

Nitric oxide An increase in shear stress due to an increase in blood velocity stimulates the production of endothelial nitric oxide (NO) via protein kinase B induced activation of the enzyme endothelial nitric oxide synthase (eNOS). NO is thereby synthesized and

released from the endothelial cells and acts to relax adjacent smooth muscle cells resulting in vasodilatation.

EDHF EDHF is an additional vasodilator, with properties different from either NO or prostacyclin, released by endothelium in response to increased shear stress (Mombouli and Vanhoutte, 1997).

1.4.2.2 Metabolic vasodilators

In order to supply oxygen to fulfill the metabolic demand of cardiac and skeletal muscle during elevated metabolism, the local blood flow to these regions increases. This increase in blood flow due to vasodilation in response to increased metabolism is called functional hyperaemia or metabolic hyperaemia. Small resistance blood vessels are most sensitive to metabolic control. The exact vasodilators causing metabolic hyperaemia may vary between tissues and are listed below:

Acidosis Carbon dioxide and lactic acid produced in metabolically active tissue causes local tissue acidosis resulting in vasodilatation. Acidosis based vasodilatation is particularly important in cerebral arteries and there is also a weak response to metabolic acidosis in skeletal and cardiac muscles.

Hypoxia is an important cause of vasodilatation but has opposing effects on the systemic and pulmonary circulation. Hypoxia dilates systemic arterioles whereas it constricts pulmonary arteries and large arteries. Hypoxia may be systemic or local. Systemic hypoxia at low oxygen pressure of <40 mmHg or 5 kPa causes vasodilation to increase tissue perfusion to restore oxygen supply. However, local hypoxia of skeletal

muscles during exercise leads to the formation of adenosine that is a contributing chemical agent to metabolic hyperaemia.

Adenosine Adenosine monophosphate is a breakdown product of ATP (adenosine triphosphate) that is largely produced during hypoxic conditions. AMP is further metabolized into adenosine by a nucleotidase in the interstitial fluid of skeletal muscle and myocardium. The adenosine formed causes vasodilation by activating adenosine receptors on vascular smooth muscle.

K⁺ ions The interstitial K⁺ concentration rises during exercise and neuronal activity and contributes to metabolic hyperemia. It is believed that during muscle contraction there is an initial rise of K⁺ concentration from 4 to 9 mM that causes hyperpolarization due to increased opening of inward rectifier potassium channels and activation of Na⁺-K⁺ pump (Levick, 2003).

1.4.2.3 Autacoids

Under various pathological conditions these chemicals are released and perform their specialized functions. These agents, called autacoids, that include histamine, bradykinin, serotonin, prostaglandins, thromboxane and leukotrienes are vasoactive agents that are released under various pathological conditions.

Histamine is released from mast cells and basophilic leukocytes under conditions such as trauma, allergic reactions and asthma. Histamine acts on H₁ and H₂ receptors of blood vessels to cause vasodilation or vasoconstriction respectively. H₁ receptor activation causes vasoconstriction via a G_q linked IP₃ signaling pathway; whereas, H₂ receptor activation causes vasodilatation via a cAMP dependent pathway.

Bradykinin causes vasospasm and is produced during inflammation from its plasma protein precursor kininogen by the action of kallikrein. Bradykinin causes vasodilatation of small resistance arteries and increases the permeability of veins. Its effect is also mediated by the release of other vasodilators like NO, EDHF and prostacyclin from endothelial cells.

Serotonin is produced from its amino acid precursor tryptophan in platelets, intestine and some neurons and is released during inflammation and causes vasoconstriction and increases the permeability of veins leading to inflammatory swelling.

Prostaglandins and thromboxanes are eicosanoids and are produced from arachidonic acid by the action of cyclooxygenase. Prostaglandins can be subdivided into the F category (PGF), which are vasoconstrictors, and the E category recognized for their inflammatory vasodilatory actions and reactive hyperaemia.

Thromboxane A₂ is a blood clotting factor synthesized by platelets and released during blood clotting by the action of cyclooxygenase. In addition to its thrombotic actions it is also a powerful vasoconstrictor and contributes to vasospasm in atheromatous coronary arteries.

Leukotrienes and platelet activation factors Leukotrienes and platelet activating factors (PAF) are important vasoconstrictors released from leukocytes in response to inflammation. The leukotrienes mainly cause constriction of venules whereas platelet activating factors cause constriction and contribute to bronchoconstriction in asthmatics and vasospasm in atheromatous coronary arteries.

UTP Uridine triphosphate is an important signaling molecule and also has an autocrine or paracrine role (Lazarowski and Boucher, 2001). UTP is released from platelets during thrombus formation and also from endothelial and vascular smooth muscle cells during shear stress, high glucose and hypoxia (Lazarowski and Boucher, 2001, Lazarowski and Harden, 1999). Mechanical stress is one of the major reasons of UTP release from nonsecretory cells (Lazarowski and Boucher, 2001). UTP is believed to activate mainly P2Y receptors, preferentially P2Y₂ and P2Y₄; whereas P2Y₆ is more likely to be activated by its metabolite UDP (Lazarowski and Boucher, 2001). Some studies, however, suggest that P2X₁ receptors can be activated by UTP (Lazarowski and Boucher, 2001).

1.4.3 The myogenic response of blood vessels

Arteries contract as a result of an increase in blood pressure and is called the myogenic response to blood pressure. Sir William Bayliss discovered the myogenic response and it is often termed the Bayliss myogenic response (Bayliss, 1902). The myogenic response is the contractile reaction of arteries and arterioles that occurs within seconds of mechanical distention in response to increased luminal pressure. The myogenic response contributes to basal tone and it is important that this tone is maintained to stabilize local blood flow and capillary filtration pressure. Little is known about the exact mechanism of the myogenic response but it involves smooth muscle depolarization and activation of Ca²⁺ channels (Omote and Mizusawa, 1996, Altura et al., 1987, Zhang et al., 2010). Myogenic constriction is reversed by increased shear stress of the blood flow which resulted in the increased production of vasodilators (e.g. nitric oxide) from endothelial cells (Levick, 2003).

1.5 Smooth muscle

Smooth muscle is the major component of several hollow organs including blood vessels (except capillaries) and represents about 2% of human body weight (Carsten, 1997). The term smooth muscle arises because of the lack of striations that are seen in skeletal and cardiac muscle. Each smooth muscle cell is 2 to 10 μm in diameter at the centre and is tapered at the end form a fusiform shape. In contrast to the T-tubules of striated muscle, smooth muscle cells have caveolae which are sac like pockets within the membrane that associate with the sarcoplasmic reticulum of the cell. The caveolae, in conjunction with the sarcoplasmic reticulum, may be involved in the regulation of intracellular Ca^{2+} (Kamishima et al., 2007); caveolin1 and caveolin3 are reported to be involved in the regulation of Ca^{2+} homeostasis in smooth muscle cells of rat cerebral arteries (Kamishima et al., 2007). There is evidence that some ion channels such as K_{ATP} channels are also associated with the caveolae in smooth muscle cells (Das and Das, 2011, Adebisi et al., 2010, Brainard et al., 2005, Cole, 2010, Sampson et al., 2007, Sampson et al., 2004). The sarcoplasmic reticulum is an intracellular store of Ca^{2+} from where Ca^{2+} can be released by IP_3 or ryanodine receptor activation following a signaling cascade. The contractile machinery of smooth muscle comprises of myosin (thick) and actin (thin) filaments but their physical arrangement is not as structured as in striated muscle. Generally, vascular smooth muscle exhibits long-lasting tonic contraction where the cross-bridges enter a latch state where contraction is maintained whilst using very little energy. In many vessels this vascular tone is maintained throughout life.

1.5.1 Smooth muscle contraction

Smooth muscle contraction results from crossbridge activity of actin and myosin. A rise in global Ca^{2+} concentration of the cytoplasm is required to activate the contractile machinery and hence it is the primary stimulus for contraction. A variety of stimuli trigger contraction by either increasing the intracellular Ca^{2+} concentration or by increasing the sensitivity of the contractile machinery to Ca^{2+} . For contraction to occur, four Ca^{2+} ions bind with one molecule of calmodulin which results in a conformational change enabling the Ca^{2+} -calmodulin complex to interact with and activate myosin light chain kinase (MLCK). The activated MLCK catalyzes the phosphorylation of a regulatory light chain on the myosin which is necessary for interaction with actin and cross-bridge cycling to occur (Kamm and Stull, 1985a, Kamm and Stull, 1985b, Sommerville and Hartshorne, 1986, Hai and Murphy, 1989a, Hai and Murphy, 1989b). The interaction between actin and myosin is stopped by de-phosphorylation of the myosin light chain by the enzyme myosin light chain phosphatase (MLCP) which is constitutively active. Thus the relative activity of these two enzymes regulates the contraction of smooth muscle (Hirano et al., 2004).

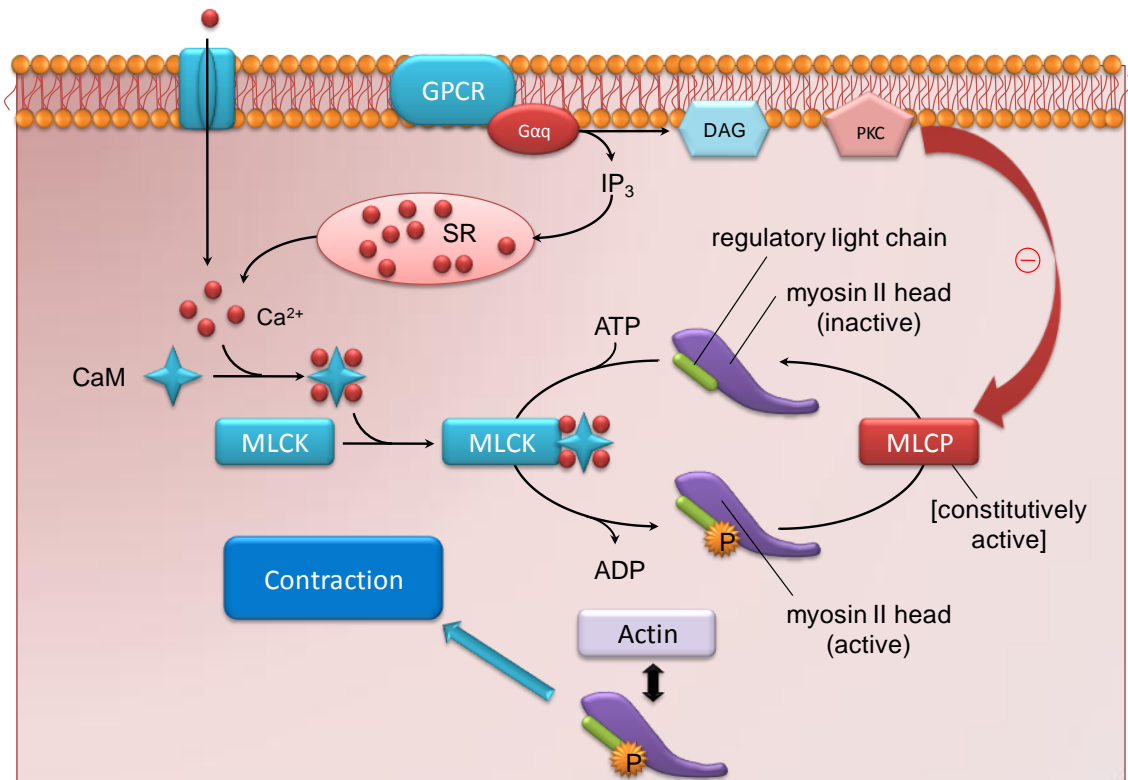


Fig: 1.3 Schematic diagram showing smooth muscle contraction

1.5.2 Regulation of contraction in vascular smooth muscle

An increase in intracellular free Ca^{2+} stimulates smooth muscle contraction whereas a decrease in intracellular Ca^{2+} leads to relaxation. The level of Ca^{2+} in the cytosol is increased due to Ca^{2+} release from intracellular stores or from Ca^{2+} entry through Ca^{2+} permeable ion channels. Vasoactive compounds initiate contraction by increasing the intracellular Ca^{2+} concentration leading to the formation of the Ca^{2+} -calmodulin complex. Agonist induced vasoconstriction mainly comprises an initial phasic contraction due to Ca^{2+} release from intracellular stores followed by a more prolonged tonic contraction maintained by Ca^{2+} entry. Various agonists are known to induce a transient contraction in vascular smooth muscle by releasing Ca^{2+} from the internal stores even in the absence of extracellular Ca^{2+} (Kanashiro and Khalil, 1998, Khalil, 2010, Khalil and van Breemen, 1988, Salamanca and Khalil, 2005). Many

vasoconstrictors also increase the sensitivity of the contractile mechanism to Ca^{2+} by decreasing the activity of MLCP, thus for a given $[\text{Ca}^{2+}]$ the balance towards the phosphorylated state of the myosin light chain will be favoured.

1.5.3 Smooth muscle membrane potential and its role in regulating contraction

Like all animal cells, smooth muscle cells are surrounded by a lipid bilayer membrane that is impermeable to ions. At rest, there is a negative charge inside the cell which is mainly due to the presence of large negatively charged protein molecules that are unable to diffuse out of the cell. A large difference in the ionic concentrations exists between the inside and outside of the membrane and typical values for smooth muscle cells are listed in table 1.1. Because of the charged nature of ions, and their separation by the membrane, an electrical force needs to be considered also. The potential at which the electrical force is equal but opposite to the diffusional (concentration gradient) force is termed the equilibrium potential which is calculated using the Nernst equation:

$$E_{ion} = \frac{RT}{zF} \ln \left\{ \frac{[ion]_{out}}{[ion]_{in}} \right\} \quad 1.2$$

Where E_{ion} is the equilibrium potential for the ion, z the charge of the ion and R , T and F have their usual thermodynamic values. Values of the equilibrium potentials are also given in table 1.1. The combination of the diffusional force and the electrical force is termed the electrochemical gradient.

The hydrophobic lipid plasma membrane stops ions diffusing down their electrochemical gradient. However, the presence of trans-membrane pores, which are

structural components of ion channels, enables such movement. Ion channels exist in either an open state, where the pore is open and allows flow of selective ions down their electrochemical gradient, or a closed state when there is no flow of ions. From table 1.1 it is seen that the concentration of K^+ is higher inside than outside and the equilibrium potential for K^+ (E_K) is -89 mV. There is, therefore, a tendency for K^+ to move down its electrochemical gradient such that the membrane potential moves closer to E_K , a potential at which there would be no net movement of K^+ . At the resting membrane potential the membrane is more permeable to K^+ than to other ions and hence K^+ ions move down their electrochemical gradient from the inside of the cell to the outside, resulting in an increase in the negative charge inside the cell. The resting membrane potential of smooth muscle *in vivo* is -40 to -55 mV (Harder, 1984, Nelson et al., 1990); however, *in vitro* the resting membrane potential ranges from -40 to -70 mV (Nelson et al., 1990, Neild and Keef, 1985). These potentials signify that the membrane potential of smooth muscle results from a relatively high permeability to K^+ ions at rest. A change in the relative permeability of the cell membrane, as a result of the alteration in the open probability of ion channels to one or more ionic species, eventually results in a change in the membrane potential because of the movement of ions down their respective electrochemical gradients.

Table 1-1 Ionic composition of vascular smooth muscle

Ion	Intracellular (mM)	Extracellular (mM)	Nernst equilibrium potential (mV)
K⁺	165	5	-89
Na⁺	9	137	+69
Ca²⁺	0.0001	1.2	+124
Cl⁻	54	134	-23
HCO³⁻	7.3	15.5	-19
pH	7.06	7.4	-20

(reproduced from (Levick, 2003))

1.5.4 Ion channels and smooth muscle contraction

The influx of Ca²⁺ from the extracellular space, either through voltage-dependent or receptor operated Ca²⁺ permeable channels, is one of the main regulators of smooth muscle contraction. Because of the presence of voltage-gated Ca²⁺ channels the amount of Ca²⁺ entry is tightly regulated by the membrane potential (Nelson et al., 1990). The following sections describe the main ion channels involved in regulating Ca²⁺ entry.

1.5.4.1 Voltage gated Ca²⁺ channels

Voltage gated Ca²⁺ channels are activated in response of membrane depolarization and mediate a subsequent Ca²⁺ influx. Voltage gated Ca²⁺ channels are composed of pore forming α subunit and many accessory subunits that regulate the pore formation and kinetic behavior of the voltage gated Ca²⁺ channels. The pore forming α subunits of voltage gated Ca²⁺ channels are large peptide molecules with four repeating segments, each with six membrane spanning domains (S1-S6) and a voltage sensing domain (S4). Because of the presence of a voltage sensor in the S4 domain of the α subunit, voltage gated Ca²⁺ channels are activated by depolarization of the plasma membrane (Catterall, 1995).

According to the electrophysiological characteristics of Ca^{2+} currents, Ca^{2+} channels can be divided into L-, T-, P/Q, R- and N-types (Horowitz et al., 1996). Among all these subclasses, L- and T- types are widely expressed in smooth muscles (Horowitz et al., 1996). L-type Ca^{2+} channels, also called long lasting Ca^{2+} channels, are widely distributed among smooth muscle cells with varying distribution between tissues. These channels are sensitive to dihydropyridines, an important class of antihypertensive drugs acting on L-type Ca^{2+} channels. The L-type Ca^{2+} channels are primarily regulated by the depolarization of smooth muscle resulting in L-type Ca^{2+} channel activation; however, maintained depolarization causes inactivation of these channels (Horowitz et al., 1996). A window current lies within the potential range where activation occurs but inactivation is incomplete. In human mesenteric arteries this window current starts at about -50 mV and peaks at -20 mV (Smirnov and Aaronson, 1992). In this physiologically important range a sustained non-inactivating Ca^{2+} influx occurs (Horowitz et al., 1996, Fleischmann et al., 1994). The important contribution of L-type Ca^{2+} channels to smooth muscle contraction has been demonstrated using dihydropyridine blockers such as nifedipine and nisoldipine which strongly inhibit depolarization induced contraction (Horowitz et al., 1996). Other voltage gated Ca^{2+} channel blockers such as verapamil and diltiazem belong to phenylalkylamine and benzothiazepine drug groups respectively (Perez-Reyes, 2003).

T-type Ca^{2+} channels, also termed low voltage activated (LVA) Ca^{2+} channels, are blocked by Ni^{2+} but are not significantly suppressed by L-type Ca^{2+} channel blockers such as nifedipine and nisoldipine (reviewed by (Horowitz et al., 1996). T-type channels possess distinct biophysical properties, such as their negative activation range, that are useful to isolate the T-type current from L-type (Horowitz et al., 1996). The T-type

current also inactivates more rapidly and at more negative potentials than the L-type Ca^{2+} current (Horowitz et al., 1996, Perez-Reyes, 2003).

1.5.4.2 TRP channels

The transient receptor potential channels or TRP channels are a large family of ion channels that are permeable to cations and many are permeable to Ca^{2+} as well as monovalent ions (Nilius et al., 2007). TRP channels, first discovered in *Drosophila* eye (Cosens and Manning, 1969) are also present on the membrane of smooth muscle cells (Chen et al., 2009, Hill et al., 2006, Minke and Cook, 2002, Tirupathi et al., 2006). Most TRP channels are non-selective in nature and are permeable to Na^+ , K^+ and Ca^{2+} ions (Soboloff et al., 2007). TRP channels are made up of six transmembrane domains (S1-S6), where the fifth and six domain forms the pore region. Four TRP subunits are required to form a functional channel (Clapham et al., 2001, Minke and Cook, 2002). The TRP channels are classified into three main groups: 1) TRPCx (short), 2) TRPVx (osm-9-like or vanilloid), and 3) TRPMx (long or melastatin). These groups can be divided further into subfamilies as shown in table 1-2.

As shown in the table 1-2, TRP channels are widely expressed in various tissues including the cardiovascular system (Clapham et al., 2001). TRP channels are often activated in conjunction with voltage gated Ca^{2+} channels and are therefore able to induce a sustained contraction in smooth muscle cells (Reading et al., 2005). Activation of TRP channels causes depolarization. Various TRP channels are involved in the regulation of important cellular functions such as Ca^{2+} influx. Dysfunction of TRP channels in cardiac myocytes is the potential cause of cardiac hypertrophy (Clapham et al., 2001). Studies on rat carotid arteries reveal that TRPC1/TRPC3 channels are

involved in depolarization induced by UTP in rat carotid arterial smooth muscle and hence are involved in maintaining the vascular tone (Chen et al., 2009).

Table 1-2 TRP channel subfamilies and their possible regulation

TRP Family	TRP subfamilies	Tissue distribution	Possible regulation
TRPC	TRPC1	Widely expressed in cells	Receptor operated, store depletion
	TRPC2	VNO, testis, heart, brain, sperm	Store depletion
	TRPC3	Brain, heart, muscle & placenta	DAG, IP3R
	TRPC4	Brain, testis, placenta, adrenal gland, endothelial cells	Receptor operated, store depletion
	TRPC5	Brain	Receptor operated, store depletion
	TRPC6	Lung, brain, muscle	DAG
	TRPC7	Heart, muscle, Lung, eye, brain	DAG
TRPV	TRPV1	Brain, spinal cord, peripheral sensory neurons	Capsaicin, heat, PKC
	TRPV2	Brain, spinal cord, spleen, lung, peripheral sensory neurons	Heat, growth factors
	TRPV4	Brain, liver, kidney, heart, fat, testis, salivary gland, trachea	Osmolarity
	TRPV5	Kidney, placenta, intestine	Low intracellular Ca ²⁺
	TRPV6	Kidney, intestine, placenta, prostate & salivary gland	Store depletion, low intracellular Ca ²⁺
	TRPV	TRPM1	Eye
TRPM2		Adult and fetal brain, placenta	ADP ribose
TRPM3		-	-
TRPM4		-	-
TRPM5		Widely expressed	-
TRPM6		Heart, brain, kidney, liver, spleen,	Phosphorylation
TRPV7		-	-
TRPV8		-	-

Table adapted from (Clapham et al., 2001)

1.5.4.3 K⁺ channels

Small resistance arteries exist in a partially contracted state and respond to changes in transmural pressure by undergoing further dilation or constriction. This is called myogenic tone that in turn depends on the membrane potential of the smooth muscle cells of these arteries. The membrane potential, an important determinant of the myogenic tone, is regulated by the open probability of potassium channels and thereby controls the arterial tone and subsequently the diameter of the small resistance blood vessels. Upon opening of K⁺ channels there is an efflux of K⁺ causing membrane hyperpolarization resulting in a closure of voltage gated Ca²⁺ channels and eventually vasodilation. Excessive activation of K⁺ channels in conditions such as endotoxic shock lead to hypotension (Landry and Oliver, 1992); whereas inhibition of K⁺ channels by vasoconstrictors lead to depolarization and vasoconstriction (Landry and Oliver, 1992, Betts and Kozlowski, 2000, Rainbow et al., 2009).

The four main types of potassium channels are voltage gated (Kv) channels; Ca²⁺ activated (BK) channels; ATP-dependent (K_{ATP}) channels; and inward rectifier (Kir) channels. Potassium channel blockers have potential therapeutic benefits in conditions including arrhythmia, cancer, stroke and some neurological disorders (Tamargo et al., 2004, Surti and Jan, 2005).

1.5.4.4 Voltage-gated K⁺ (Kv) channels

Voltage gated K⁺ channels comprise a large number of closely related ion channels which share the basic property of being activated following membrane depolarization. Structurally they are composed of four similar or identical pore forming α subunits arranged together to form a tetramer. As shown in figure 1.4, each pore forming α subunit of the Kv channel is composed of six transmembrane domains (S1 to S6) with

an inner cytoplasmic N and C terminus. The S4 transmembrane domain acts as a voltage sensor. The H5 loop lies between the fifth and sixth transmembrane domain (S5-S6) of the K α subunits (Jan and Jan, 1992) and acts as a selectivity filter and is often the interaction site for extracellular ion channel blockers (Bett and Rasmusson, 2008). K α subunits may also coexist with the ancillary subunits of Kv channels. Examples of Kv ancillary subunits are KCNEs, KChIPs and Kv β s (Bett and Rasmusson, 2008).

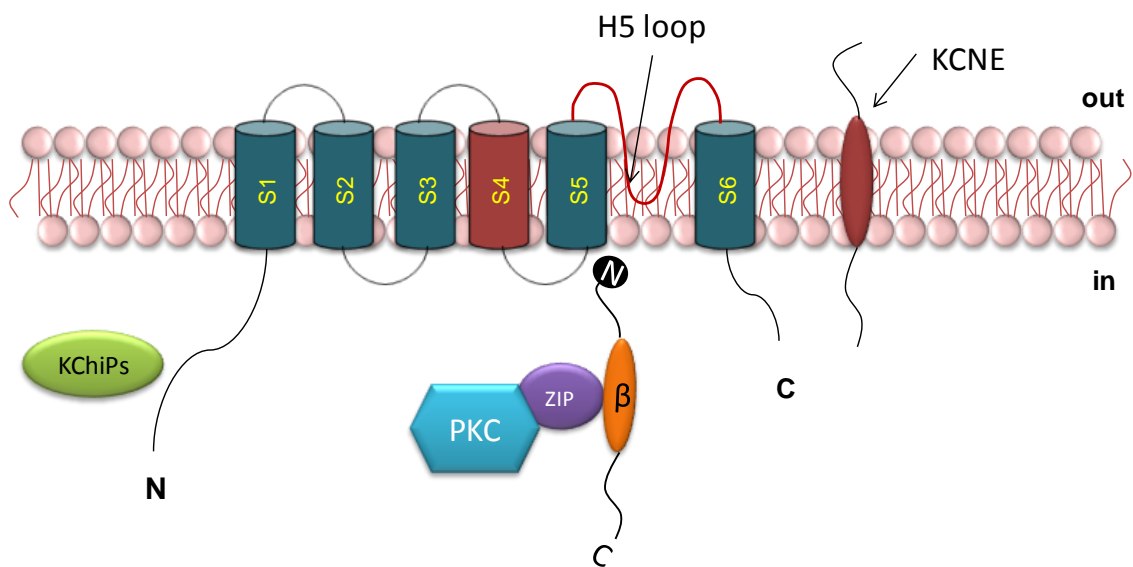


Fig: 1.4 Schematic diagram of Kv channels and its ancillary subunits.

(adapted from (Bett and Rasmusson, 2008, Cox, 2005)).

Among these ancillary subunits, the KCNEs are a family of single transmembrane domain with an intracellular C terminus and an extracellular N terminus. In contrast, to KCNEs, the KChIPs and Kv β s are cytoplasmic. KChIPs are believed to interact with the N terminus of the K α subunits whereas Kv β is known to interact with N- and C-termini of K α subunits (Bett and Rasmusson, 2008). In most cases interaction of the

ancillary subunits with α subunits of the Kv channel modulate the activity of the ion channel.

Message and protein expression of various Kv α subunits have been reported in rat mesenteric arteries, including Kv1.1 to Kv1.5; Kv2.1 to Kv2.2; Kv3.2 to Kv3.4; Kv4.1 to Kv4.3; and Kv9.3 (Cox, 2005). Coexpression of the Kv α subunits with ancillary subunits can have a dramatic effect on the kinetics of channel gating, for example coexpression of Kv β 3 (cloned from rat brain) with Kv α 1.1 introduced rapid N-type inactivation to the normally slowly inactivating Kv1.1 current (Bett and Rasmusson, 2008). Kv β 1, 2 and 3 subunits have been detected in smooth muscles (Cox, 2005). Among several Kv β subunits Kv β 1.1, 1.2 and 2.1 expression has been detected in mesenteric arteries (Cox, 2005).

Kv channels are voltage dependent, and open upon membrane depolarization allowing efflux of K⁺ and subsequent repolarization. In vascular smooth muscle at membrane potentials of -60 to -40 mV the activity of Kv channels is low, but when the membrane potential becomes more depolarized, activation of Kv channels results in K⁺ efflux which limits depolarization (Nelson et al., 1990). However, a sustained depolarization will eventually result in inactivation of many Kv channels (Panaghie et al., 2008). Activation and steady-state inactivation of Kv currents have been measured and quantified using the Boltzmann equation:

$$G = 1/[1 + \exp((V_{1/2} - V)/k)] \quad 1.3$$

Where G is the relative conductance, V the membrane potential, k is the slope factor and $V_{1/2}$ is the voltage for half maximal conductance. Typical values obtained from rat mesenteric arterial smooth muscle cells for activation are -11 and 15 mV for $V_{1/2}$ and k respectively, and for inactivation -40 and -14 mV for $V_{1/2}$ and k respectively (Cox, 2005). The kinetic behaviour and pharmacological properties of smooth muscle Kv currents reveal the presence of several components in smooth muscle from different vascular beds (Cox, 2005).

Vasoconstrictors including ET-1, Ang-II and AVP have been shown to suppress Kv currents of mesenteric arterial smooth muscle cells following PKC activation (Rainbow et al., 2009, Mackie et al., 2008), and block of Kv channels by 4-aminopyridine increases myogenic tone of rat mesenteric arteries (Plane et al., 2005). Furthermore, impaired functions of Kv channels contribute to some vascular diseases such as hypertension, pulmonary hypoxia, and subarachnoid haemorrhage (Cox, 2005).

1.5.4.5 Ca^{2+} activated K^+ channels

Ca^{2+} activated potassium channels can be divided into 3 main types depending on their size of their single channel conductance. Large conductance (BK) channels are voltage-dependent and Ca^{2+} dependent channels with a large single channel conductance of 100-250 pS; intermediate conductance (IK) channels have an intermediary single channel conductance of 18 to 50 pS; small conductance (SK) channels have a low single channel conductance of 2 to 25 pS and are voltage independent.

Like Kv channels the large conductance potassium channel (BK channel) is also expressed in vascular smooth muscle and comprises pore forming α subunits and regulatory β subunits (Ko et al., 2008, Knaus et al., 1994, Tanaka et al., 2004). Four α

subunits are closely arranged to form the tetramer where each α subunit contributes to the pore formation of the channel (Ko et al., 2008). Each α subunit is composed of 11 hydrophobic domains (S_0 to S_{10}) with an extracellular N terminus and long intracellular C terminus (Ledoux et al., 2006). The S_1 - S_6 domains are similar to those in Kv channels. In addition to S_1 - S_6 transmembrane domains the α subunit also contains an additional transmembrane domain (S_0) and four cytosolic domains S_7 - S_{10} (Ledoux et al., 2006, Ko et al., 2008). The S_4 domain contains several positive charges due to the abundance of lysine and arginine amino acids. The large C terminus also contains a Ca^{2+} sensing region termed the calcium bowl (Wei et al., 1994). The regulatory β subunits, which comprise 2 transmembrane domains, modulate the Ca^{2+} sensitivity of BK channels (Ko et al., 2008, Ko et al., 2010).

The cytosolic Ca^{2+} concentration is an important regulator of BK channel activity and an elevated level of Ca^{2+} and depolarization increases the open probability of these channels (Blatz and Magleby, 1986). BK channels play an important role in the regulation of tone in vascular smooth muscle. An increase in intracellular Ca^{2+} due to agonists activation causes release of Ca^{2+} from intracellular stores or Ca^{2+} influx through voltage gated Ca^{2+} channels. This elevated Ca^{2+} activates ryanodine receptors (RyR) leading to further local Ca^{2+} release termed Ca^{2+} sparks which causes opening of nearby BK channels leading to efflux of K^+ . The current recorded due to activation BK channel is known as spontaneous transient outward current (STOC) (Bolton and Imaizumi, 1996). BK channel activation limits depolarization and provides a negative feedback mechanism to regulate vasoconstriction (Ko et al., 2008).

1.5.4.6 ATP-dependent K⁺ (K_{ATP}) channels

These potassium channels, which are inhibited by intracellular ATP, were first described in cardiac myocytes (Noma, 1983) and later identified in a variety of other cells including vascular smooth muscle (Standen et al., 1989).

Structurally K_{ATP} channels are composed of four Kir 6.x subunits (Kir 6.1 or Kir 6.2) which are pore forming subunits and four sulphonylurea receptor (SUR1 and SUR2) subunits to form a hetero-octamer protein complex. Sulphonylurea receptors are the targets of sulphonylurea antidiabetic drugs. K_{ATP} channels expressed in smooth muscle are composed of SUR2B with either Kir6.1 or Kir6.2 subunits (Yamada and Sunaga, 1997, Koh et al., 1997, Standen and Quayle, 1998).

K_{ATP} channels are activated by an increase in the ADP: ATP ratio (Quayle and Standen, 1994) and are important regulators of membrane potential and hence control the myogenic tone of small resistance arteries (Nelson and Quayle, 1995). Many vasoconstrictors also inhibit K_{ATP} channel activity to inhibit the efflux of potassium ions resulting in depolarization, activation of L-type Ca²⁺ channels and vasoconstriction.

Based on the fact that K_{ATP} channels have important regulatory roles in various tissues their pharmacology has been studied extensively and several blockers and activators have been synthesized to date. Among these pharmacological agents pinacidil, cromakalim, levcromakalim, nicorandil, minoxidil, diazoxide, and BRL-55834 cause vasodilation (Quayle et al., 1997). However, glibenclamide, an antidiabetic agent, significantly inhibits K_{ATP} channels and causes vasoconstriction of hyperpolarized smooth muscle (Quayle et al., 1995, Quayle et al., 1997).

1.5.4.7 Inward rectifier K⁺ (Kir) channels

Kir channels were first identified in skeletal muscle and have since been found in a variety of cells including neurons, cardiac myocytes, endothelial cells, pancreatic beta cells and kidney cells (Hibino et al., 2010). Kir channels are also expressed in smooth muscle cells, in particular those of small resistance arteries such as cerebral, coronary and mesenteric arteries (Ko et al., 2008, Park et al., 2005a, Park et al., 2006, Quayle et al., 1996, Smith et al., 2008, Standen and Quayle, 1998).

The Kir current, because of its strange behavior was first named the anomalous rectifier potassium current and later called the inward rectifier K⁺ current. The activation of this channel is closely linked to the external K⁺ concentration and hence on E_K. Kir channels are more active near to and at potentials negative to E_K.

The Kir channels are, like Kv channels, tetramers but each Kir subunit contains two transmembrane regions only called TM1 and TM2, a pore forming H5 loop and intracellular N and C termini (Hibino et al., 2010). Kir channel subunits do not have a voltage sensing domain and are therefore not a voltage-gated ion channel, though their activity does depend on the K⁺ electrochemical gradient. Various (15 to date) Kir channel genes have been identified and have been grouped into families (Kir1.x - Kir7.x). According to their functional characteristics these Kir channels can be divided into four major groups: classical Kir channels (Kir2.x), G-protein gated Kir channels (Kir3.x) and ATP sensitive K⁺ channels (Kir6.x) and K⁺ transport channels (Kir1.x, Kir4.x, Kir5.x, and Kir7.x) (Hibino et al., 2010). The Kir channel subunits combine to form homomeric or heteromeric functional Kir channels where heteromerization occurs

by combination of the subunits from the same subfamily with the exception of Kir4.1 that combines with Kir5.1.

Several studies have confirmed that the mechanism of inward rectification occurs because of a block of the channel pore by intracellular polyamines and, to a lesser extent, Mg^{+} (Lopatin et al., 1994) and the membrane potential at which this block occurs is very dependent on the K^{+} concentration (Stanfield et al., 1994). In vascular smooth muscle, a modest increase in extracellular K^{+} concentration from 5 mM to 15 mM causes hyperpolarization of the membrane potential due to opening of Kir channels (Hibino et al., 2010).

Barium (Ba^{2+}) and Cesium (Cs^{+}) are the pharmacological agents most commonly used as Kir channel blockers. These blockers can be applied externally to block most Kir currents and the blocking effect is voltage dependent but the block can be relieved by raising external K^{+} concentration (Hibino et al., 2010).

1.5.5 Receptors involved in regulating smooth muscle contraction

Receptors are protein molecules, present either on the surface of the membrane or within the cytoplasm, that act as sensors to which ligands bind to initiate a signal. Some receptors termed ionotropic receptors are ligand gated ion channels containing a central pore that is opened or closed (rarely) on ligand binding. These ionotropic receptors are hence directly involved in mediating the signal of the binding ligand. However, other receptors, termed metabotropic receptors, work indirectly by transmitting the signal of the binding molecule to other enzymes or effectors.

Ligands, the molecules which bind to receptors, can be neurotransmitters, hormones, autacoids or an intracellular ligand. Ligand binding is required to induce a conformational change in the receptor which enables the receptor to exert its effects either directly by opening an intrinsic ion channels or indirectly by initiating a signaling cascade. A ligand that activates a receptor is called an agonist, whilst one that inhibits the receptor is an antagonist. Four main types of receptors and their effectors along with examples are enlisted in 1-3.

Table 1-3 Types of receptor

	Ligand gated ion channels	G-protein coupled receptors	Receptor kinase	Nuclear receptors
Location	Membrane	Membrane	Membrane	Intracellular
Effectors	Ion channel	Channel or Enzyme	Protein kinase	Gene transcription
Coupling	Direct	G protein	Direct	via DNA
Examples	nAChR, GABA receptor	Muscarinic acetylcholine receptors, adrenoceptors	Insulin, growth factors, cytokine receptors	Steroid receptors
Structure	Oligomeric assembly of subunits with a central pore	Seven transmembrane helices making a monomeric or dimeric	Single transmembrane helix make a link between extracellular domain and intracellular kinase domain	Monomeric structure with separate receptor and DNA binding domains

Table adapted from (Rang, 2007)

1.5.5.1 Ligand gated ion channels

Ligand gated ion channels are integral membrane proteins with an intrinsic pore which, when open, allows flux of the permeant ions down their electrochemical gradient. These ion channels have an extracellular domain that contains a ligand binding site. Binding of

an agonist causes a conformational change in the receptor leading to opening of the pore. Examples of ligand gated ion channels are P2X receptors, which are found on smooth muscle and activated by ATP (Cho et al., 2010, Aronsson et al., 2010, Boland et al., 1992, Dobronyi et al., 1997, Zhao et al., 2004), fast acting neurotransmitter receptors such as the nicotinic acetylcholine receptor and the intracellular IP₃ and ryanodine receptors which are Ca²⁺ release channels.

1.5.5.2 G-protein coupled receptors (GPCRs)

The β adrenoceptor, the first G-protein coupled receptor (GPCR), was cloned in 1986 (Dixon et al., 1986). GPCRs constitute a family of more than 500 members and share some common features. G-protein coupled receptors have seven transmembrane α helices; each α helix comprises 22 to 28 hydrophobic amino acids. These receptors are named as G-protein coupled receptors because of their need for an intermediary protein, a G-protein (guanosine triphosphate binding protein), to mediate their signal to the effectors or other enzymes within the cell. GPCRs are also the therapeutic target of more than 30% of all drugs; therefore much attention is focused on the understanding of this rapidly emerging field of therapeutics. P2Y receptors, where UTP acts as a ligand, also belong to this important family of receptors (Abbracchio et al., 2003). G-protein coupled receptors are the target of several vasoconstrictors as well as neurotransmitters; therefore much attention has been focused on understanding the signaling cascade triggered by these receptors.

1.6 Signaling pathways involved

1.6.1 G-protein coupled receptor (GPCR) signaling pathways

Several vasoactive compounds, hormones and neurotransmitters are dependent on GPCR activation. These ligands bind to their specific GPCR present on the membrane. Ligand binding causes a conformational change in the receptor and enables the receptor to interact with the inactive heterotrimeric G protein. G proteins are membrane resident proteins and diffuse within the plane of the bilayer membrane to pass on the message of the receptor to the effector. The G-protein in its inactive state is a complex of α , β , and γ subunits and contains a GTP binding site in α subunit. This binding site is normally occupied by GDP in its inactive state; however, as soon as the G-protein trimer interacts with the activated GPCR a conformational change in the receptor decreases the binding affinity of the GDP to the G-protein so that GDP is displaced from its binding site and is replaced by GTP. The binding of GTP causes the G-protein to dissociate into $G\alpha$ -GTP and dimer $G\beta\gamma$. The activated free form of $G\alpha$ -GTP complexes may activate or inhibit enzymes of various signaling cascades depending on the type of the α subunit ($G\alpha_s$, $G\alpha_{i/o}$, $G\alpha_{q/11}$, $G\alpha_{12/13}$) as summarized in the Table 1-4. In a similar way, the $\beta\gamma$ -dimer also has the ability to activate certain ion channels or enzymes. However, the signaling pathways activated by $\beta\gamma$ -dimers need more GPCRs to be activated (Rang, 2007).

G-protein signaling is terminated when the GTPase activity of the α -subunit hydrolyses GTP to GDP, resulting in the inactivation of the $G\alpha$ subunit that subsequently binds to the $\beta\gamma$ subunit to reform the inactive form of the G-protein (Sperelakis, 2001). It is also believed that GPCR of one type can interact with more than one type of G-protein and hence is able to initiate more than one signaling pathway. GPCRs are involved in regulating the following main signaling pathways:

1.6.1.1 Cyclic adenosine monophosphate (cAMP) signaling pathway

Cyclic AMP is an important intracellular mediator that is synthesized from ATP by the action of a membrane bound enzyme adenylate cyclase. Several drugs, hormones and neurotransmitters act on GPCRs to produce their effects by increasing or decreasing the activity of adenylyl cyclase and thereby affecting the production of cAMP. Two isoforms of G-protein α subunits modulate adenylate cyclase activity; G_s (G_s) stimulates whereas G_i inhibits adenylate cyclase.

Upon activation, the G_s -GTP complex activates the catalytic domain of the adenylyl cyclase and enables the adenylyl cyclase to convert ATP to cAMP which then acts as a second messenger to mediate the signal of the GPCR to other components of the cell. In most animal cells cAMP activates cAMP dependent protein kinase (PKA). PKA catalyzes several important functions and in its inactive form consists of a complex of two catalytic subunits and two regulatory subunits. The binding of cAMP to the regulatory subunits of PKA causes a conformational change that liberates the catalytic subunits. The catalytic subunit of PKA phosphorylates specific target proteins, for example, in patches excised from mesenteric smooth muscle PKA causes an increase in the activity of Kv channels (Hayabuchi et al., 2001b).

1.6.1.2 Phosphoinositide or Phospholipase C signaling pathway

Activation of GPCRs coupled to G_q initiates a signaling cascade via activation of the enzyme phospholipase C. Phospholipase C is a plasma membrane bound enzyme that catalyzes the hydrolysis of the phospholipid, phosphatidylinositol 4,5-bisphosphate (PIP_2) to inositol 1,4,5-trisphosphate (IP_3) and diacylglycerol (DAG). Both of these are important signaling molecules. In general, IP_3 causes release of Ca^{2+} by binding to IP_3

receptors (IP₃R) present on the membrane of the endoplasmic reticulum. DAG activates the serine threonine protein kinase C (PKC) either alone or in combination with cytosolic free Ca²⁺, which in turn catalyzes the phosphorylation of many other proteins (Somlyo and Somlyo, 2000).

Protein kinase C was formerly described as a Ca²⁺ activated phospholipid-dependent protein kinase (Salamanca and Khalil, 2005). Protein kinase C (PKC) comprises a family of various isoforms with distinct characteristics and physiological functions (Salamanca and Khalil, 2005). PKC isoforms are classified into three sub groups (Nishizuka, 1992).

The conventional PKCs (cPKC): α , βI , βII , and γ . The conventional PKC isoforms comprise four conserved regions (C1–C4) and five variable regions (V1-V5). Cysteine-rich zinc finger-like motifs are present in the C1 region of the regulatory domain. It also contains an autoinhibitory pseudosubstrate sequence. A recognition site for phosphatidylserine, DAG and phorbol ester is also present within the C1 region (Salamanca and Khalil, 2005). The C2 region contains the binding site for Ca²⁺. The C3 and C4 regions act as catalytic domains and form the ATP- and substrate-binding sites (Salamanca and Khalil, 2005).

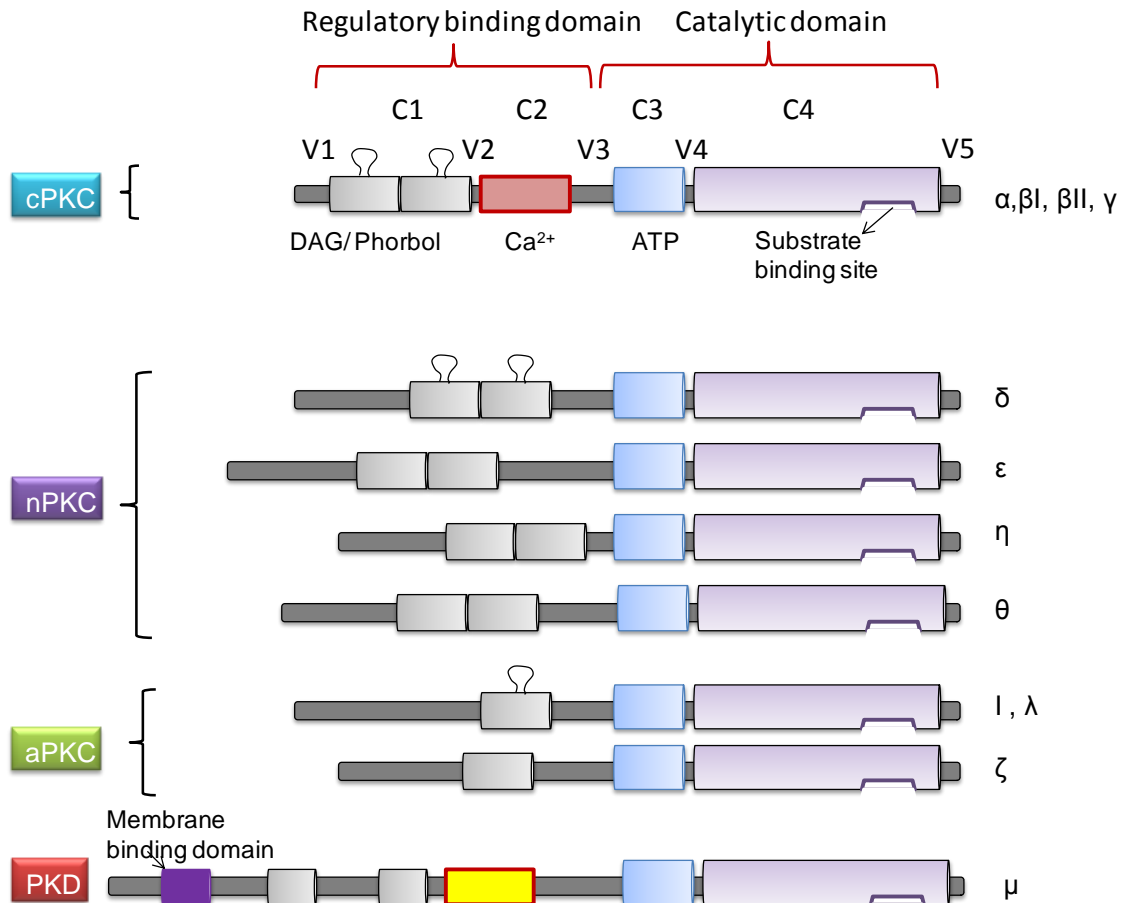


Fig: 1.5 Structure of PKC isoforms

adapted from (Salamanca and Khalil, 2005).

The novel PKCs (nPKC): δ, ε, η and θ The C2 region is not present in the novel PKC isoforms and hence these do not require Ca^{2+} for their activation (Salamanca and Khalil, 2005).

The atypical PKCs (aPKC): ζ and λ/ι The atypical PKC isoforms also lack a C2 region in their structure and also only one cysteine-rich zinc finger-like motif is present and therefore they are dependent on phosphatidylserine, but are unaffected by DAG, phorbol esters or Ca^{2+} (Salamanca and Khalil, 2005).

The PKD family comprises three structurally related isozymes i.e. PKD1 (also called PKC μ), PKD2, PKD3 (formerly called PKC ν) that also belongs to the family of serine threonine kinases. However these are classified as a subfamily of the Ca²⁺- calmodulin dependent kinases (CaMK) due to their close structural homology to CaMK and MLCK at their catalytic domain. The PKD is a DAG receptor that possesses high mobility and communicates the signal from DAG and PKC (Wang, 2006).

In mesenteric artery smooth muscle cells PKC α , γ , δ , ϵ , and ζ isoforms are expressed (Salamanca and Khalil, 2005). PKC phosphorylates important regulatory proteins in vascular smooth muscle many of which are important in the regulation of contraction (Lee and Severson, 1994, Salamanca and Khalil, 2005). Many vasoconstrictors induce contraction via activation of specific PKC isoforms, for example Ang-II and ET-1 induce contraction in rat mesenteric arteries by activating PKC ϵ and PKC α respectively (Rainbow et al., 2009). It is generally believed that most of the PKC isoforms including conventional, novel and atypical are activated via the PLC signaling pathway. Several agonists act at GPCRs and activate PLC via G_{q/11} to produce IP₃ and DAG as second messengers. The DAG, either alone or in combination with Ca²⁺ activates PKC.

PKC phosphorylates various regulatory proteins such as CPI-17 and MARCKS (myristoylated alanine-rich C-kinase substrate) (Salamanca and Khalil, 2005). PKC phosphorylates CPI-17 which interacts with myosin light chain phosphatase to decrease its activity effectively increasing the Ca²⁺ sensitivity of the contractile machinery (Mueed et al., 2005, Xie et al., 2006). It is also reported that PKC affects plasma membrane ion channels including L-type Ca²⁺, K_v, Kir; and K_{ATP} channels and pumps including the Na⁺-H⁺ exchanger (Maddali et al., 2005, Park et al., 2006, Rainbow et al., 2009, Ratz and Miner, 2009, Sampson et al., 2007, Endoh et al., 1998,

Hayabuchi et al., 2001a). PKC inhibits L-type voltage gated Ca^{2+} channels (Navedo et al., 2005, Schuhmann and Groschner, 1994) and vasoconstrictors inhibit several types of potassium channels via PKC mediated pathways (Salamanca and Khalil, 2005). Among smooth muscle K^+ channels PKC has been reported to modulate are Kv channels (Fish et al., 1988, Hayabuchi et al., 2001b), inward rectifier potassium channels (Park et al., 2007, Park et al., 2005b, Wu et al., 2007) and ATP sensitive potassium channels (Standen and Quayle, 1998, Kubo et al., 1997). PKC also suppresses the BK channel activity in pulmonary arterial smooth muscle (Barman et al., 2004). Vasoconstrictors also activate non selective cation channels through PKC dependent or independent pathways (Soboloff et al., 2007).

1.6.1.3 RhoA/ RhoA- kinase signaling pathway

Vasoconstrictors are also able to sensitize the contractile machinery by employing Rho kinase signaling pathway (Somlyo and Somlyo, 2000). Agonists binding to GPCRs recruit $\text{G}\alpha_{12/13}$ which activates guanosine nucleotide exchange factor (RhoGEFs) which changes RhoA from its inactive GDP bound form (RhoA-GDP) to its active RhoA-GTP form by the exchange of GDP with GTP (Bishop and Hall, 2000). Subsequently, RhoA-GTP activates RhoA-kinase (ROCK) which, in smooth muscle, can increase the activity of MLCP (Kimura et al., 1996, Hirano et al., 2004). $\text{G}\alpha_{12/13}$ coupled GPCRs also tend to couple to other subclasses of GPCRs, such as $\text{G}\alpha_{q/11}$ (Somlyo and Somlyo, 2000).

Rhokinase is a serine threonine kinase and among its various isoforms, ROCK-1 and ROCK-2 are expressed in vascular smooth muscle (Khalil, 2010). In addition to sensitizing the contractile machinery, ROCK is also employed in various other cellular and metabolic processes of the vascular smooth muscle including cell proliferation, cell migration and gene transcription (Khalil, 2010). Luykenaar et al provide evidence for a

role of Rhokinase in Kv current modulation by UTP (Luykenaar et al., 2004) and demonstrated that the ROCK inhibitor (Y-27632) significantly modulated the Kv current inhibition and depolarization by UTP in rat cerebral arteries.

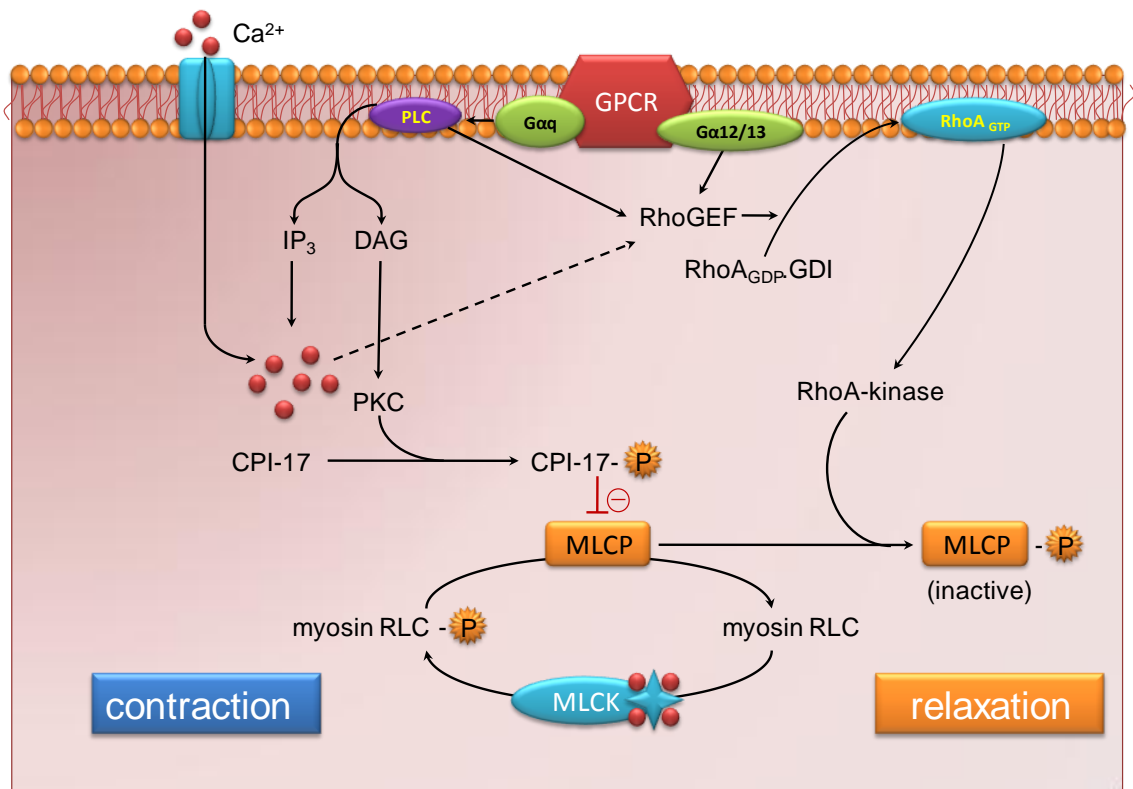


Fig: 1.6 GPCR mediated IP₃ and RhoKinase signaling pathway.

Figure modified from (Hirano et al., 2004)

1.6.1.4 Ion channels

Some ion channels can be modulated by direct interaction with the free Gβγ subunits released on activation of GPCRs. An example of this modulation follows ACh activation of M2 receptors in sinoatrial node cells of the heart which leads to the activation of G-protein regulated inwardly rectifying K⁺ channels (GIRKs); these channels are activated by the Gβγ released from the G_i-protein (Roche and Treisman,

1998, Vorobiov et al., 1998). Some voltage-gated Ca^{2+} Channels (P/Q- and N-type) are also modulated by direct $\text{G}\beta\gamma$ interaction (Tedford and Zamponi, 2006, Hernandez-Ochoa et al., 2007, Yoon et al., 2008).

Table 1-4 G-protein subtypes and their functions

G-protein subunit	GPCR	Effector	Comments
Gαs	Amines & other receptors like: histamine, catecholamine, and serotonin	Activates adenylyl cyclase \uparrow cAMP	Activated by cholera toxin
Gαi	Same as G α s; also opioid and cannabinoid receptors	Inhibits adenylyl cyclase \downarrow cAMP	Blocked by pertussis toxin
Gαo	Same as G α s; also opioid and cannabinoid receptors	Effects mainly due to $\text{G}\beta\gamma$ subunits	Blocked by pertussis toxin
Gαq	Amine, peptide and prostanoid receptors	Activates PLC, \uparrow DAG and IP3	-
G$\beta\gamma$	All GPCR	As for G α , also: Activate K^+ channel; inhibits VGCC; activate GPCR kinases and other kinases	Higher levels of GPCR activation required

Table adapted from (Rang, 2007)

1.6.2 Ca^{2+} regulation

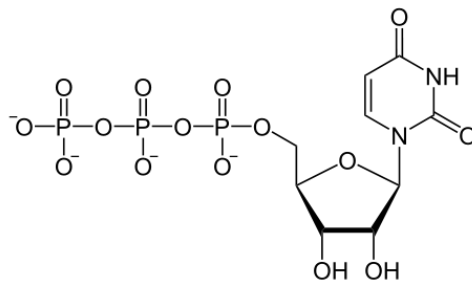
The cytosolic Ca^{2+} concentration is in the nanomolar range (50-150 nM) compared to an external concentration of 1.8 mM. However, the Ca^{2+} concentration rises to approximately 600-800 nM in response to depolarization or the action of vasoconstrictors (Horowitz et al., 1996). This small rise in Ca^{2+} concentration is sufficient to initiate contraction and comes from two main sources; external Ca^{2+} influx and Ca^{2+} release from the sarcoplasmic reticulum. Several vasoconstrictors induce a biphasic response in the smooth muscles. The initial rise in intracellular Ca^{2+}

concentration in response to vasoconstrictor occurs due to the release of Ca^{2+} from the internal stores following activation of IP_3 receptors on the sarcoplasmic reticulum (Berridge, 2009). A more sustained phase of the contraction is maintained by Ca^{2+} entry across the cell membrane through Ca^{2+} permeable channels (Khalil and van Breemen, 1988, Horowitz et al., 1996). The increased Ca^{2+} levels of the cytosol is decreased to resting levels by Ca^{2+} extrusion from the smooth muscle cell by plasma membrane Ca^{2+} ATPase and the $\text{Na}^+/\text{Ca}^{2+}$ exchanger in addition to being taken up into the sarcoplasmic reticulum via Ca^{2+} ATPase (Khalil, 2010).

1.7 Purinergic signaling

1.7.1 Introduction to purinergic signaling

The work done in this thesis concentrates on uridine 5' triphosphate, which is a pyrimidine nucleotide. UTP is a uracil nucleotide containing a uracil base which is linked to a ribose sugar that in turn contains three phosphates at its fifth carbon atom.



Among purine and pyrimidine nucleotides, adenosine compounds have been studied extensively since the discovery of a physiological role of ATP in the heart more than 80 years ago by Drury and colleagues (Drury and Szent-Gyorgyi, 1929). It is now known that nucleotides are released from platelets, endothelial cells and some other secretory

cells under normal as well as under stress conditions (Anderson and Parkinson, 1997); however, their release from non-secretory cells is as a result of tissue injury, inflammation or hypoxia. Nucleotides are released in the blood vessels from nerve terminals and from blood platelets (Boarder and Hourani, 1998). The signaling mechanism of ATP was studied in guinea pig cerebral cortex by Sattin and Rall in 1970 (Sattin and Rall, 1970) and later, in 1972, Burnstock defined ATP as a non-adrenergic and non-cholinergic neurotransmitter (Burnstock, 1976, Burnstock et al., 1978). Burnstock and coworkers classified purine receptors into P1 and P2. According to the current classification adenosine receptors are distinguished from other nucleotides and these are classified into P1 receptors and there are four adenosine receptors namely, A₁, A_{2A}, A_{2B}, and A₃. However, P2 receptors are classified into two broad categories of ionotropic P2X and metabotropic P2Y receptors (Abbracchio and Burnstock, 1994). Currently, seven subtypes of P2X and eight subtypes of P2Y receptors are recognized so far (Ralevic and Burnstock, 1998, North, 2002).

The classification was widely adopted when new receptors were identified (Ralevic and Burnstock, 1998). Within P2Y receptors, mammalian and non mammalian receptors could also be distinguished by writing the P2Y in lower case letters (p2y). The first P2Y₁ and P2Y₂ receptors were formerly named as P2U receptors. Later research based on cloning and identification discovered several P2Y receptors and hence P2Y followed by a subscript number sequentially list proteins in their chronological order of cDNA cloning with the exception of P2Y₁ and P2Y₂ that were formerly classified on the pharmacological basis (Abbracchio et al., 2006). To date eight human P2Y receptors have been cloned and identified as P2Y₁, P2Y₂, P2Y₄, P2Y₆, P2Y₁₁, P2Y₁₂, P2Y₁₃ and P2Y₁₄ (Abbracchio et al., 2003, Abbracchio et al., 2006). However, the missing

numbers are those receptors that are either non mammalian receptors and were initially grouped into this classification; or some receptors that are irresponsive to the purine or pyrimidine nucleotides. Since the pyrimidine nucleotide UTP is the focal point of this thesis the discussion will be limited to those receptors activated by pyrimidine nucleotides with especial reference to P2Y receptors.

1.7.2 Purinergic signaling

The ionotropic P2X receptor are widely stimulated by adenosine compounds with different rank orders of potency (table 1-5). UTP has also been shown to activate P2X₁ receptors at a higher concentration compared to ATP in rat tail artery (McLaren et al., 1998).

P2Y receptors, on the other hand, are G protein coupled receptors with seven transmembrane domains, an extracellular N- and intracellular C-terminus like other GPCRs and are activated upon binding of some purine and pyrimidine nucleotides. The P2Y₁ receptor, isolated from chick brain was the first in the series to be cloned and characterized as a G protein coupled receptor (Abbracchio et al., 2006). Several other P2Y receptors were isolated, cloned and characterized thereafter.

On the basis of pertussis toxin sensitivity and measurements of Ca²⁺, IP₃ and cAMP levels, P2Y receptors are believed to couple with G proteins (Abbracchio and Burnstock, 1994, Abbracchio et al., 2006). However, direct measurements of the coupling of nucleotides with G protein were done in vesicles reconstituted with various isoforms of G proteins and purified P2Y receptors. In these heterologous expression systems, G protein coupling was confirmed with P2Y₁, P2Y₂, P2Y₄, and P2Y₆ receptors (Abbracchio et al., 2006) and the signaling was via the activation of phospholipase C

and Ca^{2+} mobilization through IP_3 (Boarder and Hourani, 1998, Abbracchio et al., 2006). Furthermore, the same P_2Y receptor coupling to distinct G proteins was demonstrated in studies on HEL cells and gastric smooth muscle cells (Baltensperger and Porzig, 1997, Murthy and Makhlof, 1998). The studies on isolated gastric smooth muscle cells demonstrated that P_2Y_2 receptors couple to $\text{PLC}\beta_1$ via $\text{G}\alpha_{q/11}$ and to $\text{PLC}\beta_3$ via the $\beta\gamma$ subunit of $\text{G}\alpha_{i3}$. However, P_2Y_2 receptors also interact with integrins in astrocytoma cells to mediate the signaling cascade via G_o , not via G_q (Bagchi et al., 2005). UTP and ATP equipotently activates P_2Y_2 receptors (Lazarowski et al., 1995), however, human as well as rat P_2Y_4 receptors are potently activated by UTP (Harper et al., 1998) as well as other uracil nucleotides. UTP along with other tri and diphosphonucleotides were detected by Goetz et al (1971) in blood platelets of man, rabbit, guinea pig and cattle by chromatographic and spectrophotometric techniques (Goetz et al., 1971). Under normal physiological conditions, these purine (ATP and ADP) and pyrimidine nucleotides (UTP in small amount) are released from platelets which then act on the endothelium of the blood vessels and it is speculated that P_2Y receptor activation of the endothelium induces release of prostacyclin and nitric oxide resulting in vasodilation (Boarder and Hourani, 1998). Endothelium under normal physiological conditions acts as a barrier and nucleotides have access to the vascular smooth muscle only under various stress conditions such as subarachnoid haemorrhage and migraine (Boarder and Hourani, 1998, White et al., 2000).

It was reported that in rat mesenteric arteries UTP as well as ATP showed dual effects i.e. with intact endothelium, both nucleotides relaxed the noradrenaline induced vasoconstriction whereas in endothelium denuded arteries both of these nucleotides constricted the vessels (Ralevic and Burnstock, 1991).

Table 1-5 P2 receptor, agonists, antagonists, tissue distribution and the downstream signaling pathways

P2	Ligand	Antagonist	Tissue distribution (human)	Signaling pathway
P2Y₁	ADP >ATP	Suramin, PPADS	Endothelium, platelets, red blood cells (turkey), perivascular sensory nerves (low), perivascular sympathetic nerves (medium)	Gq11; PLCβ activation
P2Y₂	ATP =UTP	Suramin, not PPADS	Endothelium, VSMC, heart, inflammatory cells, perivascular sensory nerves (low), perivascular sympathetic nerves (possible)	Gq11; PLCβ activation
P2Y₄	UTP >ATP	Not PPADS or suramin	VSMC	Gq11; PLCβ activation
P2Y₆	UDP>ADP		Endothelium, VSMC, heart	Gq11; PLCβ activation
P2Y₁₁	ATP> >>ADP	-	Endothelium (possible), heart, inflammatory cells	Gq11; PLCβ activation
P2Y₁₂	ADP	-	VSMC, platelets, inflammatory cells	Gi/o; adenylate cyclase ↓
P2Y₁₃	ADP	-	Red blood cells, inflammatory cells	Gi/o; adenylate cyclase ↓
P2Y₁₄	UDP-glucose, UDP-galactose	UDP-glucose, UDP-galactose	-	Gi/o; adenylate cyclase ↓
P2X₁	ATP> ADP>UTP	Suramin, PPADS	VSMC, heart, platelets, inflammatory cells	Positive ion channel
P2X₂	ATP >>ADP,UTP	Suramin, PPADS	Perivascular sensory nerves, perivascular sympathetic nerves	Positive ion channel
P2X₃	ATP>ADP>UTP	Suramin, PPADS	Perivascular sensory nerves	Positive ion channel
P2X₄	ATP	Suramin, PPADS	Endothelium, heart, inflammatory cells,	Positive ion channel
P2X₅	ATP > ADP	Suramin, PPADS	-	Positive ion channel
P2X₆	ATP > ADP	Suramin, PPADS	-	Positive ion channel
P2X₇	ATP >ADP	Suramin, PPADS	VSMC (possible), red blood cells, inflammatory cells	Positive ion channel

Table adapted from (Boarder and Hourani, 1998, Erlinge and Burnstock, 2008, Abbracchio et al., 2006)

1.8 Aims and Overview of the thesis

The aim of the present study is to determine the mechanism by which UTP induces contraction of rat mesenteric arteries. The work described in this thesis focuses on two aspects: (i) measurements of contraction of rat small mesenteric arterial segments; and (ii) measurements of ionic currents in rat isolated mesenteric artery smooth muscle cells.

Chapter 3 describes the experiments done to investigate the UTP induced contraction of mesenteric arteries. The role of extracellular calcium and the downstream signaling pathways in response to UTP application were studied in this chapter. UTP induced sustained contractions of rat mesenteric arteries and my experiments were designed to investigate possible signalling mechanisms using various pharmacological agents. One aim was to use these pharmacological tools to dissect out the relative role that voltage gated Ca^{2+} channels and non-selective cation channels have in mediating the UTP induced contraction. Specific peptide blockers of selected PKC isoforms were linked to the Tat-peptide, making them highly membrane permeable, with the aim of examining possible specific roles that the PKC isoforms PKC α , β I, β II, δ and ϵ have in mediating the UTP response.

Chapter 4 describes the experiments done to determine the ionic basis of the UTP induced contraction. Using the whole cell patch clamp technique various currents were recorded in the absence and presence of UTP. The currents examined were the K_v current, the K_{ATP} current and a non-selective cation current. Many vasoconstrictors I, including Ang II and ET-1, have been shown to modulate these currents through specific PKC isoforms. The aim of the work presented here was to ascertain whether

UTP modulated these currents using specific PKC isoforms, again utilizing the specific Tat-linked PKC isoform inhibitors. An additional objective was to assess whether voltage-gated Ca^{2+} currents could be reduced directly by UTP induced signaling events. Although in my preliminary experiments I did manage to record whole-cell inward Ba^{2+} currents these were too small and labile to enable the effect of UTP to be tested on these currents.

Chapter 2 Material and Methods

2.1 Dissection of rat mesenteric arteries

Mesenteric arteries are small resistance arteries that supply blood to the small intestine. They are subdivided into branches and form the vascular mesenteric bed to provide a rich blood supply to the walls of the small intestine.

Mesenteric arteries of adult male Wistar rats (weight range 200-250 g) were used. The rats were killed by stunning followed by cervical dislocation and the mesenteric arteries were dissected out as described below.

The abdomen was cut carefully using forceps and a pair of scissors. The skin around the abdomen was lifted with the help of forceps and a small piece of the skin was cut for a short distance to expose the peritoneum. A piece of skin was cut away from the level of the pelvic region towards the bottom of the diaphragm. The peritoneal membrane was then picked up with help of forceps and carefully cut in a vertical direction from the lower abdomen towards the diaphragm. Furthermore, two small horizontal cuts at the abdominal region allowed easy access to the gut. To prevent drying of the exposed gut, zero Ca^{2+} solution was poured on to the exposed tissues. The mesenteric arteries lie in the middle of the gut and can be identified as a fat covered group of blood vessels connected with the intestine. The mesenteric arterial bed was exposed by a gentle movement of the small intestine.

The vascular bed of mesenteric arteries, along with the primary branch of the superior mesenteric artery, were dissected out carefully without stretching the arteries by cutting the mesenteric arteries away from the small intestine using a pair of micro scissors (Fig: 2.1). The arteries were then transferred to zero Ca^{2+} PSS. The dissection was

carried out under a microscope at room temperature. As shown in the Fig: 2.1 the vascular bed was transferred and pinned onto a Sylgard-based petri dish containing zero Ca^{2+} PSS such that the most visible blood vessels (mesenteric veins) were uppermost. Mesenteric veins could easily be distinguished from the mesenteric arteries due to their dark colour and fragile nature. The mesenteric veins were separated from the mesenteric arteries forceps and micro scissors. The mesenteric arteries were then cleaned of fat and adipose tissue Fig: 2.1. Following which they were clearly visualized as primary branches of the superior mesenteric artery which was branched into second, third and fourth order branches till the distal end. After dissection mesenteric arteries were either placed into some fresh ice cold normal PSS and maintained on ice for myography or were immediately enzymatically digested for cell isolation.

For enzymatic isolation of the cells the residual blood was gently squeezed out from the mesenteric bed without stretching the blood vessels; however for myography experiments stretching of the vascular bed was avoided as much as possible.

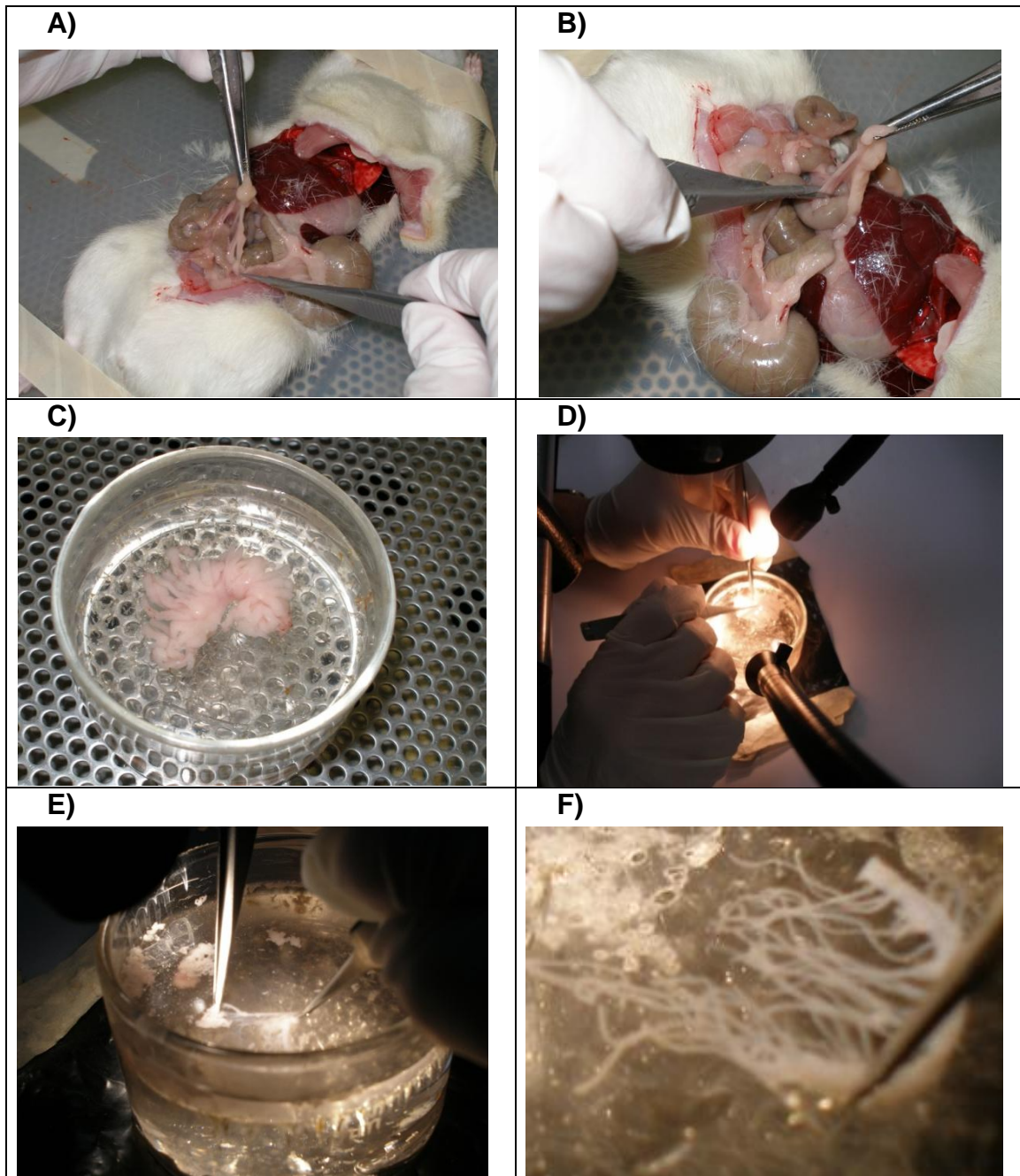


Fig: 2.1 Dissection of rat mesenteric artery

A-B) The mesenteric arterial bed from adult male Wistar rats were dissected out immediately after stunning and cervical dislocation; C) Mesenteric arteries were kept in a Sylgard petri dish containing ice cold PSS (0 Ca^{2+}) while removing adipose tissues and fat; D-E) Mesenteric arteries were cleaned of fat under microscope using forceps and micro scissors; F) The mesenteric artery with its lateral branches is seen clearly.

2.2 Myography

2.2.1 Principles of small vessel myography

Small vessel wire myography enables the force developed during isometric contraction of arterial segments to be measured. Several other parameters including the thickness of a vessel and its internal diameter could also be determined by this technique.

Before the 1980s information about the pharmacological and mechanical properties of the small resistance arteries were limited to histological examination and perfusion experiments. The myograph technique was developed by Bevan and Osher in 1972 and later adapted by Mulvany and Halpern (1976) (Bevan *et al.*, 1972) for making measurements in small vessels. The myograph mounting procedure does not rely on the direct attachment of a wire to the vessel segment; instead a mounting wire is threaded through the middle of the vessel lumen and secured under tension on both sides therefore allowing isometric contraction to occur. The arterial ring segments are stretched horizontally; hence the sheer force is the same along the length of the vessel wall.

In my myographic experiments I used a Myo-interface model 500A myograph (Fig: 2.2). This allows simultaneous measurement of two vessel segments and incorporates a system for adjusting the vessel extension, thereby enabling automatic normalization, calibration and data acquisition. Using this myograph the isometric contractile forces of mesenteric arterial segments during the application of various pharmacological agents were measured.

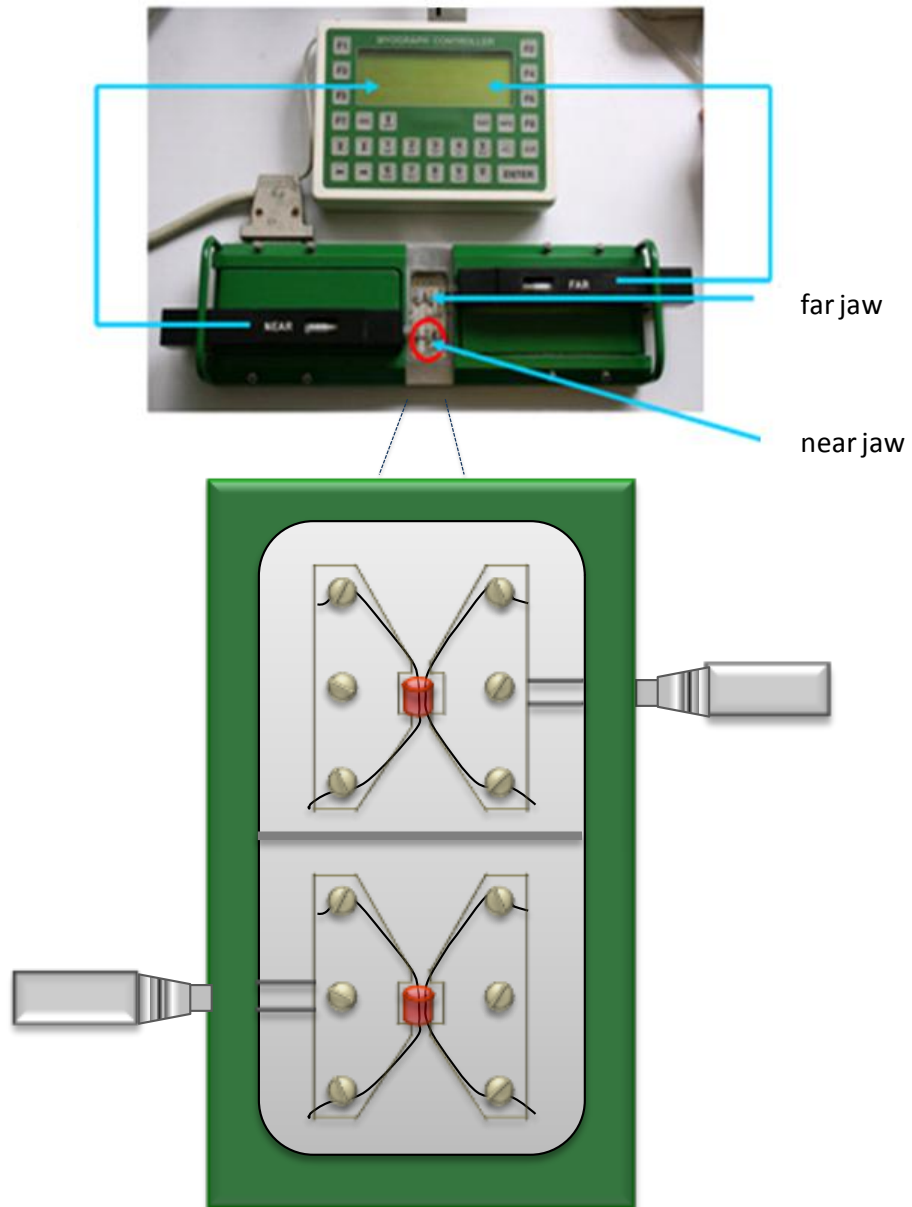


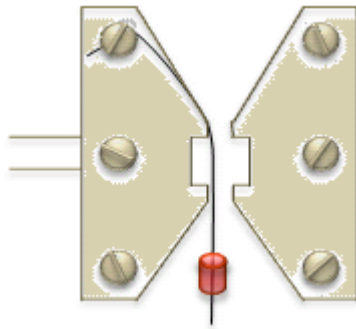
Fig: 2.2 Small vessel myograph.

The dual channel wire myograph (top);

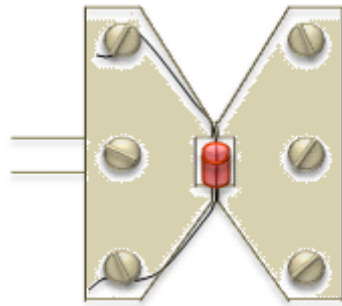
An illustrated diagram (bottom) of the wire myograph chambers, where small pieces of vessel are hanged using pieces of wires.

2.2.2 Mounting of mesenteric arterial segment

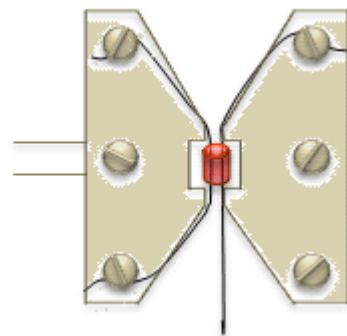
The myograph chamber was filled with ice cold physiological saline solution (PSS). One end of a 40 μm thick stainless steel wire was secured with fixing screws to the far end of the mounting jaw. The dissected mesenteric arteries were transferred into the myograph chamber and a suitable piece of third order mesenteric artery was selectively cut. This small piece of vessel was pushed gently into the near end of the screwed wire. The vessel was pulled along the wire and set at the central position of the mounting jaws Fig: 2.3A. The jaws were screwed together, the near end of the wire fixed under the fixing screws, and the jaws were moved apart slightly. Another wire was gently fed through the lumen of the vessel Fig: 2.3B and the jaws screwed together. Both ends of the wire were then fixed under fixing screws. In the wire myograph one of the jaws is movable and is attached to micropositioner whereas the other jaw is attached to a sensitive isometric transducer.



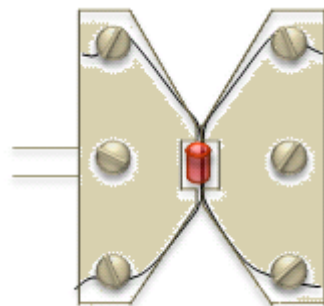
A) One end of the small piece of wire was secured under fixing screw in one of the jaw; the lumen of the mesenteric artery was passed along the wire.



B) The vessel was positioned in the middle of the mounting jaw; the free end of the wire was fixed under screw.



C) A second wire was also passed through the lumen of the same vessel and fixed under screw.



D) The free end of the second wire was also fixed under screw.

Fig: 2.3 Various steps of mounting mesenteric arterial segment in a wire myograph.

2.2.3 Normalization

Since the size of the vessel and its response to various agonists depends on the degree of stretch a normalization procedure was carried out to define the internal circumference as that when the vessel was fully relaxed and under a transmural tension equivalent to a pressure of 100 mmHg. Normalization was routinely performed after mounting the mesenteric arteries by distending the arterial segments in a step wise manner and measuring sets of micrometer readings and force readings on chart recorder or digital display. From these measurements various parameters can be calculated.

- i) The internal circumference of the vessel is calculated from the known diameter of the wire and the distance between the wires.
- ii) The wall length of the vessel is also determined in ocular divisions with the help of the eye piece of the microscope. It should also be noted that the wall length is the sum of the upper and the lower wall and is twice the segment length.
- iii) The wall tension is another parameter and is the measured force divided by the wall length.
- iv) The effective pressure, P_i is an estimate of the pressure that would be necessary to extend the vessel to the measured internal circumference and is given by the Laplace equation:

$$P_i = \text{Wall tension} / [\text{internal circumference} / (2\pi)] \quad \mathbf{2-1}$$

The effective pressure corresponding to vessel distension is therefore calculated by entering each pair of readings and the relevant calibration factors into the myograph controller. The stepwise distension of the vessel is stopped when the effective pressure exceeds 100 mmHg; where 100 mmHg = 13.3 kPa. The internal circumference is set to $IC_1 = 0.9 * IC_{100}$, since at this internal circumference the force production of the vessel

(with special reference to rat mesenteric arteries) is maximal. To the internal circumference data an exponential curve was fitted and the internal diameter of each vessel corresponding to a transmural pressure of 100 mmHg i.e. $l_{100} = IC_{100} / \pi$ was determined.

Output:

r^2 = regression coefficient for fit of (x_i, y_i) to an exponential curve; where x_i and y_i are micrometer reading (μm) and force reading (chart recorder division) respectively.

l_{100} = internal diameter corresponding to a transmural pressure of 100 mmHg and is given by IC_{100} / π .

x_1 = micrometer screw setting for which internal circumference corresponds to an internal diameter of l_1 ($l_1 = 0.9 * l_{100}$).

2.2.4 Measurement of contractile responses

After normalization the vessels were equilibrated with 6 mM K^+ normal PSS for 15 to 20 minutes to get a steady base line at 37°C. Since the endothelium was intact within the mesenteric arteries, 20 mM L-NAME was added to all solutions to inhibit the production of nitric oxide which might interfere with the contractile responses of mesenteric arteries. The solutions (maintained at 37°C in a water bath) were added or changed using a 1 ml transferring pipette in to the static bath of the myograph chamber. Contractile responses were digitized using an ADC interface (Digidata 1332A or Minidigi 1A, Axon Instruments), and stored on computer for subsequent analysis using pClamp 9 (Axon Instruments).

After obtaining a steady baseline with 6 mM K^+ PSS, the mounted mesenteric arteries were challenged with 60 mM K^+ as indicated in Fig: 2.4. A contraction on addition of 60 mM K^+ was used as a measure of the likely ability of the arterial segment to respond

to various vasoactive compounds. The contractile response of 60 mM K⁺ was washed by normal PSS as indicated by the immediate decline of the sustained phase to the base line as shown in the Fig: 2.4B. UTP (100 μM in normal PSS) was applied twice to measure the contractile response of the mesenteric arteries to UTP and to ascertain any possible desensitization of the receptor. The involvement of various ion channels or second messengers was studied using a range of pharmacological agents which were added 20 minutes prior to the third addition of UTP. Any unspecific effects were assessed by measuring the contractile response to 60 mM K⁺ in the presence of the compound at the end of the experiment. The dual channel wire myograph allows simultaneous measurements of the contractile responses of two arterial segments treated separately using a removable separator. Hence it was possible to treat one segment as a control and add the compound under test to the other segment only.

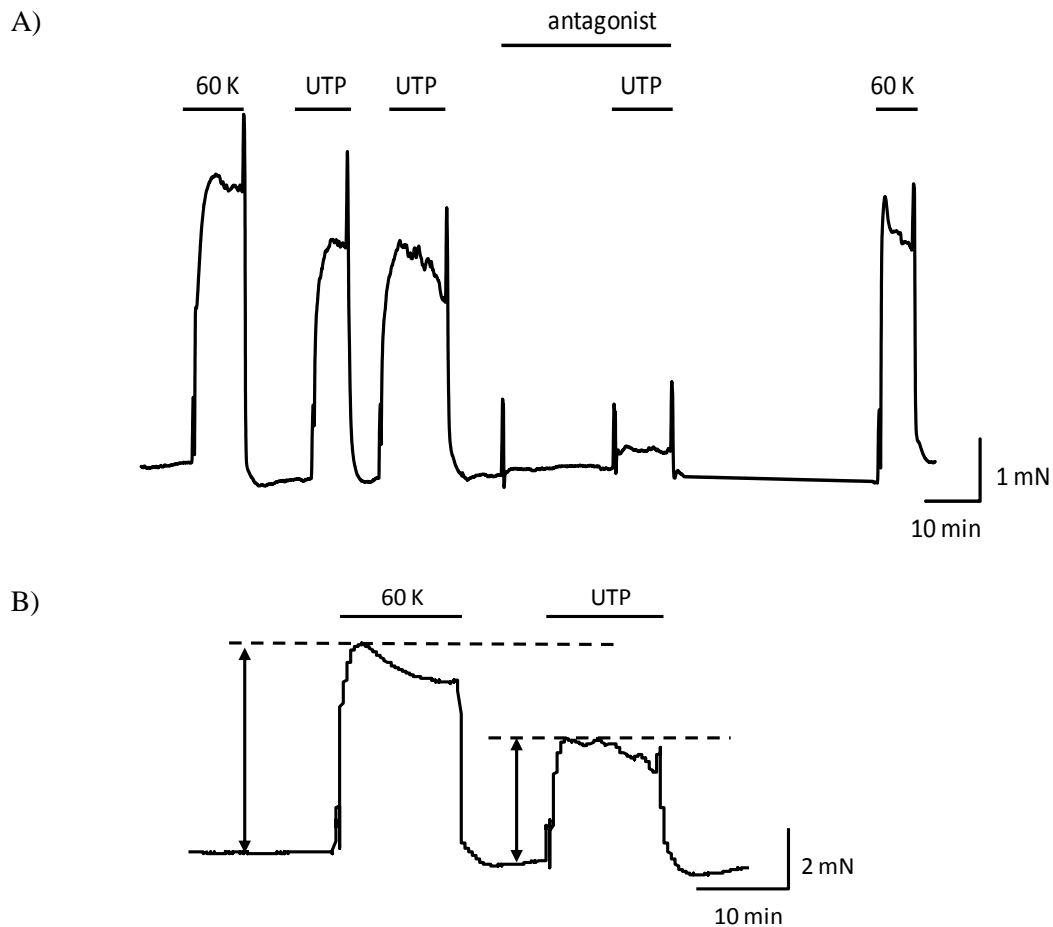


Fig: 2.4 Protocol for the measurement of contractile response

Representative traces of contractile responses of third order mesenteric arteries to the 60 mM K^+ and 100 μ M UTP in the absence and presence of antagonist.

A) The mesenteric arteries were allowed to equilibrate for about 15 minutes in normal salt Solution (PSS) after mounting in the wire myograph until steady base line was established at 37°C. To inhibit the production of NO all experiments were performed in the presence of L-NAME, an inhibitor of eNOS. The mesenteric arteries were washed with normal PSS after getting contractile response to the vasoconstrictors. The contractile response to 60 mM K^+ assured the viability of the mesenteric artery. The UTP was applied twice to assess the consistent contractile response evoked by UTP under control conditions. Mesenteric arteries were incubated for 20 minutes in antagonist; a third UTP induced contractile response was recorded and analyzed by normalizing it with the second UTP induced contraction.

B) The contractile responses of the mesenteric arteries to the vasoconstrictors were measured from the steady base line to the maximum steady contractile response to the vasoconstrictors.

2.2.5 Analysis

The contractile response to various pharmacological agents was measured relative to the nearest base line. The contraction evoked by UTP in presence of a blocker was normalized with the equivalent UTP induced contractile response in the absence of blocker (control, considered as 1 or 100 %) from the control portion of the same arterial segment. The contractile responses of UTP in the presence and absence of the blocker (control) were plotted as means \pm SEM. For analysis Student's paired *t* test was used; $P < 0.05$ was considered as significant.

The response to 60 mM K^+ in the presence of blocker was also measured in a similar way and normalized to the equivalent 60 mM K^+ evoked response in the absence of the blocker (control) from the same arterial segment and plotted as a histogram.

ET-1 induced contractions of mesenteric arteries were measured in a similar way by taking the maximal peak response relative to the nearest base line response. The ET-1 induced responses of each arterial segment were normalized to their respective 60 mM K^+ induced contractile responses. ET-1 induced contractile responses in the presence of the blocker were compared and plotted as a histogram against the contractile responses induced by ET-1 in absence of the blocker.

2.2.6 Experimental Solutions:

All chemicals were bought from Sigma-Aldrich (unless otherwise stated). Solutions (Table: 2.1) were made up in Elga deionized water and chemicals were added in solid form except for calcium chloride and magnesium chloride which were added from 1M stock solutions (both from BDH laboratory supplies). The solutions were adjusted to pH

7.4 with NaOH or HCl. The freshly made solutions were stored at 5° C in the refrigerator and used within one week. The pH of each solution was checked every day before experiments.

Table 2.1 Solutions for myography

Chemical	0 Ca²⁺ PSS	6 mM K⁺ Normal PSS	60 mM K⁺ PSS
NaCl	135 mM	135 mM	81.0 mM
KCl	6.0 mM	6.0 mM	60.0 mM
MgCl₂	1.2 mM	1.2 mM	1.2 mM
CaCl₂	—	1.8 mM	1.8 mM
Glucose	4.0 mM	4.0 mM	4.0 mM
Mannitol	6.0 mM	6.0 mM	6.0 mM
HEPES	10.0 mM	10.0 mM	10.0 mM

2.3 Patch clamp electrophysiology

2.3.1 Cell isolation:

Mesenteric arteries were dissected out and placed in Ca^{2+} free solution (4°C) containing (in mM): 137 NaCl, 5.4 KCl, 0.42 Na_2HPO_4 , 0.44 NaH_2PO_4 , 4 glucose, 6 mannitol, 10 HEPES, 1 MgCl_2 adjusted to pH 7.4 with NaOH. The mesenteric arteries were cleaned of fat and connective tissues and transferred to fresh Ca^{2+} free solution as described in section 2.1. The enzymes were added to a low Ca^{2+} solution containing bovine serum albumin (BSA, 0.9mg/ml). The composition of the low Ca^{2+} solution was the same as the Ca^{2+} free solution except that it contained 0.1 mM CaCl_2 . Two enzyme solutions were used for isolation of mesenteric arterial smooth muscle cells. The first contained (in mg/ml): 1.05 papain and 0.9 dithioerythritol and the second contained (in mg/ml): 0.45 collagenase and 0.6 hyaluronidase. The tissue was incubated in the first and second enzyme solutions (pre warmed for 10 min at 35°C) for 31 and 12.5 min respectively in a water bath at 35°C . At the end of tissue digestion, the enzyme solution was carefully drained out without disrupting the tissue and washed with low Ca^{2+} BSA to prevent further digestion and following this the tissue was washed with 2-3 ml of BSA free low Ca^{2+} solution. The tissue was then placed into a fresh bottle containing 3–4 ml of low Ca^{2+} solution and was triturated for a few min with a wide-bore pipette (glass or plastic) until the solution appeared cloudy due to the presence of isolated cells. The residual tissue was then removed and placed in a separate container and the cells were stored on ice. Healthy cells were long, thin and bright and were ready for experiments 20 to 30 minutes after isolation.

2.3.2 Principles of patch clamp electrophysiology

E. Neher and B. Sakmann first used the patch clamp technique to measure current in cell attached patches of membrane of frog skeletal muscle (Neher *et al.*, 1976a; Neher *et al.*, 1976b). The technique was subsequently refined by Hamill *et al.* (Hamill *et al.*, 1981) to enable various recording configurations including the measurement of whole cell currents in cells normally too small for conventional microelectrode recording. For this purpose a glass pipette containing suitable electrolyte solution is pressed against the membrane of the cell so that a high seal resistance is achieved between the tip of a clean glass electrode and the surface of the cell membrane. A high seal resistance of the order of $>10^9 \Omega$ (termed a gigaseal) is required for the complete isolation of the membrane patch and to ensure that the total ionic current flows from the cell membrane to the pipette which is then measured and amplified by a current sensitive headstage amplifier. With a gigaseal the distance between the pipette electrode and the cell membrane is estimated to be around 1\AA , so that small molecules are unable to diffuse through the seal (Walz, 2002). The high seal resistance is therefore effective in reducing the noise level of the recording by allowing current flow into the glass electrode rather than under the seal as shown in the Fig: 2.5.

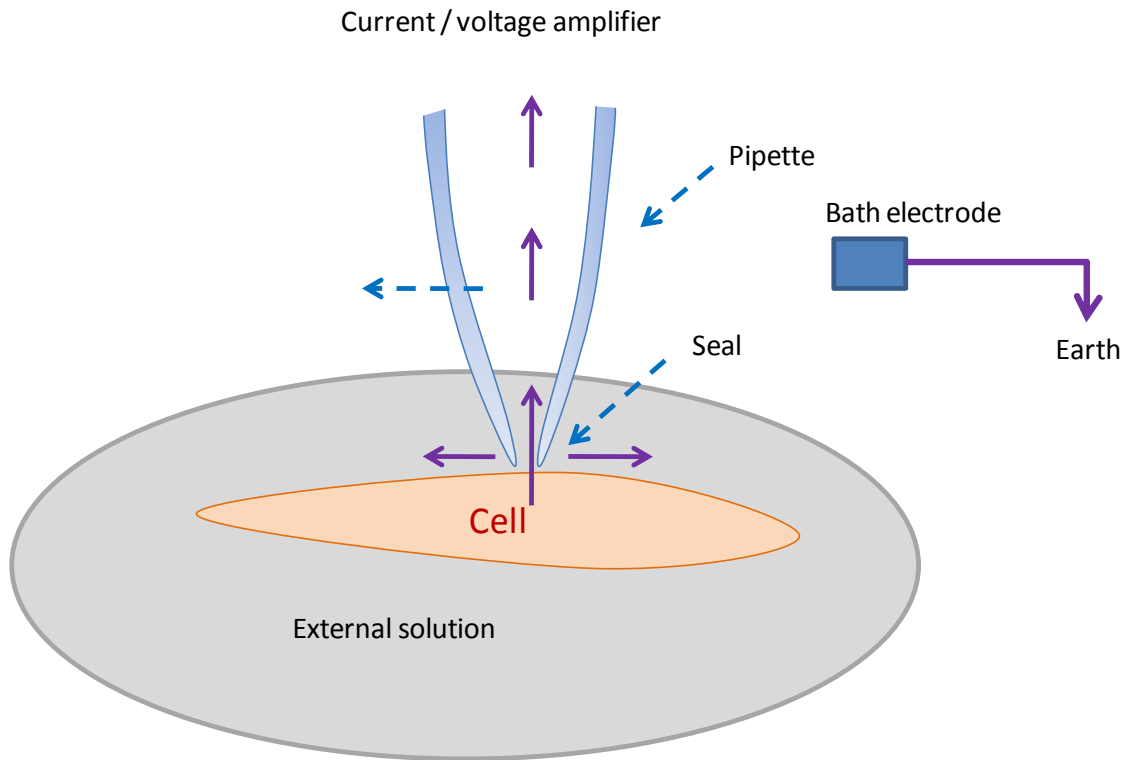


Fig: 2.5 Illustration of pipette to cell relationship and the current flow

The gigaseal formation allowed Hamill and colleagues to develop several different configurations of the patch clamp technique as shown in Fig: 2.6. The various configurations are described briefly:

The cell-attached mode is the first step of the patch clamp technique where a high seal resistance is achieved between the tip of the electrode and the patch of the membrane. In general the seal resistance increases as the tip of the pipette electrode is pressed against the surface of the membrane and a light suction to the interior of the pipette increases the seal resistance gradually to achieve a high seal resistance (Fig: 2.6). The cell attached configuration allows single channel recording from a variety of cells. From

the cell-attached mode experimenter can establish various other configurations such as inside out, whole cell, outside out and perforated patch.

The inside out configuration is used to measure single channel currents where the cytoplasmic side of the membrane patch is in contact with the bath solution. This configuration is obtained by pulling the electrode away from the cell in the cell-attached configuration so that the patch of membrane covered by the tip of the electrode is excised from the rest of the cell. The cytoplasmic side of the membrane patch is in contact with the bath solution, whereas the extracellular side of the membrane faces towards the patch pipette.

In contrast to inside out patch whole cell patch clamp configuration is used to measure the currents flowing through the ion channels of the membrane of the entire cell. Once a gigaseal is obtained, the whole-cell configuration is achieved by applying gentle suction, or a brief 1 V pulse, to rupture the membrane patch while retaining the gigaseal (Fig: 2.6). The patch pipette solution is in contact with the intracellular solution and ionic currents can be recorded from the whole cell.

The perforated patch configuration (Fig: 2.6) is an alternative method of recording from the whole cell where instead of rupturing the membrane patch a pore forming antibiotic such as amphotericin or nystatin is used in the internal pipette solution which acts on the membrane of the cell to make it permeable to monovalent ions in the cell-attached configuration. In this method the cytoplasmic contents remain intact and do not diffuse out of the cell into the patch pipette.

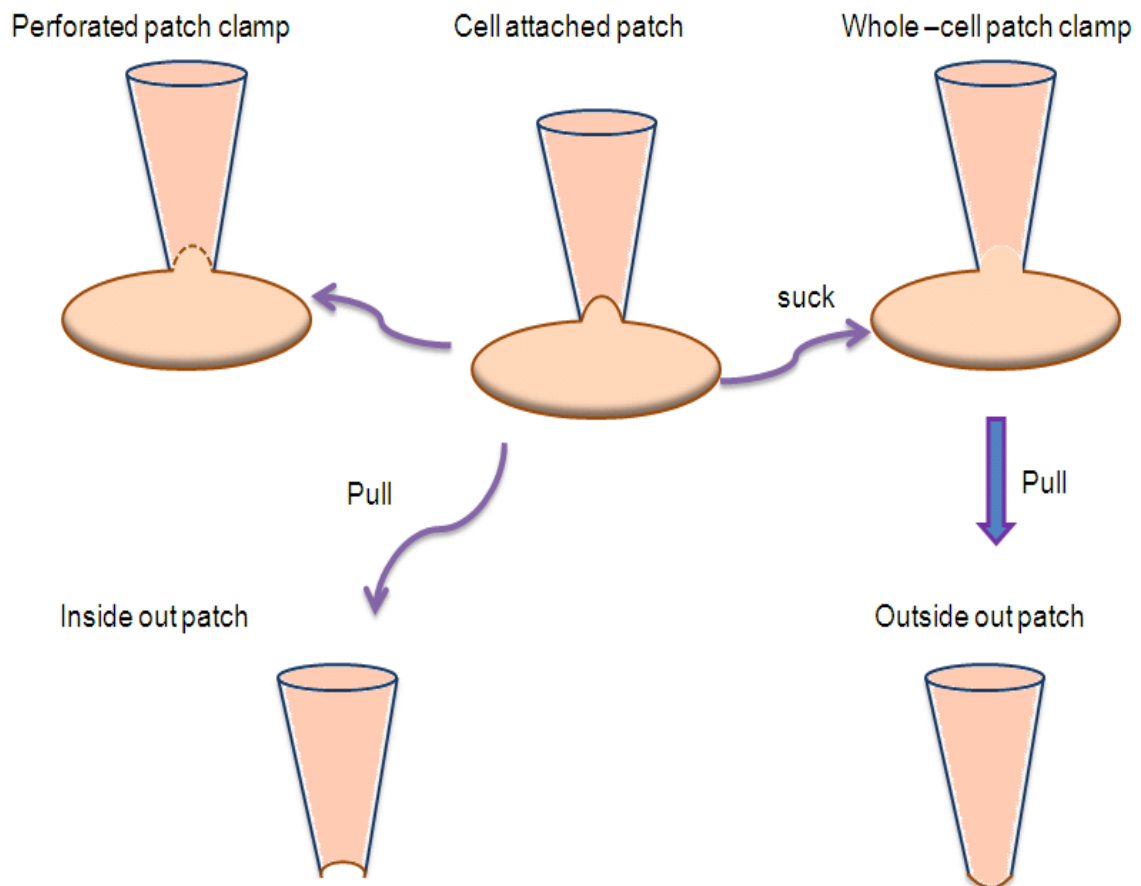


Fig: 2.6 Patch clamp configurations

Fig: 2.6 also illustrates the outside out configuration which can be used to study single channels. In the outside out configuration a neck of the membrane is pulled away after establishing the whole cell which then reseals so that the extracellular surface of the patch is bathed in the external solution and the cytoplasmic surface in contact with the pipette solution.

Among the configurations described above, and illustrated in Fig: 2.6, I used the whole cell patch clamp configuration with the aim of studying any modulation of ionic currents by UTP which may be linked to its contractile mechanisms.

2.3.3 Whole cell patch clamp configuration

A whole cell voltage clamp measurement allows recording of membrane current under constant voltage so that current is directly proportional to the conductance of permeable ions which in turn depends on channel activity.

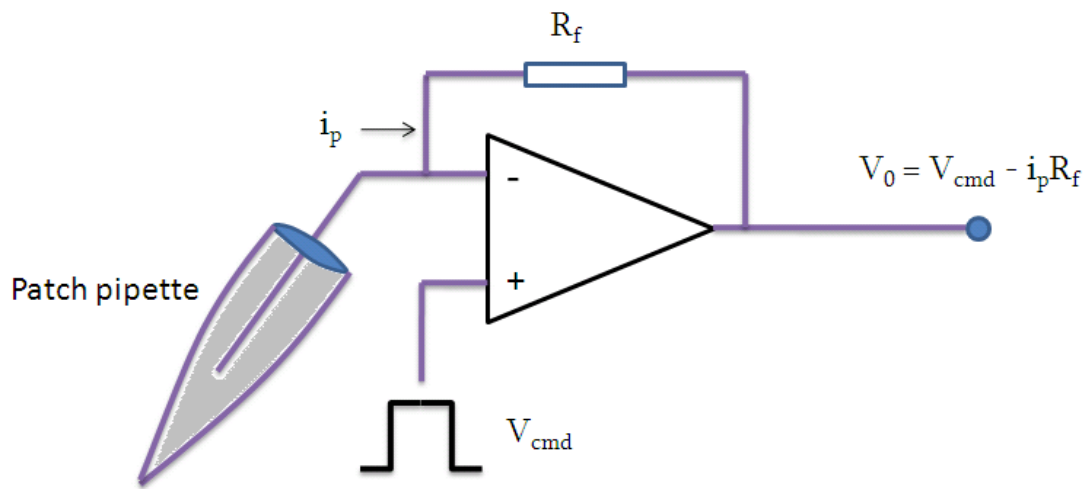


Fig: 2.7 Schematic diagram of the headstage circuit of current / voltage amplifier.

2.3.4 Practical aspects of the whole cell patch clamp technique

A) Patch clamp recording setup

The setup I used to record whole-cell currents included an inverted microscope (Nikon), a motorized manipulator (Siskiyou), an Axopatch 200A patch-clamp amplifier, an oscilloscope, a Digidata 1322A interface and computer.

The microscope was placed on an anti-vibration table (Technical manufacturing corporation USA) which was surrounded by a Faraday cage used to minimize electrical

noise. The anti-vibration table, Faraday cage and microscope were connected to the single high quality earth of the patch-clamp amplifier to minimize the introduction of earth loops and all cables were of the shielded BNC type wherever possible. All of my patch-clamp experiments were performed at $30 \pm 1^\circ\text{C}$.

B) Choice of glass for the construction of electrode

For any patch clamp measurements obtaining a high resistance seal between the patch pipette and cell membrane is a necessity and as such patch pipettes should be constructed carefully. Patch pipettes are made by drawing out glass capillaries with an electrode puller to produce a tip diameter of 1-2 μm (Aidley, 1996). The type of glass selected for making electrodes varies depending on the recording mode e.g. single channel recordings requires lower noise as compared to whole cell recordings and thick walled glass gives lower noise and is therefore preferably used for single channel recording. However, thin walled glass capillaries give a lower access resistance and are suitable for whole cell recordings. For whole cell recordings blunt and low resistance electrodes facilitate the seal formation therefore I used standard thick walled borosilicate glass tubing (GC150F-7.5) by Harvard Instruments). Several general properties of glasses must be considered for constructing patch clamp electrodes such as thermal and optical properties but one of the most important is the electrical properties of the glass which determines the background noise level. The electrical properties also determine the size of the capacity transients following a step change in potential. Thermal properties determines the optimal temperature for the fabrication of the tip, the melting point of quartz, for example, is above 1600°C and therefore cannot be pulled with ordinary electrode pullers. The chemical composition of the glass is also an

important consideration since it may lead to leaching of the chemical constituents of the glass into the pipette solution that can ultimately interfere with the currents measured.

B) Pulling electrodes

I used a vertical puller (Narishige; Tokyo, Japan) to pull electrodes from standard-walled borosilicate glass using two steps pulling setting. The vertical pullers work under gravitational force. The Narishige puller used a two stage process with two different heating steps to pull the electrodes. During the first step, the middle of the capillary was heated and pulled under gravitational force to around 7 mm with automatic settings. The second pull was used to pull the capillary apart to yield two electrodes of optimal geometry.

C) Fire polishing

Fire polishing is an additional step used often to blunt the electrode tip which aids the formation of a gigaseal. To fire polish a pipette its tip was placed near (several micrometers) a heated, glass coated, platinum wire for approximately 5 seconds. I used fire polishing in my initial experiments but later I was able to seal onto the smooth muscle cells without fire polishing and found it unnecessary.

D) Obtaining a whole-cell recording

Cells were placed in the recording chamber containing 6 mM K^+ external solution and left to settle for approximately 10 minutes. A patch electrode was back filled with the appropriate solution (see below) and tapped gently to remove air bubbles before being inserted into the holder of the headstage. After placing the patch pipette into the holder, the electrode was moved closer to the recording chamber using coarse control of the

micromanipulators. The liquid junction potential that was generated when the electrode tip was immersed into the bath was offset using the adjustment on the amplifier. The concentration and ionic composition of the internal pipette and the external bath solution are responsible for the magnitude of the junction potential. Electrode resistances, which were monitored by observing currents resulting from the application of repetitive 5 mV pulses, were in the range of 4 – 6 M Ω . As the tip of an electrode was brought near a cell, the resistance of the electrode was monitored carefully, and contact with the cell was detected as an increase of 40-50% of this resistance. At this point gentle suction using a 10 ml syringe was applied to aid seal formation. To improve the seal quality a holding potential of about -40 mV was applied; success was deemed when the resistance rose above 1 G Ω (gigaseal). During and after the process of sealing the external solution was continuously perfused at a rate of 2 ml / min.

Once a gigaseal was obtained the electrode capacitance spikes were cancelled using the fast capacitance compensation controller of the amplifier and the output gain was increased. To rupture the seal and to get the access to the whole cell further suction was applied with a 1 ml syringe. Access to the whole cell was indicated by the increased capacitance transient spikes arising from the added membrane capacitance. At this stage the membrane capacitance and series resistance were adjusted to minimize these transients. The value of the membrane capacitance after this adjustment was used as an indicator of membrane surface area and was used to give a measure of current density (pA pF⁻¹). As soon as the whole cell configuration was achieved the contents of the intracellular pipette solution equilibrated with the cell contents.

2.3.5 Data collection and analysis

2.3.5.1 Recording of Kv current – pulse protocol

Whole-cell Kv currents were recorded with 6 mM external K⁺ and 140 mM internal K⁺ in the pipette and Penitrem A (100 nM) was added to the external solution to block BK channels. Kv currents were induced by applying 400 ms depolarizing voltage pulses ranging from -40 to +60 mV from a holding potential -65 mV. Prior to these test pulses a P/6 leak subtraction protocol was used. Currents were filtered at 2 kHz, digitized at 10 kHz and stored on the hard drive of a computer for subsequent analysis.

To plot current-voltage relationships the mean current over 50 ms (between 320-370 ms) was calculated and plotted against test potential. Data are expressed as means ± SEM; and differences between currents measured under control conditions and those measured during UTP application were analyzed by ANOVA with Bonferroni's test or Student's paired or unpaired *t*-test as appropriate and a value of P < 0.05 was considered significant.

2.3.5.2 Recording of current from K_{ATP} channels

The initial establishment of the whole-cell configuration was done in 6 mM external K⁺. Following this, steady state whole cell currents were recorded at a holding potential -65 mV and the external solution changed to one containing 140 mM K⁺. Pinacidil (10 μM) was used to open K_{ATP} channels further and reversal of the current by glibenclamide (10 μM) was used to assess the amount of K_{ATP} current present. Currents were filtered at 2 kHz and digitized at 10 kHz.

Total K_{ATP} current, which included the steady-state plus pinacidil activated current, was measured from the baseline current with 6 mM K^+ (adjusted manually to zero) to the maximum amplitude of the pinacidil activated current (see Fig. 4.11). UTP inhibition was measured as the current remaining in the presence of UTP normalized to the maximum total K_{ATP} current. Data were plotted as means \pm SEM and intergroup differences were analyzed by ANOVA or Students paired or unpaired t -test as appropriate. $P < 0.05$ was considered as significant.

2.3.5.3 Recording of current from non selective cation channels (NSCC)

1. Steady state current

When recording non-selective cation currents K^+ was replaced by Cs^+ in the patch pipette to minimize contamination from K^+ currents. Steady-state currents were recorded at -65 mV, and the current was filtered at 2 kHz and digitized at 10 kHz.

2. Ramps

Whole cell current ramps were recorded by applying symmetrical ramps, first from -100 to +30 mV in 400 ms and back to -100 mV again in 400 ms. Ramps were applied every 5 seconds from a holding potential of -65 mV. Currents were filtered at 2 kHz and sampled at 10 kHz. The ramps were used to generate instantaneous current-voltage relationships of the non-specific cation current (see section 4.5).

2.3.5.4 Recording of current from voltage gated Calcium channels

To record Ca^{2+} currents the pipette solution contained 140 mM Cs^+ instead of K^+ to minimize contamination by K^+ currents. Cells were clamped at -65 mV and currents

were elicited by applying 150 ms voltage pulses ranging from -40 to +50 mV. Currents were filtered at 2 kHz and sampled at 10 kHz.

2.3.6 Chemicals

Uridine 5' triphosphate, cadmium chloride, (+)-cis-diltiazem hydrochloride, Gö6983, myristoylated PKC20-28-IP, gadolinium chloride, pinacidil, glibenclamide, penitrem A, endothelin-1, angiotensin-II, chelerythrine chloride and L-NAME (*N*_ω-Nitro-L-arginine methyl ester hydrochloride) were bought from Sigma-Aldrich. Stock concentrations of all chemicals were made by dissolving them in Elga / MilliQ water (double distilled deionized water) except chelerythrine and U73122 which were dissolved in DMSO. Aliquots of all stock solutions were kept at -20°C in a freezer (except L-NAME that was kept in a refrigerator and used within few weeks), thawed on the day of an experiment and diluted to the desired concentration in 6 mM physiological salt solution. BQ123 and myristoylated PKC20-28-IP were bought from Calbiochem and dissolved in Elga / MilliQ water to make the stock concentration. Small aliquots were kept in a freezer for further use.

The general and isoform-specific PKC inhibitor peptides were also linked to a HIV derived Tat peptide (Tat-PKC20-28-IP, Tat-PKC α -IP, Tat-PKC δ -IP, Tat-PKC β IV5-3-IP and Tat-PKC β II-IP) rendering them membrane permeable. Linking these inhibitory peptides to the Tat peptide was done by Dr. R.I. Norman of the Department of Cardiovascular Sciences, University of Leicester.

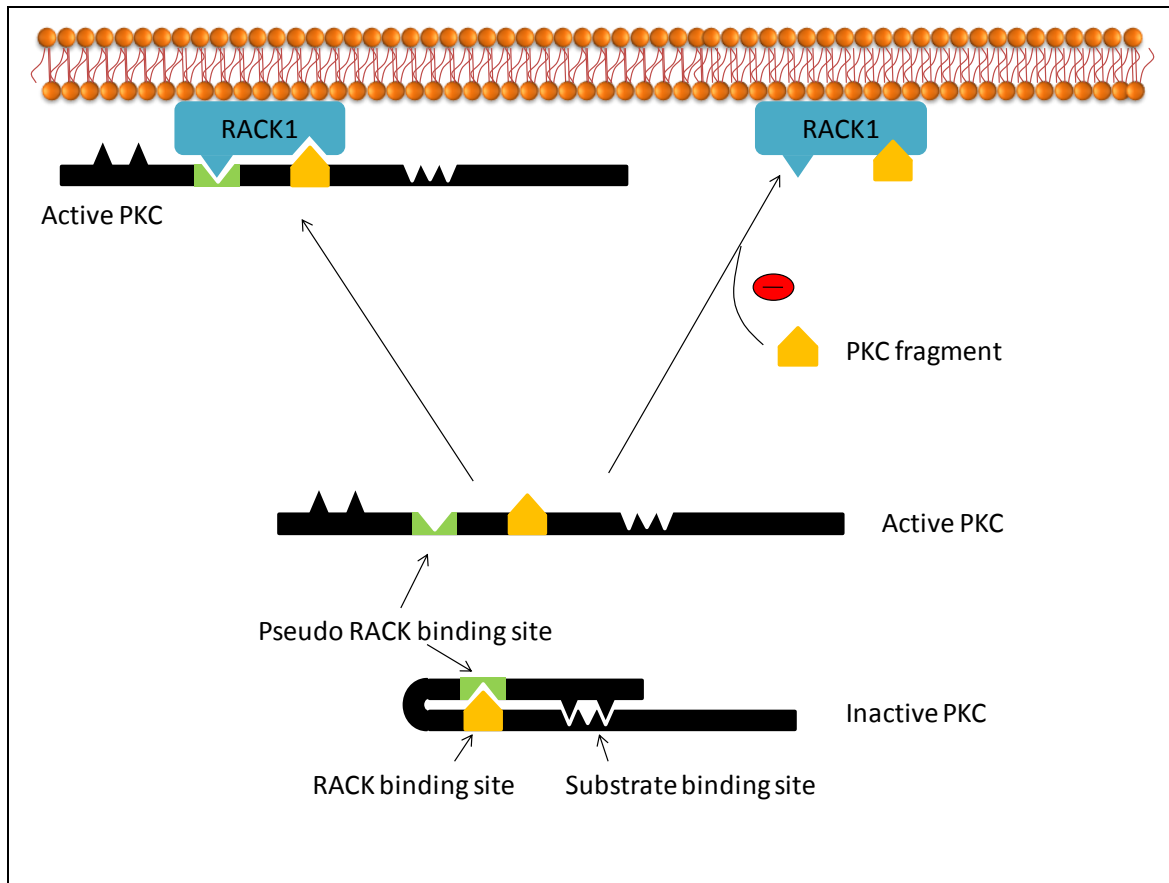
2.3.7 PKC inhibitor peptides:

To date many PKC inhibitors have been developed that compete at different binding sites of PKCs. PKC inhibitors such as chelyrethrine, Gö6983, staurosporine and H-7 compete with ATP at the C3 region of the catalytic domain of PKC and are non specific in their action. Chelyrethrine is known as a competitive inhibitor with histone H3 but is less competitive with ATP (Herbert *et al.*, 1990) whereas Gö6983 is a non-selective PKC inhibitor that competitively inhibits various PKC isoforms at different IC₅₀ values. Some PKC inhibitors, for example calphostin C and sphingosine, specifically compete with the DAG, phorbol ester or phosphatidylserine binding sites of PKC and hence are more specific in their action.

The amino acid sequence of the regulatory domain of PKCs between amino acid residues 19 and 36 resembles the PKC substrate and is bound to the substrate binding site when the enzyme is in its inactive conformation and hence are useful targets for inhibiting the PKC –substrate phosphorylation. Therefore, investigators have developed the peptides (19-36) and (19-31) based on pseudosubstrate sequences which possess the capability of inhibiting the PKC by binding at the PKC–substrate binding site to specifically inhibit the PKC-substrate phosphorylation. This inhibition occurs without interfering with the ATP binding site (House *et al.*, 1987). Since these peptide inhibitors are not permeable through the hydrophobic lipid bilayer various approaches have been employed to make permeable PKC inhibitor peptides.

Introduction of a fatty acid (myristoyl group) makes the PKC pseudosubstrate peptide inhibitor more permeable. Myristoylated PKC20-28 inhibitor peptide is such an example where a myristoylated nonapeptide sequence, based on the pseudosubstrate

domain of PKC- α and PKC- β , was shown to inhibit TPA (12-*O*-tetradecanoyl-phorbol-13 acetate) induced phosphorylation of MARCKS (myristoylated alanine rich C kinase substrate protein) (Eichholtz *et al.*, 1993). To understand the role of different PKC isozymes another approach has been adopted to develop isoform specific peptide inhibitors.



2 Schematic diagram representing the mechanism of PKC binding to its RACK binding protein and PKC isoform inhibition (e.g. RACK1 (β)).

As mentioned before in chapter 1, several PKC isozymes exist and many of these may be present within a single cell type. In their inactive state these PKC isozymes are differentially localized within sub cellular compartments, and upon activation translocate either to the plasma membrane or to the various intracellular organelles,

depending on their corresponding anchoring proteins (Mochly-Rosen, 1995). Several protein molecules have been shown to act as anchoring proteins, being involved in translocating the PKC isoforms either in their inactive or active state (Mochly-Rosen *et al.*, 1998; Mochly-Rosen *et al.*, 1991). Examples of these anchoring proteins are RACK_S (receptor for activated C kinase) and RICK_S (receptor for inactive C kinase) (Mochly-Rosen *et al.*, 1998). To achieve PKC isoform selective inhibition, peptide fragments have been developed, based on these RACK binding sites (Mochly-Rosen *et al.*, 1998), to compete with the PKC isoform for its particular membrane bound RACK binding protein (e.g. RACK1 (β) as shown in the figure: 2.8). The peptide-RACK binding is of such a high affinity that it mimics the PKC docking with its specific RACK protein (Mochly-Rosen *et al.*, 1998).

In 1994, Fawell and colleagues first demonstrated the ability of HIV derived Tat peptide 37-72 to deliver large protein molecules such as RNAase, β -galactosidase and peroxidase into cells from the extracellular solution (Fawell *et al.*, 1994). Mochly-Rosen's group utilized this approach to deliver PKC isoform selective peptide inhibitors by linking them with Tat peptides (Begley *et al.*, 2004) and recently results from our lab demonstrated the ability of Tat linked PKC α -IP and Tat linked PKC ϵ -IP to inhibit selectively ET-1 and Ang-II modulation of Kv currents respectively in rat mesenteric arterial smooth muscle cells (Rainbow *et al.*, 2009). The HIV derived Tat peptide, which is able to deliver several large molecules across the membrane, contains arginine and lysine in abundance and is highly cationic. This high polarity of Tat peptides is known to be responsible for their ability to deliver large molecules across the membrane (Brooks *et al.*, 2005).

Table: 2.2 lists the Tat PKC inhibitor peptides that I have used in my thesis, along with their corresponding amino acid sequences. Tat peptide 47-57 is a 11 amino acid peptide which was utilized to deliver the PKC peptide inhibitors. Tat peptide 47-57 and the various PKC peptide inhibitors (listed in table: 2.2) were obtained from Pepceuticals Ltd. Each peptide inhibitor was reversibly coupled to the Tat peptide by a disulphide bond through N-terminal cysteine residues with a coupling efficiency of 40%. This was done by Dr Bob Norman, Department of Cardiovascular Science, University of Leicester, to whom I am very grateful. The resulting cell permeable Tat linked peptides enter the cell where the Tat carrier peptide is released by the splitting of the disulphide bond due to the reducing intracellular environment of the cell (Begley *et al.*, 2004; Brooks *et al.*, 2005; Hallbrink *et al.*, 2001)

Table 2.2 Tat PKC inhibitor peptides

Tat	47-57	YGRKKRRQRRR Cys at N-terminal		(Begley <i>et al.</i> , 2004; Vives <i>et al.</i> , 1997)
αC2-4		SLNPQWNET	α PKC antagonist	(Xiao <i>et al.</i> , 2003)
βI V5-3		KLFIMN	β IPKC antagonist	(Xiao <i>et al.</i> , 2003)
βII V5-3		QEVIRN	β IIPKC antagonit	(Xiao <i>et al.</i> , 2003)
δ V1-1	8-17	SFNSYELGSL RACK binding site PKC δ V1/C2 domain	PKC δ antagonist	(Chen <i>et al.</i> , 2001)
ϵ V1-2	14-21	EAVSLKPT RACK binding site V1/C2	PKC ϵ antagonist	(Johnson <i>et al.</i> , 1996)
PKC20-28		N-Myr-FARKGALRQ-NH ₂ pseudosubstrate	PKC inhibitor	(Eichholtz <i>et al.</i> , 1993; Ward <i>et al.</i> , 1993)

2.3.8 Experimental solutions for electrophysiology

All solutions listed in tables 2.3, 2.4 and 2.5 were made using doubled distilled deionized water either from Elga or MilliQ deionizer from chemicals bought from Sigma-Aldrich except CaCl_2 and MgCl_2 , both of which were from BDH laboratory supplies in the form of 1 M stock solutions. Solutions were made and stored in refrigerator for further use except internal pipette solutions listed in table 2.5; that were stored in freezer in small bijou bottles for further use. As shown in the table 2.5, internal pipette solutions contain 3.9 mM Ca^{2+} which was buffered with 10 mM EGTA (as listed in table 2.5) giving a total free $[\text{Ca}^{2+}]$ of 100 nM as calculated using <http://www.stanford.edu/~cpatton/webmaxcS.htm>. For 20 nM free Ca^{2+} the internal pipette solution contained 1 mM CaCl_2 along with 10 mM EGTA.

Table 2.3 Solutions for dissection and isolation of smooth muscle cells

Chemical (mM)	Zero Ca^{2+} solution	Low Ca^{2+} solution
KCl	5.4	5.4
NaCl	137.0	137.0
Na_2HPO_4	0.42	0.42
NaH_2PO_4	0.44	0.44
Glucose	4.0	4.0
Mannitol	6.0	6.0
HEPES	10.0	10.0
MgCl_2	1.0	1.0
CaCl_2	-	0.1

pH was adjusted to 7.4 with NaOH/HCl.

Table 2.4 External solutions for whole cell patch clamp recording

Chemicals (mM)	6 mM K ⁺ (K _V / K _{ATP} / NSCC)	140 mM K ⁺ (K _{ATP})	I _{Ba} ²⁺
NaCl	135	-	135
HEPES	10	10	10
CaCl ₂	0.1	0.1	-
BaCl ₂	-	-	10
MgCl ₂	1.0	1.0	1.0
KCl	6.0	140	6.0
Glucose	4.0	4.0	4.0
Mannitol	6.0	6.0	6.0

pH was adjusted to 7.4 with NaOH / HCl every day.

Table 2.5 Internal pipette solution

Chemicals (mM)	K _V	K _{ATP}	NSCC	I _{Ca} ²⁺
KCl	110	110	-	-
KOH	30	30	-	-
CsCl	-	-	110	110
CsOH	-	-	30	30
MgCl ₂	1.0	1.0	1.0	1.0
†CaCl ₂	3.9	3.9	3.9	3.9
†EGTA	10.0	10.0	10.0	10.0
HEPES	10.0	10.0	10.0	10.0
Na ₂ ATP*	1.0	1.0	1.0	1.0
GTP*	0.5	0.5	0.5	0.5
ADP*	-	0.1	-	-

* Added (solid) on the day of experiment and pH was adjusted to 7.2 with NaOH/HCl.

† The free [Ca²⁺] was 100 nM as calculated from <http://www.stanford.edu/~cpatton/webmaxcS.htm>; for 20 nM free Ca²⁺, 1 mM CaCl₂ and 10 mM EGTA was used in some experiments (also calculated from <http://www.stanford.edu/~cpatton/webmaxcS.htm>).

Chapter 3 UTP induced contractile response of rat mesenteric arteries

3.1 Introduction

3.1.1 Uridine 5' triphosphate

Uridine 5' triphosphate (UTP) is a pyrimidine nucleotide which shares the property, along with several other nucleotides, of being a potent vasoconstrictor. UTP has been implicated in several physiological and pathological situations; for example it has been shown to have a role in regulating vascular tone of cerebral arteries under conditions such as subarachnoid hemorrhage or migraine (Ralevic and Burnstock, 1998, Debdi et al., 1993). The role of UTP in cardiomyocytes under stress conditions was studied by Yitzhaki (2005) who found that UTP protects cultured cardiomyocytes of newborn rat against hypoxic damage (Yitzhaki et al., 2005).

To exert its biological effects in resistance arteries, UTP activates membrane bound P2Y receptors (Erlinge and Burnstock, 2008). However, the constriction or relaxation of resistance arteries by pyrimidine nucleotides depends on the type of P2Y receptor activated (Horiuchi et al., 2001, Miyagi et al., 1996). Among various subtypes, P2Y₂ and P2Y₄ receptors are potently activated by UTP and blocked by suramin and PPADS respectively. UTP stimulates two different subtypes of P2Y receptors in cerebral arteries; activation of P2Y₆ receptors causes vasoconstriction, whereas endothelial P2Y₂ receptor activation is responsible for vasodilation of cerebral arteries (Horiuchi et al., 2001). The P2Y₆ receptors are distributed widely within the heart, brain and blood vessels; it is preferentially activated by UDP rather than UTP.

UTP is thought to exert its contractile effects by the activation of membrane bound P2Y₂ and P2Y₄ receptors that are G-protein coupled receptors (G_{q/11} and possibly G_i). Activation of G_q linked receptors causes activation of phospholipase C leading to

hydrolysis of plasma membrane phosphatidylinositol 4, 5 bisphosphate (PIP₂) to yield inositol 1, 4, 5-trisphosphate (IP₃) and diacylglycerol (DAG) (Kanashiro and Khalil, 1998, Nishizuka, 1992). IP₃ stimulates Ca²⁺ release from the sarcoplasmic reticulum and initiates contraction in smooth muscle (Sima et al., 1997, Strobaek et al., 1996). UTP induces contraction of rat basilar arteries by increasing the frequency of Ca²⁺ waves and inhibiting Ca²⁺ spark frequency (Jaggar and Nelson, 2000) that occurs due to Ca²⁺ release from the sarcoplasmic reticulum (SR) through IP₃R activation (Syyong et al., 2009). IP₃R1 activation has been shown to be involved in generating a UTP induced cation current in cerebral arteries, leading to elevated intracellular global Ca²⁺ concentration and vasoconstriction (Zhao et al., 2008). UTP also activates TRPC3 and TRPC7 in rat cardiomyocytes via activation of DAG (Alvarez et al., 2008).

Several studies have been undertaken on UTP signaling mechanism in rat aorta, cerebral and basilar arteries; however little is known about the mechanism underlying the UTP induced contractile response of mesenteric arteries. The objective of the present study was to understand the underlying mechanisms involved in the UTP induced contraction of mesenteric arterial smooth muscle with the aim of dissecting out the role of protein kinase C in this response. The contractile responses of mesenteric arteries to UTP were measured using the dual channel wire myograph technique.

3.2 General conditions

3.2.1 Contractile response

Contractions of rat mesenteric arterial segments to 60 mM K⁺ and UTP were measured in the absence and presence of antagonists (as described in the methods chapter) at 37°C and in the presence of L-NAME, an eNOS inhibitor, to inhibit the production of nitric oxide from the intact endothelium of the mesenteric artery. At the start of the experiment a steady baseline with 6 mM K⁺ PSS was established followed by addition of 60 mM K⁺ containing saline (see methods) to ascertain the viability of the mesenteric arteries. Subsequently, mesenteric arterial segments were challenged twice with UTP (100 μM) and then washed. Following these initial procedures the arteries were exposed to the test compound for 20 minutes (unless stated otherwise) followed by addition of 100 μM UTP in the continued presence of the test compounds. At the end of the experiments the response to 60 mM K⁺ was determined to assess whether the experimental procedure had affected the ability of the artery to contract to depolarization.

3.2.2 Analysis

Contractile responses were measured as the difference between the baseline and the peak response of the contraction induced by the vasoconstrictors (e.g. 60 mM K⁺, UTP). The change in UTP induced contraction following pre-treatment of the artery with a compound was recorded and expressed as a percentage of the contraction induced by the second application of UTP (UTP2) under control conditions (see Fig: 2.4).

The normalized data are expressed as means \pm SEM. Student's paired *t*- test was used to assess statistical significance of the data. Student's *t*- test was performed on non normalized data. A value of $P < 0.05$ was considered significant.

3.3 Results

3.3.1 UTP induced contraction was sustained and reproducible

Application of 100 μ M UTP to mesenteric arteries resulted in a rapid and maintained contraction that returned readily to base line on washing. The sustained nature of the UTP induced constriction is indicative of P2Y receptor activation that is in contrast to P2X receptor activation, where ATP is known to elicit transient constrictions.

To assess whether UTP induced contractions were consistent and reproducible mesenteric arteries were challenged with repeated applications of 100 μ M UTP. UTP was applied directly into the bath for 5 minutes in the presence of L-NAME, followed by a 10 minute wash before the next application as shown in Fig. 3.1A. Such repeated applications of UTP produced robust and consistent contractions. Mean normalized contractions (to the first UTP response) from 4 arterial segments plotted against time of application is shown in Fig. 3.1B. The consistent contractile responses of UTP under control conditions suggested that there was little or no desensitization of the receptors activated by UTP under these conditions. Therefore, subsequent myograph experiments were designed such that responses to UTP in the absence and presence of a pharmacological agent were observed in the same arterial segment.

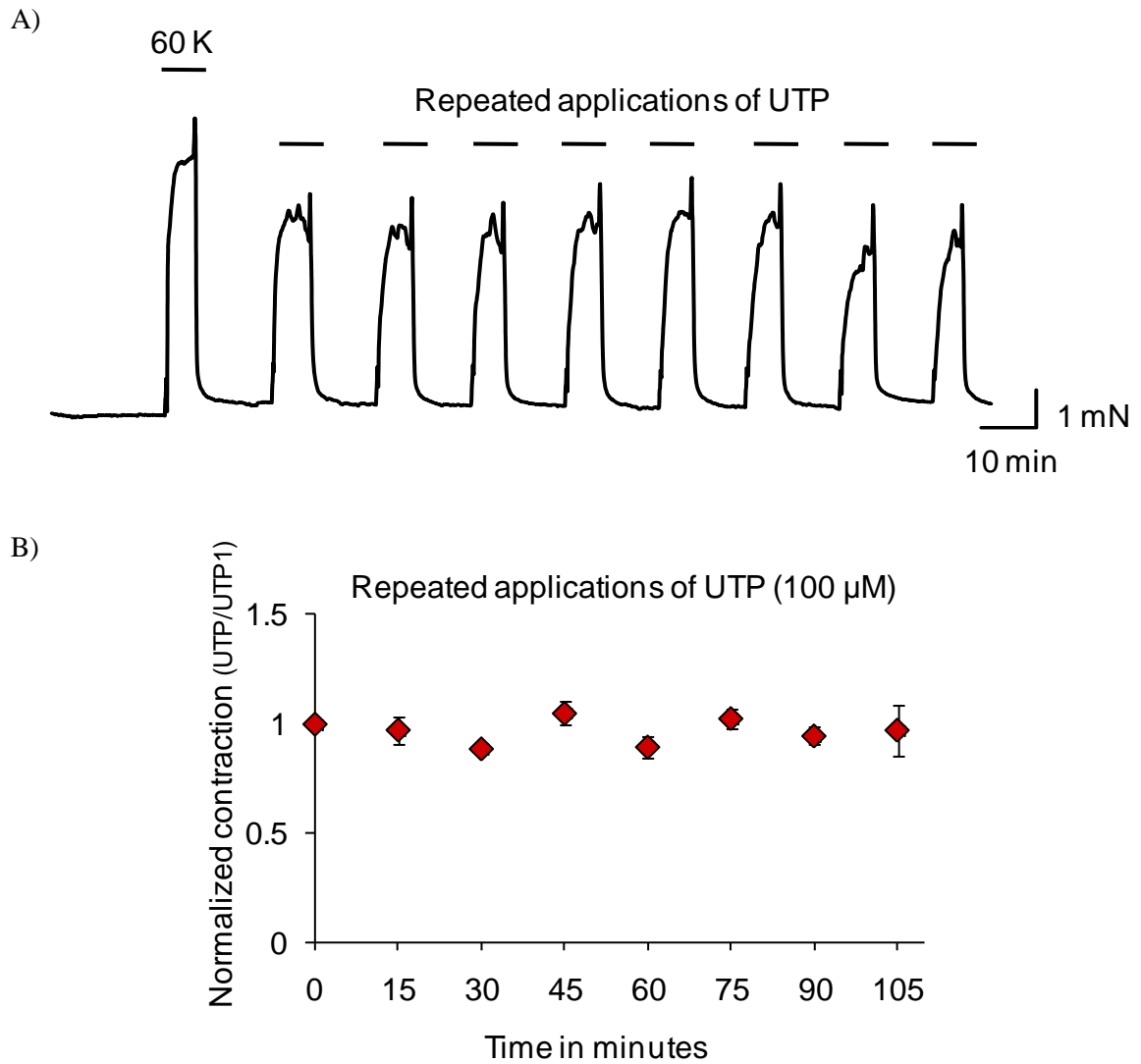


Fig: 3.1 Time course of UTP induced contraction

A) Representative traces showing the contractile response of a mesenteric artery segment to repeated applications of UTP. 100 μ M UTP was applied each time for 5 min and washed off with 6 mM PSS. The time interval between each UTP application was 10 min. All solutions contained L-NAME.

B) UTP induced contractile responses were measured and normalized with their first UTP induced response and mean normalized responses were plotted against time of application. The responses to repeated applications of UTP were consistent over time.

3.3.2 Cumulative dose response curve for UTP

The contractile responses of mesenteric arterial segments following applications of a range of concentrations of UTP were measured to ascertain an appropriate concentration of UTP to use in my experiments. After obtaining a contractile response to 60 mM K⁺, mesenteric arteries were challenged with increasing concentrations of UTP (1 μM to 300 μM). UTP was added in a cumulative manner without washing between applications. The response to each concentration of UTP was measured from the plateau response relative to the baseline (before first application of UTP). The cumulative addition of UTP constricts rat mesenteric arteries in a dose dependent manner. To quantify these results equation 3.1 was fitted to the data obtained from each arterial segment

$$R = R_{max}[UTP]^n / ([UTP]^n + EC_{50}^n) \quad 3.1$$

where R is the contractile response to UTP, R_{max} the maximum contractile response, n the Hill coefficient and EC_{50} the excitatory concentration needed to produce 50% of the maximal response. The value for R_{max} returned by the fitting routine for each arterial segment was then used to normalize the data for that particular segment. The normalized data for 3 segments were then averaged and equation 3.1 was fitted to this data with R_{max} constrained to 1. The fit returned a value of 52 μM for EC_{50} and n of 2.10. A sub-maximal excitatory concentration of 100 μM was found to induce a consistent response and was therefore used in all the experiments in this thesis.

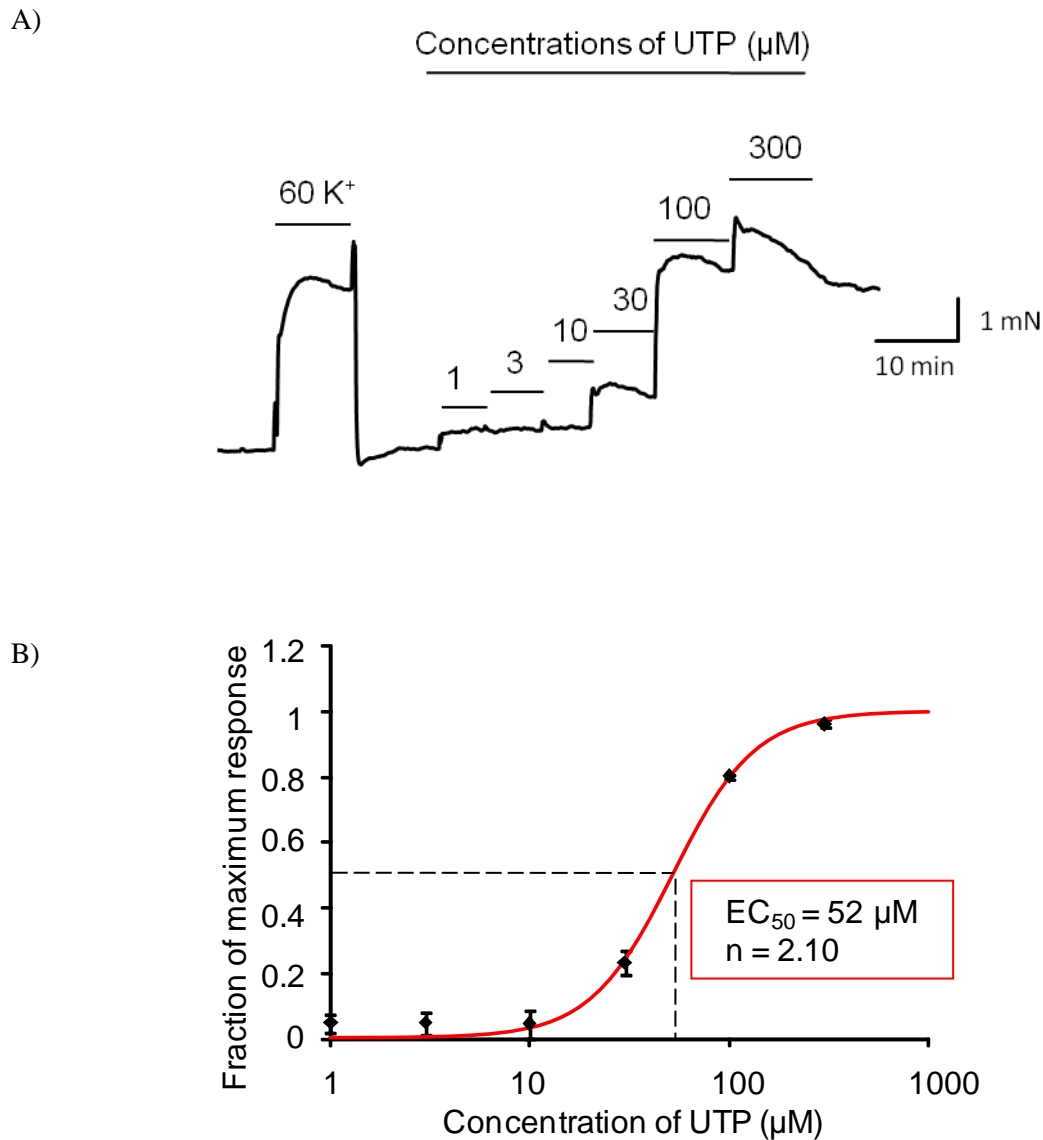


Fig: 3.2 Cumulative dose response curve

A) Representative recording of the effects of various concentrations of UTP on the contractile response of a mesenteric artery. Following a 60 mM K evoked contraction, the mesenteric artery was challenged with UTP ranging from 1 μM to 300 μM (cumulative addition) to contract the mesenteric artery in a dose dependent manner.

B) UTP induced responses from 3 arterial segments were normalized as explained in the text and a cumulative dose response curve was constructed. The curve shows the fit with equation 3.1, giving values of 52 μM for EC_{50} and 2.1 for n .

3.3.3 Role of extracellular Ca^{2+} influx in UTP induced contraction

To investigate the signaling pathway and to examine the role of extracellular Ca^{2+} influx in evoking UTP induced contractions, responses to UTP were measured in Ca^{2+} free solution. Following 20 minutes incubation in Ca^{2+} free solution the response to UTP was measured. As shown in Fig. 3.3, removal of extracellular Ca^{2+} prevented UTP induced contraction ($P < 0.001$; $n=4$). However, the contractile response to UTP recovered when 1.8 mM Ca^{2+} was returned to the bath. These results indicate that Ca^{2+} influx plays a large contribution to the UTP induced contraction of mesenteric artery.

In addition to its effect on UTP induced contraction, removing extracellular Ca^{2+} also abolished the contraction resulting from application of 60 mM K^+ Fig. 3.3. As was the case with UTP, the 60 mM K^+ induced contraction recovered upon addition of Ca^{2+} to the extracellular solution.

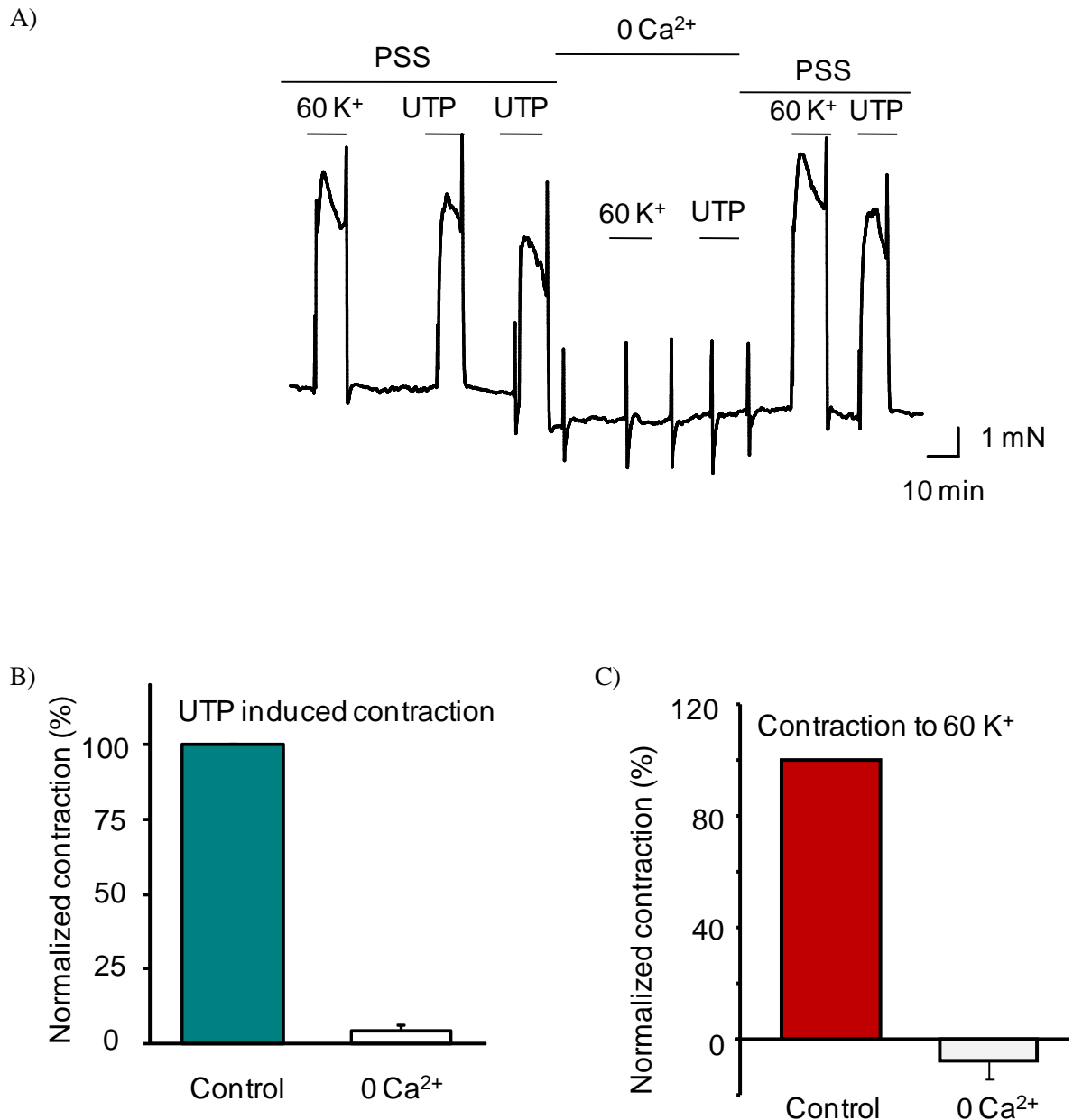


Fig: 3.3 Effect of extracellular Ca²⁺ on UTP induced contraction

A) Representative traces of UTP induced contraction in the presence and absence of extracellular Ca²⁺. In the absence of extracellular Ca²⁺, neither UTP nor 60 mM K⁺ induced a contraction. These contractions recovered on addition of Ca²⁺.

B) Mean normalized UTP (100 μM) induced contraction in the absence of extracellular Ca²⁺ as indicated. Removal of extracellular Ca²⁺ reduced the UTP induced contraction to 4.1 ± 2.4% (P < 0.001; n=4)

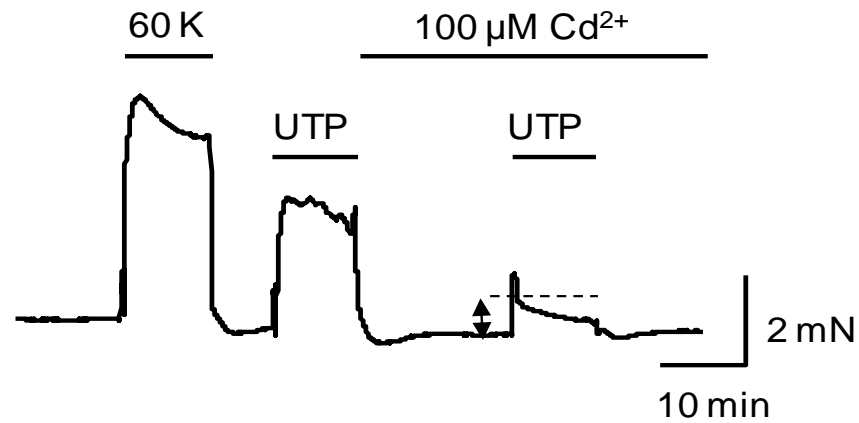
C) Mean normalized 60 mM K⁺ induced contraction in the absence of extracellular Ca²⁺ as indicated (n=4).

3.3.4 Involvement of voltage gated Ca^{2+} channels

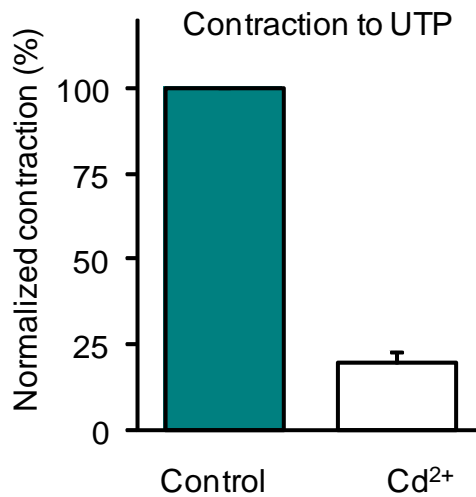
As indicated in the previous section UTP evoked contraction was mainly dependent on Ca^{2+} influx from the extracellular space. To investigate this further I studied the involvement of Ca^{2+} entry pathways using a variety of Ca^{2+} channel blockers. Initial experiments were done using Cd^{2+} , a non selective Ca^{2+} channel blocker. As expected, application of 100 μM Cd^{2+} markedly reduced the contractile response to 60 mM K^+ (Fig. 3.4). As shown in Fig: 3.4, pretreatment of mesenteric arteries with 100 μM Cd^{2+} reduced UTP induced contractions to $19.3 \pm 3.7\%$ ($n = 4$); suggesting the involvement of Ca^{2+} channels. Because of the non selectivity of Cd^{2+} further studies were needed to dissect out the role of voltage gated Ca^{2+} channels in UTP induced contractions. Among various subtypes of voltage gated Ca^{2+} channels, the L- and T- types are highly expressed and heterogeneously distributed in smooth muscle cells, both of which are blocked by Cd^{2+} .

To test whether L-type voltage gated Ca^{2+} channels are involved the effect of d-cis-diltiazem, a blocker of these channels, on UTP induced contractions was examined. Pretreatment of mesenteric arteries with 50 μM diltiazem inhibited UTP induced contractions by $41 \pm 6\%$ ($n = 15$, $P < 0.001$, see Fig.3-5). In contrast, contractions induced by 60 mM K^+ , in the same arterial segments, were blocked substantially by diltiazem (Fig. 3.5C).

A)



B)



C)

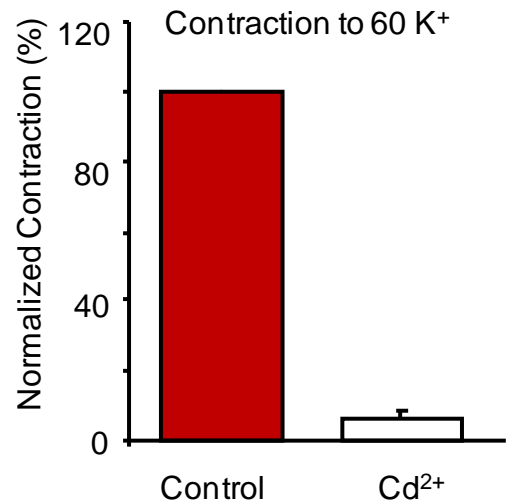


Fig: 3.4 Effect of Cd²⁺ on UTP induced contractile response.

A) A representative trace showing the effect of Cd²⁺ on the contractile response of a mesenteric artery to UTP.

B) The response to UTP in the presence of Cd²⁺ was normalized with that in its absence (control) and plotted as a percentage of the control contraction.

C) Contraction to 60 mM K⁺ in the absence and presence of Cd²⁺ was also measured in a parallel experiment and the response were normalized and plotted as a percentage of the response to 60 mM K⁺ in the absence of Cd²⁺.

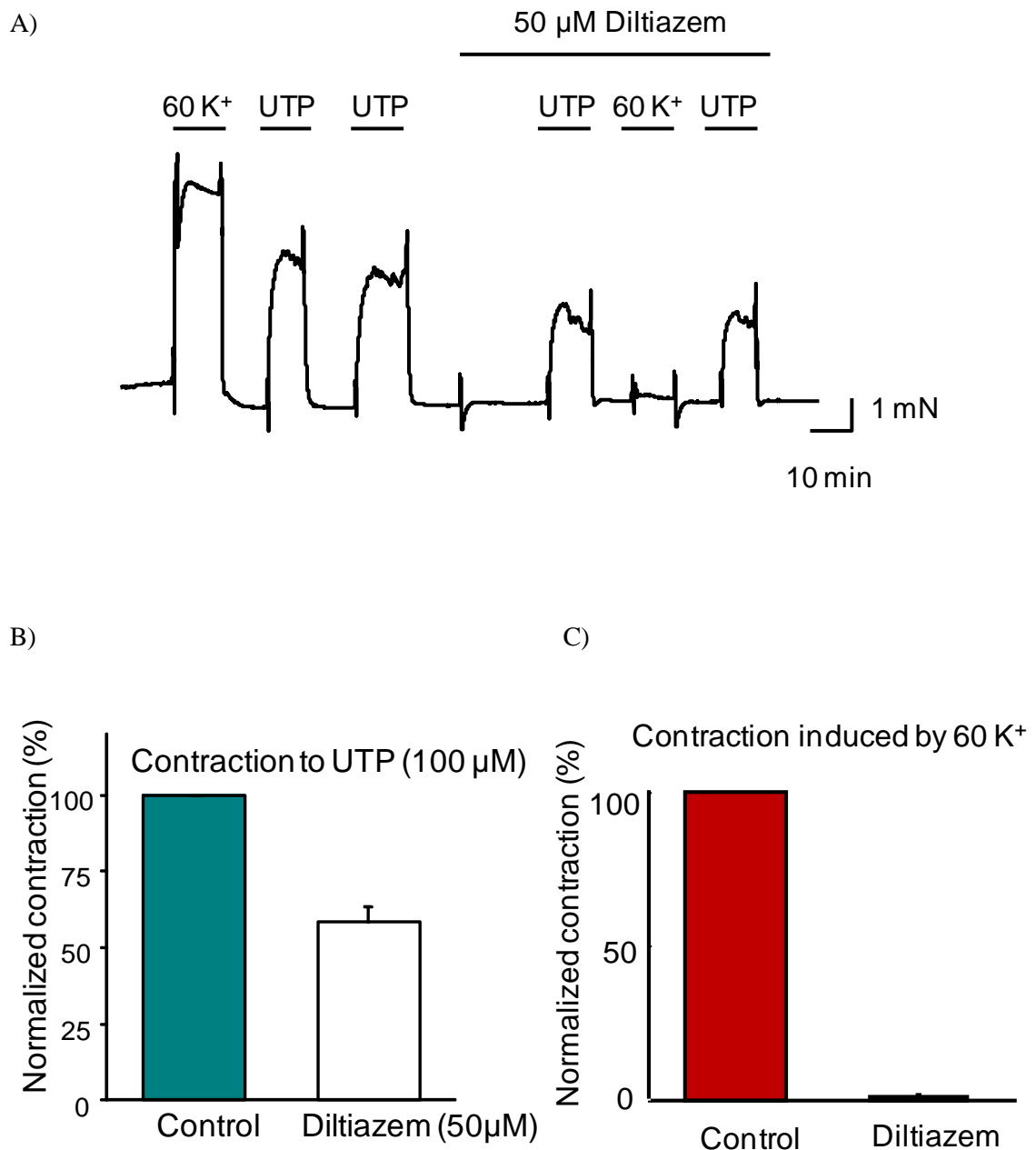


Fig: 3.5 Effect of diltiazem on UTP and 60 mM K⁺ induced contractions.

A) Trace showing the effect of 50 μ M diltiazem on contractions induced by 100 μ M UTP and 60 mM K⁺ as indicated. UTP induced contractions were only partly inhibited by diltiazem; whereas the contractile response to 60 mM K⁺ was abolished.

B) Mean normalized data showing that UTP induced contractions were inhibited by $41 \pm 6\%$ ($n = 15$; $**P < 0.001$) in the presence of 50 μ M diltiazem.

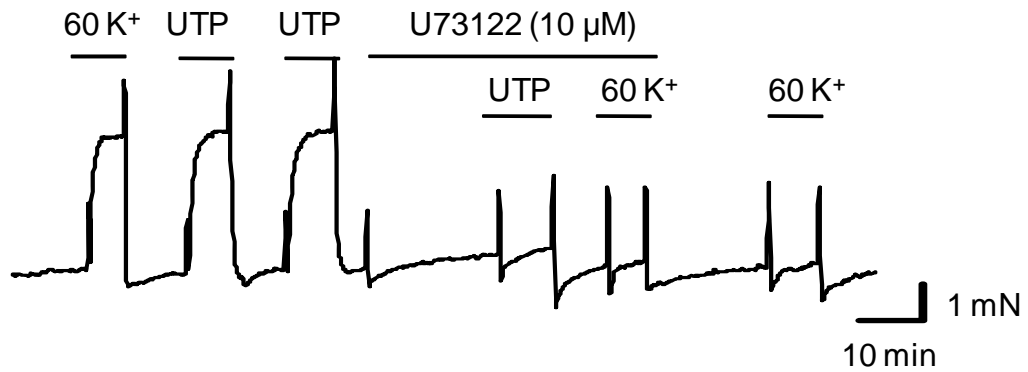
C) Mean normalized data showing that 60 mM K⁺ induced contractions were inhibited to $1.1 \pm 0.5\%$; $**P < 0.001$) in the presence of 50 μ M diltiazem.

3.3.5 UTP induced contractions and activation of PLC

Among several P2Y receptors expressed in vascular smooth muscle P2Y₂ and P2Y₄ potently respond to UTP (Morris et al., 2010, Luykenaar et al., 2004). Since P2Y receptors are G protein coupled receptors it was therefore postulated that UTP induced responses are mediated by activation of phospholipase C.

To assess the possible role of PLC in mediating UTP induced contractions in mesenteric arteries I used the PLC inhibitor U73122 (Helliwell and Large, 1997, Smith et al., 1990) to abolish any signaling downstream of PLC. Pre-treatment of mesenteric arterial rings for 20 minutes with 10 μ M U73122 caused a significant block of the UTP induced response to $0.8 \pm 1.8\%$ of control values (n= 5; P < 0.01), consistent with the hypothesis that UTP acts via a G_q coupled receptor pathway. However, pre-treatment with U73122 also irreversibly abolished the contractile response to 60 mM K⁺.

A)



B)

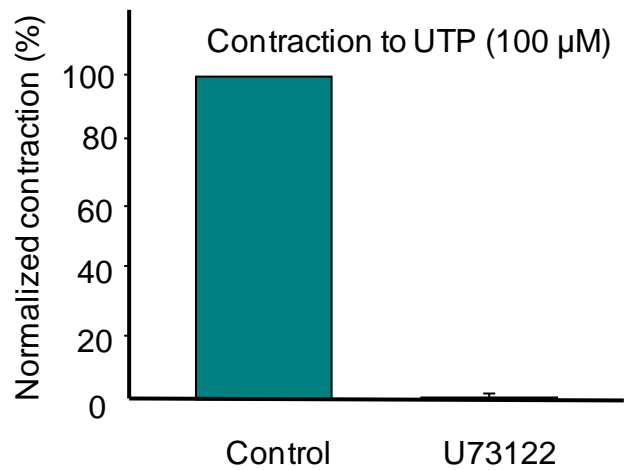


Fig: 3.6 Effect of U73122 on UTP induced contractions.

A) Typical traces showing the effects of the PLC inhibitor U73122 on UTP induced contraction of a mesenteric arterial ring segment. 20 minutes incubation with 10 μM U73122 prevented UTP from evoking a contraction 60 mM K⁺ induced contraction was also observed in the presence and absence of U73122 within same arterial segment. U73122 irreversibly blocked the 60 mM K⁺ to induce contraction ($0.8 \pm 1.8\%$; $n= 5$; $P < 0.01$).

3.3.6 PKC involvement in the contractile response of mesenteric arteries to UTP

Protein kinase C (PKC) is a family of serine/threonine kinase and is involved in the mechanism of agonist induced contraction. PKC, by altering the phosphorylation state of key proteins of the contractile machinery, performs distinct role in the Ca^{2+} signaling that leading to contraction. Because of the potential role of PKC in receptor mediated constriction, its contribution was examined by using a selection of non peptide and peptide PKC inhibitors.

Chelerythrine is a naturally occurring plant alkaloid isolated from *Chelidonium majus* L (family Papaveraceae) and is a non selective PKC inhibitor that also exerts a wide range of biological activities from antimicrobial, antifungal, anti-inflammatory, sympatholytic, adrenergic and local anesthetic (Colombo and Bosisio, 1996). As shown in Fig. 3.7A & B, pre-treatment of arterial segments with 5 μM chelerythrine for 20 minutes attenuated the contractile response to UTP by $85.7 \pm 1.9\%$ of the control ($n=3$; $P<0.05$). Chelerythrine also showed unspecific blocking effects on 60 mM K^+ induced contraction within the same arteries as shown in Fig. 3.7A.

In view of the unspecific blocking effects of chelerythrine, the effects of a more selective inhibitor, Gö6983, that inhibits the Ca^{2+} dependent PKC isoforms PKC α ($\text{IC}_{50}=7$ nM), PKC β ($\text{IC}_{50}=6$ nM) and PKC γ ($\text{IC}_{50}=6$ nM). Gö6983 also inhibits the Ca^{2+} or DAG independent PKC isoenzyme PKC ζ ($\text{IC}_{50}=10$ nM); however, it poorly suppressed the PKC μ activity at slightly higher concentration (Gschwendt et al., 1996).

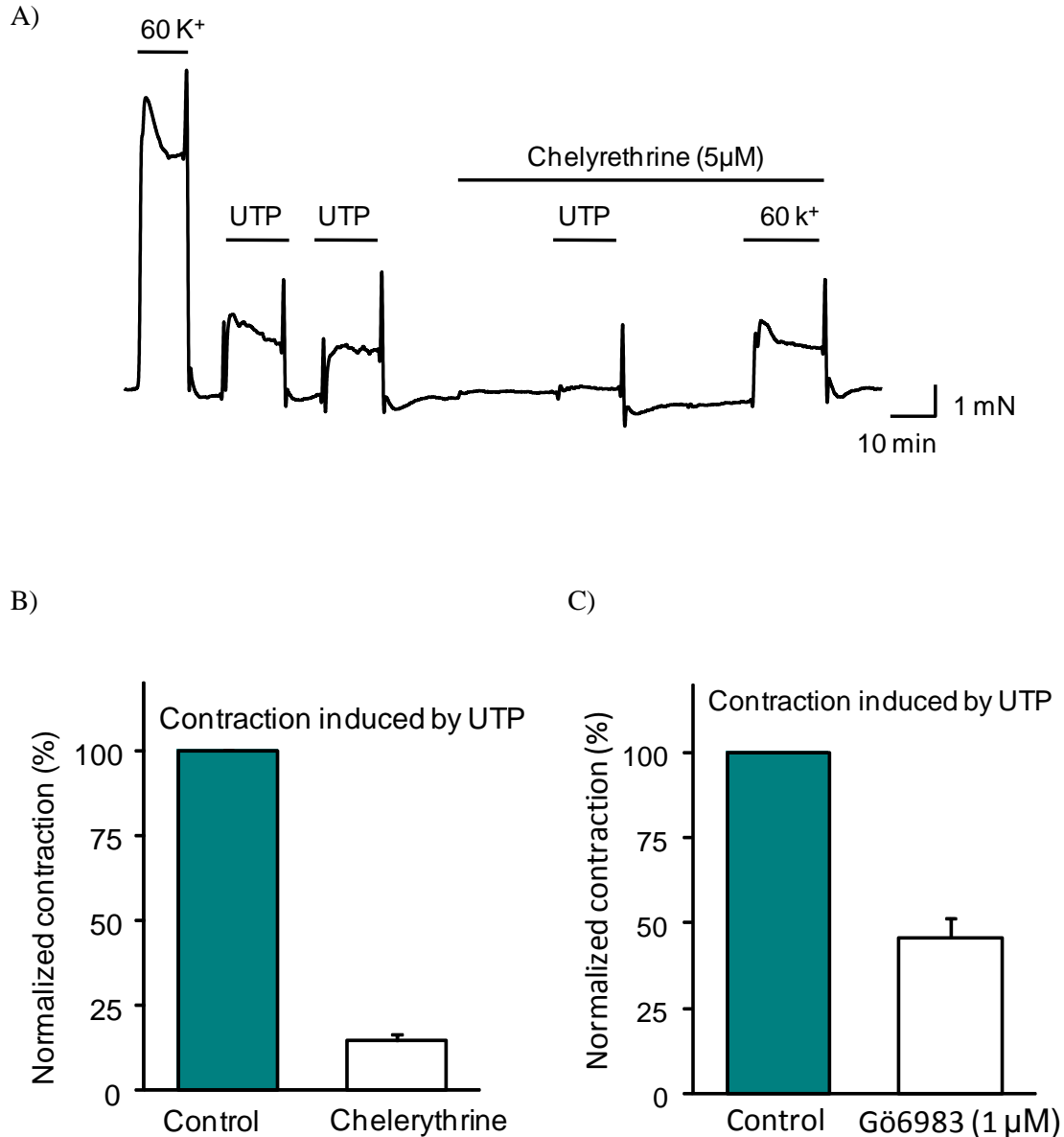


Fig: 3.7 Effect of chelerythrine and Gö6983 on UTP induced contraction.

A) Representative trace showing mesenteric arterial response to 60 mM K⁺ and 100 μM UTP in the absence and presence of 5 μM chelerythrine.

B) Mean normalized contraction to UTP (100 μM) under control conditions and after treatment with chelerythrine (5 μM). Chelerythrine reduced UTP induced contraction by $85.7 \pm 1.9\%$ of control. (n = 3; P<0.05).

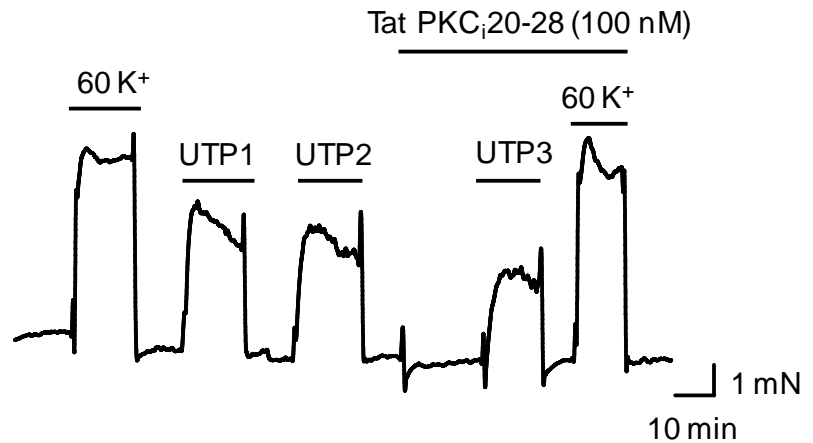
C) Mean normalized contraction to UTP (100 μM) under control conditions and after treatment with Gö6983 (1 μM). Gö6983 reduced UTP induced contraction by $54.3 \pm 5.8\%$ of control. (n = 3; P<0.005).

Since at a concentration of 1 μM Gö6983 inhibits almost all Ca^{2+} dependent PKC isoforms, therefore 1 μM Gö6983 was used to dissect out the involvement of Ca^{2+} dependent PKC isoforms in UTP induced contraction. As shown in the in Fig. 3.7C Gö6983 partly inhibited the contractile response to 100 μM UTP by $22.4 \pm 3.1\%$ ($P < 0.005$, $n = 5$).

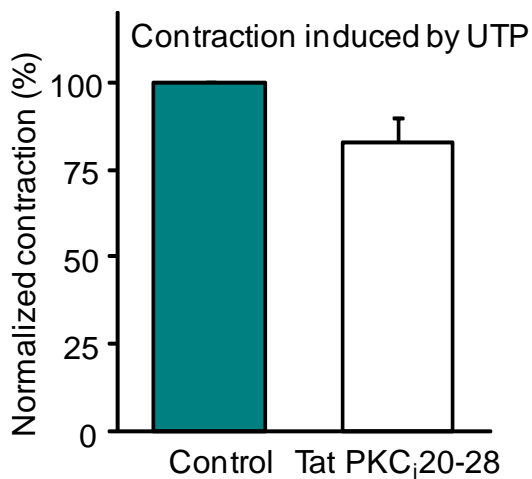
To investigate the role of PKC in more detail I used several PKC inhibitor peptides (PKC-IP), including the general PKC inhibitor PKC20-28-IP, and peptide inhibitors specific for PKC isoforms α , β , δ and ϵ . PKC inhibitors are less permeable, therefore, in order to make them membrane permeable, they were linked with HIV tat- derived peptide. The HIV tat-derived peptide is a small peptide i.e. 86 amino acid peptide which has been shown to successively deliver a large variety of molecules, from small particles to proteins (Brooks et al., 2005, Vives et al., 1997). In addition to these Tat-linked peptides the membrane permeable myristoylated PKC20-28-IP was used.

Pre-treatment of mesenteric arteries for 20 min with 40 μM myristoylated PKC20-28-IP reduced the UTP evoked contraction by only 21% in two arterial ring segments. The tat linked PKC20-28-IP (Tat-PKC20-28-IP), applied at 100nM for 20 minutes which has been shown to be effective at this concentration (Rainbow et al., 2009), reduced the UTP induced contraction by a similar amount, $17.1 \pm 6.8\%$; ($P < 0.05$; $n = 7$). In a parallel series of experiments, Tat-PKC20-28-IP reduced ET-1 evoked contractions by 40% in four arterial ring segments ($P < 0.05$).

A)



B)



C)

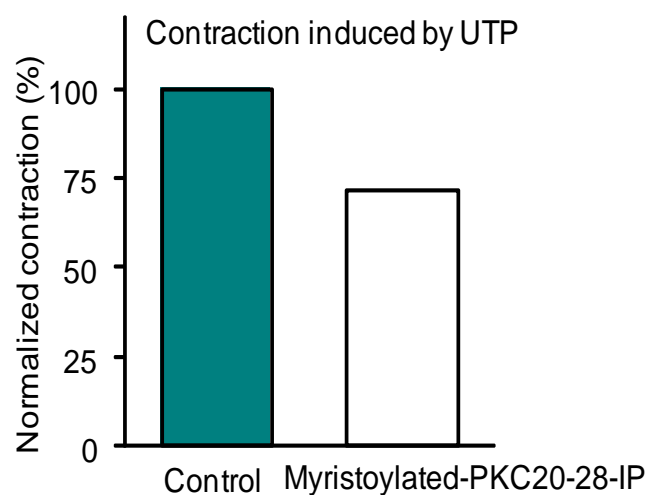


Fig: 3.8 Effect of PKC20-28-IP on UTP induced contraction

A) An example trace showing the contractions induced by 60 mM K⁺ and 100 μM UTP before and after the addition of 100 nM Tat-PKC20-28-IP as indicated.

B) Mean normalized data of the UTP induced contractions in the absence and presence of 100 nM Tat-PKC20-28-IP. The response to UTP was reduced by 17.1±6.8% (P<0.05; n=7).

C) Mean normalized data of the UTP induced contractions in the absence and presence of 40 μM myristoylated-PKC20-28-IP. The response to UTP was reduced by 28.8% (n=2).

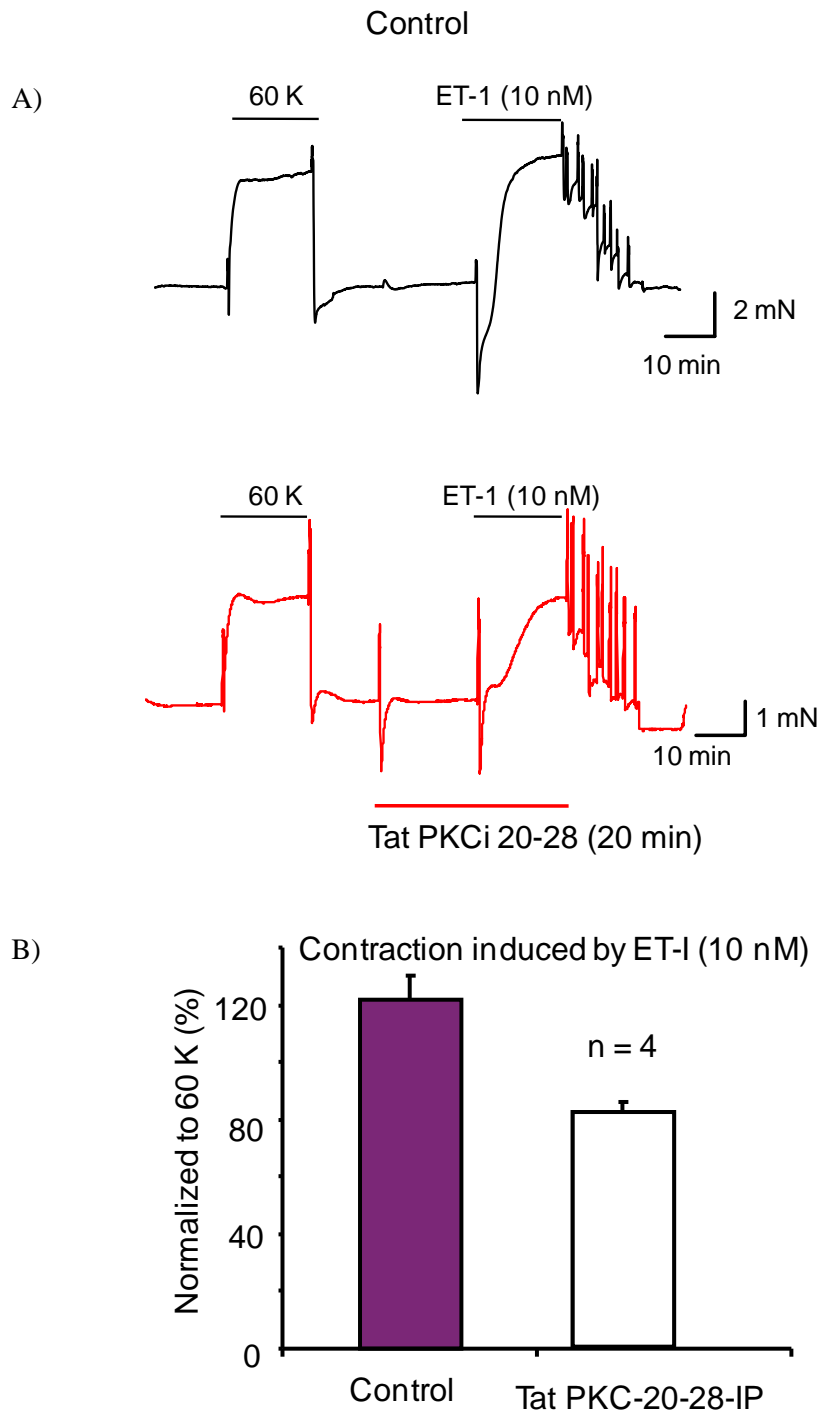


Fig: 3.9 Effect of Tat-PKC20-28-IP on ET-1 induced contraction.

A) Traces showing the contractions induced by 60 mM K^+ and 10 nM ET-1 in control (black trace) and in 100 nM Tat-PKC20-28-IP (red trace) as indicated.

B) Mean contraction to ET-1 (10 nM) as percentage of 60 mM K^+ induced contraction under control conditions and in the presence of Tat-PKC20-28-IP (100 nM). ET-1 induced contraction was reduced from 120% to 80% ($P < 0.05$; $n = 4$).

Since the effect of the general PKC20-28-IP was not clear more selective PKC isoform inhibitors were used in an attempt to dissect out the role of specific PKC isoforms in UTP induced contractions. Pre-treatment of arterial segments with 100nM Tat PKC α C2-4-IP for 20 minutes did not affect UTP induced contractions as shown in Fig. 3.10. However, a parallel experiment was designed to check the effectiveness of Tat PKC α C2-4-IP (100 nM) to UTP (30 μ M) as well as ET-1 (3 nM) induced contractions. Tat PKC α C2-4-IP effectively blocked the contraction induced by ET-1, previously reported by (Rainbow et al., 2009).

Using similar experimental conditions Tat-PKC δ -IP (50 nM), Tat-PKC ϵ -IP (100 nM), Tat-PKC β I-IP (100 nM) and Tat-PKC β II-IP (100 nM) were all unable to reduce UTP induced contractions significantly, see Fig. 3.14 and a summary of the effects of PKC inhibitors is shown in Fig. 3.16. Rainbow et al. (2009) reported the Ang-II induced contraction was significantly inhibited by Tat PKC ϵ -IP under experimental conditions similar to those where I found no significant reduction in UTP induced contraction of mesenteric arteries pretreated for 20 minutes with Tat PKC ϵ -IP. Therefore a parallel experiment was performed, using the Ang II induced contraction, to check the effectiveness of Tat PKC ϵ -IP in my experiments. As shown in Fig. 3.15, the Ang-II induced contraction was reduced by 45% (n=1) after pretreatment for 20 minutes with 100 nM Tat-PKC ϵ -IP (bottom traces).

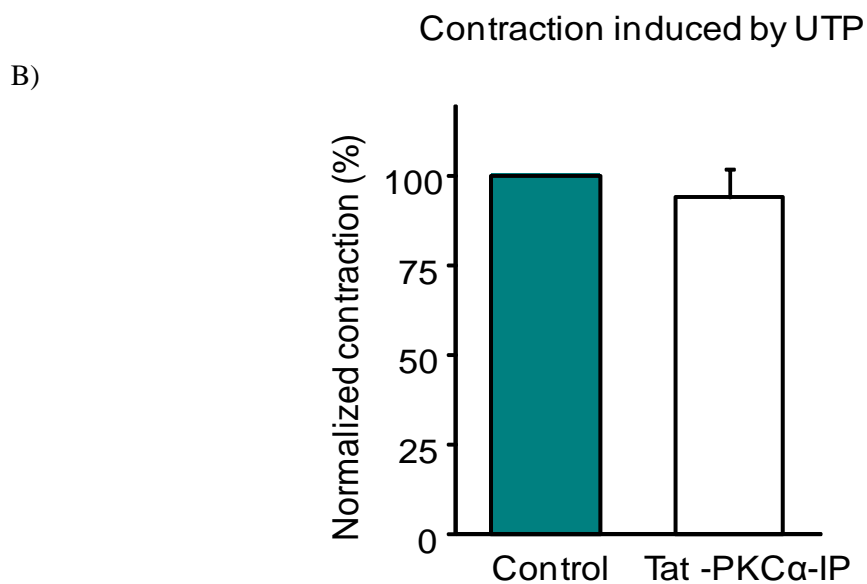
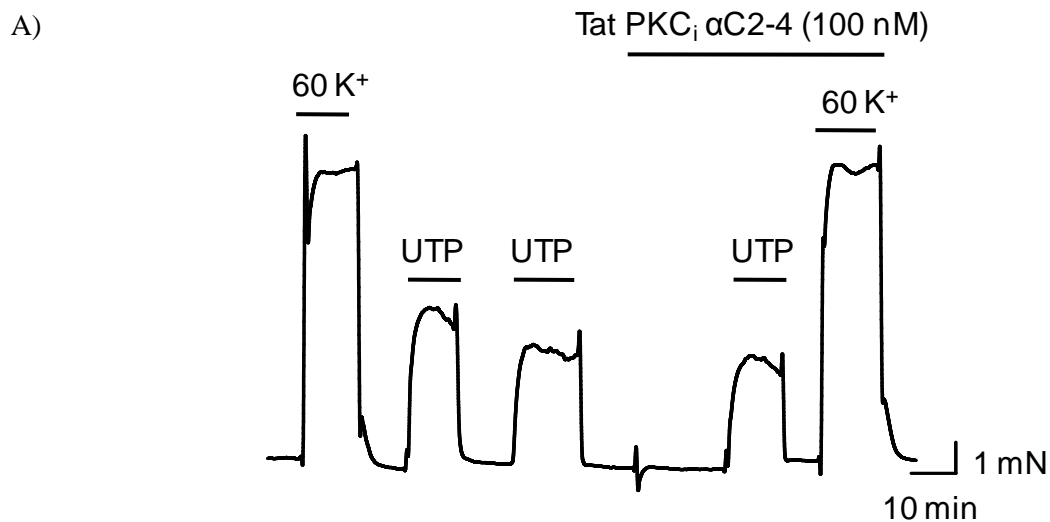


Fig: 3.10 Effect of Tat-PKC α C2-4-IP on contractile response of mesenteric arteries.

A) Representative traces showing the effect of Tat-PKC α C2-4-IP (100 nM) on UTP (100 nM) induced contraction. Following 60 mM K⁺ induced contraction arterial segment was challenged with repeated applications of UTP under control conditions and subsequently UTP induced contraction was observed after pretreatment of the arterial segment with Tat PKC α C2-4-IP (100 nM). Tat-PKC α C2-4-IP was unable to prevent the UTP to induce contraction.

B) Mean normalized data of UTP induced contraction is expressed as percentage (\pm SEM). No significant reduction in the UTP induced contraction was obtained (n=3).

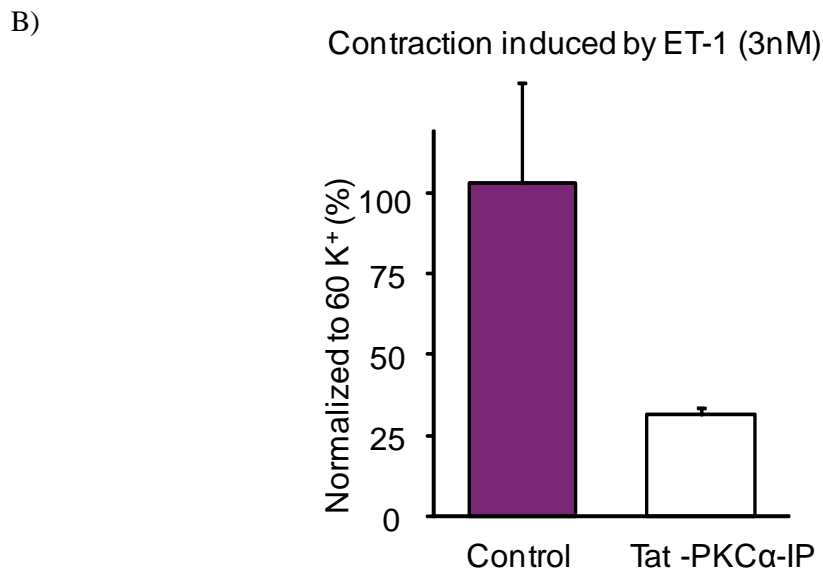
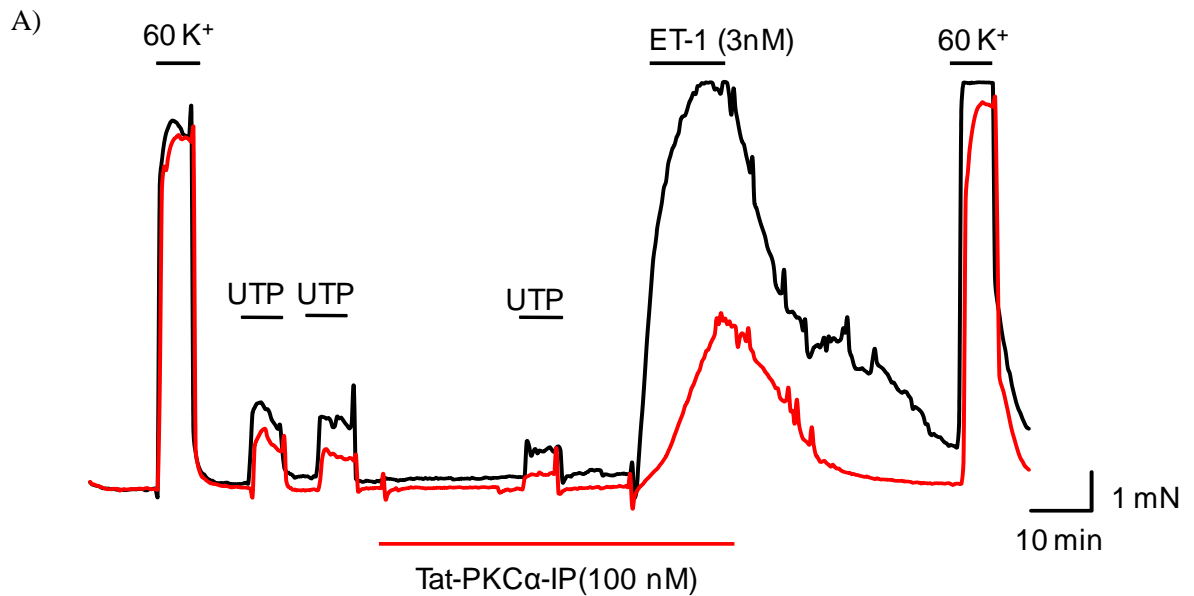
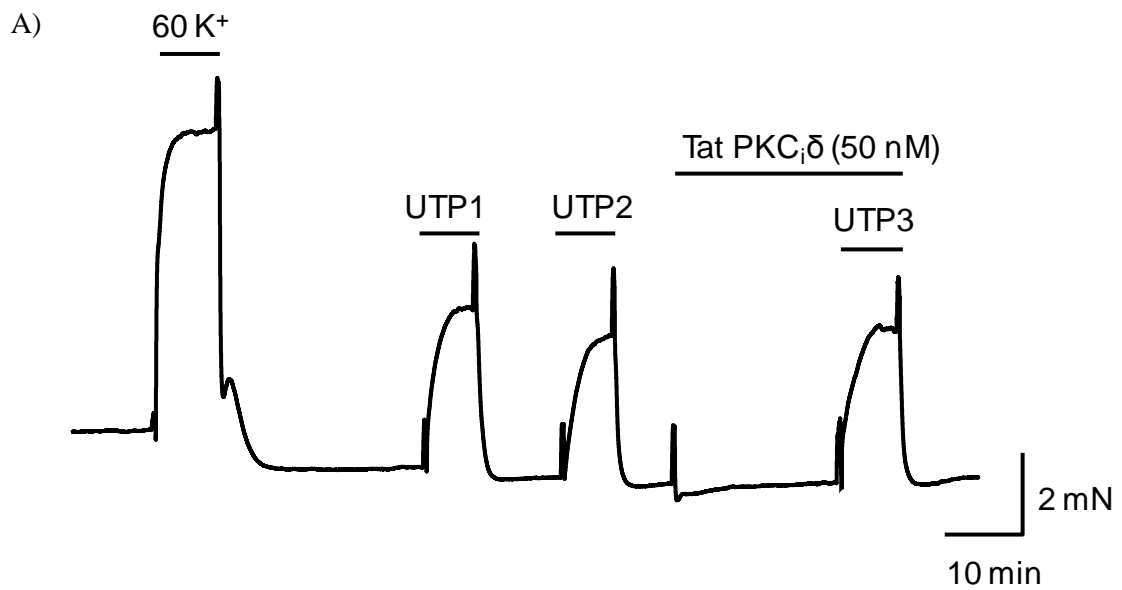


Fig: 3.11 Effect of Tat -PKC α -IP on UTP (30 μ M) and ET-1 (3 nM) induced contraction

A) Typical tracings of a myograph experiment showing the effect of Tat PKC α -IP (100 nM) on ET-I (3 nM) induced contraction. Upper control traces (black) shows the contraction of a mesenteric arterial ring to 60 mM K⁺ and subsequently to repeated applications of UTP (30 μ M) and later to ET-1 (3 nM); Bottom traces (red) indicate the recording from a paired ring as in the upper trace, but with 20 min exposure to 3 nM Tat-PKC α -IP (100 nM) before application of ET-I (3 nM).

B) Plot of mean contraction to ET-1 (3 nM) as percentage of 60 mM K⁺ induced contraction under control conditions and after treatment of Tat-PKC α -IP (100 nM). Tat-PKC α -IP reduced the ET-1 response by 69% (n=3).



B)

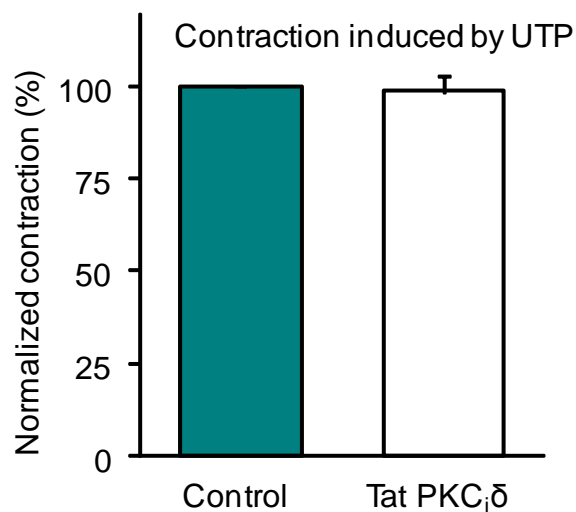


Fig: 3.12 Contractile response of UTP in the presence of Tat PKC_δ-IP

A) Myograph recording of contraction of mesenteric arterial ring segment to 60 mM K⁺ and subsequently to 100 μM UTP in the absence and presence of 50 nM Tat PKC_δ-IP. Response to third UTP after pretreatment of Tat PKC_δ-IP was normalized to second UTP induced response (in the absence of Tat PKC_δ-IP) and mean normalized data was plotted as percentage of the control.

B) Histogram plotted from the above experiment showed no profound reduction in UTP induced contraction in six arterial ring segments.

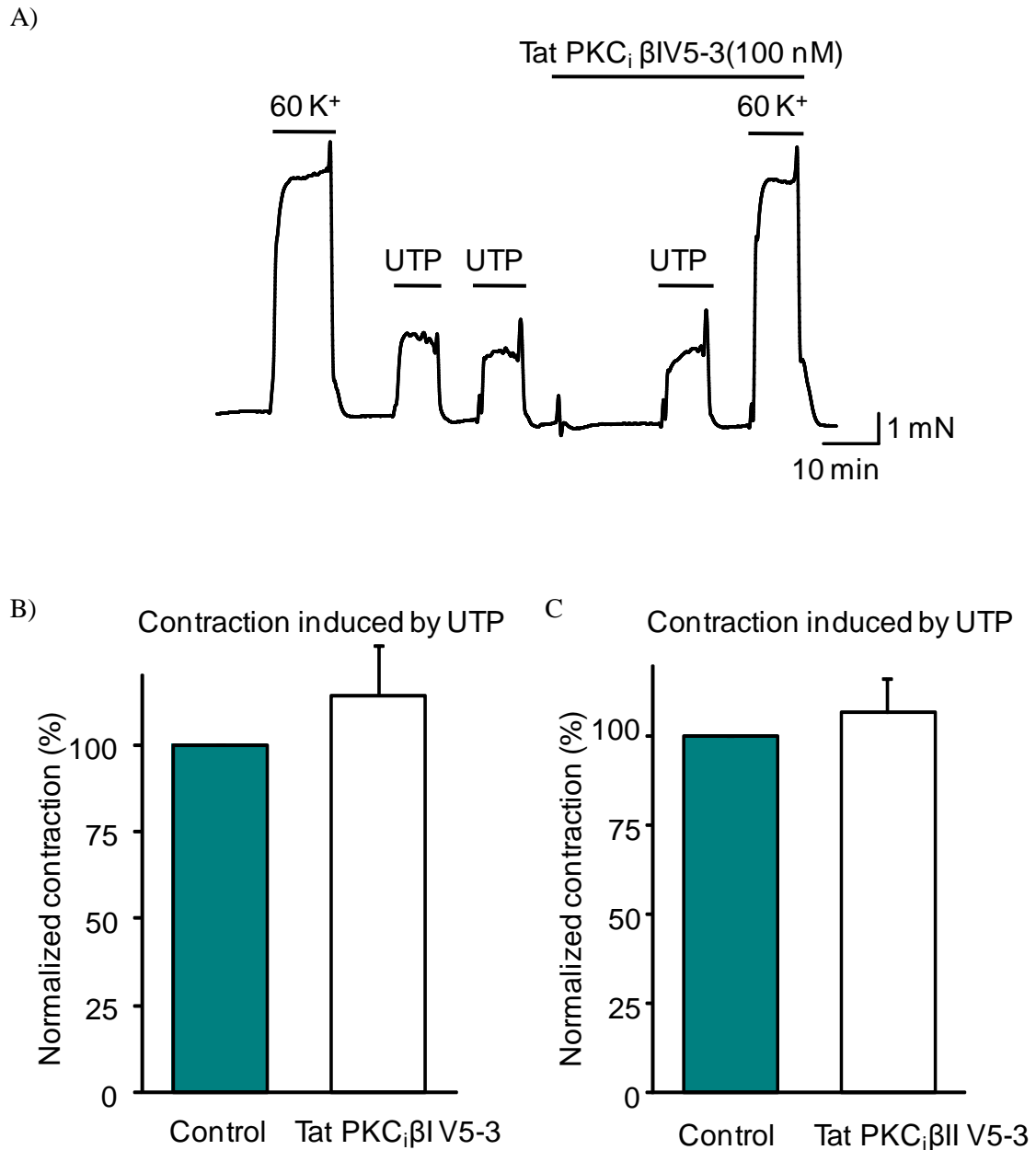


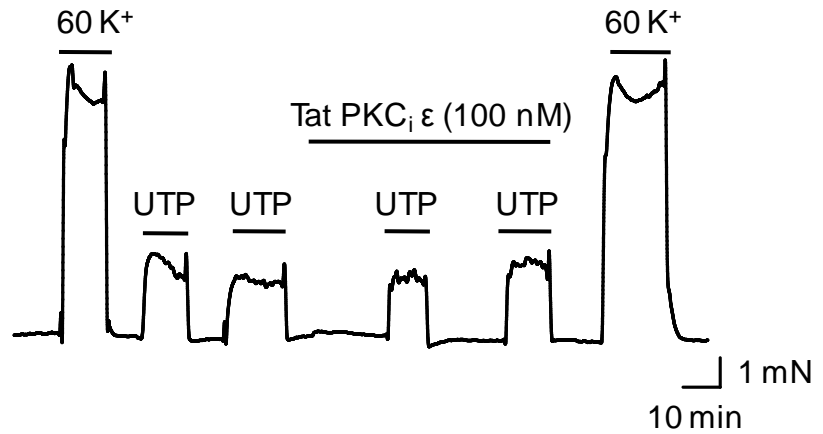
Fig: 3.13 Effect of Tat-PKC β -IP on UTP induced contraction.

A) Typical traces of a myograph experiment showing the effect of Tat-PKC β -IP (100 nM) on UTP (100 μ M) induced contraction. No reduction in the contraction was observed.

B) Mean normalized data plotted as histogram shows no reduction in UTP induced contraction when arterial ring segment was pretreated for 20 minutes in Tat-PKC β -IP (n=4).

C) Mean normalized data plotted as histogram shows no reduction in UTP induced contraction when arterial ring segment was pretreated for 20 minutes in Tat-PKC β -IP (n=3).

A)



B)

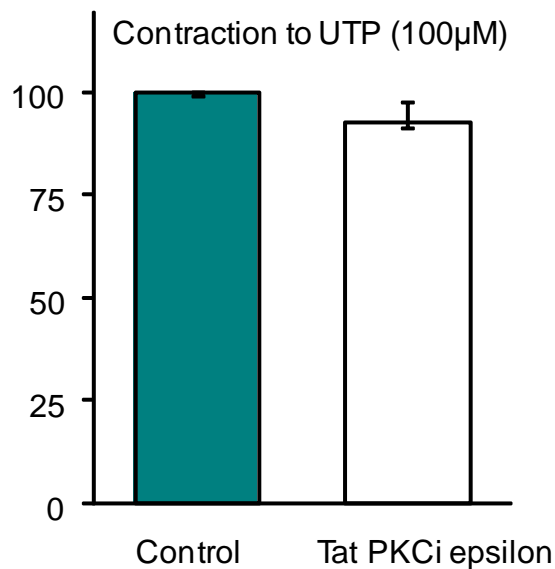


Fig: 3.14 Response of mesenteric artery to UTP in the presence of Tat PKC_ε-IP.

A) Typical tracings of a myograph experiment showing the effect of Tat PKC_ε-IP (100 nM) on UTP induced contraction. Response of mesenteric arterial segment to 60 mM K⁺, UTP was assessed prior to addition of Tat-PKC_ε-IP (100 nM). After 20 minutes of pretreatment of Tat PKC_ε-IP, UTP (100 μM) induced contraction was determined.

B) There was no profound reduction of UTP induced contraction was seen in four mesenteric arterial ring segments.

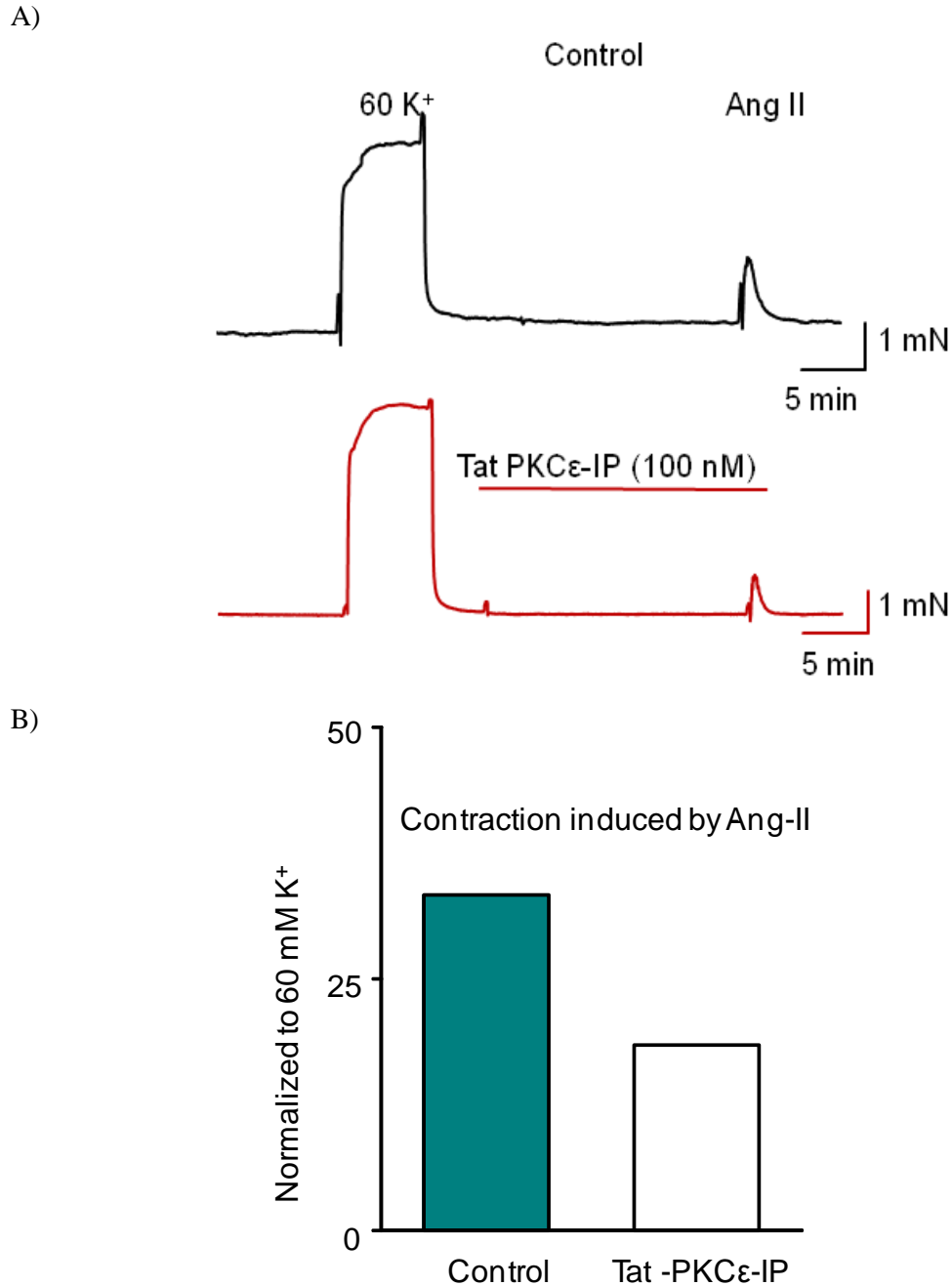


Fig: 3.15 Effect of Tat-PKC ϵ -IP on Ang-II induced contraction.

A) Typical tracings of a myograph experiment showing the effect of Tat PKC ϵ -IP (100 nM) on Ang-II induced contraction. Upper traces (control) shows the contraction of a third order mesenteric arterial ring to 60 mM K⁺ and subsequently to Ang-II; Bottom traces indicate the recording from a paired ring as in the upper trace, but with 20 min pretreatment to 100 nM Tat-PKC ϵ -IP before application of Ang-II.

B) Ang-II induced contraction was expressed as percentage of the 60 mM K⁺ induced contraction (n=1).

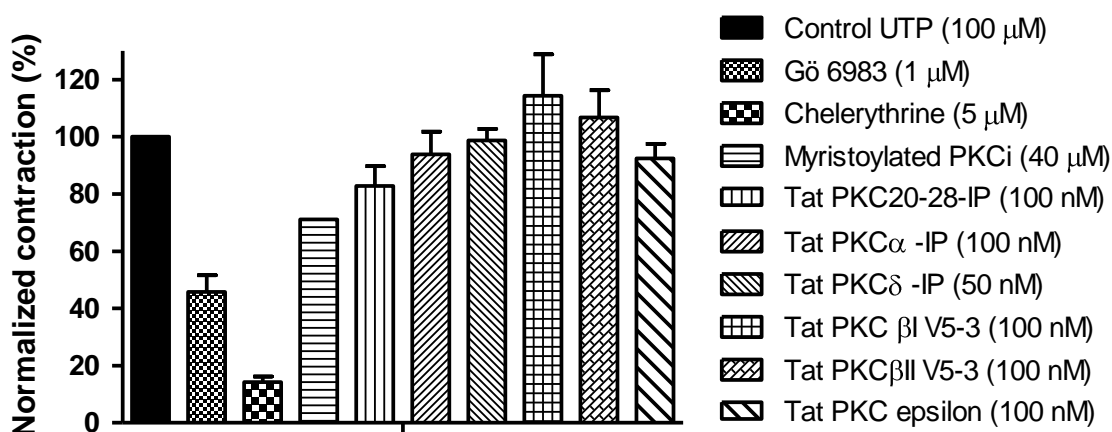


Fig: 3.16 Summary of the effects of various PKC inhibitors on UTP induced contraction.

Plot of mean normalized data of UTP induced contractions in the absence (control) and presence of various PKC inhibitors.

	Mean normalized contraction (%)	SEM	P-value
Gö6983 (1 μM)	45.7	5.8	P<0.005
Chelerythrine (5 μM)	14.3	1.9	P<0.05
Myristoylated PKCi (40 μM)	71.2	0	-
Tat PKC20-28-IP (100 nM)	82.8	6.8	P<0.05
Tat PKC α -IP (100 nM)	93.9	7.8	ns
Tat PKC δ -IP (50 nM)	98.7	4.0	ns
Tat PKC β I V5-3-IP (100 nM)	114.3	14.5	ns
Tat PKC β II V5-3-IP (100 nM)	106.8	9.5	ns
Tat PKC ϵ -IP (100 nM)	92.5	5.1	-

3.3.7 Are non-selective cation channels involved in UTP induced contraction?

To examine whether Ca^{2+} influx via non-selective cation channels is involved in UTP induced contraction the effect of Gd^{3+} , a non-selective cation channel blocker, was examined. Following normal contractile responses to 60 mM K^+ and UTP, mesenteric arterial segments were pretreated with various concentrations of Gd^{3+} for 20 minutes and contractile responses to UTP were recorded in the presence of Gd^{3+} . The UTP induced contraction was virtually abolished in the presence of 100 μM Gd^{3+} and reduced by 85% in 10 μM Gd^{3+} (Fig.3.17). The effect of Gd^{3+} was concentration dependent as observed in some parallel experiments with varying concentrations of Gd^{3+} . Normalized contractile responses of mesenteric arteries to 100 μM UTP in the presence of 1, 10, 30 and 100 μM Gd^{3+} are plotted in Fig. 3.18. Maximum inhibition of UTP induced contraction was observed with 100 μM Gd^{3+} ; however at this concentration it also inhibited the 60 mM K^+ induced contraction of mesenteric arteries.

During the time course of these recordings the inhibition of UTP induced contractions by Gd^{3+} did not recover. However, a recovery of 60 mM K^+ induced contractions was observed. These results suggest a possible involvement of non-selective cation channels in eliciting the contraction of UTP.

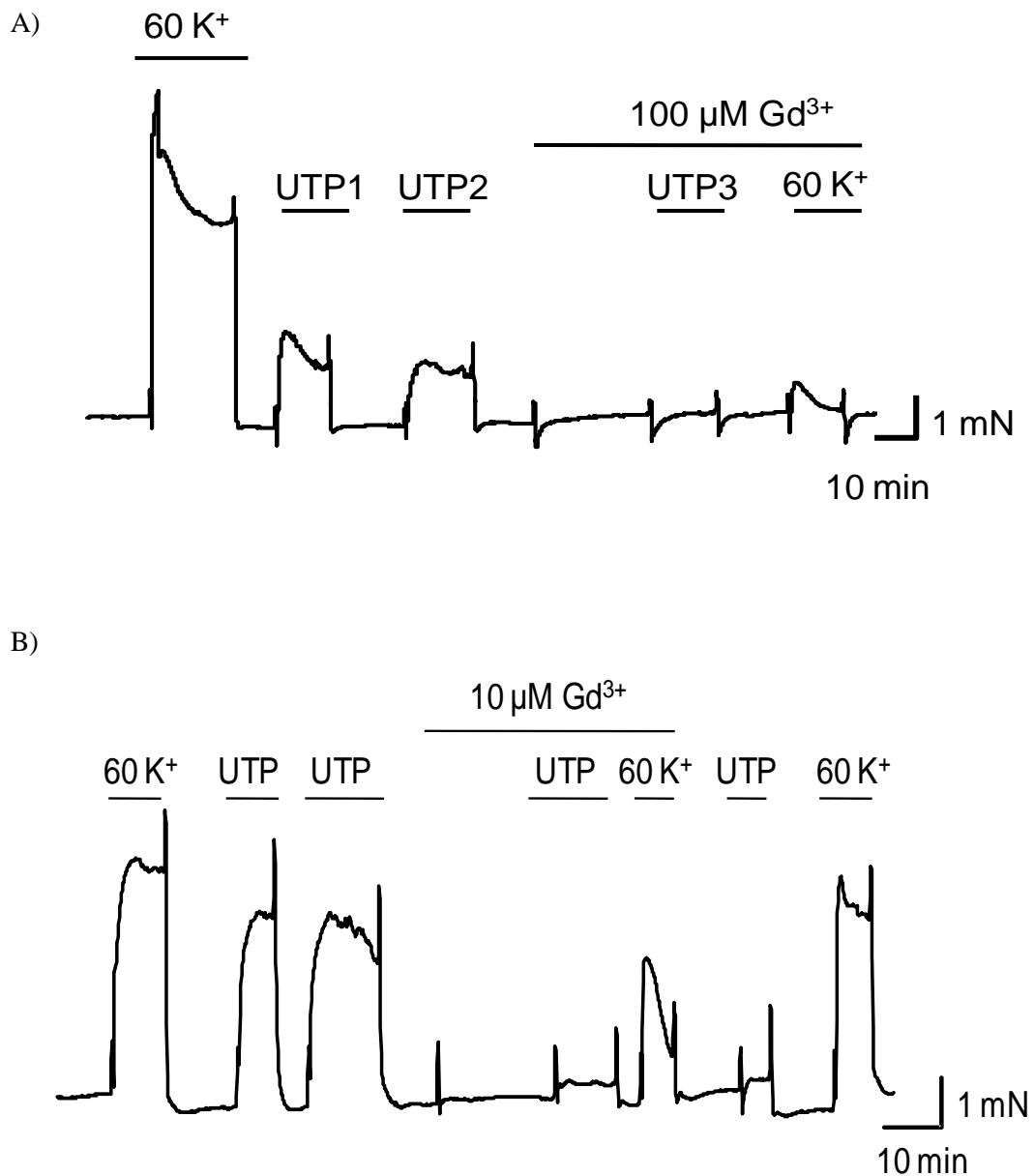


Fig: 3.17 Effect of Gd³⁺ on UTP induced contraction.

A) Recording of the response of a mesenteric arterial segment challenged with 60 mM K⁺ and 100 μM UTP in the absence and presence of 100 μM Gd³⁺ as indicated.

B) Recording of the response of a mesenteric arterial segment challenged with 60 mM K⁺ and 100 μM UTP in the absence and presence of 10 μM Gd³⁺ as indicated. At a concentration of 10 μM Gd³⁺ still blocked the UTP induced contraction, but was much less effective at inhibiting the contraction evoked by 60 mM K⁺.

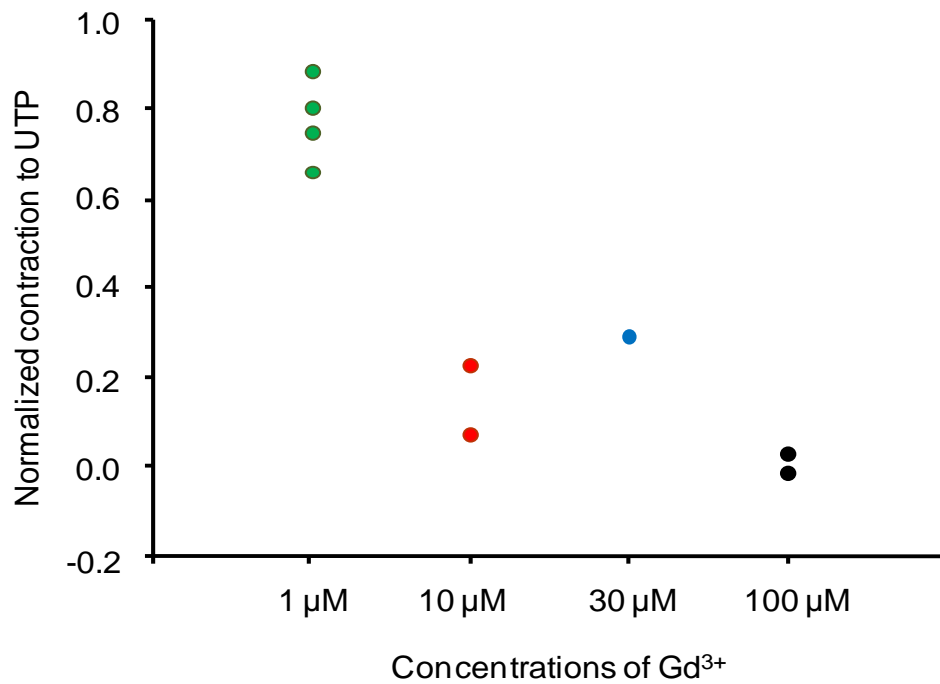


Fig: 3.18 Effect of different concentrations of Gd³⁺ on UTP induced contraction.

The effect of various concentrations (1, 10, 30 and 100 μM) of Gd³⁺ on UTP (100 μM) induced contractions. Maximum reduction in UTP induced contraction was observed when arterial segments were pretreated with 100 μM Gd³⁺.

3.4 Discussion

3.4.1 UTP induced sustained contraction depends on extracellular Ca^{2+} influx

The results of the myograph experiments presented here show that the UTP induced contraction of rat mesenteric arteries is sustained in nature and is likely to result from activation of P2Y receptors (Gitterman and Evans, 2000). However, more recently Sugihara and coworkers reported a P2X₁-like receptor activation in addition to P2Y receptor activation in response to UTP application in rat aorta (Sugihara et al., 2011). In my experiments, UTP elicited a concentration dependent contraction with an EC₅₀ of 52 μM and a Hill coefficient of 2.1 in three arterial ring segments. A similar EC₅₀ value (28 μM) for mesenteric arteries was found by Morris et al (2011). A comparison of the effect of UTP on rat mesenteric artery segments of different diameters yielded variable results which depended not only on the diameter but also on the measurement technique (Gitterman and Evans, 2000). Using wire myography the EC₅₀ and Hill coefficient values for different diameter segments were 1.6 mM and 0.9 for medium (131-342 μm) and 1.4 mM and 1.3 for large (386-806 μm) diameter segments respectively. However, UTP was more potent when vessel diameter was measured using the diamtrak technique, with EC₅₀ values of 15 μM and 88 μM for small and medium arteries and corresponding Hill coefficient values of 1.1 and 2.2 respectively (Gitterman and Evans, 2000). The vessel diameters (265 ± 4 μm ; n=86) in my experiments were within the medium range defined by Gitterman and Evans but I found a greater potency in the UTP induced response (EC₅₀: 52 μM and Hill coefficient: 2.1). This variation could result from the inclusion of L-NAME in my solutions to inhibit endothelial nitric oxide synthase thus limiting the production of nitric oxide. It is interesting to note that the Hill coefficient for UTP I found (2.1) agrees closely with the 2.2 reported by Gitterman and

Evans (2000) using the diamtrak technique in medium sized arteries. UTP potency is higher in coronary and cerebral arteries with EC₅₀ values of 3.2 and 3.1 μM respectively (Welsh and Brayden, 2001; Luykenaar et al., 2004). The sensitivity of the response of rat mesenteric arteries to UTP and suramin indicates the presence of P2Y₂ receptors in this tissue (Gitterman and Evans, 2000).

Furthermore, UTP induced contractions were reproducible even with several repeated applications of UTP. The contractions were largely dependent on extracellular Ca²⁺ influx. The potential sources of Ca²⁺ that contribute to agonist induced contractions in arterial smooth muscle cells are: Ca²⁺ influx from the extracellular space and Ca²⁺ release from internal stores. UTP was unable to induce contraction of mesenteric arteries in a Ca²⁺ free solution. My results are consistent with Sy Yong's findings who reported that in cerebral arteries only one minute incubation period in Ca²⁺ free external solution significantly suppressed UTP induced Ca²⁺ waves (Sy Yong et al., 2009). Furthermore, I also found that UTP induced contractions in rat mesenteric arteries returned as soon as the extracellular Ca²⁺ was replenished. In contrast to my findings, Lopez et al (2000) found that the contraction induced by UTP was not affected even 30 min after depleting extracellular Ca²⁺ and in the presence of EGTA (Lopez et al., 2000). This difference in the sensitivity of UTP induced contractions to external Ca²⁺ may be due to variation between aortic and mesenteric arterial smooth muscle, possibly reflecting the size and the amount of Ca²⁺ present in the sarcoplasmic reticulum.

3.4.2 Voltage gated L-type Ca²⁺ channels and UTP induced vasoconstriction

Because of the sustained contractile behavior and the role of extracellular Ca²⁺ in UTP induced contraction, it was expected that the Ca²⁺ influx occurred via voltage gated Ca²⁺ channels. Voltage gated Ca²⁺ channels are highly expressed in smooth muscle (Horowitz et al., 1996). UTP induced contractions were significantly reduced but not abolished by diltiazem, suggesting that Ca²⁺ entry was at least partially dependent on L-type Ca²⁺ channel activity. This is consistent with the results reported by Luykenaar (2004) in rat cerebral arteries where UTP induced contraction was partly reduced by diltiazem (Luykenaar et al., 2004). The more potent L-type Ca²⁺ channel blocker, nifedipine, also reduced, but did not abolish, the UTP induced Ca²⁺ wave frequency as well as tonic contractile responses in rat basilar arteries (Syyong et al., 2009).

3.4.3 UTP activates PLC to initiate a signaling cascade leading to contraction.

UTP has been shown to exert its effects by activating G-protein coupled P2Y receptors (Abbracchio et al., 2006, Burnstock, 1997, Burnstock, 2007, Burnstock, 1976, Erlinge and Burnstock, 2008, Gitterman and Evans, 2000). In general, GPCRs activate PLC via G_q which in turn hydrolyzes PIP₂ to DAG and IP₃. IP₃ causes activation of IP₃R and Ca²⁺ release from the sarcoplasmic reticulum. Ca²⁺ binds to calmodulin and the resulting Ca²⁺-calmodulin complex activates myosin light chain kinase which phosphorylates MLC, leading to actin-myosin interaction and contraction. DAG, either alone or in combination with calcium, activates several protein kinase C isoforms. Various PKC isoforms have been shown to have roles in agonists induced contractile processes for example causing Ca²⁺ sensitization of the contractile machinery and inhibition of K⁺ channels (Rainbow et al., 2009). The signaling molecules of the

phosphoinositide pathway have important roles in the activation of non-selective cation channels. DAG plays a central role in the noradrenalin activated cation current which involves TRPC6 via a protein kinase C-independent mechanism (Helliwell and Large, 1997). Whereas, stimulation of ET(A) and ET(B) receptors activate PKC-dependent TRPC1 channels in rabbit coronary artery (Saleh et al., 2009). Stimulation of IP₃R1 contributes to UTP-induced vasoconstriction and non-selective cation current activation in rat cerebral arteries (Zhao et al., 2008). The complete inhibition of the UTP induced contraction I observed with the PLC inhibitor U73122 indicates that UTP induced contraction is mediated by a receptor mediated pathway, possibly P2Y₂, which is a Gq linked receptor that activates PLC/DAG/IP₃ signaling. However, U73122 also abolished the contractile response to 60 mM K⁺. Nonspecific blocking effects of this compound has been reported by other groups. For instance a nonspecific blocking effects of higher concentrations (10 μM) of U73122 on contractions evoked by 50 mM K⁺ in rat mesenteric arteries have been reported during an attempt to titrate the minimal effective concentration of U73122 needed to inhibit noradrenaline and endothelin 1 induced contractions of rat mesenteric arteries (Clarke et al., 2008). Other authors have also reported nonspecific effects of U73122 including its interference with adenosine A1 receptor signaling (Walker et al., 1998).

3.4.4 Contribution of PKC to UTP induced vasoconstriction

Vasoconstrictors such as ET-1 and Ang II, activate serine-threonine protein kinase C (PKC) to exert their contractile response. PKC comprises a family of isoenzymes; which are classified into three groups. The conventional PKC isoforms are: α, β_I, β_{II} and γ; all these require both Ca²⁺ and DAG for their activation. However, the novel isoenzymes δ, ε, η and θ do not need Ca²⁺ for their activation; they are activated by

DAG alone, while the atypical isoenzymes ζ and λ/ι need neither Ca^{2+} nor DAG phorbol esters for their activation. Among various PKC isoforms α , β , γ , δ , ϵ , and ζ have been reported in vascular smooth muscle (Salamanca and Khalil, 2005). The PKC isoforms may be activated differentially in response to various agonists (Rainbow et al., 2009). Vasoconstrictors can cause activation of non-selective cation channels through PKC dependent or PKC independent pathways (Saleh et al., 2009, Soboloff et al., 2007). The inhibition of various types of K^+ channels via PKC in vascular smooth muscle have also been reported (Kubo et al., 1997, Hayabuchi et al., 2001, Park et al., 2006, Jaggar and Nelson, 2000, Fujita et al., 2007, Park et al., 2005a, Rainbow et al., 2009, Rainbow et al., 2006, Park et al., 2007, Standen and Quayle, 1998, Ko et al., 2008, Xiao et al., 2003, Park et al., 2005b). PKC by means of phosphorylation of CPI-17 can cause Ca^{2+} sensitization of the contractile machinery (Mueed et al., 2005, Erlinge and Burnstock, 2008); this in turn inhibits myosin light chain phosphatase resulting in the increase in light chain phosphorylation.

Because of the potential role of PKC in the contractile action of UTP in mesenteric arteries I used a selection of peptide as well as non-peptide PKC inhibitors. The UTP induced contractions of mesenteric arterial segments were attenuated significantly by the general PKC inhibitors Gö6983 and chelerythrine. UTP induced contraction was partly inhibited by the cell permeable myristoylated PKC20-28-IP. To confirm these results I used Tat-PKC20-28-IP (synthesized and kindly provided by Dr R.I. Norman) which is actively accumulated in the cell by a, to date, undetermined transport process. The involvement of various PKC isoforms were also investigated using Tat-linked PKC inhibitor peptides. Rat mesenteric arteries express PKC α , β , δ , and ϵ and the particulate levels of these isoforms were increased by ET-1 (Mueed et al., 2005). Tat-linked PKC

inhibitor peptides against the α and ϵ isoforms differentially inhibit the contractile responses of mesenteric arteries to ET-1 and Ang-II respectively (Rainbow et al., 2009). ET-1 was used as a pharmacological tool for comparison purpose; therefore I have also observed ET-1 induced contractile response of mesenteric artery. The ET-1 response was significantly blocked (~40%, n=4) by Tat linked PKC20-28-IP. However, similar experiments showing a comparatively bigger block of ET-1 induced contraction by Tat-PKC α -IP has been reported previously (Rainbow et al., 2009). Moreover, in my experiments UTP induced contractions were not inhibited by Tat PKCi α , β I, β II or δ isoforms. Since it has been shown that the effects of two vasoconstrictors are mediated by different PKC isoforms, it may be possible that several PKC isoforms, with different effects on the contractile machinery, are activated in response to agonist stimulation.

3.4.5 Are non-selective cation channels involved in UTP induced contractions?

Canonical transient receptor potential protein (TRP) is a family of seven (TRPC1–TRPC7) non-selective cation channels. TRPCs are expressed widely in mammalian tissues and are activated by G protein ($G_{q/11}$) coupled receptors. TRPCs are involved in several cardiovascular functions and diseases. The TRPC group can be divided into four subfamilies (TRPC1, TRPC4, 5, TRPC3, 6, 7 and TRPC2) on the basis of sequence homology and functional similarities. The TRPC1 and TRPC6 expression were detected in mesenteric arterial smooth muscle cells and found to be involved in responses of vascular smooth muscle to α 1-adrenoceptor (Hill et al., 2006). In cerebral arteries UTP stimulates TRPC3 channels via IP₃R activation, leading to membrane depolarization by Na⁺ influx, opening of voltage-gated Ca²⁺ channel and vasoconstriction (Zhao et al., 2008). Because of the potential for activation of these non selective cation channels via PLC, IP₃ or DAG activation, during UTP induced contraction I investigated the possible

role of these channels in the UTP induced contraction by using the non selective cation channel blocker Gd^{3+} . A significant block of non selective cation channels by 10 μM Gd^{3+} prevented the UTP induced vasoconstriction. The trivalent Gd^{3+} also had an inhibitory effect at higher concentrations on the contraction of mesenteric arteries by 60 mM K, which may reflect a blocking effect of Gd^{3+} on voltage gated Ca^{2+} channels. Although Gd^{3+} is a blocker of non selective cation channels, I observed its unspecific blocking effects at 100 μM concentration on 60 K⁺ induced contractile response of mesenteric artery.

3.5 Summary

UTP induced a sustained dose dependent and reproducible contraction of mesenteric arteries. The contraction induced by UTP depends on the extracellular Ca^{2+} influx. UTP induced contraction was abolished by Cd^{2+} , however partly inhibited by L-type voltage gated Ca^{2+} channels blocker, diltiazem. L-type voltage gated Ca^{2+} seems to be partly involved in the UTP induced contraction in mesenteric arteries. The non selective cation channels were also studied using Gd^{3+} . Nonselective cation channels are involved in Ca^{2+} influx and contraction of mesenteric arteries. The involvement of G_q coupled receptor signaling pathway was studied by blocking one of the signaling molecule i.e. PLC_{β} . The inhibition of phospholipase C_{β} blocked the UTP induced contractile response and therefore it can be concluded that UTP activates signaling cascade of G_q coupled receptor pathway leading to the production of IP3 and DAG. The involvement of Protein kinase C was also studied using a range of PKC blockers. It was found that PKC is only partly involved in UTP induced vasoconstriction in mesenteric arteries.

Chapter 4 Investigation of the modulation of ionic currents by UTP

4.1 Introduction

Ion channels play an important role in the regulation of membrane potential and are hence involved in the mechanism of inducing contraction in the vasculature. Potassium ion efflux from smooth muscle cells in response to opening of various potassium channels including K_V , K_{ATP} , BK_{Ca} and K_{ir} channels, hyperpolarize the membrane potential resulting in smooth muscle relaxation. However, inhibition of these potassium channels by vasoconstrictors or modulators ultimately result in contraction of smooth muscle. These potassium channels are in turn activated or inhibited by several mechanisms including phosphorylation by PKA or PKC (Cole et al., 1996, Hayabuchi et al., 2001b, Kubo et al., 1997, Park et al., 2007). In contrast to potassium channels, non-selective cation channels or voltage gated Ca^{2+} channels are involved in smooth muscle contraction.

In this chapter the effects of UTP on several ionic currents in rat mesenteric arterial smooth muscle cells were studied using the whole cell patch clamp technique. The currents investigated were K_V , K_{ATP} , I_{NSCC} and, to a lesser extent, I_{Ca} . The involvement of PLC and PKC in the modulation of K_V and K_{ATP} current by UTP were studied using the pharmacological inhibitors U73122 (PLC inhibitor) and Tat-linked PKC inhibitory peptides. Data from my contractile experiments inferred that UTP induced contraction also depends on Ca^{2+} influx through non selective cation channels. Therefore non selective cation channels were examined on the basis of the functional myography experiments.

4.2 **Kv current and UTP**

4.2.1 **Isolation of Kv current**

Voltage-gated K⁺ currents were recorded from acutely isolated rat mesenteric arterial smooth muscle cells with 140 mM intracellular K⁺ and 6 mM extracellular K⁺. Outward currents were evoked by 400 ms depolarizing pulses ranging from -40 to +60 mV in 10 mV increments from a holding potential of -65 mV. The contribution of other ionic currents, mainly resulting from BK channel activity, was minimized by several approaches. A P/6 leak subtraction protocol was used to remove any linear leak components. BK channel activity was seen at positive potentials despite the relatively low intracellular Ca²⁺ concentration in the pipette (100 nM free Ca²⁺ with 10 mM EGTA). In order to completely remove BK channel activity at more depolarizing voltages 100 nM penitrem A, a selective BK channel blocker, was added to the external solution. Under these experimental conditions the time-course of the currents had the characteristics expected for Kv currents.

The average cell capacitance of the mesenteric arterial smooth muscle cells was 13.9 ± 0.7 pF and the average current recorded from these cells in 6 mM K⁺ control solution was 290.7 ± 52.3 pA at + 60 mV.

4.2.2 **Modulation of Kv current by UTP**

Voltage gated potassium channels are widely expressed in vascular smooth muscle cells including rat mesenteric arteries and it is reported that vasoconstrictors induced contraction is partly due to Kv current inhibition in a variety of tissues (Luykenaar et al., 2004).

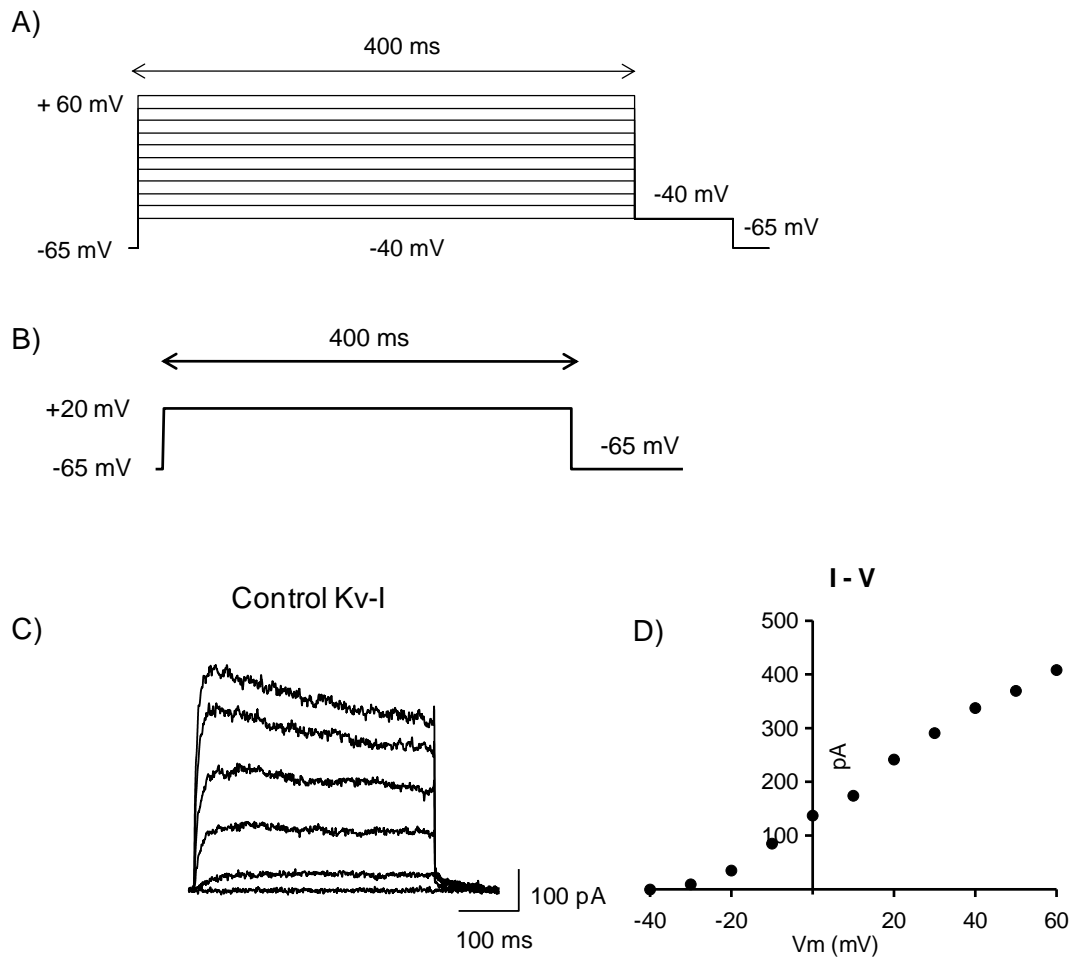


Fig: 4.1 Kv-I protocol

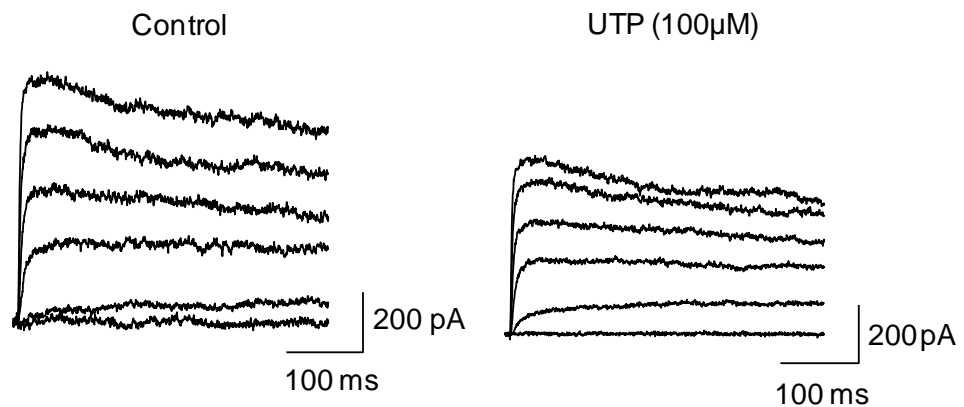
A) Protocol used for whole cell recording from mesenteric arterial smooth muscle cells. Cells were clamped at -65 mV and currents were evoked by 400 ms voltage pulses from -40 to +60 mV using 10 mV increments. A brief voltage step to -40 mV was applied after each 400 ms voltage step to repolarize the cell. The current was measured at 2 kHz and sampled at 10 kHz; B) Voltage protocol designed to measure the stability of the Kv current over time. The cells were held at -65 mV and 400 ms voltage pulses were applied to +20 mV every 20 seconds; C) Example traces of Kv current recording from mesenteric arterial smooth muscle cells in control. Mesenteric arterial smooth muscle cells with an average membrane capacitance 13.4 ± 0.8 were clamped at -65 mV and currents were recorded as described in protocol (A).

D) Current voltage plot from the cell shown in part (C). The current value for each pulse was taken as the mean current between 320-370 ms. The average Kv current recorded from mesenteric arterial smooth muscle cells in 6 mM K^+ was 290.7 ± 52.3 pA at +60 mV.

In the present study the effect of UTP on Kv channel activity was studied. Initially, whole-cell Kv currents were recorded under control conditions using the protocol shown in Fig. 4.1. Following this, the cells were exposed to external solution containing 100 μ M UTP and Kv currents were recorded after 3, 6, 9 and 12, and occasionally 15, 18 and 21 minutes after UTP application. A comparison of the whole cell current recorded under control conditions and after application of UTP revealed that UTP inhibited the Kv current, especially at more depolarized voltages, as shown in figure 4.2A. To generate a current-voltage (I-V) curve the mean currents over 50 ms towards the end of the 400 ms voltage pulses (320 - 370 ms) were measured. An example of an I-V curve is shown in Fig. 4.1. To compare the inhibition produced by UTP over many cells I-V curves were normalized to the maximum control current at +60 mV. Plotting the normalized I-V curves revealed that 100 μ M UTP inhibited Kv currents, especially at more depolarized voltages. As shown in figure 4.3A, the mean Kv current in the presence of UTP at +60 mV was reduced to $59.8 \pm 7.3\%$ of the control value (n= 9, ***P< 0.001).

UTP reduced the Kv current further to $55.9 \pm 2.3\%$ (n=4) within 12 minutes of addition of UTP as shown by the I-V curve of figure 4.3B. To test whether the reduction in current observed following UTP application was not simply a result of run-down the stability of the Kv current over time was assessed by applying a 400 ms depolarizing step to +20 mV every 20 sec from a holding potential of -65 mV (protocol as shown in the 4.1B). A plot of the current amplitude, normalized to that of the first pulse, against time is shown in figure 4.2B.

A)



B)

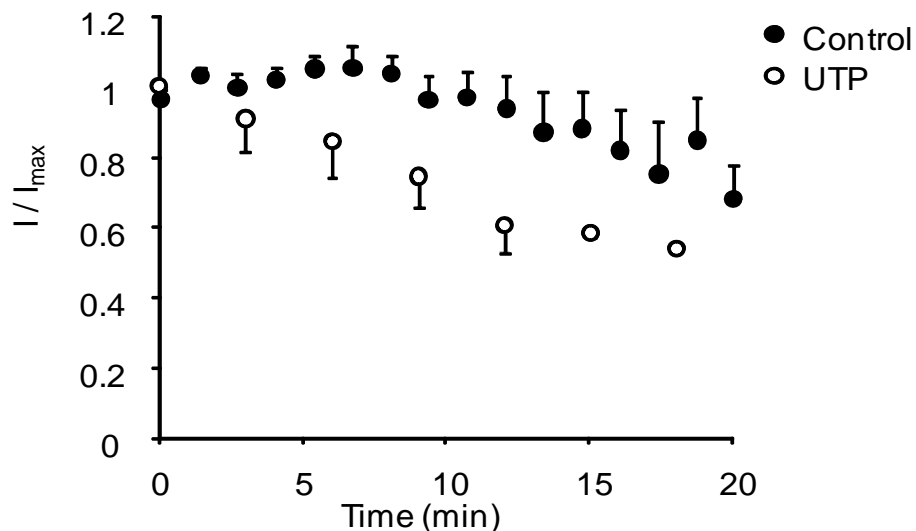


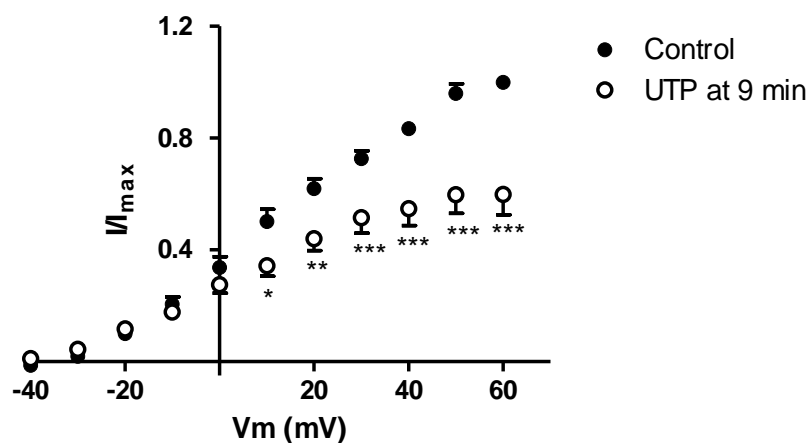
Fig: 4.2 modulation of Kv current by UTP

Currents were recorded from mesenteric arterial smooth muscle cells using conventional whole-cell recording with an external $[K^+]$ of 6 mM and a pipette solution containing a free $[Ca^{2+}]$ of 100 nM (using 10 mM EGTA as a chelator) and 140 mM K^+ . Voltage pulses were applied from -40 to +60 mV in 10 mV increments from a holding potential -65 mV. Currents were recorded in the presence of Penitrem A to block BK channels.

A) Example traces of Kv current recordings in control (6 mM K^+) and after addition of 100 μ M UTP.

B) Mean Kv current amplitudes at +20 mV, normalized to the amplitude of the first pulse, plotted against time in control (\bullet , n=6). Pulses were applied every 20 s from a holding potential of -65 mV. The values in the presence of 100 μ M UTP are also shown (\circ , n=5) where the current at +20 were measured as part of an I-V protocol given every 3 minutes and are normalized to the corresponding first pulse in control conditions.

A) n = 9



B) n = 3

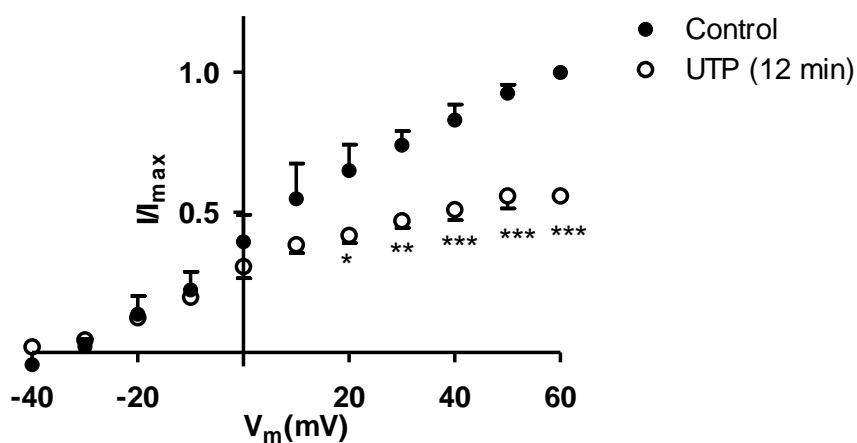


Fig: 4.3 Effects of UTP on Kv current recording.

Mean current-voltage curves, normalized to the current measured at +60 mV in control conditions (\bullet) and in the presence of 100 μ M UTP (\circ) for 9 minutes (n=9) and 12 minutes (C, n=3). The voltage protocols used to generate these I-V curves were as shown in Fig 4.1A and the current for each pulse was taken as the mean current between 320 and 370 ms. Significant difference from control is expressed as * $P < 0.05$, ** $P < 0.01$ and *** $P < 0.001$.

It can be seen that the Kv current amplitude was quite stable up to 12-15 minutes of recording; however, current rundown was observed from 15 minutes onwards. Figure 4.2B also shows the time course of the reduction in Kv current induced by 100 μ M UTP (protocol as in figure 4.1A). As can be seen the Kv current was suppressed within 3 to 9 minutes of UTP application with maximum reduction occurring after 12 to 18 minutes (figure 4.2B). In view of the possible rundown of Kv currents due to dialysis of cellular contents with the passage of time after going to whole cell, unless stated otherwise the effect of UTP on Kv currents were measured after 9 minutes of UTP application.

To study the effect of UTP on Kv channel activation parameters, activation curves were constructed by measuring tail current amplitudes on repolarization to -40 mV after 400 ms voltage pulses (from -40 to +60 mV). Activation curves give information about the relative channel open probability at a given voltage. The tail current after each depolarizing pulse was fitted with an exponential function and the value of this, extrapolated to the beginning of the tail current, was used as the magnitude of the tail current (see Fig.4.4A, figure with the tail current fits). This method of obtaining the amplitude of the tail currents minimizes possible measurement artifacts resulting from current noise and any capacitative transients remaining. The tail current amplitudes thus obtained were normalized with the maximum tail current amplitude ($I_{tail}/ \max I_{tail}$) and plotted against test pulse potential. The activation plots were fitted with Boltzmann distributions of the form:

$$\frac{I_{tail}}{\max I_{tail}} = \frac{1}{(1 + \exp (V_{1/2} - V)/k))} \quad 4.1$$

Where, I_{tail} is the magnitude of the tail current; V is the membrane potential; $maxI_{tail}$ is the magnitude of the maximum tail current; $V_{1/2}$ is the membrane potential required for half maximal activation and k determines the voltage dependence of activation.

Activation plots of the Kv current in control conditions and in the presence of UTP are shown in Fig. 4.4B. The lines are drawn to the Boltzmann equation (4.1) with values for $V_{1/2}$ and k of -14.8 and 9.36 in control and -26.3 and 5.27 in the presence of 100 μ M UTP respectively.

Since UTP clearly reduced the Kv current at more depolarized voltages the activation curve in the presence of UTP was re-plotted whereby the tail current amplitudes in the presence of UTP were normalized with the maximum tail current amplitude in control conditions (Fig.4.4A). This plot was fitted with a modification of equation 4.1:

$$\frac{I_{tail}(UTP)}{maxI_{tail} (control)} = \frac{f}{(1 + \exp(V_{1/2} - V)/k)} \quad 4.2$$

Where $I_{tail} (UTP)$ is the magnitude of the tail current in the presence of UTP, $maxI_{tail} (control)$ is the maximum tail current in the absence of UTP and f is the fractional reduction in the tail currents caused by UTP. The control line of Fig.4.4C shows the fit to equation 4.1 where $V_{1/2}$ and k are -15.4 and 8.05 mV respectively, while the UTP line shows the fit to equation (4.2); where $V_{1/2}$, k and f are -26.0, 6.42, and 0.69 respectively.

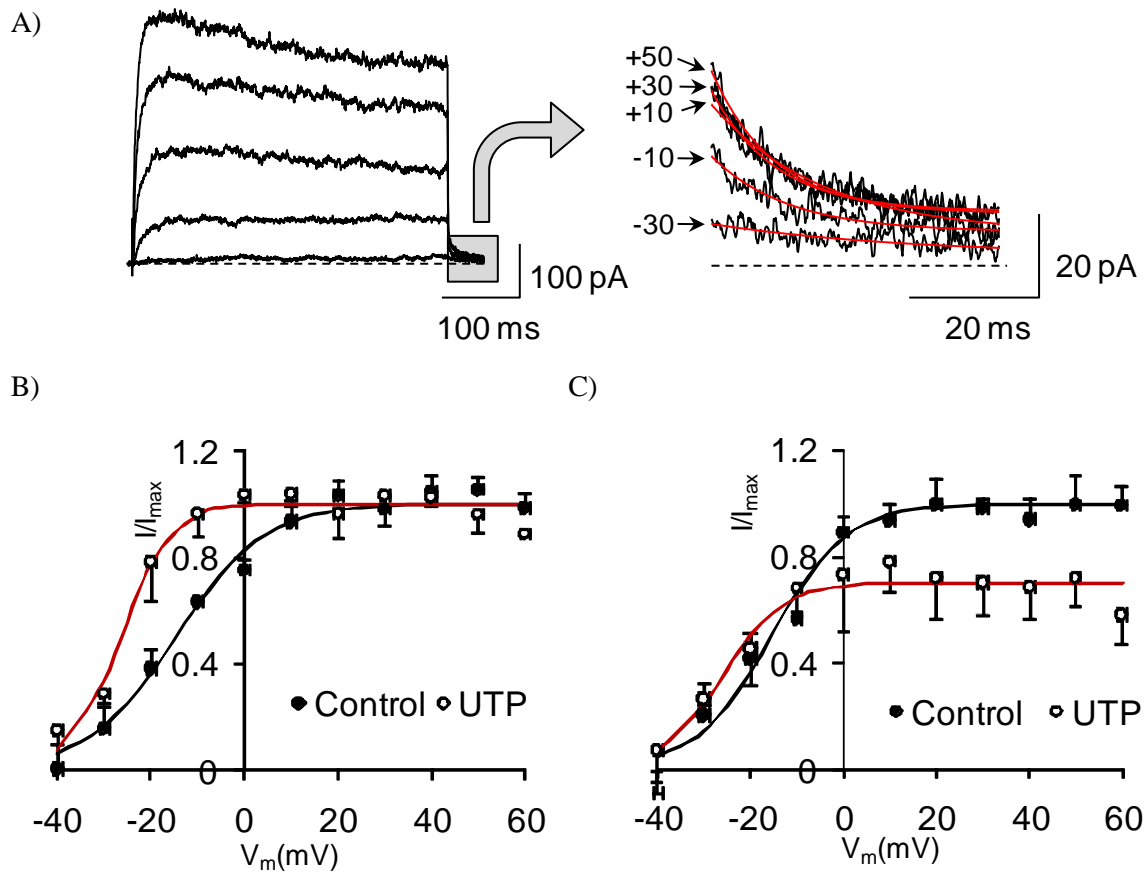


Fig: 4.4 Effect of UTP on Kv current activation curve.

Example traces of Kv currents recorded in control solution to measure the tail current. The tail current after each depolarizing pulse was fitted with an exponential function and the value of this, extrapolated to the beginning of the tail current, was used as the magnitude of the tail current.

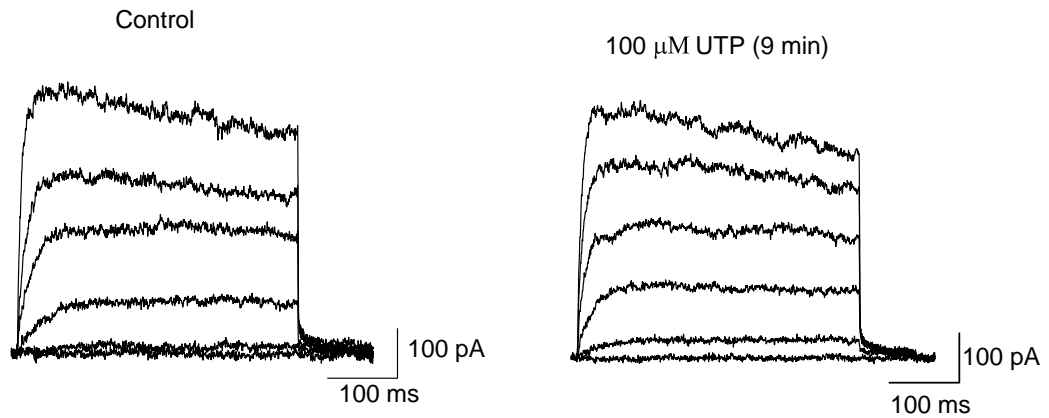
Activation curves for the Kv current recorded under control conditions (●) and after 9 minutes in the presence of 100 μ M UTP (○). Tail currents were measured as described in the text and in Fig. 4.4 A). Mean tail currents were normalized with the maximum tail current in either control or UTP (B) or with the maximum tail current in control for both control and UTP (C) before averaging. Data are expressed as means \pm SEM. In part (B) the lines are drawn to equation (4.1) with $V_{1/2}$ and $k = -14.8$ and 9.36 mV in control and -26.3 and 5.27 mV in UTP; and in part (C) the lines are drawn to equation (4.2) with $V_{1/2}$, k and f being -15.4 mV, 8.05 mV and 1 in control and -26.0 mV, 6.42 mV, and 0.69 in UTP.

4.2.3 Effect of low intracellular Ca^{2+} on K_v current modulation by UTP

Whole cell K_v currents were recorded from single cells held at -65 mV with an intracellular pipette solution containing 0 Ca^{2+} and 10 mM EGTA. Recording protocol was same as in figure 4.1A i.e. currents were recorded by applying 400 ms pulses between -40 to $+60$ mV ($V_h = -65$) in control (6 mM K^+ solution) and after addition of 100 μM UTP as shown in figure 4.5A. 100 nM penitrem A was also included in the external solution to block currents from BK_{Ca} channels. Net I-V relationship was plotted in the absence and presence of UTP (after 9 min) by measuring the average current from 320 to 370 ms of the voltage steps (-40 to 60 mV) and normalizing them with maximum control current at $+60$ mV (figure 4.5B). Current-voltage relationship (I-V curve) revealed that when the pipette solution contained 10 mM EGTA and no added Ca^{2+} UTP was unable to modulate the K_v current (at 60 mV K_v current in response to UTP at 9 minute was 95%).

Figure 4.6A shows examples of K_v currents in control and 9 minutes after the application of 100 μM UTP in a cell where the intracellular free Ca^{2+} was calculated to be 20 nM (1 mM Ca^{2+} and 10 mM EGTA) using the pulse protocol described in figure 4.1A. As can be seen, UTP was less effective at inhibiting the current. Mean normalized I-V curves (figure 4.6B) revealed similar results to those obtained with zero internal Ca^{2+} . UTP was unable to suppress the K_v current with low intracellular Ca^{2+} (20 nM free Ca^{2+}). Using 20 nM free Ca^{2+} mean normalized current in the presence of UTP was $93.9 \pm 11.2\%$ of control at 60 mV.

A)



B)

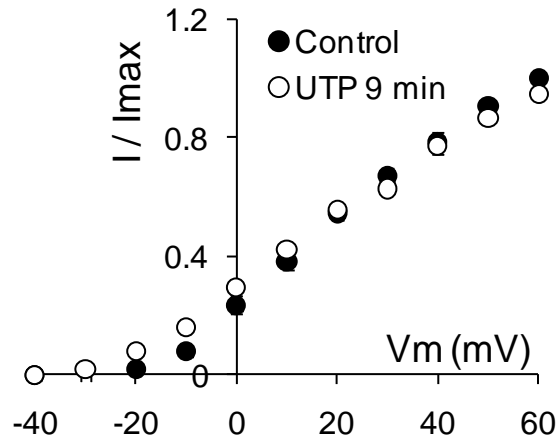
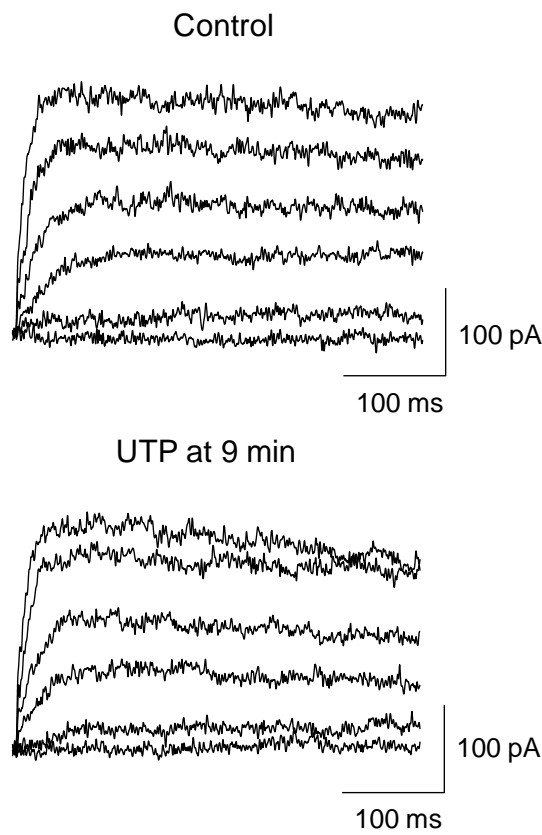


Fig: 4.5 Effect of zero internal Ca^{2+} on Kv current suppression by UTP

Currents recorded from mesenteric arterial smooth muscle cell using conventional whole-cell recording with an external K^+ of 6 mM and a pipette solution containing no added Ca^{2+} and 10 mM EGTA and 140 mM K^+ . Voltage protocol is same as in figure 4.1A; pulses were applied from -40 to +60 mV with a 10 mV increment to the whole cells held at a holding potential -65 mV. To block BK channel activity penitrem A was included in the external solution. Kv current was recorded in the absence and presence of UTP; A) Trace showing the whole cell current recording in a nominally zero Ca^{2+} internal pipette solution in control (n=3) and after 9 min addition of 100 μM UTP (n=1). For simplicity only 20 mV increments of 400 ms voltage pulses are shown in the trace.

B) Net current voltage relationship (I-V curve) was constructed from mean currents obtained from last 50 ms voltage pulses (i.e. 320 to 370 ms) in control (●) and after 9 min of UTP (○). In each case, currents were normalized with the maximum control current at +60 mV.

A) 20 nM Intracellular Ca^{2+}



B) Normalized I-V curve

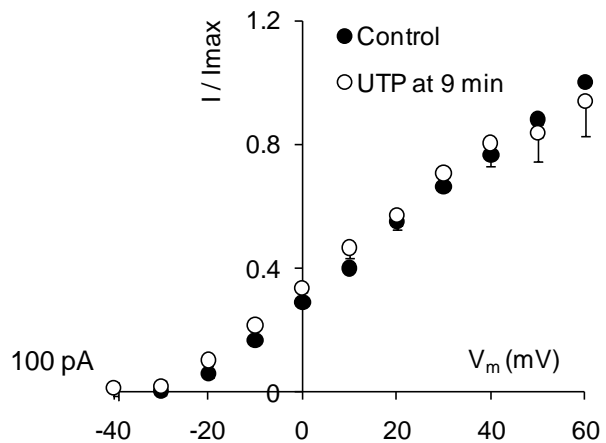


Fig: 4.6 Effect of low intracellular Ca^{2+} (20 nM) on Kv current suppression by UTP

(A) Whole cell currents recorded from a cell with an external K^+ of 6 mM and a pipette solution containing 20 nM free Ca^{2+} and 140 mM K^+ . The voltage protocol is same as in figure 4.1A; pulses were applied from -40 to +60 mV with a 10 mV increment to the cells from a holding potential -65 mV (currents are displayed at 20 mV increments). To block BK channel activity penitrem A (100 nM) was included in the external solution. Kv currents were recorded in the absence and presence of UTP as indicated.

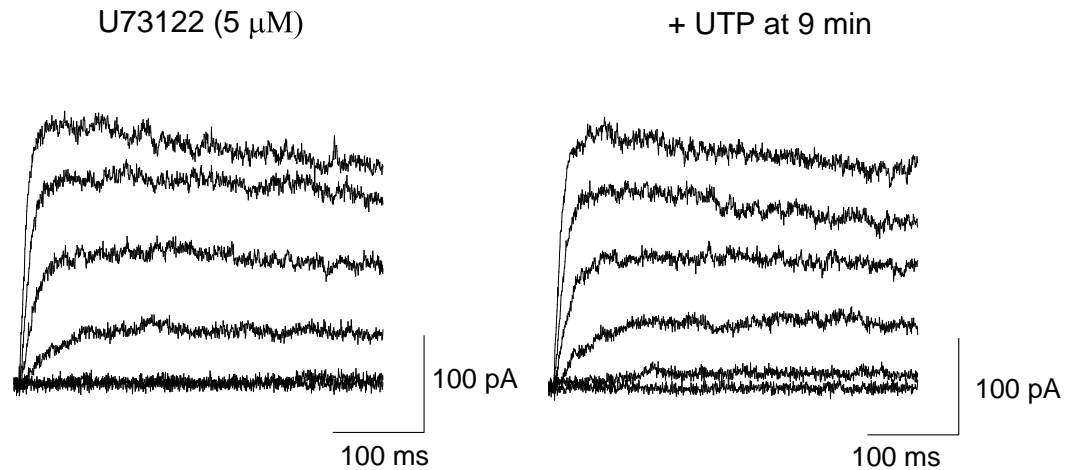
B) Mean normalized I-V curves in control (●) and after 9 min of UTP (○). In each case, currents were normalized with the maximum control current at +60 mV.

4.2.4 Effect of PLC on Kv current modulation by UTP

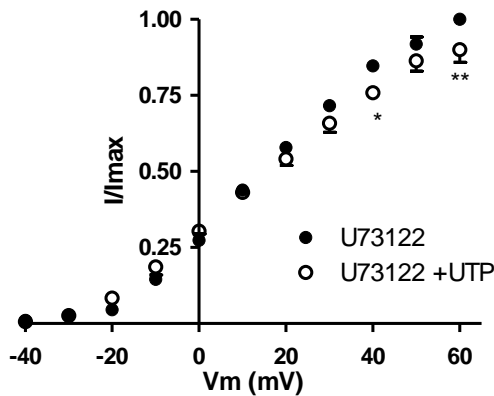
To determine the role of PLC in Kv current suppression by UTP, the effect of the PLC inhibitor, U73122, on the ability of UTP to inhibit Kv currents was assessed. Currents were recorded in the absence (control) and presence of 100 μM UTP while cells were dialyzed with a 140 mM K^+ internal pipette solution containing 5 μM U73122. Because of the unspecific blocking effects of U73122 (10 μM), observed in functional myograph experiments, a slightly lower concentration of this inhibitor was used in these experiments. Furthermore, the potential contamination and toxicity of U73122 in the perfusion system was avoided by including U73122 in the pipette solution. The addition of U73122 was not practically favorable due to its oily nature which would make the surface of the cells slippery and difficult to seal.

Representative traces showing the effect of U73122 on Kv current in control and 9 minutes after UTP (100 μM) application are shown in Fig. 4.7. Inclusion of 5 μM U73122 in the pipette solution reduced the ability of UTP to suppress the Kv current. Normalized I-V curves obtained with U73122 in the pipette in the absence and presence of 100 μM UTP are shown in figure 4.7B. The currents were normalized to that measured at +60 mV in the absence of UTP. At this potential, in the presence of U73122, 100 μM UTP reduced the Kv current to $90 \pm 4.2\%$ ($n=6$, $P < 0.01$). However, U73122 also inhibited the Kv current as shown in the bar chart (figure 4.7C).

A)



B)



C)

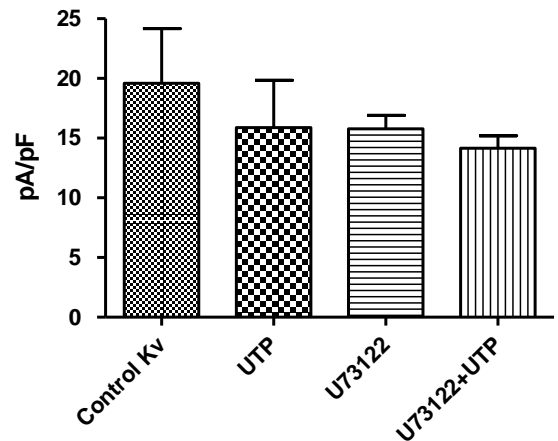


Fig: 4.7 Effect of U73122 on UTP inhibited Kv current

Currents recorded from a cell with an external K^+ of 6 mM and a pipette solution containing 5 μ M U73122 (PLC inhibitor) in addition to 100 nM free Ca^{2+} and 140 mM K^+ . Pulses were applied from -40 to +60 mV in 10 mV increments from a holding potential -65 mV. To block BK channel activity penitrem A was included in the external solution. Kv current was recorded in the absence and presence of UTP.

A) Example traces showing the currents recorded at -40 to +60 mV in 20 mV increments in the absence (control) and 9 minutes after the addition of 100 μ M UTP as indicated; B) Normalized I-V curves in control (●) and 9 minutes after the application of 100 μ M UTP (○). In each case, currents were obtained as the mean current measured from 320 to 370 ms of each pulse and normalized with the maximum control current observed for each cell at +60 mV; C) Currents normalized to their cell capacitance and plotted as a histogram. U73122 also reduced the Kv current.

4.2.5 Does UTP modulate Kv current via PKC?

Vasoconstrictors such as Ang-II and ET-1 constrict smooth muscle by the activation of protein kinase C which in turn regulates the Kv channels (Hayabuchi et al., 2001b, Cole et al., 1996, Ko et al., 2008, Park et al., 2005, Rainbow et al., 2006, Rainbow et al., 2009, Standen and Quayle, 1998, Xiao et al., 2003). To study whether PKC has a role in Kv current modulation by UTP, whole cell currents were recorded from arterial smooth muscle cells pretreated with 100 nM Tat-PKC20-28-IP. The cells, which were initially bathed in 6 mM K⁺ external solution to settle, were pretreated with 100 nM Tat PKC20-28-IP for at least 10 minutes before Kv current recording. The voltage protocol (400 ms steps to -40 to +60 mV from a holding potential of -65 mV) used to generate the Kv currents was as described earlier 4.2.1 and Fig: 4.1, using an intracellular pipette solution containing 140 mM K⁺ and 100 nM free Ca²⁺. The currents were recorded after pretreatment with Tat PKC20-28-IP and 9 minutes following the addition of UTP to the bath (Fig: 4.8).

To examine the role of different PKC isoforms in the mediation of Kv current suppression by UTP, currents were recorded from cells pretreated with either 50 nM Tat PKC ϵ -IP or 100 nM Tat PKC α -IP for at least 10 minutes before the Kv current was recorded (Fig: 4.9A, B & C). The voltage protocol (400 ms steps to -40 to +60 mV from a holding potential of -65 mV) used to activate Kv currents was as described earlier in Fig: 4.1 and using an intracellular pipette solution containing 140 mM K⁺ and 100 nM free Ca²⁺. The currents were recorded after pretreatment with Tat PKC ϵ -IP and 9 minutes following the addition of UTP to the bath (Fig: 4.9A & B). Similarly currents were also recorded from cells pretreated with Tat PKC α -IP for at least 10 minutes using the same voltage protocol (Fig: 4.9C).

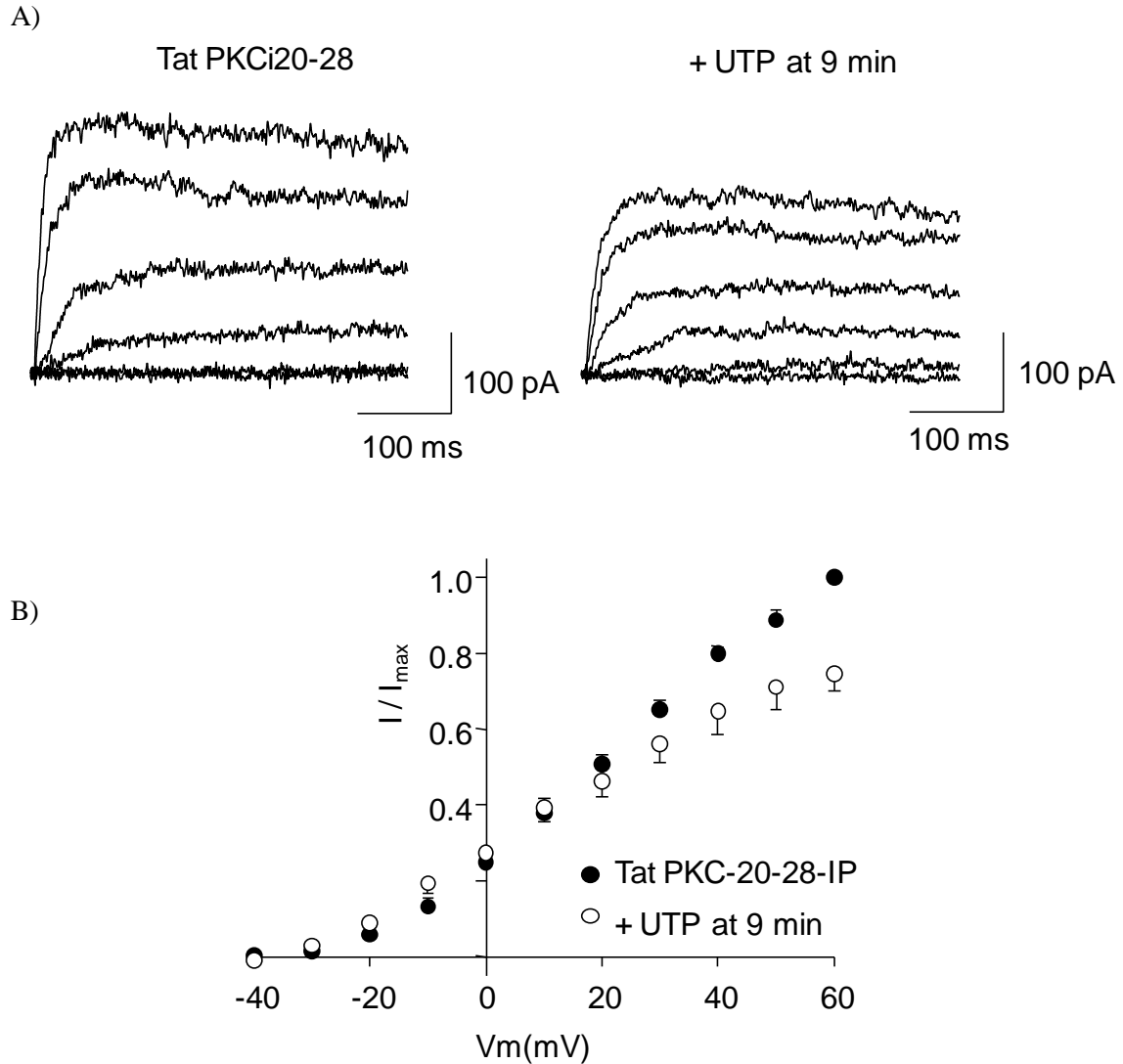


Fig: 4.8 Effect of Tat PKC-20-28-IP on UTP modulated K_v current

Whole cell currents recorded from a cell bathed in an external K⁺ of 6 mM containing 100 nM Tat PKC20-28-IP and a pipette solution containing 100 nM free Ca²⁺ and 140 mM K⁺. Pulses were applied in 10 mV increments from -40 to +60 mV from a holding potential -65 mV. To block BK channel activity penitrem A was included in the external solution and K_v currents were recorded in the absence and presence of UTP.

A) Example traces showing the currents recorded at -40 to +60 mV in 20 mV increments in the absence (control) and 9 minutes after the addition of 100 μM UTP as indicated in cells pretreated with 100 nM Tat PKC20-28-IP.

B) Normalized I-V curves in control (●, cells pretreated with Tat-PKC20-28-IP) and 9 minutes after the application of 100 μM UTP (○). In each case, currents were obtained as the mean current measured from 320 to 370 ms of each pulse and normalized with the maximum control current observed for each cell at +60 mV. Data are the mean ± SEM from 7 cells.

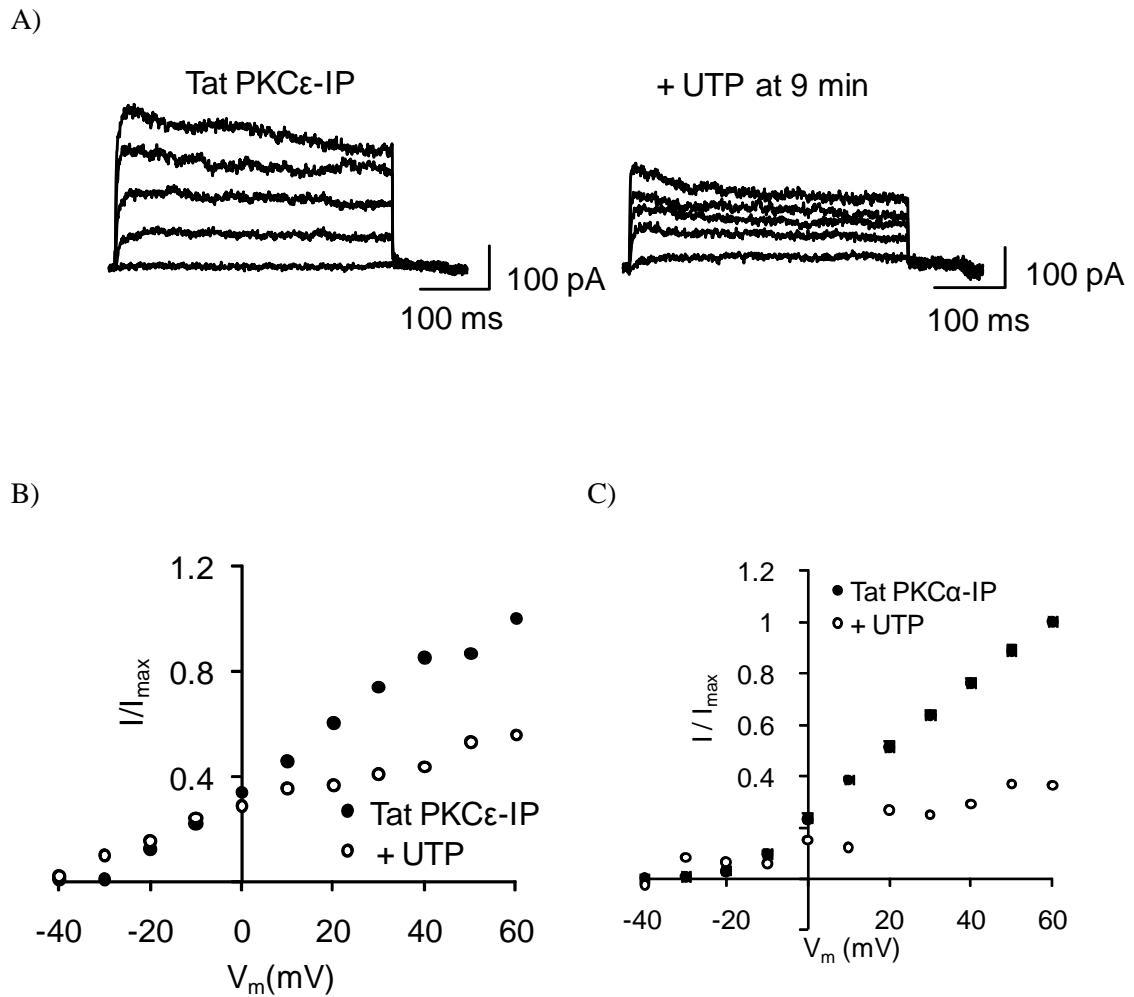


Fig: 4.9 Effect of Tat PKC-IP isoforms on UTP modulated Kv current.

Whole cell currents recorded from single cells pretreated with Tat PKC-IP for <10 min in the absence and presence of UTP (after 9 min). Voltage protocol is same as in figure 4.1A. For plotting I-V curve, mean currents obtained from 320 to 370 ms voltage pulses from -40 to 60 mV in Tat PKC-IP (●) and after 9 min perfusion of UTP (○). In each case, currents were normalized with the maximum control current at +60 mV.

A) Representative traces showing the effect of 50 nM Tat PKC ϵ -IP on Kv currents in the absence and presence of 100 μ M UTP (after 9 min);

B) Net I-V curve of Tat PKC- ϵ -IP (●) and after 9 min perfusion of UTP (○) (n=1);

C) Net I-V plot Tat PKC α -IP (●) and after 9 min perfusion of UTP (○). Data are the mean from 2 cells.

4.2.6 K_{ATP} current and UTP

K_{ATP} channels are widely distributed among smooth muscle cells and play an important role in vasodilation and regulation of vascular tone. Many vasodilators activate K_{ATP} channels whereas inhibition of K_{ATP} channels by vasoconstrictors causes constriction of the vasculature. The effect of UTP on K_{ATP} channels was investigated using whole-cell recording of steady-state K_{ATP} current.

K_{ATP} channel activity depends on the metabolic state of the cell and is generally increased by a fall in the intracellular concentration of ATP and a rise in ADP (Beech et al., 1993, Quayle et al., 1995, Nelson and Quayle, 1995). Therefore, to record K_{ATP} current from mesenteric arterial smooth muscle an intracellular pipette solution containing suitable proportions of intracellular metabolites was used. The pipette solution contained (mM): 110 KCl, 30 KOH, 1 MgCl₂, *3.9 CaCl₂, 10 EGTA, 10 HEPES, †1 Na₂ATP, †0.5 GTP, †0.1 ADP (*free Ca²⁺ was 100 nM; †added on the day of experiment and pH was adjusted to 7.2). Recordings were made at 29 to 30°C.

Steady-state K_{ATP} currents were recorded at -60 mV with symmetrical 140 mM K⁺ containing solutions, with 100 nM free Ca²⁺ in the pipette. These conditions minimized contamination by voltage-gated currents whilst giving a large, inwardly directed, electrochemical gradient for K⁺. Initially, sealing was done in 6 mM K⁺ external solution which was exchanged to 140 mM K⁺ solution soon after a whole-cell configuration was achieved. When the external K⁺ concentration was raised from 6 to 140 mM there was an increase in the inward current that reflected the increased driving force for K⁺ and the basal activity of K_{ATP} channels. Pinacidil (10 µM), a synthetic activator of K_{ATP} channels, was applied to increase the K_{ATP} current. Pinacidil activated current (e.g. 258 pA in figure 4.10) was quite stable for up to 10 minutes and thereafter

declined slowly. Glibenclamide, a sulphonylurea antidiabetic drug, is often used to isolate and characterize K_{ATP} currents because of its ability to selectively inhibit K_{ATP} channels. In my experiments I added 10 μM glibenclamide to check that the current observed was the K_{ATP} current. Currents were measured after subtracting the baseline current observed in glibenclamide. Currents were normalized with the maximum pinacidil activated current.

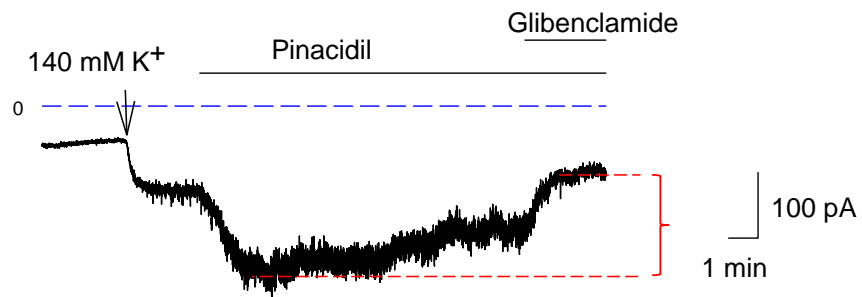


Fig: 4.10 Pinacidil activated K_{ATP} current.

Whole cell currents recorded from acutely isolated mesenteric arterial smooth muscle cell voltage clamped at -60 mV with 140 mM internal K^+ . The extracellular K^+ was raised from 6 to 140 mM at the point indicated by the arrow. Pinacidil (10 μM) and glibenclamide (10 μM) were applied as indicated by the bars. Pinacidil activated an inward current which was reversed by the addition glibenclamide. The bars indicate the estimated time the drugs reach the bath after subtracting the dead space. The top dashed line (blue) indicates the zero current level and the bottom dashed line indicates the pinacidil activated current.

4.3 Modulation of K_{ATP} current by UTP

The effect of UTP on the K_{ATP} current was assessed at -60 mV in symmetrical 140 mM K^+ with 100 nM free Ca^{2+} in the pipette; under these conditions ($E_K = 0$) the K_{ATP} current is inward. K_{ATP} channels were activated with 10 μ M pinacidil, as describe in section 4.3.6 above and 100 μ M UTP was then applied. As shown in figure 4.11, pinacidil (10 μ M) caused a significant activation of the K_{ATP} current, which reached a plateau (230 pA in the example traces shown in figure: 4.11A) within 30 - 60 seconds of application. The average current density at -60 mV in the presence of pinacidil was 204 ± 37 pA (n=7). Once the K_{ATP} current had remained stable for about 1 minute 100 μ M UTP was added. UTP caused a substantial inhibition of the pinacidil activated current and application of 10 μ M glibenclamide reduced the remaining current further (Fig. 4.11A). To quantify these effects the baseline current in glibenclamide was subtracted and all currents were then normalized to the maximum pinacidil induced current. Mean normalized currents are plotted in figure 4.11B. Pinacidil significantly activated the K_{ATP} current as expected, whereas UTP significantly reduced the K_{ATP} current to $15 \pm 7\%$ of the pinacidil value (n=8; ***P<0.0001).

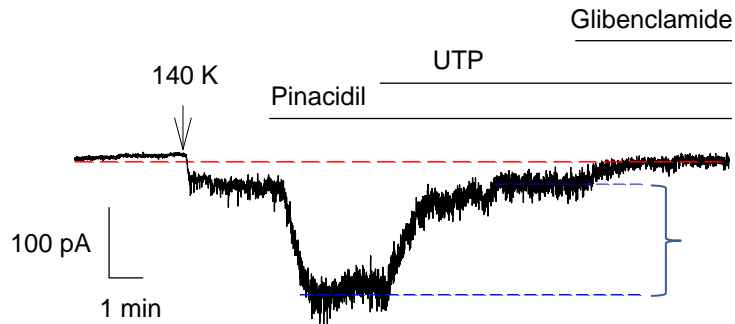
4.3.1 Effect of Ca^{2+} on K_{ATP} current modulation by UTP

K_{ATP} currents were recorded as described in section 4.2.6 and 4.3 with a slight change in the pipette solution. The free $[Ca^{2+}]_i$ was lowered from 100 nM to 20 nM (1mM Ca^{2+} and 10 mM EGTA). As shown in figure 4.12, the activation of the K_{ATP} current by pinacidil was relatively slow with 20 nM internal Ca^{2+} compared to that with 100 nM Ca^{2+} in the pipette solution. The effect of 100 μ M UTP was much less pronounced, reducing the pinacidil activated current to $77 \pm 2.9\%$ (n= 4; not significant). In low

internal Ca^{2+} , the effect of UTP was quite slow and maximum inhibition of the K_{ATP} current was only obtained several minutes after UTP application.

100 nM free Ca²⁺ internal solution

A)



B)

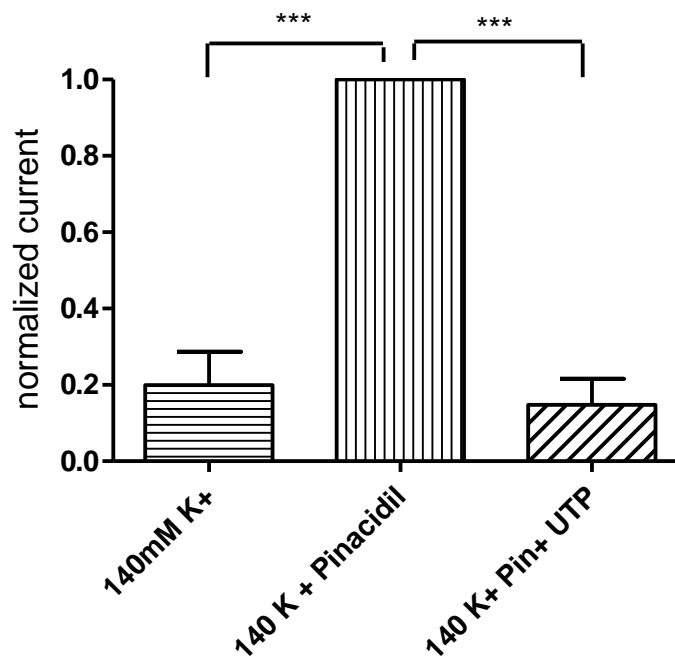
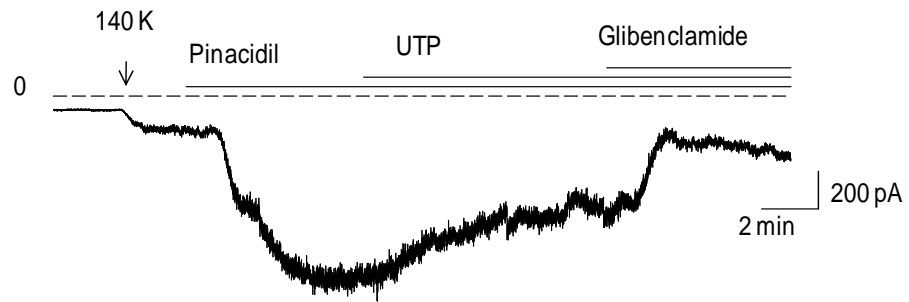


Fig: 4.11 K_{ATP} current modulation by UTP

UTP inhibits pinacidil (10 μ M) activated K_{ATP} currents in rat mesenteric arterial smooth muscle cells. Currents were recorded at -60 mV with a pipette solution containing 100 nM free Ca²⁺; A) An example trace showing the pinacidil activation of glibenclamide sensitive K⁺ currents in a mesenteric arterial smooth muscle cell. External 6 mM K⁺ was exchanged for 140 mM K⁺ at the time indicated by the arrow; all other drug applications are indicated by the bars. All currents were measured from the baseline current, taken as that in the presence of glibenclamide as indicated by the dashed horizontal red line. B) Currents normalized to those in the presence of pinacidil and plotted as a histogram. The fractional pinacidil induced current remaining in UTP was 0.15 ± 0.07 (n=8; ***P<0.0001).

A)



B)

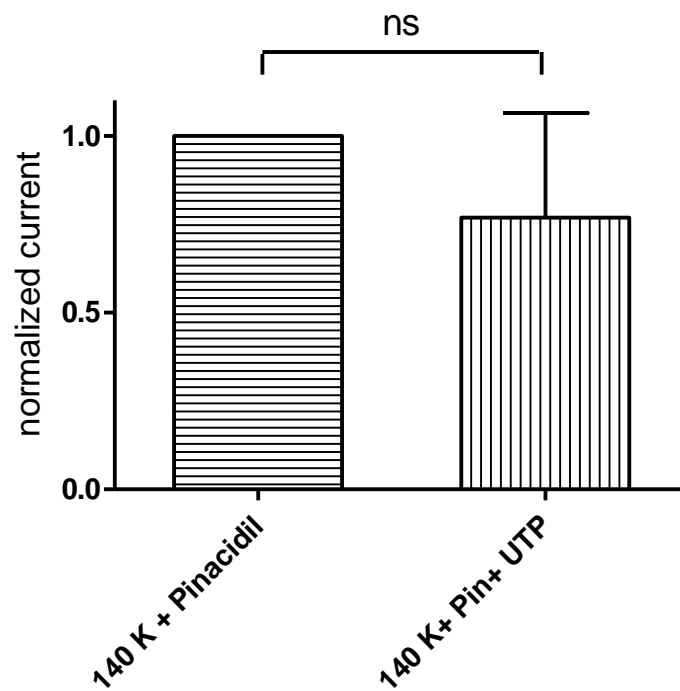


Fig: 4.12 K_{ATP} current modulation by UTP in low internal Ca^{2+} solution

Currents were recorded at -60 mV with a pipette solution containing 20 nM free Ca^{2+} .

A) An example trace showing the K_{ATP} current recording from mesenteric arterial smooth muscle cell. External 6 mM K^+ was exchanged for 140 mM K^+ at the time indicated by the arrow; all other drug applications are indicated by the bars. The dashed line shows the zero current level. All currents were measured from the baseline current measured in glibenclamide. B) Currents normalized to those in the presence of pinacidil and plotted as a histogram. The fractional amount of the pinacidil induced current remaining in 100 μ M UTP was 0.77 ± 0.29 ($n=4$). The effect of UTP was not significant.

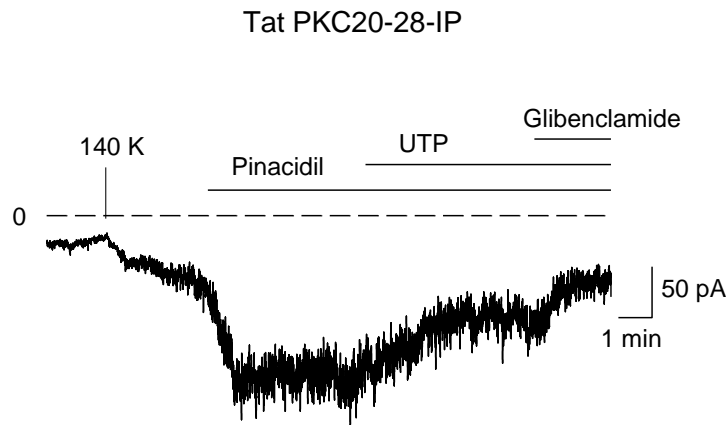
4.3.2 Does UTP modulate K_{ATP} current via PKC

To evaluate the role of PKC in K_{ATP} current modulation by UTP, mesenteric arterial smooth muscle cells were pretreated in 100 nM Tat PKC20-28-IP for more than 10 minutes. Figure 4.13A shows an example of a current recorded from a cell pretreated with Tat PKC20-28-IP (100 nM) at a holding potential of -60 mV and a pipette solution containing 100 nM free Ca^{2+} . After switching to an external 140 mM K^+ solution, pinacidil (10 μ M) was added to activate the K_{ATP} current further. It can be seen that addition of 100 μ M UTP was still able to suppress the K_{ATP} current and the remaining current was inhibited further by 10 μ M glibenclamide. As described previously, the currents in response to various drugs were measured and the basal current (with glibenclamide) was subtracted. These values are plotted as a fraction of the current in pinacidil current. As shown in figure 4.13B, there was no significant difference in UTP inhibition of K_{ATP} current between Tat-PKC20-28-IP treated and untreated cells (n=8 in each case).

To test whether the effect of Tat PKC20-28-IP on the inhibition of K_{ATP} current by UTP was dependent on intracellular $[Ca^{2+}]$ a similar set of experiments were done with a lower free $[Ca^{2+}]$ (20 nM) in the pipette. Although cells were pretreated with Tat-PKC20-28-IP, it was also included in the solutions during recording. As shown in figure 4.14, the inhibition of the K_{ATP} current by UTP was not significant in 20 nM Ca^{2+} and inclusion of Tat-PKC20-28-IP did not alter the effect of UTP.

100 nM free Ca²⁺

A)



B)

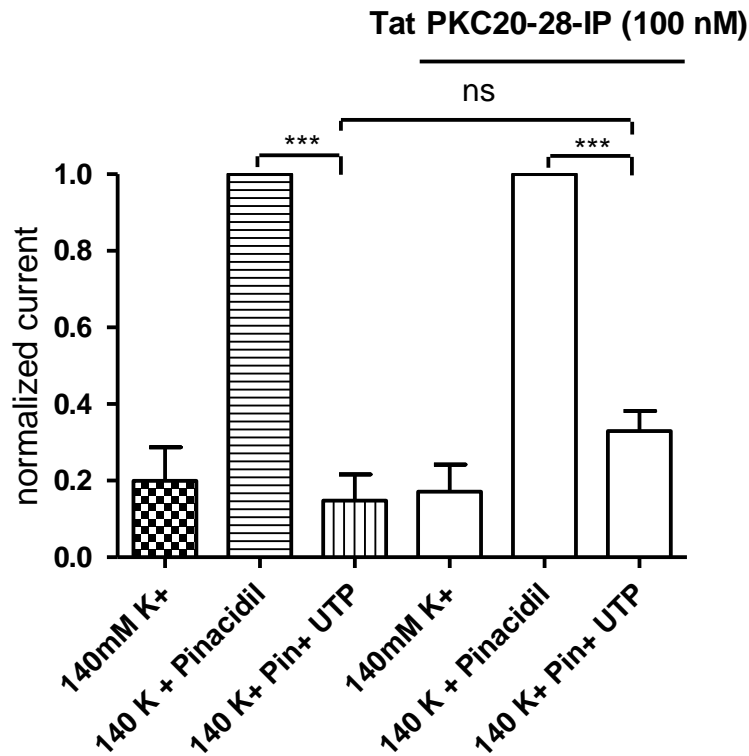


Fig: 4.13 Effect of Tat PKC20-28-IP on UTP modulated K_{ATP} current.

A) Example traces showing K_{ATP} current recorded from a cell pre-treated with Tat PKC20-28-IP (100 nM) for more than 10 minutes. The pipette solution contained 100 nM free Ca²⁺. All drugs were applied as indicated by the bars and the arrow indicates the exchange of 6 mM K⁺ with 140 mM K⁺; B) Histogram of the currents normalized to the maximum current in pinacidil in response to various drugs in the absence and after pre-treatment with Tat PKC20-28-IP (n =8 in each case). No significant difference was observed in the suppression of K_{ATP} current by UTP before and after treatment of Tat PKC20-28-IP.

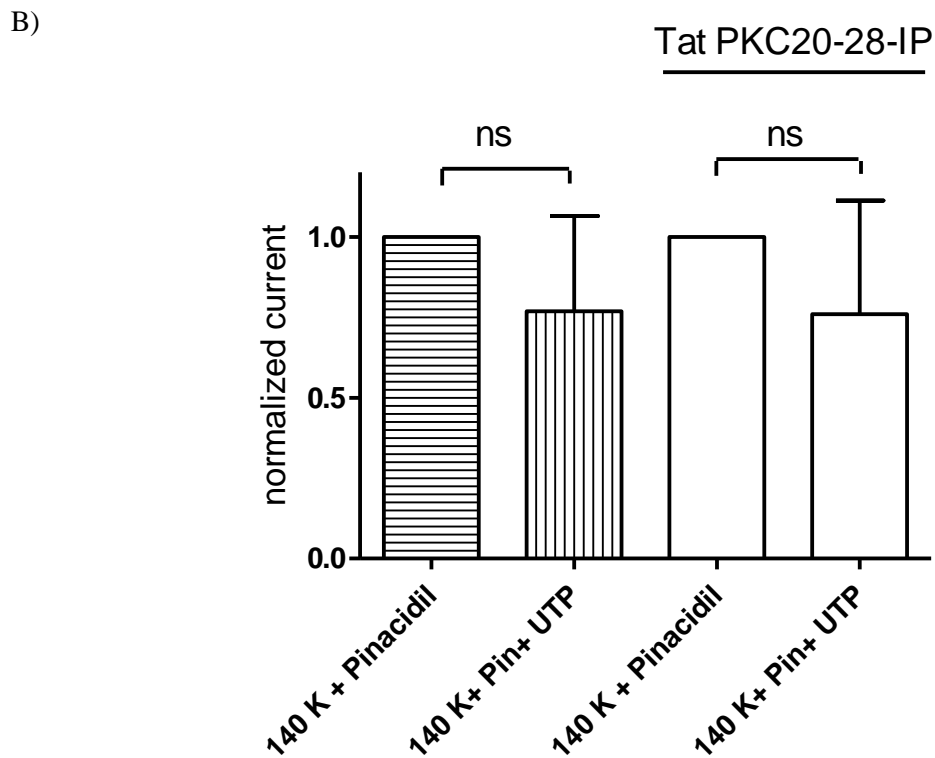
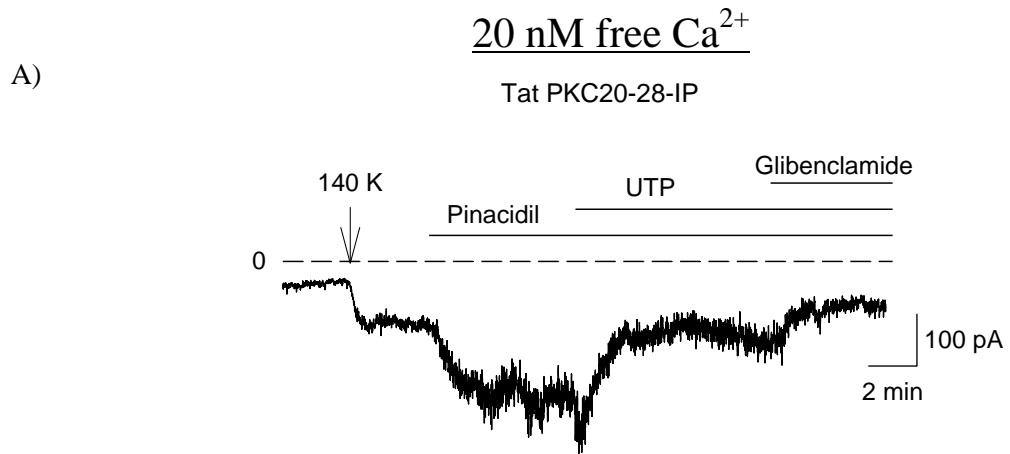


Fig: 4.14 Effect of Tat PKC20-28-IP on UTP inhibited K_{ATP} current.

A) Example traces showing K_{ATP} current recorded from a cell pre-treated with Tat PKC20-28-IP (100 nM) for more than 10 minutes. The pipette solution contained 20 nM free Ca²⁺. All drugs were applied as indicated by the bars and the arrow indicates the exchange of 6 mM K⁺ with 140 mM K⁺. The holding potential was -60 mV.

B) Histogram showing the effect of Tat PKC20-28-IP (n=3) on UTP inhibited K_{ATP} current in the absence (n=5) and presence of Tat PKC20-28-IP. There was no significant difference between Tat PKC20-28-IP treated (n=3) and untreated cells (n=4).

4.4 Nonselective cation current evoked by UTP

The isometric contraction of mesenteric arteries in response to UTP was effectively blocked by the trivalent cation Gd^{3+} (see section 3.3.7), which is a widely used blocker of non-selective cation channels (Hill et al., 2006). Whole-cell recordings were made to evaluate whether UTP activated non-selective cation channels in isolated mesenteric artery smooth muscle cells.

Whole cell steady state currents were recorded from mesenteric arterial smooth muscle cells voltage clamped at -65 mV with an external $[K^+]$ of 6 mM and a pipette solution containing 140 mM Cs^+ instead of K^+ and a free $[Ca^{2+}]$ of 100 nM. Cs^+ was used internally because it will minimize K^+ currents yet is able to pass through the non-selective channel (Hill et al., 2006). As shown in Fig. 4.15, at a holding potential of -65 mV UTP (100 μ M) induced a noisy inward current that was blocked on addition of Gd^{3+} (10 μ M, Fig 4.15A & B).

To evaluate the characteristics of this inward current further, 400 ms ramps from -100 to +30 mV and back were applied at regular intervals from a holding potential of -60 mV (figure 4.16A). The cells were bathed in 6 mM K^+ for control recordings and 100 μ M UTP was applied after several control ramps were recorded. The UTP induced current was obtained by subtracting the mean ramp current in the absence of UTP from that in its presence, as shown in Fig.4.16. The current was normalized to cell capacitance and the resulting I-V relationship was that of the UTP induced current. The current reversed around 0 mV and showed inwardly rectifying properties similar to that reported previously for this type of current (Hill et al., 2006, Helliwell and Large, 1997, Alvarez et al., 2008).

The effects of gadolinium on ion channels other than non selective cation channels were also studied to ascertain the blocking effects of gadolinium to K_v and K_{ATP} channels. To study the effects of gadolinium on K_{ATP} channels steady state currents were recorded from mesenteric arterial smooth muscle cell at -65 mV using 20 nM free Ca²⁺ in the pipette solution. Penitrem A was also included in the external solution to block BK channels. As described before, when measuring K_{ATP} current pipette sealing was done in 6 mM [K⁺] and this was raised to 140 mM [K⁺] once the whole-cell configuration was established. Following activation of K_{ATP} currents by 10 μM pinacidil application of 10 μM Gd³⁺ significantly inhibited this pinacidil activated current to 62 ± 7% of control (n = 3; *P < 0.05) as shown in Fig. 4.17.

The effect of Gd³⁺ on the K_v current in these cells was also assessed. K_v currents were induced by 400 ms depolarizing steps from -40 to +60 mV in 10 mV increments from a holding potential of -65 mV. K_v currents were recorded in control (6 mM K⁺) and in the presence of 10 μM Gd³⁺ (Fig 4.18A). Mean currents measured from -60 to +40 mV were normalized to their cell capacitance and plotted to give an I-V relation. A comparison of the I-V relations revealed no significant difference in control and in presence of Gd³⁺.

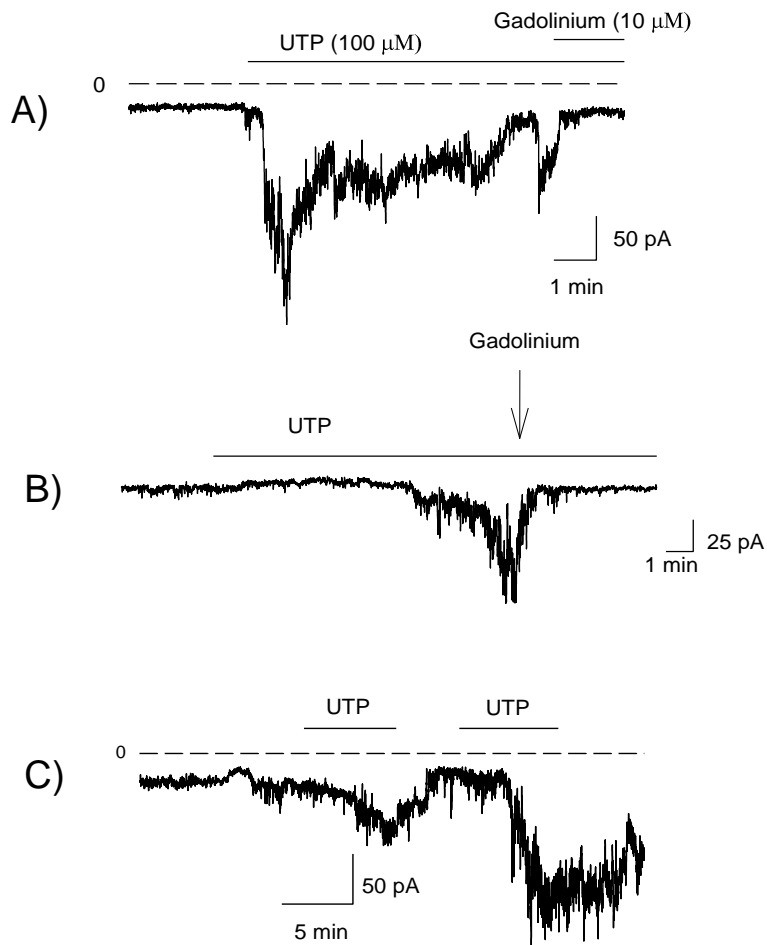


Fig: 4.15 Effect of UTP on nonselective cation channels

Mesenteric arterial smooth muscle cells were clamped at -65 mV and whole-cell recordings were obtained with an external $[K^+]$ of 6 mM and a pipette solution containing 140 mM Cs^+ instead of K^+ and a free $[Ca^{2+}]$ of 100 nM (using 10 mM EGTA as a chelator). Penitrem A was added to the external bath solution to prevent activation of BK channels. A) Steady-state current recorded at -65 mV; application of UTP (100 μ M) induced an inward current that was reversed by Gd^{3+} (10 μ M); B) Another trace showing an inward current induced by UTP (100 μ M) that was reversed by Gd^{3+} (10 μ M); C) Trace showing repeated applications of UTP induced inward currents.

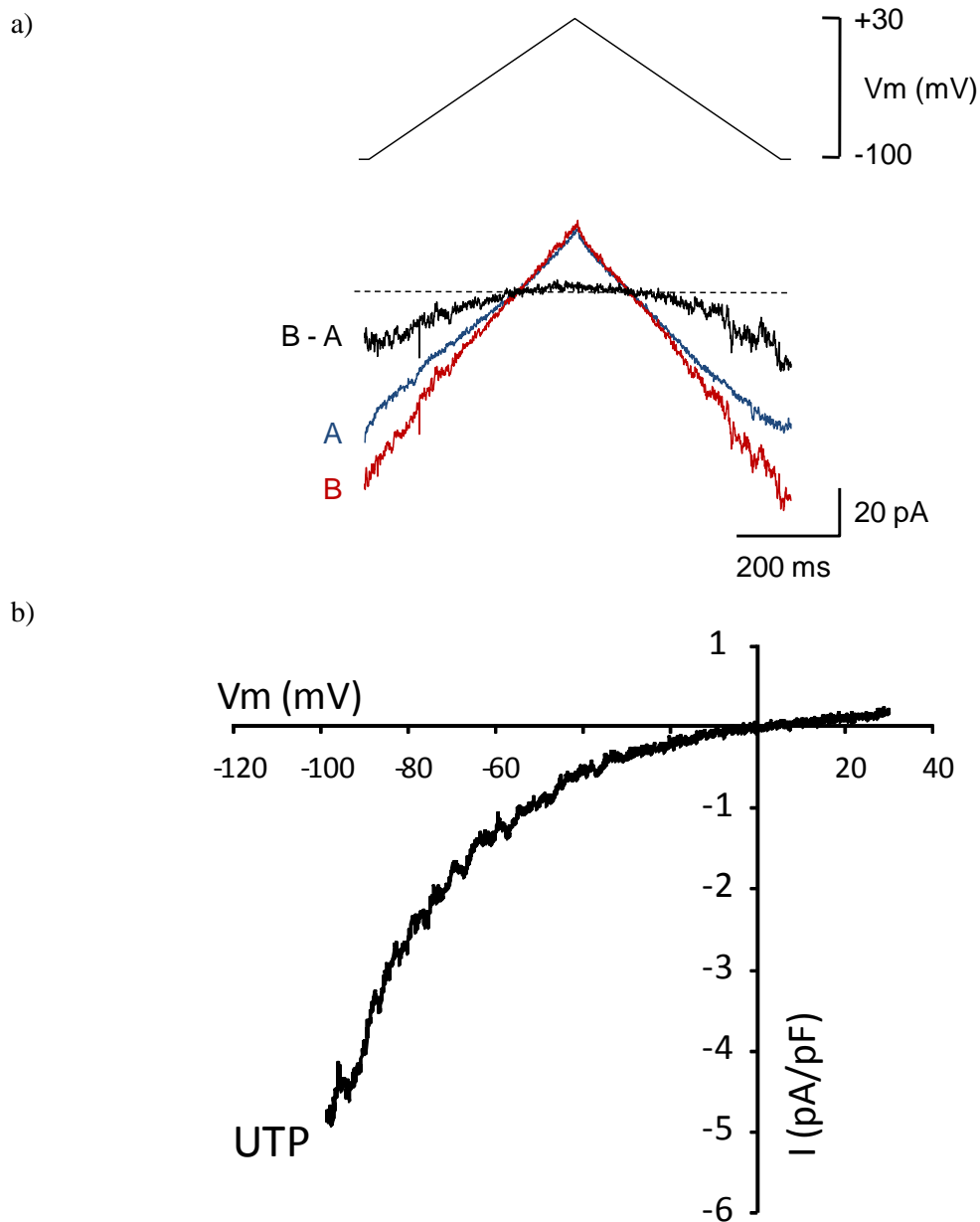
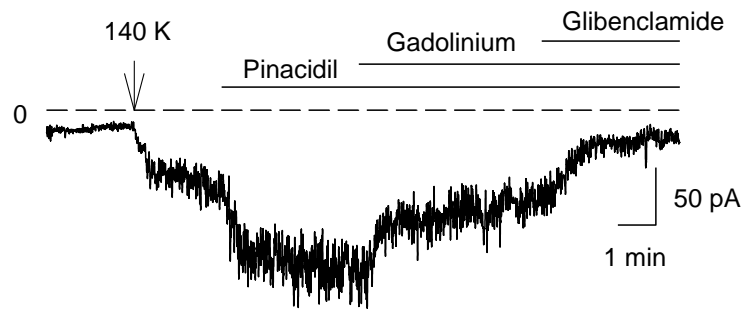


Fig: 4.16 UTP induced non selective cation current

a) Whole-cell currents elicited in response to voltage ramps from -100 to +30 mV and back as indicated by the protocol (top). Control currents and those in the presence of 100 μM UTP are shown in A and B respectively. The current activated by UTP was given by B-A as indicated.

b) Net I-V relationship of the mean UTP activated current from two cells obtained by averaging the current produced by 0.4 s ramps from -100 to +30 mV after subtracting the mean ramp current in the absence of UTP from that obtained during the UTP induced current.

A)



B)

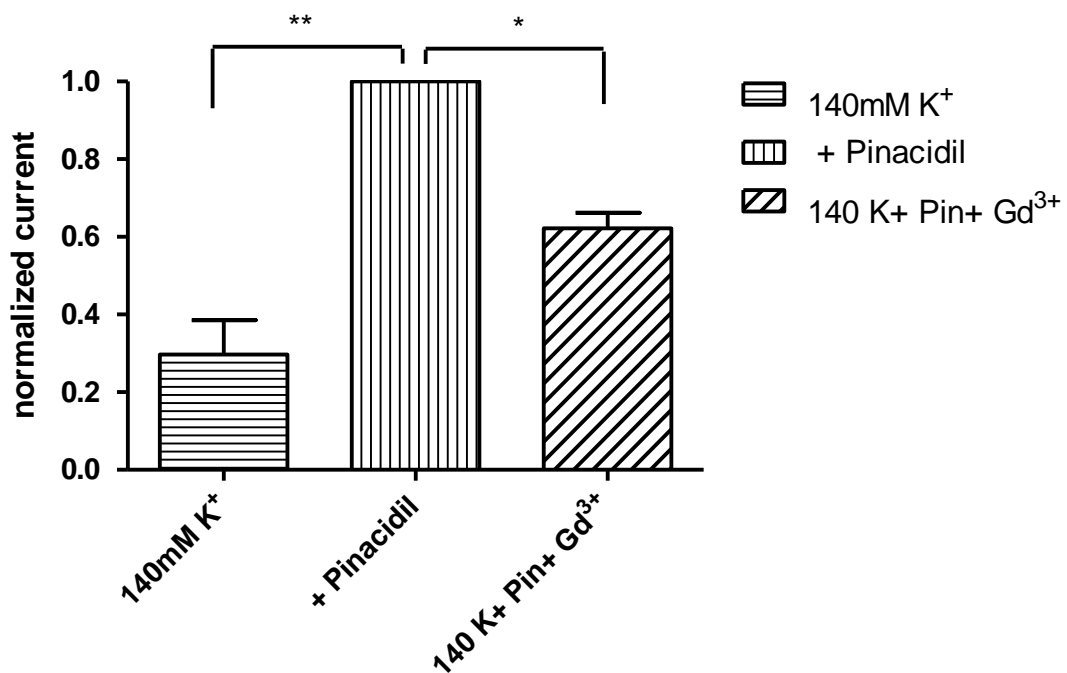
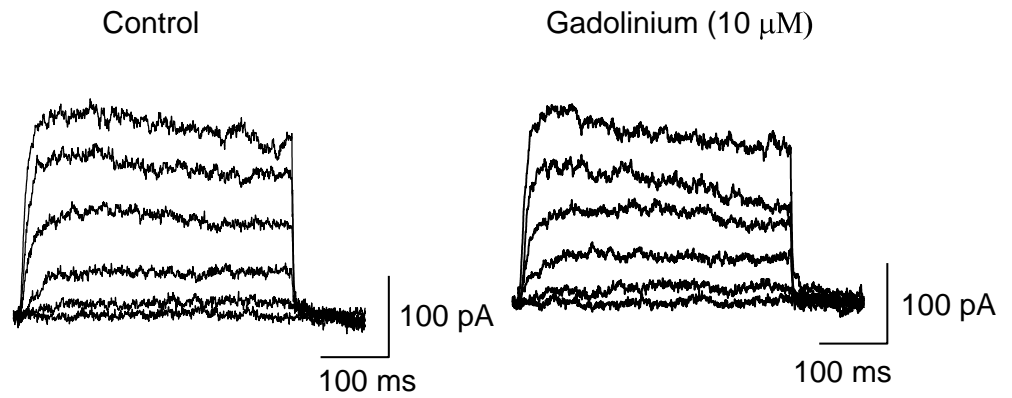


Fig: 4.17 Effect of gadolinium on K_{ATP} channels

The effect of gadolinium on K_{ATP} current was recorded from mesenteric arterial smooth muscle cells held at -65 mV; A) Whole cell steady state currents were recorded from cell with a pipette solution containing 140 mM K⁺ and a free [Ca²⁺] of 20 nM. Penitrem A was added to the external bath solution to prevent activation of BK channels. The current was recorded with 6 mM K followed by addition of 140 mM K as indicated by the arrow. Gadolinium (10 μM) reduced the pinacidil activated current and glibenclamide reversed the residual current to baseline. The glibenclamide sensitive current was taken as the baseline current and all the currents were measured from this baseline and normalized to the pinacidil activated current; B) Histograms showing the effect of gadolinium (10 μM) on the current in the presence of pinacidil. The mean fractional current remaining in 10 μM gadolinium was 0.62 ± 0.07 (n = 3; *P < 0.05).

A)



B)

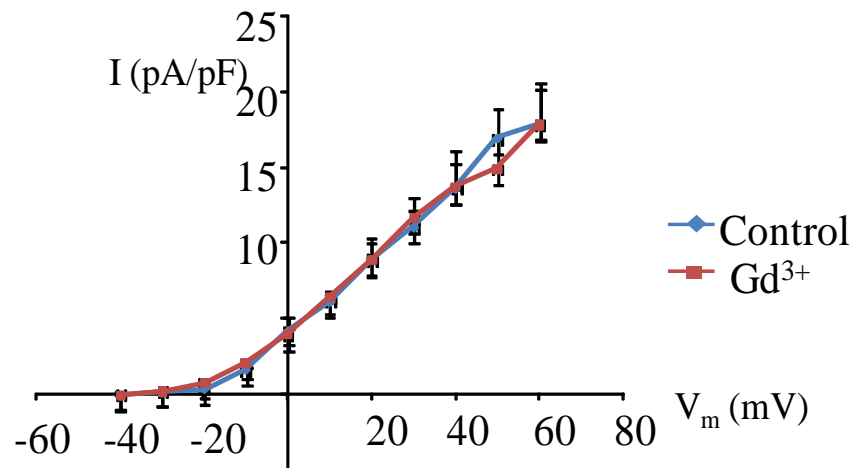


Fig: 4.18 Effect of gadolinium on Kv currents.

A) Kv currents recorded from a single cell held at -65 mV in control and after addition of gadolinium ($10 \mu\text{M}$). Currents were recorded from by applying 400 ms voltage pulses between -40 to $+60$ mV. The external solution contained 6 mM K^+ and the pipette solution contained $100 \text{ nM free Ca}^{2+}$. Penitrem A was included in the external solution to inhibit BK currents.

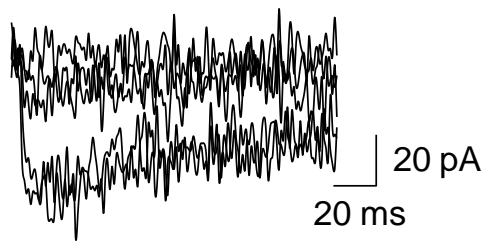
B) Mean I-V curves were constructed from currents measured between 320 and 370 ms of each pulse and normalized to cell capacitance ($n = 3$).

4.5 Isolation of voltage gated Ca^{2+} current

An attempt was made to measure voltage gated calcium currents from single smooth muscle cells enzymatically isolated as described in the methods chapter. The smooth muscle cells were voltage clamped at -60 mV and recordings were done in external solution containing 10 BaCl_2 and internal solution containing 140 mM Cs^+ and 100 nM free Ca^{2+} . The internal Cs^+ virtually abolished all outward K^+ currents and using Ba^{2+} as a charge carrier maximized any currents flowing through Ca^{2+} channels.

Whole cell currents were recorded from cells by applying 150 ms voltage pulses from -40 to +50 mV from a holding potential -65 mV. Most cells investigated had no detectable Ba^{2+} current and in the few cells where I observed a current it was very small (see Fig. 4.19). For this reason I did not pursue this any further.

A)



B)

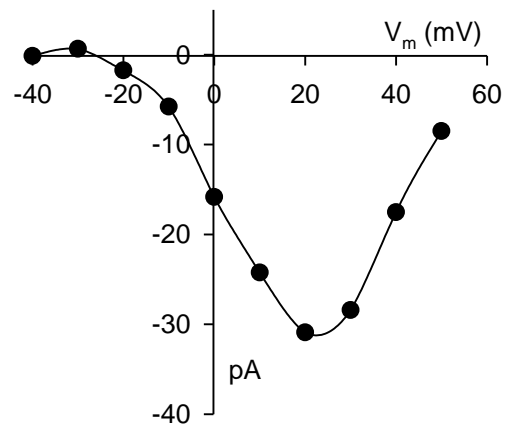


Fig: 4.19 Voltage gated Ca^{2+} channel activation.

A) Trace showing whole cell Ba^{2+} currents recorded from a mesenteric arterial smooth muscle cell. Depolarizing voltage steps were given from -40 to +50 mV from a holding potential of -65 mV.

B) Plot of the I-V relationship for the cell shown in part (A). A maximum inward current of -30 pA was obtained at +20 mV.

4.6 Discussion

4.6.1 Kv current and effect of UTP

Whole cell voltage gated potassium (Kv) currents recorded from mesenteric arterial smooth muscle cells were suppressed by UTP at depolarizing voltages. The outward potassium current in control recordings was quite stable over time with a slow current rundown occurring after 12-15 minutes. Because of the presence of a BK channel blocker there was no contamination of the Kv currents with BK channel activity so the resulting current modulated by UTP under these conditions was the Kv current only. In rat cerebral arteries, Luykenaar reported a similar inhibition of smooth muscle Kv currents by UTP (Luykenaar et al., 2004). The amount of inhibition of the Kv current by UTP was reduced by the PLC blocker, U73122, suggesting a role for PLC activation, although it must be stressed that U73122 also unexpectedly reduced the contractile response to 60 mM K⁺ observed in my myography experiments. I also observed that U73122 inhibited the Kv current itself to some extent.

It was an interesting observation that in the virtual absence of free Ca²⁺ in the pipette (10 mM EGTA, no added Ca²⁺) UTP was unable to inhibit the Kv current. A similarly small reduction in the Kv current by UTP persisted when the free Ca²⁺ concentration in the pipette solution was increased to 20 nM. However, raising free [Ca²⁺] in the pipette to 100 nM resulted in pronounced inhibition of Kv currents by UTP. This Ca²⁺ dependence of modulation of Kv channels by UTP indicates that UTP is likely to be more effective at inhibiting K⁺ currents when the intracellular [Ca²⁺] is raised, such as during a high state of myogenic tone.

Kv channels contribute to the regulation of membrane potential in several arterial beds as shown by an increase in vessel tone following application of Kv channel blockers such as 4-AP (Cole et al., 1996, Prior et al., 1998, Shimoda et al., 1998, Cox, 2005). These channels open as a result of depolarization and their role could be to limit the extent of depolarization thereby limiting contraction. Many vasoconstrictors such as Ang-II and ET-1 have been shown to inhibit potassium channels, including Kv channels, via PKC dependent mechanisms (Rainbow et al., 2009, Xiao et al., 2003). However, UTP induced contraction was partially dependent on the inhibition of Kv current via a PKC independent Rho kinase pathway in rat cerebral arteries (Luykenaar et al., 2004). Luykenaar et al (2004) demonstrated that the PKC inhibitors calphostin C and bisindolylmaleimide I, failed to inhibit the K_v current modulation by UTP whereas a Rho kinase inhibitor (Y-27632) inhibited this modulation in rat cerebral arterial smooth muscle cells. They, therefore, argued that instead of PKC the small GTP RhoA / Rhokinase is involved in UTP modulation of Kv current in rat cerebral arteries.

In this study the role of PKC in mediating the inhibition of mesenteric artery Kv currents by UTP was investigated using several cell permeable Tat-linked PKC inhibitor peptides. These Tat linked peptide inhibitors are more selective and isoform specific, and due to their linkage with Tat peptide 47-57 possessed the ability to cross the hydrophobic lipid bilayer. Within the cell the internal reducing environment causes the cleavage of the bonding between the Tat peptide and its cargo PKC inhibitor protein. Our lab demonstrated the effectiveness of these Tat linked PKC peptide inhibitors at distinguishing between the PKC isoforms involved in the modulation of Kv current by ET-1 and Ang-II (Rainbow et al., 2009). Pretreatment of cells with Tat linked PKC peptide inhibitors for more than 10 minutes was shown to be sufficient to enable

effective accumulation of PKC inhibitor peptides within the cells (Rainbow et al, 2009). Based on the observation that UTP inhibition of Kv current appeared unaffected by these PKC inhibitors it is unlikely that PKC has a major role in the modulation of the Kv current by UTP in mesenteric artery smooth muscle cells. Hence my results in rat mesenteric arterial smooth muscle agree with those reported by Luykenaar et al (2004) that UTP modulation of Kv currents depends on a pathway other than PKC, possibly a Rho-kinase pathway and this needs to be explored further in mesenteric arteries.

4.6.2 K_{ATP} current and UTP

UTP also inhibited the pinacidil activated K_{ATP} current in rat mesenteric smooth muscle cells. The inhibition of the K_{ATP} current was dependent on free $[Ca^{2+}]$ in the pipette solution. With 100 nM free Ca^{2+} the UTP reduced the current to $15 \pm 7\%$ of the control value, but with only 20 nM Ca^{2+} in the pipette the reduction was only to $77 \pm 2.9\%$ of the control and was not significant.

As is the case with vascular Kv channels, K_{ATP} channels are also inhibited by several vasoconstrictors in a PKC dependent manner (Hayabuchi et al., 2001a, Kubo et al., 1997, Standen and Quayle, 1998, Moon et al., 2004, Ko et al., 2008). However, as was the case with the Kv current inhibition by UTP, the inhibition of the K_{ATP} current by UTP was also insensitive to PKC inhibition by the Tat-linked PKC20-28-IP, either in 100nM or in 20 nM free internal Ca^{2+} . It should be noted that these Tat-linked peptide inhibitors are effective at blocking the ET-1 and Ang II induced reduction of both Kv and K_{ATP} currents in this preparation (Rainbow et al., 2009).

Like the Kv inhibition, K_{ATP} channel modulation by UTP was also dependent on intracellular Ca^{2+} which suggests that UTP is more likely to inhibit the potassium

channels under conditions where the concentration of Ca^{2+} is high. It is likely that a Ca^{2+} dependent signaling pathway is involved in UTP modulation of both K_v and K_{ATP} channels. However, inhibition of Ca^{2+} dependent PKC isoforms were generally ineffective, thus it could be proposed that Ca^{2+} dependent RhoKinase signaling might be involved.

4.6.3 NSCC current and UTP

Since Gd^{3+} , a known blocker of non-selective channels (Hill et al., 2006), was effective at blocking the contraction induced by UTP the ability of UTP to activate non-selective cation current was investigated. In these experiments K^+ was replaced by Cs^+ which would block K^+ currents but permeate non-selective channels (Albert et al., 2003, Hill et al., 2006). As shown in the results section, UTP did induce a current with properties similar to those reported previously for a non-selective current (Alvarez et al., 2008). The I-V relation of the current, obtained using voltage ramps, reversed close to 0 mV and displayed a fairly marked inward rectification (Fig.4.16) and steady-state recordings of the current at -60 mV were blocked by the application of Gd^{3+} . The activation of this current, however, was quite variable and often transient.

The blocking effects of Gd^{3+} on K_v and K_{ATP} currents were also studied and although Gd^{3+} had no significant effect on K_v currents it did inhibit K_{ATP} current by nearly 40%.

4.6.4 Voltage gated Ca^{2+} current

These channels respond to membrane depolarization and mediate calcium influx resulting in an inward current. Voltage gated calcium channels play important roles in several intracellular processes including smooth muscle contraction. I attempted to investigate the effects of UTP on these channels but I found that the ability to observe

Ca²⁺ channel currents, even with 10 mM Ba²⁺ as the charge carrier, was too unreliable. In my preliminary experiments, I did manage to record whole cell inward currents Ba²⁺ currents but was unable to test the effect of UTP on these currents.

Chapter 5 Overall Discussion

5.1 Discussion

The work presented in this thesis was focused on investigating the possible mechanisms leading to UTP induced contraction in rat mesenteric arteries. UTP is not only a building block of cellular RNA but also acts as an extracellular signaling molecule and plays an important role in conditions such as migraine and hypertension (Lazarowski and Boucher, 2001). Extracellular UTP triggers a signaling cascade by activating membrane bound P2Y receptors that are members of the G protein coupled receptor family. UTP, ATP and ADP are secreted from platelets, neuronal and endothelial cells (Daniel et al., 1998). In the cardiovascular system, UTP is secreted from endothelial cells during ischemia and hypoxia (Erlinge et al., 2005).

In the vasculature UTP is released to the luminal side of the blood vessel and has little or limited interaction with the intact smooth muscle cells that are wrapped in the layers of the walls of the vessel. However, as a result of inflammation or disruption of the endothelial cells, UTP has access to the smooth muscle cells and thereby causes vasoconstriction (Boarder and Hourani, 1998). Because of the role of UTP in subarachnoid hemorrhage and migraine (Lazarowski and Boucher, 2001) many research groups have focused their attention on understanding the mechanisms whereby UTP induces contraction of cerebral arteries (Jaggar and Nelson, 2000, Lacza et al., 2001, Marrelli et al., 1999, Ralevic and Burnstock, 1991, Schilling et al., 1995, Sugihara et al., 2011, Sy Yong et al., 2009, Zhao et al., 2008). However, less work has been done investigating the contraction produced by UTP in other vascular beds. The research I have presented in this thesis was focused on understanding the range of possible

mechanisms leading to the UTP induced contraction of rat mesenteric arterial smooth muscle.

5.1.1 UTP induced contraction depends largely on extracellular Ca^{2+} influx

UTP is a ligand for P2Y receptors and in smooth muscle these are likely to be P2Y₂ and possibly P2Y₄ and P2Y₆ receptors (Bultmann et al., 1999, Buvinic et al., 2002, Chootip et al., 2005, Gitterman and Evans, 2000, Harper et al., 1998, Hill and Sturek, 2002, Kumari et al., 2003, Morris et al., 2010, Erlinge et al., 2005). However, a recent report suggests the possibility of a dual signaling pathway leading to vasoconstriction by UTP in rat aorta, where UTP activates P2X₁-like receptors in addition to P2Y receptors (Sugihara et al., 2011). If the P2Y receptors are located on the endothelial cells, nucleotides causes a relaxation of the blood vessels, otherwise, if they are located on smooth muscles then contraction occurs (Miyagi et al., 1996).

In my experiments I found UTP to be a potent vasoconstrictor that induced a sustained and concentration-dependent contraction of mesenteric arteries. The vasoconstriction induced by 100 μM UTP was reproducible even after several applications.

UTP induced contraction was abolished in the absence of extracellular Ca^{2+} , however, contraction was restored upon returning Ca^{2+} to the bath solution. As expected, the contraction evoked by 60 mM K^+ , which occurs because of membrane depolarization, was also completely abolished in the absence of Ca^{2+} . UTP induced contraction that is largely due to Ca^{2+} influx has been reported previously in mesenteric arteries (Juul et al., 1992).

5.1.2 Voltage gated Ca^{2+} channels are partly involved in UTP induced contraction

Agonist induced contraction often depends on depolarization of the membrane potential and Ca^{2+} influx from the extracellular space either through voltage gated Ca^{2+} channels or non-selective cation channels (Horowitz et al., 1996, Khalil and van Breemen, 1988, Le et al., 1993). Some vasoconstrictors, including noradrenaline, have the ability to increase the open probability of voltage gated Ca^{2+} channels (Horowitz et al., 1996). Noradrenaline activates L-type current only in rabbit mesenteric arterial smooth muscle cells and was unable to modulate the T- type Ca^{2+} current (Helliwell and Large, 1997). To examine possible Ca^{2+} influx pathways contributing to UTP induced contraction I focused my research on investigating the roles of L-type Ca^{2+} channels and non-selective cation channels in this response. Electrophysiological studies on smooth muscle cells have revealed two major components to the Ca^{2+} current, namely L- and T-type Ca^{2+} channels (Horowitz et al., 1996). Currents flowing through these channels can be distinguished by their activation and inactivation profiles. The T-type current activated differentially than L-type currents and activated as well as inactivated at more negative potentials(Horowitz et al., 1996) (Benham et al., 1987). Both L- and T- type channels are blocked by cadmium, however, the L-type Ca^{2+} channel is much more sensitive to dihydropyridines, benzothiazepines, and phenylalkylamines (Bean et al., 1986, Loirand et al., 1986, Benham et al., 1987). In my experiments cadmium effectively blocked the UTP induced contraction by 81%; whereas application of the diltiazem (benzothiazepine) reduced the contraction by 41% only. However, Diltiazem significantly blocked the 60 mM K^+ induced contraction within same experimental conditions. Despite the differential results it appears that UTP induced contraction partly depends voltage gated Ca^{2+} channels. Similar results have been reported for rat

cerebral arteries where UTP induced contraction is only partly dependent on depolarization and activation of voltage gated Ca^{2+} channels (Luykenaar et al., 2004).

5.1.3 UTP mediates contraction via PLC activation

The phospholipase C signaling pathway is often the initial trigger of a vasoconstrictor induced contraction in vascular smooth muscle (Clarke et al., 2008b) (Delarue et al., 2005, Montmayeur et al., 2011). UTP activates P2Y receptors and possibly the P2Y₂ receptor in mesenteric arteries which is a Gq linked receptor that activates PLC (Iwamuro et al., 1999) with the subsequent formation of IP₃ and DAG from PIP₂. UTP has been shown to increase the concentration of intracellular Ca^{2+} and IP₃ levels in mesenteric artery smooth muscle cells (Nelson et al., 2008, Morris et al., 2010).

Phospholipase C (PLC) is a family of 11 isoenzymes and in vascular smooth muscle β_1 , β_2 , δ_1 , and γ_1 have been identified (Hyun et al., 2002). To ascertain whether UTP activates PLC in mesenteric arteries I examined the effect that pharmacologically inhibiting PLC had on the UTP induced contraction. The blocker I used was U73122 which has been used frequently to dissect out the role of PLC in agonist stimulated signaling (Peppiatt-Wildman et al., 2007). Both UTP and 60 mM K^+ induced responses were significantly blocked after pre-incubating mesenteric arteries with 10 μM U73122. The block of the UTP response is in agreement with the hypothesis that UTP activates PLC via activation of a Gq linked receptor; however, the inhibition of the 60 mM K^+ induced contraction by U73122 was unexpected and suggests the possibility that U73122 has effects additional to blocking PLC.

Agonist stimulated Ca^{2+} release from internal stores following IP₃ formation is often characterized by Ca^{2+} waves and Ca^{2+} oscillations (Berridge, 2008). Jaggar et al

investigated UTP induced contraction and its relationship with Ca^{2+} sparks and Ca^{2+} waves and reported that UTP increases the frequency of calcium waves in rat basilar arteries whereas it inhibits Ca^{2+} spark frequency in the same tissue (Jaggar and Nelson, 2000).

5.1.4 Is PKC involved in generating the UTP induced contraction?

Protein kinase C, a family of related isoenzymes, plays an important role in agonist induced contraction by various mechanisms including increasing the sensitivity of the myofilaments to intracellular Ca^{2+} (Khalil, 2010, Khalil and van Breemen, 1988, Salamanca and Khalil, 2005) and inhibiting K^+ channels leading to depolarization (Khalil, 2010, Khalil and van Breemen, 1988). PKC catalyzes the phosphorylation of the regulatory protein CPI-17 to increase the sensitivity of the contractile filaments by suppressing the activity of MLC phosphatase and increases vascular smooth muscle contraction (Kanashiro and Khalil, 1998, Khalil, 2010, Khalil and van Breemen, 1988). Activation of PKC α is reported to phosphorylate a regulatory protein, calponin, that is a thin filament protein associated with actin and is involved in the regulation of smooth muscle contraction (Kaneko et al., 2000, Nagumo et al., 1994, Parker et al., 1994, Winder et al., 1998, Winder and Walsh, 1993, Winder et al., 1993). PKC mediated phosphorylation of the calponin could also enhance vascular smooth muscle contraction (Bi et al., 2005, Patil et al., 2004, Sohn et al., 2001, Somara and Bitar, 2008, Tani and Matsumoto, 2004, Woodsome et al., 2001).

Because of the potential role of PKC in UTP stimulated contraction, I studied UTP induced contraction in rat mesenteric arteries using a range of PKC inhibitors. Unfortunately, the results obtained with different PKC inhibitors were very mixed

making it difficult to reach any conclusions about the involvement of PKC in UTP induced contraction. A commonly used PKC inhibitor, chelerythrine, was used initially and this reduced the UTP induced contraction significantly. Since chelerythrine, reduced the 60 mM K⁺ induced contraction also, a more specific blocker of PKC was used. Gö6983 is another broad spectrum PKC inhibitor that inhibits the isoforms PKC α , PKC β , PKC γ , PKC δ , PKC ζ and PKC μ with IC₅₀ values of 7, 7, 6, 10, 60 and 20000 nM respectively (Gschwendt et al., 1996). Gö6983 (1 μ M) significantly blocked the UTP induced contraction by more than 50% in 3 mesenteric arterial segments without any effect on 60 mM K⁺ induced contraction, suggesting a role for at least one of the isoforms of PKC blocked by Gö6983.

To investigate the role of PKC in more detail I used a range of peptide inhibitors, many of which target specific PKC isoforms (Rainbow et al., 2009). PKC20-28 is a pseudosubstrate sequence that acts as a PKC inhibitor. Pretreatment of arterial segments with a cell permeable form of this peptide PKC inhibitor, myristoylated-PKC20-28-IP only inhibited the UTP induced contraction by 28.8%. PKC20-28-IP has been used previously in our lab to block PKC sensitive modulation of K⁺ currents in mesenteric smooth muscle cells (Hayabuchi et al., 2001a, Hayabuchi et al., 2001b, Rainbow et al., 2006).

To further investigate the role of PKC in UTP induced contraction I used an alternative Tat peptide-mediated method of making the PKC inhibitor peptides cell permeable (Brooks et al., 2005). In this method the PKC inhibitor peptides were conjugated with the HIV Tat-derived peptide (47-57) using disulphide conjugation at the N terminal of the cysteine residues (Rainbow et al., 2009). Only very low concentrations of this

carrier Tat peptide is required to translocate into the cell and in the reducing environment of the cell the conjugated peptide is released thereby accumulating the unconjugated PKC inhibitors in the cell (Rainbow et al., 2009, Brooks et al., 2005). Linking the PKC inhibitor peptides with the Tat peptide sequence was done by Dr. R.I. Norman of the Department of Cardiovascular Sciences at the University.

The effects of the myristoylated PKC20-28-IP (40 μ M) as well as its Tat linked chimera Tat-PKC20-28-IP (100 nM) reduced the UTP induced contraction by a similar amount, 21% and 17 % respectively. Under the same conditions the Tat-PKC20-28-IP reduced the ET-1 induced contraction by 40%, suggesting that PKC has a smaller role in the UTP induced contraction.

Among various PKC isoforms PKC α , β , δ , and ϵ are found in mesenteric arteries (Mueed et al., 2005). In cultured mesenteric smooth muscle cells GFP-linked PKC α , PKC δ and PKC ϵ have all been shown to be translocated to the membrane following application of either Ang II, ET-1 or UTP (Nelson et al., 2008). PKC α and PKC ϵ have been shown to mediate contractions, and the inhibition of Kv current, induced by ET-1 and Ang-II respectively in rat mesenteric arteries (Rainbow et al., 2009). These results indicate that each of these vasoconstrictors can target a distinct PKC isoform to mediate contraction of mesenteric arteries. To evaluate the role of different PKC isoforms in mediating UTP induced contraction, various Tat-PKC inhibitor peptides against PKC α , β 1, β 11, δ , and ϵ were used. No significant reduction of UTP induced contraction was seen after pre-incubation of mesenteric arteries with either of these Tat PKC inhibitor peptides. Tat-PKC α and Tat-PKC ϵ , under conditions similar to those used in my experiments, significantly reduced the contraction induced by ET-1 and Ang-II

respectively (Rainbow et al., 2009). In the experiments presented in this thesis I found that Tat-PKC α -IP blocked the ET-1 induced contraction by almost 70%, but its effect on the UTP induced contraction was not significant.

It is difficult to interpret my results regarding the involvement of PKC in mediating the UTP induced contraction of mesenteric arteries. The results as they stand indicate that PKC has only a limited role in producing the UTP induced contraction, although obtaining a clear control that can overcome possible variations in the concentration of PKC inhibitors inside the cells is lacking. It should, however, be noted that Luykenaar et al. (2004) report that the UTP induced contraction of rat cerebral arteries is independent of PKC and they suggest that Rho kinase plays a major role in this tissue (Luykenaar et al., 2004).

5.1.5 UTP activates non selective cation channel

Various studies have suggested that UTP activates non selective cation channels (Alvarez et al., 2008, Baek et al., 2008, Reading et al., 2005). Electrophysiological studies reveal that UTP induces a sustained, non selective cation current in rat cardiomyocytes by the activation of TRPC3/7 via a PLC mediated pathway (Alvarez et al., 2008).

My result showing that 100 μM Gd^{3+} , a known blocker of non-selective cation channels (Hill et al., 2006), blocks the UTP induced contraction is consistent with an activation of a non-selective depolarizing current by UTP. This rather high concentration also blocked the 60 mM K^+ induced contraction, whereas 10 μM Gd^{3+} effectively blocked the UTP induced contraction with little or no effect on the 60 mM K^+ induced contraction (Figure 3-17). In the light of these observations, and of the incomplete block

of the response by the L-type Ca^{2+} channel blocker diltiazem, it appears that UTP induced contraction may be mediated, at least partly, by Ca^{2+} influx via non selective cation channels. The activation of a non-selective cation current by UTP was confirmed using whole-cell current measurements. During some of these measurements voltage-ramps were applied and the resulting instantaneous I-V curves obtained had a similar rectification profile and reversal potential (near 0 mV) to those recorded in vascular smooth muscle cells previously (Albert et al., 2003).

5.1.6 UTP modulates Kv current

Vasoconstrictors such as 4-AP, ET-1 and Ang-II induced contraction is partly due to the inhibition of voltage gated potassium channels which may in turn cause membrane depolarization, an increase in intracellular Ca^{2+} concentration and force generation. Several voltage gated potassium channel blockers have been identified so far that prove themselves as effective therapeutic agents. The voltage gated potassium channel blockers could be used in a variety of pathological conditions like hypertension, cardiac arrhythmia, stroke. (Beech, 1997, Dohi et al., 1994, Goonetilleke and Quayle, 2010, Mackie et al., 2008, Surti and Jan, 2005).

Luykenaar and colleagues report that UTP induced contraction and depolarization in rat cerebral arteries are partly mediated by the suppression of a Kv current (Surti and Jan, 2005, Luykenaar and Welsh, 2007, Luykenaar et al., 2004). To study the possible involvement of Kv channel inhibition by UTP I measured whole-cell Kv currents. The Kv currents recorded with 100 nM free Ca^{2+} in the pipette revealed that UTP suppressed the Kv current at potentials more positive than -10 mV. The activation curve for the Kv current also revealed the ability of UTP to suppress the Kv current at more positive

potentials, while surprisingly at potentials negative to -10 mV the Kv current was increased. Because of the range of Kv subunits expressed in smooth muscle (Cox, 2005) there is the possibility that UTP may modulate the different channel types differentially.

Studies on the mechanism of vasoconstriction often reveal that vasoconstrictors such as 5-HT, ET-1, and Ang-II modulate K⁺ channels by the PLC and PKC signaling pathways and that inhibition of K⁺ channels, including Kv channels, leads to depolarization and contraction (Ko et al., 2010). Including 5 μM of the PLC inhibitor U73122 in the pipette attenuated the reduction of Kv currents by UTP provided there was sufficient Ca²⁺ (100 nM) in the pipette. There was also a slight reduction in the average currents observed with U73122 in the pipette compared to control currents (figure 4.7C), suggesting that U73122 has effects in addition to blocking PLC. Potential additional effects of U73122 were also hinted at by its ability to abolish the contraction induced by 60 mM K⁺. Although U73122 has been used widely to study the signaling mediated by phospholipase C there have been reports by some research groups on its nonspecific blocking effects (Walker et al., 1998).

Ion channels and pumps are known to be regulated by the various isoforms of PKC in smooth muscle cells (Salamanca and Khalil, 2005). Vasoconstrictors in several preparations such as airway smooth muscle, cerebral and mesenteric arteries exert their effect partly through inhibiting Kv channel activity in a PKC dependent manner (Hayabuchi et al., 2001b, Cheng et al., 2007, Cole et al., 1996, Ko et al., 2008, Mackie et al., 2008, Park et al., 2005a, Poole and Furness, 2007, Rainbow et al., 2006, Rainbow et al., 2009, Standen and Quayle, 1998). In contrast to many of these reports, pretreating mesenteric smooth muscle cells with 100 nM Tat PKC20-28-IP for at least 10 minutes

did not significantly prevent UTP suppression of the Kv current. Similarly pretreating the cells with either Tat PKC ϵ -IP or Tat PKC α -IP did not prevent the effects of UTP on Kv current. Similarly Luykenaar (2004) reported that in rat cerebral arteries UTP contraction, as well as its effect on Kv current suppression, was mediated by a PKC independent signaling mechanism which was proposed to be a RhoKinase mediated signaling pathway (Luykenaar et al., 2004, Luykenaar and Welsh, 2007).

5.1.7 UTP modulates K_{ATP} current

ATP sensitive potassium channels are widely expressed in smooth muscle including mesenteric arterial smooth muscle cells and play an important role in the regulation of membrane potential (Standen et al., 1989, Nelson et al., 1990, Nelson and Quayle, 1995, Quayle et al., 1997, Quayle and Standen, 1994). Ang-II and some other vasoconstrictors possess the ability to suppress the K_{ATP} channel activity causing depolarization of smooth muscle. Standen et al (1989) were the first to report these channels in smooth muscle and recorded single channel K_{ATP} currents from rabbit mesenteric arterial smooth muscle cells (Standen et al., 1989).

K_{ATP} channels are activated by a fall in the intracellular ATP and a rise in ADP but they are also the target of several vasoactive compounds, being inhibited by vasoconstrictors such as Ang II and ET-1 in a PKC dependent manner (Kubo et al., 1997, Hayabuchi et al., 2001a) and activated by vasodilators such as calcitonin gene related peptide via activation of PKA (Wellman et al., 1998).

In this investigation I examined whether UTP was able to inhibit the K_{ATP} current in mesenteric smooth muscle cells and whether this involved PKC. The experimental conditions used to isolate the K_{ATP} current were similar to those used previously where

modest internal ATP (1 mM) and ADP (0.1 mM) concentrations enabled background K_{ATP} channel activity whilst maintaining enough ATP for any phosphorylation reactions to occur (Hayabuchi et al., 2001a). In addition, a holding potential of -60 mV and a low intracellular free Ca^{2+} (100 nM) ensured that contamination of the K_{ATP} current recorded by BK and Kv channels was minimal. To examine the inhibition of the K_{ATP} current it was necessary to increase its amplitude over the background activity by using pinacidil, which is a well known activator of these channels. This pinacidil activated K_{ATP} current was quite stable over time but on application of UTP it was significantly reduced. The effect of UTP on K_{ATP} current suppression was quite robust when 100 nM free Ca^{2+} was used in the pipette solution. However, the effect of UTP on K_{ATP} current suppression was less in low (20 nM) intracellular free Ca^{2+} .

Similar to Kv channels of vascular smooth muscle, many vasoconstrictors suppress K_{ATP} channel activity in a PKC dependent manner (Kubo et al., 1997, Standen and Quayle, 1998, Moon et al., 2004, Ko et al., 2008). In contrast to this the inhibition of the K_{ATP} current by UTP appeared insensitive to PKC inhibition by the Tat-linked PKC_{20-28} -IP, either in 100 nM or in 20 nM free internal Ca^{2+} . However, inclusion of PKC_{20-28} -IP in the pipette has been shown to block K_{ATP} modulation by Ang II (Hayabuchi et al., 2001a) and both Tat- PKC_{α} -IP and Tat- PKC_{ϵ} -IP at 100nM blocked the Kv inhibition by ET-1 and Ang II respectively in this tissue (Rainbow et al., 2009). These results, together with those obtained for the Kv current suggest that inhibition of Kv and K_{ATP} currents by UTP are not mediated through PKC.

5.2 Conclusion and future perspectives

UTP induced a sustained and dose dependent contraction in rat mesenteric arteries which was reproducible on repeated applications and abolished upon removal of extracellular Ca^{2+} . The UTP induced sustained contraction was partly dependent on voltage gated Ca^{2+} channels as shown by the partial block of contraction with diltiazem; however, non selective cation channels seem involved as UTP induced contraction was greatly reduced by Gd^{3+} , a known blocker of non selective cation channels. Additionally, whole cell current recordings revealed that UTP induced a non selective cation current which, under the conditions I used, had a reversal potential close to 0 mV; hence it appears that non selective cation channels are largely involved in UTP induced contraction.

Kv channels regulate membrane potential and are activated due to depolarization and therefore have a negative feedback role limit the extent of depolarization and hence contraction (Cole et al., 1996, Prior et al., 1998, Shimoda et al., 1998, Cox, 2005). UTP suppressed the Kv current at more depolarized potentials with 100 nM free Ca^{2+} in the pipette. However, little or no suppression of the Kv current by UTP was observed at low intracellular free Ca^{2+} (20 nM). My results are consistent with those reported by Luykenaar et al (2004), who reported similar Kv current suppression by UTP in rat cerebral arteries (Luykenaar et al., 2004). In addition to the inhibitory effect of UTP at positive potentials, it was seen that UTP elevates the current slightly at membrane potentials negative to -10 mV. The activation curve also revealed that UTP has potentiating effects at negative potentials which could reflect the possibility that UTP

modulates certain Kv channel subunits differently (Cox, 2005). It would be interesting to further dissect the effect of UTP on other Kv channel subunits.

The results obtained from measuring UTP induced contraction as well as modulation of ionic currents suggest that PLC activation is important in mediating these effects. This is also supported by previous reports that UTP activates P2Y receptors (possibly P2Y₂ and P2Y₄) which are G-protein coupled receptor (Abbracchio et al., 2003) which activates PLC and mobilizes the intracellular Ca²⁺ from the intracellular stores by the activation of IP₃.

An inhibitory effect of UTP on K_{ATP} channel activity was also observed and was more pronounced than its effects on the Kv current. UTP significantly blocked the pinacidil activated K_{ATP} current in the presence of 100 nM free Ca²⁺ which suggests that suppression of K_{ATP} channel activity may be one of the reasons for the sustained contraction induced by UTP. However, this sustained contraction as well as the modulation of Kv and K_{ATP} channel activity by UTP seems independent of PKC activation. This is also in agreement with the results of Luykenaar et al (2004) who report that UTP induced depolarization, as well as Kv current suppression, was independent of PKC activation. Luykenaar and colleagues also proposed that Rhokinase partly mediates the UTP induced constriction of rat cerebral arteries by modulating Kv current (Luykenaar et al., 2004, Luykenaar and Welsh, 2007). It would be interesting to investigate whether Rhokinase has a role in the UTP induced contraction of rat mesenteric arteries. Other potassium channels such as BK and Kir also regulate the membrane potential and thus contraction and it would be interesting to study the effect of UTP on these ion channels in rat mesenteric arteries.

Chapter 6 References

- ABBRACCHIO, M. P., BOEYNAEMS, J. M., BARNARD, E. A., BOYER, J. L., KENNEDY, C., MIRAS-PORTUGAL, M. T., KING, B. F., GACHET, C., JACOBSON, K. A., WEISMAN, G. A. & BURNSTOCK, G. (2003) Characterization of the UDP-glucose receptor (re-named here the P2Y₁₄ receptor) adds diversity to the P2Y receptor family. *Trends Pharmacol Sci*, 24, 52-5.
- ABBRACCHIO, M. P. & BURNSTOCK, G. (1994) Purinoceptors: Are there families of P2X and P2Y purinoceptors? *Pharmacology & Therapeutics*, 64, 445-475.
- ABBRACCHIO, M. P., BURNSTOCK, G., BOEYNAEMS, J. M., BARNARD, E. A., BOYER, J. L., KENNEDY, C., KNIGHT, G. E., FUMAGALLI, M., GACHET, C., JACOBSON, K. A. & WEISMAN, G. A. (2006) International Union of Pharmacology LVIII: update on the P2Y G protein-coupled nucleotide receptors: from molecular mechanisms and pathophysiology to therapy. *Pharmacol Rev*, 58, 281-341.
- ADEBIYI, A., NARAYANAN, D. & JAGGAR, J. H. (2010) Caveolin-1 assembles type 1 inositol 1,4,5-trisphosphate receptors and canonical transient receptor potential 3 channels into a functional signaling complex in arterial smooth muscle cells. *J Biol Chem*, 286, 4341-8.
- AIDLEY, D. J. D. J. (1996) *Ion channels : molecules in action / David J. Aidley, Peter R. Stanfield.*, Cambridge, Cambridge University Press.
- ALBERT, A. P., PIPER, A. S. & LARGE, W. A. (2003) Properties of a constitutively active Ca²⁺-permeable non-selective cation channel in rabbit ear artery myocytes. *J Physiol*, 549, 143-56.
- ALTURA, B. M., ALTURA, B. T., CARELLA, A., GEBREWOLD, A., MURAKAWA, T. & NISHIO, A. (1987) Mg²⁺-Ca²⁺ interaction in contractility of vascular smooth muscle: Mg²⁺ versus organic calcium channel blockers on

- myogenic tone and agonist-induced responsiveness of blood vessels. *Can J Physiol Pharmacol*, 65, 729-45.
- ALVAREZ, J., COULOMBE, A., CAZORLA, O., UGUR, M., RAUZIER, J. M., MAGYAR, J., MATHIEU, E. L., BOULAY, G., SOUTO, R., BIDEAUX, P., SALAZAR, G., RASSENDREN, F., LACAMPAGNE, A., FAUCONNIER, J. & VASSORT, G. (2008) ATP/UTP activate cation-permeable channels with TRPC3/7 properties in rat cardiomyocytes. *Am J Physiol Heart Circ Physiol*, 295, H21-8.
- ANDERSON, C. M. & PARKINSON, F. E. (1997) Potential signalling roles for UTP and UDP: sources, regulation and release of uracil nucleotides. *Trends Pharmacol Sci*, 18, 387-92.
- ARONSSON, P., ANDERSSON, M., ERICSSON, T. & GIGLIO, D. (2010) Assessment and characterization of purinergic contractions and relaxations in the rat urinary bladder. *Basic Clin Pharmacol Toxicol*, 107, 603-13.
- BAEK, E. B., YOO, H. Y., PARK, S. J., KIM, H. S., KIM, S. D., EARM, Y. E. & KIM, S. J. (2008) Luminal ATP-induced contraction of rabbit pulmonary arteries and role of purinoceptors in the regulation of pulmonary arterial pressure. *Pflugers Arch*, 457, 281-91.
- BAGCHI, S., LIAO, Z., GONZALEZ, F. A., CHORNA, N. E., SEYE, C. I., WEISMAN, G. A. & ERB, L. (2005) The P2Y₂ nucleotide receptor interacts with alphav integrins to activate Go and induce cell migration. *J Biol Chem*, 280, 39050-7.
- BALTENSPERGER, K. & PORZIG, H. (1997) The P2U purinoceptor obligatorily engages the heterotrimeric G protein G16 to mobilize intracellular Ca²⁺ in human erythroleukemia cells. *J Biol Chem*, 272, 10151-9.

- BARMAN, S. A., ZHU, S. & WHITE, R. E. (2004) PKC activates BK_{Ca} channels in rat pulmonary arterial smooth muscle via cGMP-dependent protein kinase. *Am J Physiol Lung Cell Mol Physiol*, 286, L1275-81.
- BAYLISS, W. M. (1902) On the local reactions of the arterial wall to changes of internal pressure. *J Physiol*, 28, 220-31.
- BEAN, B. P., STUREK, M., PUGA, A. & HERMSMEYER, K. (1986) Calcium channels in muscle cells isolated from rat mesenteric arteries: modulation by dihydropyridine drugs. *Circ Res*, 59, 229-35.
- BEECH, D. J. (1997) Actions of neurotransmitters and other messengers on Ca²⁺ channels and K⁺ channels in smooth muscle cells. *Pharmacol Ther*, 73, 91-119.
- BEECH, D. J., ZHANG, H., NAKAO, K. & BOLTON, T. B. (1993) K channel activation by nucleotide diphosphates and its inhibition by glibenclamide in vascular smooth muscle cells. *Br J Pharmacol*, 110, 573-82.
- BEGLEY, R., LIRON, T., BARYZA, J. & MOCHLY-ROSEN, D. (2004) Biodistribution of intracellularly acting peptides conjugated reversibly to Tat. *Biochem Biophys Res Commun*, 318, 949-54.
- BENHAM, C. D., HESS, P. & TSIEN, R. W. (1987) Two types of calcium channels in single smooth muscle cells from rabbit ear artery studied with whole-cell and single-channel recordings. *Circ Res*, 61, I10-6.
- BERRIDGE, M. J. (2008) Inositol trisphosphate and calcium signalling mechanisms. *Biochim Biophys Acta*, 1793, 933-40.
- BERRIDGE, M. J. (2009) Inositol trisphosphate and calcium signalling mechanisms. *Biochim Biophys Acta*, 1793, 933-40.
- BETT, G. C. & RASMUSSEN, R. L. (2008) Modification of K⁺ channel-drug interactions by ancillary subunits. *J Physiol*, 586, 929-50.

- BETTS, L. C. & KOZLOWSKI, R. Z. (2000) Electrophysiological effects of endothelin-1 and their relationship to contraction in rat renal arterial smooth muscle. *Br J Pharmacol*, 130, 787-96.
- BEVAN, J. A. & OSHER, J. V. (1972) A direct method for recording tension changes in the wall of small blood vessels in vitro. *Agents Actions*, 2, 257-60.
- BI, D., NISHIMURA, J., NIRO, N., HIRANO, K. & KANAIDE, H. (2005) Contractile properties of the cultured vascular smooth muscle cells: the crucial role played by RhoA in the regulation of contractility. *Circ Res*, 96, 890-7.
- BISHOP, A. L. & HALL, A. (2000) Rho GTPases and their effector proteins. *Biochem J*, 348 Pt 2, 241-55.
- BLATZ, A. L. & MAGLEBY, K. L. (1986) Single apamin-blocked Ca-activated K⁺ channels of small conductance in cultured rat skeletal muscle. *Nature*, 323, 718-20.
- BOARDER, M. R. & HOURANI, S. M. (1998) The regulation of vascular function by P2 receptors: multiple sites and multiple receptors. *Trends Pharmacol Sci*, 19, 99-107.
- BOLAND, B., HIMPENS, B., VINCENT, M. F., GILLIS, J. M. & CASTEELS, R. (1992) ATP activates P2x-contracting and P2y-relaxing purinoceptors in the smooth muscle of mouse vas deferens. *Br J Pharmacol*, 107, 1152-8.
- BOLTON, T. B. & IMAIZUMI, Y. (1996) Spontaneous transient outward currents in smooth muscle cells. *Cell Calcium*, 20, 141-52.
- BRAINARD, A. M., MILLER, A. J., MARTENS, J. R. & ENGLAND, S. K. (2005) Maxi-K channels localize to caveolae in human myometrium: a role for an actin-channel-caveolin complex in the regulation of myometrial smooth muscle K⁺ current. *Am J Physiol Cell Physiol*, 289, C49-57.

- BROOKS, H., LEBLEU, B. & VIVES, E. (2005) Tat peptide-mediated cellular delivery: back to basics. *Adv Drug Deliv Rev*, 57, 559-77.
- BULTMANN, R., KLEBROFF, W. & STARKE, K. (1999) A contraction-mediating receptor for UTP, presumably P2Y₂, in rat vas deferens. *Naunyn Schmiedebergs Arch Pharmacol*, 360, 196-201.
- BURNSTOCK, G. (1976) Purine nucleotides. *Adv Biochem Psychopharmacol*, 15, 225-35.
- BURNSTOCK, G. (1997) The past, present and future of purine nucleotides as signalling molecules. *Neuropharmacology*, 36, 1127-39.
- BURNSTOCK, G. (2007) Purine and pyrimidine receptors. *Cell Mol Life Sci*, 64, 1471-83.
- BURNSTOCK, G., COCKS, T., KASAKOV, L. & WONG, H. K. (1978) Direct evidence for ATP release from non-adrenergic, non-cholinergic ("purinergic") nerves in the guinea-pig taenia coli and bladder. *Eur J Pharmacol*, 49, 145-9.
- BUVINIC, S., BRIONES, R. & HUIDOBRO-TORO, J. P. (2002) P2Y(1) and P2Y(2) receptors are coupled to the NO/cGMP pathway to vasodilate the rat arterial mesenteric bed. *Br J Pharmacol*, 136, 847-56.
- CARSTEN, C. Y. K. M. E. (1997) *Cellular Aspects of Smooth Muscle Function*, Cambridge University Press.
- CATTERALL, W. A. (1995) Structure and function of voltage-gated ion channels. *Annu Rev Biochem*, 64, 493-531.
- CHEN, J., CROSSLAND, R. F., NOORANI, M. M. & MARRELLI, S. P. (2009) Inhibition of TRPC1/TRPC3 by PKG contributes to NO-mediated vasorelaxation. *Am J Physiol Heart Circ Physiol*, 297, H417-24.

- CHEN, L., HAHN, H., WU, G., CHEN, C. H., LIRON, T., SCHECHTMAN, D., CAVALLARO, G., BANCI, L., GUO, Y., BOLLI, R., DORN, G. W., 2ND & MOCHLY-ROSEN, D. (2001) Opposing cardioprotective actions and parallel hypertrophic effects of delta PKC and epsilon PKC. *Proc Natl Acad Sci U S A*, 98, 11114-9.
- CHENG, D., XU, Y., LIU, X., ZHAO, L., XIONG, S. & ZHANG, Z. (2007) The effects of protein kinase C (PKC) on the tension of normal and passively sensitized human airway smooth muscle and the activity of voltage-dependent delayed rectifier potassium channel (Kv). *J Huazhong Univ Sci Technolog Med Sci*, 27, 153-6.
- CHO, Y. R., JANG, H. S., KIM, W., PARK, S. Y. & SOHN, U. D. (2010) P2X and P2Y Receptors Mediate Contraction Induced by Electrical Field Stimulation in Feline Esophageal Smooth Muscle. *Korean J Physiol Pharmacol*, 14, 311-6.
- CHOOTIP, K., GURNEY, A. M. & KENNEDY, C. (2005) Multiple P2Y receptors couple to calcium-dependent, chloride channels in smooth muscle cells of the rat pulmonary artery. *Respir Res*, 6, 124.
- CLAPHAM, D. E., RUNNELS, L. W. & STRUBING, C. (2001) The TRP ion channel family. *Nat Rev Neurosci*, 2, 387-96.
- CLARKE, C. J., FORMAN, S., PRITCHETT, J., OHANIAN, V. & OHANIAN, J. (2008a) Phospholipase C-delta1 modulates sustained contraction of rat mesenteric small arteries in response to noradrenaline, but not endothelin-1. *Am J Physiol Heart Circ Physiol*, 295, H826-34.
- CLARKE, C. J., FORMAN, S., PRITCHETT, J., OHANIAN, V. & OHANIAN, J. (2008b) Phospholipase C{delta}1 modulates sustained contraction of rat mesenteric small arteries in response to noradrenaline, but not endothelin-1. *Am J Physiol Heart Circ Physiol*.

- COLE, W. C. (2010) Silencing vascular smooth muscle ATP-sensitive K⁺ channels with caveolin-1. *J Physiol*, 588, 3133-4.
- COLE, W. C., CLEMENT-CHOMIENNE, O. & AIELLO, E. A. (1996) Regulation of 4-aminopyridine-sensitive, delayed rectifier K⁺ channels in vascular smooth muscle by phosphorylation. *Biochem Cell Biol*, 74, 439-47.
- COLOMBO, M. L. & BOSISIO, E. (1996) Pharmacological activities of Chelidonium majus L. (Papaveraceae). *Pharmacol Res*, 33, 127-34.
- COSENS, D. J. & MANNING, A. (1969) Abnormal electroretinogram from a *Drosophila* mutant. *Nature*, 224, 285-7.
- COX, R. H. (2005) Molecular determinants of voltage-gated potassium currents in vascular smooth muscle. *Cell Biochem Biophys*, 42, 167-95.
- DANIEL, J. L., DANGELMAIER, C., JIN, J., ASHBY, B., SMITH, J. B. & KUNAPULI, S. P. (1998) Molecular basis for ADP-induced platelet activation. I. Evidence for three distinct ADP receptors on human platelets. *J Biol Chem*, 273, 2024-9.
- DAS, M. & DAS, D. K. (2011) Caveolae, caveolin, and cavins: Potential targets for the treatment of cardiac disease. *Ann Med*.
- DEBDI, M., SEYLAZ, J. & SERCOMBE, R. (1993) Increased influence of calcium and nifedipine on rabbit basilar artery reactivity after brief subarachnoid hemorrhage. *J Cardiovasc Pharmacol*, 21, 754-9.
- DELARUE, C., JOUET, I. R., GRAS, M., GALAS, L., FOURNIER, A. & VAUDRY, H. (2005) Activation of endothelinA receptors in frog adrenocortical cells stimulates both calcium mobilization from intracellular stores and calcium influx through L-type calcium channels. *Endocrinology*, 146, 119-29.

- DIXON, R. A., KOBILKA, B. K., STRADER, D. J., BENOVIC, J. L., DOHLMAN, H. G., FRIELLE, T., BOLANOWSKI, M. A., BENNETT, C. D., RANDS, E., DIEHL, R. E., MUMFORD, R. A., SLATER, E. E., SIGAL, I. S., CARON, M. G., LEFKOWITZ, R. J. & STRADER, C. D. (1986) Cloning of the gene and cDNA for mammalian beta-adrenergic receptor and homology with rhodopsin. *Nature*, 321, 75-9.
- DOBRONYI, I., HUNG, K. S., SATCHELL, D. G. & MAGUIRE, M. H. (1997) Evidence for a novel P2X purinoceptor in human placental chorionic surface arteries. *Eur J Pharmacol*, 320, 61-4.
- DOHI, Y., CRISCIONE, L., PFEIFFER, K. & LUSCHER, T. F. (1994) Angiotensin blockade or calcium antagonists improve endothelial dysfunction in hypertension: studies in perfused mesenteric resistance arteries. *J Cardiovasc Pharmacol*, 24, 372-9.
- DRURY, A. N. & SZENT-GYORGYI, A. (1929) The physiological activity of adenine compounds with especial reference to their action upon the mammalian heart. *J Physiol*, 68, 213-37.
- EICHHOLTZ, T., DE BONT, D. B., DE WIDT, J., LISKAMP, R. M. & PLOEGH, H. L. (1993) A myristoylated pseudosubstrate peptide, a novel protein kinase C inhibitor. *J Biol Chem*, 268, 1982-6.
- ENDO, M., FUJITA, S., YANG, H. T., TALUKDER, M. A., MARUYA, J. & NOROTA, I. (1998) Endothelin: receptor subtypes, signal transduction, regulation of Ca²⁺ transients and contractility in rabbit ventricular myocardium. *Life Sci*, 62, 1485-9.
- ERLINGE, D. & BURNSTOCK, G. (2008) P2 receptors in cardiovascular regulation and disease. *Purinergic Signal*, 4, 1-20.

- ERLINGE, D., HARNEK, J., VAN HEUSDEN, C., OLIVECRONA, G., JERN, S. & LAZAROWSKI, E. (2005) Uridine triphosphate (UTP) is released during cardiac ischemia. *Int J Cardiol*, 100, 427-33.
- FAWELL, S., SEERY, J., DAIKH, Y., MOORE, C., CHEN, L. L., PEPINSKY, B. & BARSOUM, J. (1994) Tat-mediated delivery of heterologous proteins into cells. *Proc Natl Acad Sci U S A*, 91, 664-8.
- FISH, R. D., SPERTI, G., COLUCCI, W. S. & CLAPHAM, D. E. (1988) Phorbol ester increases the dihydropyridine-sensitive calcium conductance in a vascular smooth muscle cell line. *Circ Res*, 62, 1049-54.
- FLEISCHMANN, B. K., MURRAY, R. K. & KOTLIKOFF, M. I. (1994) Voltage window for sustained elevation of cytosolic calcium in smooth muscle cells. *Proc Natl Acad Sci U S A*, 91, 11914-8.
- FUJITA, R., KIMURA, S., KAWASAKI, S., WATANABE, S., WATANABE, N., HIRANO, H., MATSUMOTO, M. & SASAKI, K. (2007) Electrophysiological and pharmacological characterization of the K(ATP) channel involved in the K⁺-current responses to FSH and adenosine in the follicular cells of *Xenopus* oocyte. *J Physiol Sci*, 57, 51-61.
- GITTERMAN, D. P. & EVANS, R. J. (2000) Properties of P2X and P2Y receptors are dependent on artery diameter in the rat mesenteric bed. *Br J Pharmacol*, 131, 1561-8.
- GOETZ, U., DA PRADA, M. & PLETSCHER, A. (1971) Adenine-, guanine- and uridine-5'-phosphonucleotides in blood platelets and storage organelles of various species. *J Pharmacol Exp Ther*, 178, 210-5.
- GOONETILLEKE, L. & QUAYLE, J. (2010) TREK-1 K(+) Channels in the Cardiovascular System: Their Significance and Potential as a Therapeutic Target. DOI: 10.1111/j.1755-5922.2010.00227.x [Epub ahead of print]. *J Cardiovasc Therapeutics*, Blackwell Publishing Ltd.

- GREGGER, R. (1996) *Comprehensive human physiology : from cellular mechanisms to integration*
- GSCHWENDT, M., DIETERICH, S., RENNECKE, J., KITTSSTEIN, W., MUELLER, H. J. & JOHANNES, F. J. (1996) Inhibition of protein kinase C mu by various inhibitors. Differentiation from protein kinase c isoenzymes. *FEBS Lett*, 392, 77-80.
- HAI, C. M. & MURPHY, R. A. (1989a) Ca^{2+} , crossbridge phosphorylation, and contraction. *Annu Rev Physiol*, 51, 285-98.
- HAI, C. M. & MURPHY, R. A. (1989b) Crossbridge phosphorylation and the energetics of contraction in the swine carotid media. *Prog Clin Biol Res*, 315, 253-63.
- HALLBRINK, M., FLOREN, A., ELMQUIST, A., POOGA, M., BARTFAI, T. & LANGEL, U. (2001) Cargo delivery kinetics of cell-penetrating peptides. *Biochim Biophys Acta*, 1515, 101-9.
- HAMILL, O. P., MARTY, A., NEHER, E., SAKMANN, B. & SIGWORTH, F. J. (1981) Improved patch-clamp techniques for high-resolution current recording from cells and cell-free membrane patches. *Pflugers Arch*, 391, 85-100.
- HARDER, D. R. (1984) Pressure-dependent membrane depolarization in cat middle cerebral artery. *Circ Res*, 55, 197-202.
- HARPER, S., WEBB, T. E., CHARLTON, S. J., NG, L. L. & BOARDER, M. R. (1998) Evidence that P2Y₄ nucleotide receptors are involved in the regulation of rat aortic smooth muscle cells by UTP and ATP. *Br J Pharmacol*, 124, 703-10.
- HAYABUCHI, Y., DAVIES, N. W. & STANDEN, N. B. (2001a) Angiotensin II inhibits rat arterial K_{ATP} channels by inhibiting steady-state protein kinase A activity and activating protein kinase Ce. *J Physiol*, 530, 193-205.

- HAYABUCHI, Y., STANDEN, N. B. & DAVIES, N. W. (2001b) Angiotensin II inhibits and alters kinetics of voltage-gated K(+) channels of rat arterial smooth muscle. *Am J Physiol Heart Circ Physiol*, 281, H2480-9.
- HELLIWELL, R. M. & LARGE, W. A. (1997) Alpha 1-adrenoceptor activation of a non-selective cation current in rabbit portal vein by 1,2-diacyl-sn-glycerol. *J Physiol*, 499 (Pt 2), 417-28.
- HERBERT, J. M., AUGEREAU, J. M., GLEYE, J. & MAFFRAND, J. P. (1990) Chelerythrine is a potent and specific inhibitor of protein kinase C. *Biochem Biophys Res Commun*, 172, 993-9.
- HERNANDEZ-OCHOA, E. O., GARCIA-FERREIRO, R. E. & GARCIA, D. E. (2007) G protein activation inhibits gating charge movement in rat sympathetic neurons. *Am J Physiol Cell Physiol*, 292, C2226-38.
- HIBINO, H., INANOBE, A., FURUTANI, K., MURAKAMI, S., FINDLAY, I. & KURACHI, Y. (2010) Inwardly rectifying potassium channels: their structure, function, and physiological roles. *Physiol Rev*, 90, 291-366.
- HILL, A. J., HINTON, J. M., CHENG, H., GAO, Z., BATES, D. O., HANCOX, J. C., LANGTON, P. D. & JAMES, A. F. (2006) A TRPC-like non-selective cation current activated by alpha 1-adrenoceptors in rat mesenteric artery smooth muscle cells. *Cell Calcium*, 40, 29-40.
- HILL, B. J. & STUREK, M. (2002) Pharmacological characterization of a UTP-sensitive P2Y nucleotide receptor in organ cultured coronary arteries. *Vascul Pharmacol*, 39, 83-8.
- HIRANO, K., HIRANO, M. & KANAIDE, H. (2004) Regulation of myosin phosphorylation and myofilament Ca²⁺ sensitivity in vascular smooth muscle. *J Smooth Muscle Res*, 40, 219-36.

- HORIUCHI, T., DIETRICH, H. H., TSUGANE, S. & DACEY, R. G., JR. (2001) Analysis of purine- and pyrimidine-induced vascular responses in the isolated rat cerebral arteriole. *Am J Physiol Heart Circ Physiol*, 280, H767-76.
- HOROWITZ, A., MENICE, C. B., LAPORTE, R. & MORGAN, K. G. (1996) Mechanisms of smooth muscle contraction. *Physiol Rev*, 76, 967-1003.
- HOUSE, C. & KEMP, B. E. (1987) Protein kinase C contains a pseudosubstrate prototope in its regulatory domain. *Science*, 238, 1726-8.
- HYUN, J. S., BIVALACQUA, T. J., BAIG, M. R., YANG, D. Y., LEUNGWATTANAKIJ, S., ABDEL-MAGEED, A., KIM, K. D. & HELLSTROM, W. J. (2002) Localization of peripheral dopamine D1 and D2 receptors in rat corpus cavernosum. *BJU Int*, 90, 105-12.
- IWAMURO, Y., MIWA, S., ZHANG, X. F., MINOWA, T., ENOKI, T., OKAMOTO, Y., HASEGAWA, H., FURUTANI, H., OKAZAWA, M., ISHIKAWA, M., HASHIMOTO, N. & MASAKI, T. (1999) Activation of three types of voltage-independent Ca^{2+} channel in A7r5 cells by endothelin-1 as revealed by a novel Ca^{2+} channel blocker LOE 908. *Br J Pharmacol*, 126, 1107-14.
- JAGGAR, J. H. & NELSON, M. T. (2000) Differential regulation of Ca^{2+} sparks and Ca^{2+} waves by UTP in rat cerebral artery smooth muscle cells. *Am J Physiol Cell Physiol*, 279, C1528-39.
- JAN, L. Y. & JAN, Y. N. (1992) Structural elements involved in specific K^+ channel functions. *Annu Rev Physiol*, 54, 537-55.
- JOHNSON, J. A., GRAY, M. O., CHEN, C. H. & MOCHLY-ROSEN, D. (1996) A protein kinase C translocation inhibitor as an isozyme-selective antagonist of cardiac function. *J Biol Chem*, 271, 24962-6.

- JUUL, B., PLESNER, L. & AALKJAER, C. (1992) Effects of ATP and UTP on $[Ca^{2+}]_i$, membrane potential and force in isolated rat small arteries. *J Vasc Res*, 29, 385-95.
- KAMISHIMA, T., BURDYGA, T., GALLAGHER, J. A. & QUAYLE, J. M. (2007) Caveolin-1 and caveolin-3 regulate Ca^{2+} homeostasis of single smooth muscle cells from rat cerebral resistance arteries. *Am J Physiol Heart Circ Physiol*, 293, H204-14.
- KAMM, K. E. & STULL, J. T. (1985a) The function of myosin and myosin light chain kinase phosphorylation in smooth muscle. *Annu Rev Pharmacol Toxicol*, 25, 593-620.
- KAMM, K. E. & STULL, J. T. (1985b) Myosin phosphorylation, force, and maximal shortening velocity in neurally stimulated tracheal smooth muscle. *Am J Physiol*, 249, C238-47.
- KANASHIRO, C. A. & KHALIL, R. A. (1998) Signal transduction by protein kinase C in mammalian cells. *Clin Exp Pharmacol Physiol*, 25, 974-85.
- KANEKO, T., AMANO, M., MAEDA, A., GOTO, H., TAKAHASHI, K., ITO, M. & KAIBUCHI, K. (2000) Identification of calponin as a novel substrate of Rho-kinase. *Biochem Biophys Res Commun*, 273, 110-6.
- KHALIL, R. A. (2010) Regulation of vascular smooth muscle function. IN D. NEIL GRANGER, L. S. U. H. S. C. J. P. G. & CENTER, U. O. M. M. (Eds.). Boston, Massachusetts, Morgan & Claypool.
- KHALIL, R. A. & VAN BREEMEN, C. (1988) Sustained contraction of vascular smooth muscle: calcium influx or C-kinase activation? *J Pharmacol Exp Ther*, 244, 537-42.
- KIMURA, K., ITO, M., AMANO, M., CHIHARA, K., FUKATA, Y., NAKAFUKU, M., YAMAMORI, B., FENG, J., NAKANO, T., OKAWA, K., IWAMATSU, A.

- & KAIBUCHI, K. (1996) Regulation of myosin phosphatase by Rho and Rho-associated kinase (Rho-kinase). *Science*, 273, 245-8.
- KITAZONO, T., FARACI, F. M. & HEISTAD, D. D. (1993) Effect of norepinephrine on rat basilar artery in vivo. *Am J Physiol*, 264, H178-82.
- KNAUS, H. G., EBERHART, A., GLOSSMANN, H., MUNUJOS, P., KACZOROWSKI, G. J. & GARCIA, M. L. (1994) Pharmacology and structure of high conductance calcium-activated potassium channels. *Cell Signal*, 6, 861-70.
- KO, E. A., HAN, J., JUNG, I. D. & PARK, W. S. (2008) Physiological roles of K⁺ channels in vascular smooth muscle cells. *J Smooth Muscle Res*, 44, 65-81.
- KO, E. A., PARK, W. S., FIRTH, A. L., KIM, N., YUAN, J. X. J. & HAN, J. (2010) Pathophysiology of voltage-gated K⁺ channels in vascular smooth muscle cells: Modulation by protein kinases. *Progress in Biophysics and Molecular Biology*, 103, 95-101.
- KOH, S. D., DICK, G. M. & SANDERS, K. M. (1997) Small-conductance Ca(2+)-dependent K⁺ channels activated by ATP in murine colonic smooth muscle. *Am J Physiol*, 273, C2010-21.
- KUBO, M., QUAYLE, J. M. & STANDEN, N. B. (1997) Angiotensin II inhibition of ATP-sensitive K⁺ currents in rat arterial smooth muscle cells through protein kinase C. *J Physiol*, 503 (Pt 3), 489-96.
- KUMARI, R., GOH, G., NG, L. L. & BORDER, M. R. (2003) ATP and UTP responses of cultured rat aortic smooth muscle cells revisited: dominance of P2Y2 receptors. *Br J Pharmacol*, 140, 1169-76.
- LACZA, Z., KALDI, K., KOVECS, K., GORLACH, C., NAGY, Z., SANDOR, P., BENYO, Z. & WAHL, M. (2001) Involvement of prostanoid release in the

- mediation of UTP-induced cerebrovascular contraction in the rat. *Brain Res*, 896, 169-74.
- LANDRY, D. W. & OLIVER, J. A. (1992) The ATP-sensitive K⁺ channel mediates hypotension in endotoxemia and hypoxic lactic acidosis in dog. *J Clin Invest*, 89, 2071-4.
- LAZAROWSKI, E. R. & BOUCHER, R. C. (2001) UTP as an extracellular signaling molecule. *News Physiol Sci*, 16, 1-5.
- LAZAROWSKI, E. R. & HARDEN, T. K. (1999) Quantitation of extracellular UTP using a sensitive enzymatic assay. *Br J Pharmacol*, 127, 1272-8.
- LAZAROWSKI, E. R., WATT, W. C., STUTTS, M. J., BOUCHER, R. C. & HARDEN, T. K. (1995) Pharmacological selectivity of the cloned human P2U-purinoceptor: potent activation by diadenosine tetraphosphate. *Br J Pharmacol*, 116, 1619-27.
- LE, S. Q., WASSERSTRUM, N., MOMBOULI, J. V. & VANHOUTTE, P. M. (1993) Role of extracellular calcium and calcium channels in the response of human placental venous smooth muscle to endothelin-1. *Am J Obstet Gynecol*, 169, 1427-30.
- LEDOUX, J., WERNER, M. E., BRAYDEN, J. E. & NELSON, M. T. (2006) Calcium-activated potassium channels and the regulation of vascular tone. *Physiology (Bethesda)*, 21, 69-78.
- LEE, M. W. & SEVERSON, D. L. (1994) Signal transduction in vascular smooth muscle: diacylglycerol second messengers and PKC action. *Am J Physiol*, 267, C659-78.
- LEVICK, J. R. (2003) *An introduction to cardiovascular physiology / J. Rodney Levick.*, London, Arnold,.

- LOIRAND, G., PACAUD, P., MIRONNEAU, C. & MIRONNEAU, J. (1986) Evidence for two distinct calcium channels in rat vascular smooth muscle cells in short-term primary culture. *Pflugers Arch*, 407, 566-8.
- LOPATIN, A. N., MAKHINA, E. N. & NICHOLS, C. G. (1994) Potassium channel block by cytoplasmic polyamines as the mechanism of intrinsic rectification. *Nature*, 372, 366-9.
- LOPEZ, C., SANCHEZ, M., HIDALGO, A. & GARCIA DE BOTO, M. J. (2000) Mechanisms involved in UTP-induced contraction in isolated rat aorta. *Eur J Pharmacol*, 391, 299-303.
- LUYKENAAR, K. D., BRETT, S. E., WU, B. N., WIEHLER, W. B. & WELSH, D. G. (2004) Pyrimidine nucleotides suppress KDR currents and depolarize rat cerebral arteries by activating Rho kinase. *Am J Physiol Heart Circ Physiol*, 286, H1088-100.
- LUYKENAAR, K. D. & WELSH, D. G. (2007) Activators of the PKA and PKG pathways attenuate RhoA-mediated suppression of the KDR current in cerebral arteries. *Am J Physiol Heart Circ Physiol*, 292, H2654-63.
- MACKIE, A. R., BRUEGGEMANN, L. I., HENDERSON, K. K., SHIELS, A. J., CRIBBS, L. L., SCROGIN, K. E. & BYRON, K. L. (2008) Vascular KCNQ potassium channels as novel targets for the control of mesenteric artery constriction by vasopressin, based on studies in single cells, pressurized arteries, and in vivo measurements of mesenteric vascular resistance. *J Pharmacol Exp Ther*, 325, 475-83.
- MADDALI, K. K., KORZICK, D. H., THARP, D. L. & BOWLES, D. K. (2005) PKCdelta mediates testosterone-induced increases in coronary smooth muscle Cav1.2. *J Biol Chem*, 280, 43024-9.

- MARRELLI, S. P., KHOROVETS, A., JOHNSON, T. D., CHILDRES, W. F. & BRYAN, R. M., JR. (1999) P2 purinoceptor-mediated dilations in the rat middle cerebral artery after ischemia-reperfusion. *Am J Physiol*, 276, H33-41.
- MCLAREN, G. J., SNEDDON, P. & KENNEDY, C. (1998) Comparison of the actions of ATP and UTP and P(2X1) receptors in smooth muscle of the rat tail artery. *Eur J Pharmacol*, 351, 139-44.
- MINKE, B. & COOK, B. (2002) TRP channel proteins and signal transduction. *Physiol Rev*, 82, 429-72.
- MIYAGI, Y., KOBAYASHI, S., NISHIMURA, J., FUKUI, M. & KANAIDE, H. (1996) Dual regulation of cerebrovascular tone by UTP: P2U receptor-mediated contraction and endothelium-dependent relaxation. *Br J Pharmacol*, 118, 847-56.
- MOCHLY-ROSEN, D. (1995) Localization of protein kinases by anchoring proteins: a theme in signal transduction. *Science*, 268, 247-51.
- MOCHLY-ROSEN, D. & GORDON, A. S. (1998) Anchoring proteins for protein kinase C: a means for isozyme selectivity. *FASEB J*, 12, 35-42.
- MOCHLY-ROSEN, D., KHANER, H. & LOPEZ, J. (1991) Identification of intracellular receptor proteins for activated protein kinase C. *Proc Natl Acad Sci U S A*, 88, 3997-4000.
- MOMBOULI, J. V. & VANHOUTTE, P. M. (1997) Endothelium-derived hyperpolarizing factor(s): updating the unknown. *Trends Pharmacol Sci*, 18, 252-6.
- MONTMAYEUR, J. P., BARR, T. P., KAM, S. A., PACKER, S. J. & STRICHARTZ, G. R. (2011) ET-1 induced Elevation of intracellular calcium in clonal neuronal and embryonic kidney cells involves endogenous endothelin-A receptors linked to phospholipase C through Galpha(q/11). *Pharmacol Res*, 64, 258-67.

- MOON, C. H., KIM, M. Y., KIM, M. J., KIM, M. H., LEE, S., YI, K. Y., YOO, S. E., LEE, D. H., LIM, H., KIM, H. S., LEE, S. H., BAIK, E. J. & JUNG, Y. S. (2004) KR-31378, a novel benzopyran analog, attenuates hypoxia-induced cell death via mitochondrial KATP channel and protein kinase C-epsilon in heart-derived H9c2 cells. *Eur J Pharmacol*, 506, 27-35.
- MORRIS, G. E., NELSON, C. P., EVERITT, D., BRIGHTON, P. J., STANDEN, N. B., CHALLISS, R. A. & WILLETS, J. M. (2010) G protein-coupled receptor kinase 2 and arrestin2 regulate arterial smooth muscle P2Y-purinoceptor signalling. *Cardiovasc Res*, 89, 193-203.
- MUEED, I., ZHANG, L. & MACLEOD, K. M. (2005) Role of the PKC/CPI-17 pathway in enhanced contractile responses of mesenteric arteries from diabetic rats to alpha-adrenoceptor stimulation. *Br J Pharmacol*, 146, 972-82.
- MURTHY, K. S. & MAKHLOUF, G. M. (1998) Coexpression of ligand-gated P2X and G protein-coupled P2Y receptors in smooth muscle. Preferential activation of P2Y receptors coupled to phospholipase C (PLC)-beta1 via Galphaq/11 and to PLC-beta3 via Gbetagamma3. *J Biol Chem*, 273, 4695-704.
- NAGUMO, H., SAKURADA, K., SETO, M. & SASAKI, Y. (1994) Phosphorylation of calponin by PKC is blocked by F-actin in vitro. *Biochem Biophys Res Commun*, 203, 1502-7.
- NAVEDO, M. F., AMBERG, G. C., VOTAW, V. S. & SANTANA, L. F. (2005) Constitutively active L-type Ca²⁺ channels. *Proc Natl Acad Sci U S A*, 102, 11112-7.
- NEHER, E. & SAKMANN, B. (1976a) Noise analysis of drug induced voltage clamp currents in denervated frog muscle fibres. *J Physiol*, 258, 705-29.
- NEHER, E. & SAKMANN, B. (1976b) Single-channel currents recorded from membrane of denervated frog muscle fibres. *Nature*, 260, 799-802.

- NELLD, T. O. & KEEF, K. (1985) Measurements of the membrane potential of arterial smooth muscle in anesthetized animals and its relationship to changes in artery diameter. *Microvasc Res*, 30, 19-28.
- NELSON, C. P., WILLETS, J. M., DAVIES, N. W., CHALLISS, R. A. & STANDEN, N. B. (2008) Visualizing the temporal effects of vasoconstrictors on PKC translocation and Ca^{2+} signaling in single resistance arterial smooth muscle cells. *Am J Physiol Cell Physiol*, 295, C1590-601.
- NELSON, M. T., PATLAK, J. B., WORLEY, J. F. & STANDEN, N. B. (1990) Calcium channels, potassium channels, and voltage dependence of arterial smooth muscle tone. *Am J Physiol*, 259, C3-18.
- NELSON, M. T. & QUAYLE, J. M. (1995) Physiological roles and properties of potassium channels in arterial smooth muscle. *Am J Physiol*, 268, C799-822.
- NILIUS, B., OWSIANIK, G., VOETS, T. & PETERS, J. A. (2007) Transient receptor potential cation channels in disease. *Physiol Rev*, 87, 165-217.
- NISHIZUKA, Y. (1992) Intracellular signaling by hydrolysis of phospholipids and activation of protein kinase C. *Science*, 258, 607-14.
- NOMA, A. (1983) ATP-regulated K^+ channels in cardiac muscle. *Nature*, 305, 147-8.
- NORTH, R. A. (2002) Molecular physiology of P2X receptors. *Physiol Rev*, 82, 1013-67.
- OMOTE, M. & MIZUSAWA, H. (1996) Interaction between the L-type Ca^{2+} channel and the Ca^{2+} -activated K^+ channel in the fluctuating myogenic contraction in the rabbit basilar artery. *Jpn J Physiol*, 46, 353-6.
- PANAGHIE, G., PURTELL, K., TAI, K. K. & ABBOTT, G. W. (2008) Voltage-dependent C-type inactivation in a constitutively open K^+ channel. *Biophys J*, 95, 2759-78.

- PARK, W. S., HAN, J., KIM, N., YOUM, J. B., JOO, H., KIM, H. K., KO, J. H. & EARM, Y. E. (2005a) Endothelin-1 inhibits inward rectifier K⁺ channels in rabbit coronary arterial smooth muscle cells through protein kinase C. *J Cardiovasc Pharmacol*, 46, 681-9.
- PARK, W. S., KIM, N., YOUM, J. B., WARDA, M., KO, J. H., KIM, S. J., EARM, Y. E. & HAN, J. (2006) Angiotensin II inhibits inward rectifier K⁺ channels in rabbit coronary arterial smooth muscle cells through protein kinase Calpha. *Biochem Biophys Res Commun*, 341, 728-35.
- PARK, W. S., KO, J. H., KIM, N., SON, Y. K., KANG, S. H., WARDA, M., JUNG, I. D., PARK, Y. M. & HAN, J. (2007) Increased inhibition of inward rectifier K⁺ channels by angiotensin II in small-diameter coronary artery of isoproterenol-induced hypertrophied model. *Arterioscler Thromb Vasc Biol*, 27, 1768-75.
- PARK, W. S., SON, Y. K., KO, E. A., KO, J. H., LEE, H. A., PARK, K. S. & EARM, Y. E. (2005b) The protein kinase C inhibitor, bisindolylmaleimide (I), inhibits voltage-dependent K⁺ channels in coronary arterial smooth muscle cells. *Life Sci*, 77, 512-27.
- PARKER, C. A., TAKAHASHI, K., TAO, T. & MORGAN, K. G. (1994) Agonist-induced redistribution of calponin in contractile vascular smooth muscle cells. *Am J Physiol*, 267, C1262-70.
- PATIL, S. B., PAWAR, M. D. & BITAR, K. N. (2004) Direct association and translocation of PKC-alpha with calponin. *Am J Physiol Gastrointest Liver Physiol*, 286, G954-63.
- PEPPIATT-WILDMAN, C. M., ALBERT, A. P., SALEH, S. N. & LARGE, W. A. (2007) Endothelin-1 activates a Ca²⁺-permeable cation channel with TRPC3 and TRPC7 properties in rabbit coronary artery myocytes. *J Physiol*, 580, 755-64.
- PEREZ-REYES, E. (2003) Molecular physiology of low-voltage-activated t-type calcium channels. *Physiol Rev*, 83, 117-61.

- PLANE, F., JOHNSON, R., KERR, P., WIEHLER, W., THORNELOE, K., ISHII, K., CHEN, T. & COLE, W. (2005) Heteromultimeric Kv1 channels contribute to myogenic control of arterial diameter. *Circ Res*, 96, 216-24.
- POOLE, D. P. & FURNESS, J. B. (2007) PKC delta-isoform translocation and enhancement of tonic contractions of gastrointestinal smooth muscle. *Am J Physiol Gastrointest Liver Physiol*, 292, G887-98.
- PRIOR, H. M., YATES, M. S. & BEECH, D. J. (1998) Functions of large conductance Ca²⁺-activated (BK_{Ca}), delayed rectifier (K_v) and background K⁺ channels in the control of membrane potential in rabbit renal arcuate artery. *J Physiol*, 511 (Pt 1), 159-69.
- QUAYLE, J. M., BONEV, A. D., BRAYDEN, J. E. & NELSON, M. T. (1994) Calcitonin gene-related peptide activated ATP-sensitive K⁺ currents in rabbit arterial smooth muscle via protein kinase A. *J Physiol*, 475, 9-13.
- QUAYLE, J. M., BONEV, A. D., BRAYDEN, J. E. & NELSON, M. T. (1995) Pharmacology of ATP-sensitive K⁺ currents in smooth muscle cells from rabbit mesenteric artery. *Am J Physiol*, 269, C1112-8.
- QUAYLE, J. M., DART, C. & STANDEN, N. B. (1996) The properties and distribution of inward rectifier potassium currents in pig coronary arterial smooth muscle. *J Physiol*, 494 (Pt 3), 715-26.
- QUAYLE, J. M., NELSON, M. T. & STANDEN, N. B. (1997) ATP-sensitive and inwardly rectifying potassium channels in smooth muscle. *Physiol Rev*, 77, 1165-232.
- QUAYLE, J. M. & STANDEN, N. B. (1994) KATP channels in vascular smooth muscle. *Cardiovasc Res*, 28, 797-804.

- RAINBOW, R. D., HARDY, M. E., STANDEN, N. B. & DAVIES, N. W. (2006) Glucose reduces endothelin inhibition of voltage-gated potassium channels in rat arterial smooth muscle cells. *J Physiol*, 575, 833-44.
- RAINBOW, R. D., NORMAN, R. I., EVERITT, D. E., BRIGNELL, J. L., DAVIES, N. W. & STANDEN, N. B. (2009) Endothelin-I and angiotensin II inhibit arterial voltage-gated K⁺ channels through different protein kinase C isoenzymes. *Cardiovasc Res*, 83, 493-500.
- RALEVIC, V. & BURNSTOCK, G. (1991) Effects of purines and pyrimidines on the rat mesenteric arterial bed. *Circulation Research*, 69, 1583-1590.
- RALEVIC, V. & BURNSTOCK, G. (1998) Receptors for purines and pyrimidines. *Pharmacol Rev*, 50, 413-92.
- RANG, D. (2007) *Rang and Dale's Pharmacology*, Edinburgh, Churchill Livingstone.
- RATZ, P. H. & MINER, A. S. (2009) Role of protein kinase C ζ and calcium entry in KCl-induced vascular smooth muscle calcium sensitization and feedback control of cellular calcium levels. *J Pharmacol Exp Ther*, 328, 399-408.
- READING, S. A., EARLEY, S., WALDRON, B. J., WELSH, D. G. & BRAYDEN, J. E. (2005) TRPC3 mediates pyrimidine receptor-induced depolarization of cerebral arteries. *Am J Physiol Heart Circ Physiol*, 288, H2055-61.
- ROCHE, J. P. & TREISTMAN, S. N. (1998) Ca²⁺ channel β_3 subunit enhances voltage-dependent relief of G-protein inhibition induced by muscarinic receptor activation and Gbetagamma. *J Neurosci*, 18, 4883-90.
- SALAMANCA, D. A. & KHALIL, R. A. (2005) Protein kinase C isoforms as specific targets for modulation of vascular smooth muscle function in hypertension. *Biochem Pharmacol*, 70, 1537-47.

- SALEH, S. N., ALBERT, A. P. & LARGE, W. A. (2009) Activation of native TRPC1/C5/C6 channels by endothelin-1 is mediated by both PIP(3) and PIP(2) in rabbit coronary artery myocytes. *J Physiol*, 587, 5361-75.
- SAMPSON, L. J., DAVIES, L. M., BARRETT-JOLLEY, R., STANDEN, N. B. & DART, C. (2007) Angiotensin II-activated protein kinase C targets caveolae to inhibit aortic ATP-sensitive potassium channels. *Cardiovasc Res*, 76, 61-70.
- SAMPSON, L. J., HAYABUCHI, Y., STANDEN, N. B. & DART, C. (2004) Caveolae localize protein kinase A signaling to arterial ATP-sensitive potassium channels. *Circ Res*, 95, 1012-8.
- SATTIN, A. & RALL, T. W. (1970) The effect of adenosine and adenine nucleotides on the cyclic adenosine 3', 5'-phosphate content of guinea pig cerebral cortex slices. *Mol Pharmacol*, 6, 13-23.
- SCHILLING, L., PARSONS, A. A. & WAHL, M. (1995) Effects of potassium channel activators on isolated cerebral arteries of large and small diameter in the cat. *J Neurosurg*, 83, 123-8.
- SCHUHMANN, K. & GROSCHNER, K. (1994) Protein kinase-C mediates dual modulation of L-type Ca²⁺ channels in human vascular smooth muscle. *FEBS Lett*, 341, 208-12.
- SHIMODA, L. A., SYLVESTER, J. T. & SHAM, J. S. (1998) Inhibition of voltage-gated K⁺ current in rat intrapulmonary arterial myocytes by endothelin-1. *Am J Physiol*, 274, L842-53.
- SIMA, B., WEIR, B. K., MACDONALD, R. L. & ZHANG, H. (1997) Extracellular nucleotide-induced [Ca²⁺]_i elevation in rat basilar smooth muscle cells. *Stroke*, 28, 2053-8; discussion 2059.

- SMIRNOV, S. V. & AARONSON, P. I. (1992) Ca²⁺-activated and voltage-gated K⁺ currents in smooth muscle cells isolated from human mesenteric arteries. *J Physiol*, 457, 431-54.
- SMITH, P. D., BRETT, S. E., LUYKENAAR, K. D., SANDOW, S. L., MARRELLI, S. P., VIGMOND, E. J. & WELSH, D. G. (2008) KIR channels function as electrical amplifiers in rat vascular smooth muscle. *J Physiol*, 586, 1147-60.
- SMITH, R. J., SAM, L. M., JUSTEN, J. M., BUNDY, G. L., BALA, G. A. & BLEASDALE, J. E. (1990) Receptor-coupled signal transduction in human polymorphonuclear neutrophils: effects of a novel inhibitor of phospholipase C-dependent processes on cell responsiveness. *J Pharmacol Exp Ther*, 253, 688-97.
- SOBOLOFF, J., SPASSOVA, M., HEWAVITHARANA, T., HE, L. P., LUNCSFORD, P., XU, W., VENKATACHALAM, K., VAN ROSSUM, D., PATTERSON, R. L. & GILL, D. L. (2007) TRPC channels: integrators of multiple cellular signals. *Handb Exp Pharmacol*, 575-91.
- SOHN, U. D., CAO, W., TANG, D. C., STULL, J. T., HAEBERLE, J. R., WANG, C. L., HARNETT, K. M., BEHAR, J. & BIANCANI, P. (2001) Myosin light chain kinase- and PKC-dependent contraction of LES and esophageal smooth muscle. *Am J Physiol Gastrointest Liver Physiol*, 281, G467-78.
- SOMARA, S. & BITAR, K. N. (2008) Direct association of calponin with specific domains of PKC- α . *Am J Physiol Gastrointest Liver Physiol*, 295, G1246-54.
- SOMLYO, A. P. & SOMLYO, A. V. (2000) Signal transduction by G-proteins, rho-kinase and protein phosphatase to smooth muscle and non-muscle myosin II. *J Physiol*, 522 Pt 2, 177-85.
- SOMMERVILLE, L. E. & HARTSHORNE, D. J. (1986) Intracellular calcium and smooth muscle contraction. *Cell Calcium*, 7, 353-64.

- SPERELAKIS, N. (2001) *Cell physiology : source book : a molecular approach / edited by Nicholas Sperelakis.*, San Diego, Calif. ; London Academic Press.
- STANDEN, N. B. & QUAYLE, J. M. (1998) K⁺ channel modulation in arterial smooth muscle. *Acta Physiol Scand*, 164, 549-57.
- STANDEN, N. B., QUAYLE, J. M., DAVIES, N. W., BRAYDEN, J. E., HUANG, Y. & NELSON, M. T. (1989) Hyperpolarizing vasodilators activate ATP-sensitive K⁺ channels in arterial smooth muscle. *Science*, 245, 177-80.
- STANFIELD, P. R., DAVIES, N. W., SHELTON, P. A., KHAN, I. A., BRAMMAR, W. J., STANDEN, N. B. & CONLEY, E. C. (1994) The intrinsic gating of inward rectifier K⁺ channels expressed from the murine IRK1 gene depends on voltage, K⁺ and Mg²⁺. *J Physiol*, 475, 1-7.
- STROBAEK, D., OLESEN, S. P., CHRISTOPHERSEN, P. & DISSING, S. (1996) P2-purinoceptor-mediated formation of inositol phosphates and intracellular Ca²⁺ transients in human coronary artery smooth muscle cells. *Br J Pharmacol*, 118, 1645-52.
- SUGIHARA, M., MORITA, H., MATSUDA, M., UMEBAYASHI, H., KAJIOKA, S., ITO, S., NISHIDA, M., INOUE, R., FUTATSUKI, T., YAMAZAKI, J., MORI, Y., ITO, Y., ABE, K. & HIRATA, M. (2011) Dual signaling pathways of arterial constriction by extracellular uridine 5'-triphosphate in the rat. *J Pharmacol Sci*, 115, 293-308.
- SURTI, T. S. & JAN, L. Y. (2005) A potassium channel, the M-channel, as a therapeutic target. *Curr Opin Investig Drugs*, 6, 704-11.
- SY Yong, H. T., Yang, H. H., Trinh, G., Cheung, C., Kuo, K. H. & Van Breemen, C. (2009) Mechanism of asynchronous Ca(2+) waves underlying agonist-induced contraction in the rat basilar artery. *Br J Pharmacol*, 156, 587-600.

- TAMARGO, J., CABALLERO, R., GOMEZ, R., VALENZUELA, C. & DELPON, E. (2004) Pharmacology of cardiac potassium channels. *Cardiovasc Res*, 62, 9-33.
- TANAKA, Y., KOIKE, K. & TORO, L. (2004) MaxiK channel roles in blood vessel relaxations induced by endothelium-derived relaxing factors and their molecular mechanisms. *J Smooth Muscle Res*, 40, 125-53.
- TANI, E. & MATSUMOTO, T. (2004) Continuous elevation of intracellular Ca^{2+} is essential for the development of cerebral vasospasm. *Curr Vasc Pharmacol*, 2, 13-21.
- TEDFORD, H. W. & ZAMPONI, G. W. (2006) Direct G protein modulation of Cav2 calcium channels. *Pharmacol Rev*, 58, 837-62.
- TIRUPPATHI, C., AHMMED, G. U., VOGEL, S. M. & MALIK, A. B. (2006) Ca^{2+} signaling, TRP channels, and endothelial permeability. *Microcirculation*, 13, 693-708.
- VIVES, E., BRODIN, P. & LEBLEU, B. (1997) A truncated HIV-1 Tat protein basic domain rapidly translocates through the plasma membrane and accumulates in the cell nucleus. *J Biol Chem*, 272, 16010-7.
- VOROBIOV, D., LEVIN, G., LOTAN, I. & DASCAL, N. (1998) Agonist-independent inactivation and agonist-induced desensitization of the G protein-activated K^{+} channel (GIRK) in *Xenopus* oocytes. *Pflugers Arch*, 436, 56-68.
- WALKER, E. M., BISPHAM, J. R. & HILL, S. J. (1998) Nonselective effects of the putative phospholipase C inhibitor, U73122, on adenosine A1 receptor-mediated signal transduction events in Chinese hamster ovary cells. *Biochemical Pharmacology*, 56, 1455-1462.
- WALZ, W. (2002) *Patch-clamp analysis : advanced techniques / edited by Wolfgang Walz, Alan A. Boulton and Glen B. Baker* Totowa, N.J., Humanal.

- WANG, Q. J. (2006) PKD at the crossroads of DAG and PKC signaling. *Trends Pharmacol Sci*, 27, 317-23.
- WARD, N. E. & O'BRIAN, C. A. (1993) Inhibition of protein kinase C by N-myristoylated peptide substrate analogs. *Biochemistry*, 32, 11903-9.
- WEI, A., SOLARO, C., LINGLE, C. & SALKOFF, L. (1994) Calcium sensitivity of BK-type K_{Ca} channels determined by a separable domain. *Neuron*, 13, 671-81.
- WELLMAN, G. C., QUAYLE, J. M. & STANDEN, N. B. (1998) ATP-sensitive K^+ channel activation by calcitonin gene-related peptide and protein kinase A in pig coronary arterial smooth muscle. *J Physiol*, 507 (Pt 1), 117-29.
- WELSH, D. G. & BRAYDEN, J. E. (2001) Mechanisms of coronary artery depolarization by uridine triphosphate. *Am J Physiol Heart Circ Physiol*, 280, H2545-53.
- WHITE, P. J., KUMARI, R., PORTER, K. E., LONDON, N. J., NG, L. L. & BOARDER, M. R. (2000) Antiproliferative effect of UTP on human arterial and venous smooth muscle cells. *Am J Physiol Heart Circ Physiol*, 279, H2735-42.
- WINDER, S. J., ALLEN, B. G., CLEMENT-CHOMIENNE, O. & WALSH, M. P. (1998) Regulation of smooth muscle actin-myosin interaction and force by calponin. *Acta Physiol Scand*, 164, 415-26.
- WINDER, S. J. & WALSH, M. P. (1993) Calponin: thin filament-linked regulation of smooth muscle contraction. *Cell Signal*, 5, 677-86.
- WINDER, S. J., WALSH, M. P., VASULKA, C. & JOHNSON, J. D. (1993) Calponin-calmodulin interaction: properties and effects on smooth and skeletal muscle actin binding and actomyosin ATPases. *Biochemistry*, 32, 13327-33.
- WOODSOME, T. P., ETO, M., EVERETT, A., BRAUTIGAN, D. L. & KITAZAWA, T. (2001) Expression of CPI-17 and myosin phosphatase correlates with Ca^{2+}

- sensitivity of protein kinase C-induced contraction in rabbit smooth muscle. *J Physiol*, 535, 553-64.
- WU, B. N., LUYKENAAR, K. D., BRAYDEN, J. E., GILES, W. R., CORTELING, R. L., WIEHLER, W. B. & WELSH, D. G. (2007) Hyposmotic challenge inhibits inward rectifying K⁺ channels in cerebral arterial smooth muscle cells. *Am J Physiol Heart Circ Physiol*, 292, H1085-94.
- XIAO, G. Q., MOCHLY-ROSEN, D. & BOUTJDIR, M. (2003) PKC isozyme selective regulation of cloned human cardiac delayed slow rectifier K current. *Biochem Biophys Res Commun*, 306, 1019-25.
- XIE, Z., SU, W., GUO, Z., PANG, H., POST, S. R. & GONG, M. C. (2006) Up-regulation of CPI-17 phosphorylation in diabetic vasculature and high glucose cultured vascular smooth muscle cells. *Cardiovasc Res*, 69, 491-501.
- YAMADA, Y. & SUNAGA, Y. (1997) [ATP-sensitive potassium channel--sulfonylurea receptor]. *Nippon Rinsho*, 55 Suppl, 458-62.
- YITZHAKI, S., SHNEYVAYS, V., JACOBSON, K. A. & SHAINBERG, A. (2005) Involvement of uracil nucleotides in protection of cardiomyocytes from hypoxic stress. *Biochemical Pharmacology*, 69, 1215-1223.
- YOON, E. J., HAMM, H. E. & CURRIE, K. P. (2008) G protein betagamma subunits modulate the number and nature of exocytotic fusion events in adrenal chromaffin cells independent of calcium entry. *J Neurophysiol*, 100, 2929-39.
- ZHANG, J., REN, C., CHEN, L., NAVEDO, M. F., ANTOS, L. K., KINSEY, S. P., IWAMOTO, T., PHILIPSON, K. D., KOTLIKOFF, M. I., SANTANA, L. F., WIER, W. G., MATTESON, D. R. & BLAUSTEIN, M. P. (2010) Knockout of Na⁺/Ca²⁺ exchanger in smooth muscle attenuates vasoconstriction and L-type Ca²⁺ channel current and lowers blood pressure. *Am J Physiol Heart Circ Physiol*, 298, H1472-83.

- ZHAO, G., ADEBIYI, A., BLASKOVA, E., XI, Q. & JAGGAR, J. H. (2008) Type 1 inositol 1,4,5-trisphosphate receptors mediate UTP-induced cation currents, Ca²⁺ signals, and vasoconstriction in cerebral arteries. *Am J Physiol Cell Physiol*, 295, C1376-84.
- ZHAO, X., FALCK, J. R., GOPAL, V. R., INSCHO, E. W. & IMIG, J. D. (2004) P2X receptor-stimulated calcium responses in preglomerular vascular smooth muscle cells involves 20-hydroxyeicosatetraenoic acid. *J Pharmacol Exp Ther*, 311, 1211-7.
- ZSCHAUER, A., UUSITALO, H. & BRAYDEN, J. E. (1992) Characteristics of CGRP-induced relaxation in rabbit ophthalmic artery. *Ann N Y Acad Sci*, 657, 507-9.